

**STUDY OF CORROSION INHIBITION EFFICIENCY, MECHANISM AND  
APPLICATION OF CHROMONES AS CORROSION INHIBITORS ON ALUMINIUM,  
ZINC AND MILD STEEL IN ACETIC AND SULPHURIC ACIDS**

**Ratshikombo Rinae**

**(15015809)**

A dissertation submitted in the fulfilment of the requirements of the Master of Science in the

**Department of Chemistry**

School of Mathematical and Natural Sciences

Supervisor: Dr L.C Murulana, PhD

Co-Supervisor: S.J Moema, MSc


**January 2021**

## DECLARATION

---

I, Ratshikombo Rinae, hereby declare this dissertation for Master of Science degree at University Of Venda to be my original work and to the best of my knowledge has not been submitted for any Diploma or degree at any University. No part or portion of this dissertation has been reproduced without acknowledgement.

**Signature:**



**Date:** January 2021

## DEDICATION

I dedicate this dissertation to my son, **Ratshikombo Miracle Akhodiwe**, his presence always boost my strength and encourage me to work day and night to achieved my dreams and goal

## Table of contents

---

NO	CONTENTS	PAGE NO
	Acknowledgements	i
	Abstract	ii
	List of Abbreviations	iii
	List of figures	v
	List of tables	xiv
	Chapter 1: Introduction	
1	Introduction	1
1.1	Definition of corrosion	2
1.2	General metallic corrosion	2
1.3	Corrosion problem areas	6
1.4	Significance of the study	7
1.5	Aim and objectives	8
	Chapter 2: Literature Review	
2	Corrosion protection	9
2.1	Methods of corrosion protection	9
2.1.1	Selection of materials	9
2.1.2	Non-metallic piping, coatings and lining	9
2.1.3	Protecting through cathodic	10
2.1.4	Controlling through inhibitors	10
2.2	Corrosion inhibitors	10
2.2.1	The anode corrosion inhibitors	10

2.2.2	The cathode corrosion inhibitors	11
2.2.3	Combined type corrosion inhibitors	11
2.2.4	Interface corrosion inhibitors	11
2.2.5	Passivation anodic corrosion inhibitors	12
2.2.6	Precipitation corrosion inhibitors	12
2.2.7	Adsorption corrosion inhibitors	13
2.3	Factors affecting the characteristics of inhibitors	13
2.4	Environmental conditioners	14
2.4.1	Environment	14
2.4.2	Material corrosion of zinc	14
2.5	Corrosion mechanisms in acid solutions	15
2.6	Corrosion	15
2.6.1	Corrosion rate and conditions affecting it	15
2.6.2	Corrosion in different media	17
2.6.3	Importance of corrosion	17
2.6.4	Consequences of corrosion	18
2.7	Thermodynamics of corrosion	18
2.8	Electrochemical approaches	19
2.9	Chromones as corrosion inhibitors	22

Chapter 3: Experimental Details	
3.1 Metals utilized	26
3.2 Solutions	26
3.3 Corrosion inhibitors utilized	26
3.4 Electrochemical measurements	27
3.4.1 Potentiodynamic Polarization (PDP)	27
3.4.2 Electrochemical Impedance Spectroscopy (EIS)	27
3.5 3D Optical Microscopy (3DOM)	28
3.6 Atomic Absorption Spectroscopy (AAS)	28
3.7 Fourier Transform Infrared Spectroscopy (FTIR)	28
3.8 Weight loss measurements	28
Chapter 4: Results and Discussions	
4.1 Potentiodynamic Polarization (PDP) results	29
4.2 Electrochemical Impedance Spectroscopy (EIS) results	41
4.3 3D Optical Microscopy (3DOM) results	60
4.4 Atomic Absorption Spectroscopy (AAS) results	71
4.5 Fourier Transform Infrared Spectroscopy (FTIR) results	76
4.6 Weight loss measurements results	85
Chapter 5: conclusions and recommendations	128
Chapter 6: Future work	132
Chapter 7: References	



## Acknowledgements

---

Wisdom comes from the creator of heaven and earth (Almighty God) but knowledge comes from studying. These wise words encourage me to thank almighty God for life and wisdom that originate in myself.

I am deeply indebted to my supervisor **Dr L C Murulana** for his support, guidance, technical assistance making sure that all techniques used in this project become easier and understandable, reading my work and always available to assist me in any challenge related to this project. Without your supervision this work would not be what it is today. I wish to acknowledge my co-supervisor **Mr J Moema** from Mintek, his contribution toward this work make it possible to conduct 3D Optical Microscopy at Mintek, with the technical assistance from **Mrs ND Masia**.

I extend my thank you and appreciation to my research colleagues, **Mr T Sithuba, Ms F Tshikhudo, Mr T Nesane, Mr NM Dube-Johnstone**, and the **Corrosion Science Research Group (CoRRoSci)** for their emotional support

I am also highly grateful to Department of Chemistry of the University of Venda for admitting and affording me a space to carry out this research project. I am also grateful towards NRF and SASOL Foundation for funding, without their financial support none of this would have been possible.

This study focuses on investigating three chromone derivatives namely; 3-cyanochromone (3CYC), 6-methylchromone-2-carboxylic acid (6MC2C), and 6methylchromone hydrate (6MCH) as corrosion inhibitor for three metals namely, mild steel, zinc, and aluminium in 1.5 M of acetic acid, sulphuric acid, and nitric acid solution at 303K–333K. Techniques adopted in this study were electrochemical impedance spectroscopy (EIS), Potentiodynamic Polarization (PDP), Atomic Absorption Spectroscopy (AAS), and weight loss measurements to study the inhibition efficiency, corrosion mechanism, and the adsorption behaviour of chromone to metal surface. Fourier Transform Infrared spectrometry (FTIR) was useful to reveal the functional groups formed and disappeared during the interaction between the inhibitors and metal surface. 3D Optical Microscopic (3DOP) was utilised to investigate the surface morphology of metal in the presence and absence of corrosion inhibitors.

These chromone compounds inhibited corrosion of zinc, mild steel, and aluminium in 1.5 M sulphuric acid, acetic acid, and nitric acid at 303K–333K. The effect of temperature on zinc, mild steel, and aluminium on inhibition efficiency obtained from PDP, EIS, AAS, and weight loss measurements shows that mild steel was affected severely with lower inhibition efficiency, however, these techniques shows that when the concentration of inhibitors increases, the inhibition efficiency also increases. A decrease in surface coverage occurs when temperature increases.

EIS display an increase in the  $R_{ct}$  value which lead towards an increase in the surface coverage of metal by the inhibitors. PDP reveals that the inhibitors successful affect cathodic and anodic half reactions almost equally. Weight loss measurements through  $\Delta G^\circ$  values reveal that the interactions of Al–inhibitor possess covalent nature and monolayer characteristics indicating chemisorption. It further shows physisorption character on Zn–inhibitor and MS–inhibitor. FTIR spectra displayed the disappeared and formed functional group bonds occurred when inhibitors interact with the metal surface. This implies that corrosion was minimised through this interaction forming Zn-inhibitor, MS-inhibitor, and Al-inhibitor complexes. 3DOP display rough metal surface when zinc, mild steel, and aluminium were exposed in sulphuric acid, acetic acid and nitric acid. The roughness when 3CYC, 6MCH, and 6MC2C were introduced was minimal, indicating the protection offered by these inhibitors to the metal surface. The





information gathered shows that these three chromone derivatives successfully reduce the melting of zinc, mild steel, and aluminium in acidic medium

**Keywords:** aluminium, zinc, mild steel, chromones, inhibition efficiency, adsorption.

## List of Abbreviations Used

---

<b>6MCH</b>	6-methylchromone hydrate
<b>6MC2C</b>	6-methylchromone-2-carboxylic acid
<b>3CYC</b>	3-cyanochromones
<b>AC</b>	Alternating current
<b>Al</b>	Aluminum
<b>MS</b>	Mild steel
<b>Zn</b>	Zinc
<b>CPE</b>	Constant Phase Element
<b>EIS</b>	Electrochemical Impedance Spectroscopy
<b>FT-IR</b>	Fourier Transform Infrared Spectroscopy
<b>HCl</b>	Hydrochloric Acid
<b>HNO<sub>3</sub></b>	Nitric acid
<b>H<sub>2</sub>SO<sub>4</sub></b>	Sulphuric acid
<b>IBP</b>	Intermediate Bode Plots
<b>IE</b>	Inhibition Efficiency
<b>IR</b>	Infrared radiator
<b>LPR</b>	Linear Polarization Resistance
<b>MINTEK</b>	Council for Mineral Technology
<b>OCP</b>	Open Circuit Potential
<b>PCE</b>	Platinum Counter Electrode
<b>PDP</b>	Potentiodynamic Polarization
<b>PGSTAT302N</b>	Metrohm Autolab Potentiostat/Galvanostat
<b>R<sub>ct</sub></b>	Charge Transfer Resistance
<b>RE</b>	Reference Electrode
<b>R<sub>p</sub></b>	Polarization Resistance

<b><math>R_s</math></b>	Solution Resistance
<b>SA</b>	South Africa
<b>SCC</b>	Stress Corrosion Cracking
<b>SCE</b>	Saturated Calomel Electrode
<b>WE</b>	Working Electrode
<b>SE</b>	Secondary Electrons
<b>3DOP</b>	3D Optical Microscopy

## List of figures

No	Description	PAGE No
1.1	Corroded zinc metal used for roofing purpose	3
2.1	Structure of 3-cyanochromones (3CYC)	24
2.2	Structure of 6-Methylchromone hydrate (6MCH)	24
2.3	Structure of 6-methylchromone-2-carboxylic acid (6MC2C)	25
3.1	Structures of chromone to be used as corrosion inhibitors	26
4.1	Tafel plots for mild steel in 1.5 M H <sub>2</sub> SO <sub>4</sub> in the absence and presence of different concentrations of 3CYC	29
4.2	Tafel plots for mild steel in 1.5 M H <sub>2</sub> SO <sub>4</sub> in the absence and presence of different concentrations of 6MCH	30
4.3	Tafel plots for mild steel in 1.5 M H <sub>2</sub> SO <sub>4</sub> in the absence and presence of different concentrations of 6MC2C	30
4.4	Tafel plots for zinc in 1.5 M H <sub>2</sub> SO <sub>4</sub> in the absence and presence of different concentrations of 3CYC	31
4.5	Tafel plots for zinc in 1.5 M H <sub>2</sub> SO <sub>4</sub> in the absence and presence of different concentrations of 6MCH	31
4.6	Tafel plots for zinc in 1.5 M H <sub>2</sub> SO <sub>4</sub> in the absence and presence of different concentrations of 6MC2C	32
4.7	Tafel plots for mild steel in 1.5 M acetic acid in the absence and presence of different concentrations of 3CYC	32
4.8	Tafel plots for mild steel in 1.5 M CH <sub>3</sub> COOH in the absence and presence of different concentrations of 6MCH	33
4.9	Tafel plots for mild steel in 1.5 M CH <sub>3</sub> COOH in the absence and presence of different concentrations of 6MC2C	33
4.10	Tafel plots for zinc in 1.5 M CH <sub>3</sub> COOH in the absence and presence of different concentrations of 3CYC	34
4.11	Tafel plots for zinc in 1.5 M CH <sub>3</sub> COOH in the absence and presence of different concentrations of 6MCH	34

4.12	Tafel plots for zinc in 1.5 M $\text{CH}_3\text{COOH}$ in the absence and presence of different concentrations of 6MC2C	35
4.13	Tafel plots for aluminium in 1.5 M $\text{HNO}_3$ in the absence and presence of different concentrations of 3CYC	35
4.14	Tafel plots for aluminium in 1.5 M $\text{HNO}_3$ in the absence and presence of different concentrations of 6MC2C	36
4.15	Tafel plots for aluminium in 1.5 M $\text{HNO}_3$ in the absence and presence of different concentrations of 6MCH	36
4.16	Nyquist plot of mild steel metal in sulphuric acid in the presence of various concentrations of 3CYC	42
4.17	Bode diagrams of the impedance for MS in 1.5 M sulphuric acid without and with different concentration of 3CYC	42
4.18	Nyquist plot of mild steel metal in sulphuric acid in the presence of various concentrations of 6MC2C	43
4.19	Bode diagrams of the impedance for MS in 1.5 M sulphuric acid without and with different concentration of 6MC2C	43
4.20	Nyquist plot of mild steel metal in sulphuric acid in the presence of various concentrations of 6MCH	44
4.21	Bode diagrams of the impedance for MS in 1.5 M sulphuric acid without and with different concentration of 6MCH	44
4.22	Nyquist plot of Aluminium metal in nitric acid in the presence of various concentrations of 3CYC	45
4.23	Bode diagrams of the impedance for Al in 1.5 M nitric acid without and with different concentration of 3CYC	45
4.24	Nyquist plot of Aluminium metal in nitric acid in the presence of various concentrations of 6MC2C	46
4.25	Bode diagrams of the impedance for Al in 1.5 M nitric acid without and with different concentration of 6MC2C	46
4.26	Nyquist plot of Aluminium metal in nitric acid in the presence of various concentrations of 6MCH	47
4.27	Bode diagrams of the impedance for Al in 1.5 M nitric acid without and with different concentration of 6MCH	47
4.28	Nyquist plot of zinc metal in sulphuric acid in the presence of various concentrations of 3CYC	48
4.29	Bode diagrams of the impedance for Zn in 1.5 M sulphuric acid without and with different concentration of 3CYC	48

4.30	Nyquist plot of zinc metal in sulphuric acid in the presence of various concentrations of 6MC2C	49
4.31	Bode diagrams of the impedance for Zn in 1.5 M sulphuric acid without and with different concentration of 6MC2C	49
4.32	Nyquist plot of zinc metal in sulphuric acid in the presence of various concentrations of 6MCH	50
4.33	Bode diagrams of the impedance for Zn in 1.5 M sulphuric acid without and with different concentration of 6MCH	50
4.34	Nyquist plot of mild steel metal in acetic acid in the presence of various concentrations of 6MCH	51
4.35	Bode diagrams of the impedance for MS in 1.5 M sulphuric acid without and with different concentration of 6MCH	51
4.36	Nyquist plot of mild steel metal in acetic acid in the presence of various concentrations of 6MC2C	52
4.37	Bode diagrams of the impedance for MS in 1.5 M sulphuric acid without and with different concentration of 6MC2C	52
4.38	Nyquist plot of mild steel metal in acetic acid in the presence of various concentrations of 3CYC	53
4.39	Bode diagrams of the impedance for MS in 1.5 M acetic acid without and with different concentration of 3CYC	53
4.40	Nyquist plot of zinc metal in acetic acid in the presence of various concentrations of 3CYC	54
4.41	Bode diagrams of the impedance for Zn in 1.5 M acetic acid without and with different concentration of 3CYC	54
4.42	Nyquist plot of zinc metal in acetic acid in the presence of various concentrations of 6MCH	55
4.43	Bode diagrams of the impedance for Zn in 1.5 M acetic acid without and with different concentration of 6MCH	55
4.44	Nyquist plot of zinc metal in acetic acid in the presence of various concentrations of 6MC2C	56
4.45	Bode diagrams of the impedance for Zn in 1.5 M acetic acid without and with different concentration of 6MC2C	56
4.46	Equivalent circuit used to fit the impedance spectra	57
4.47	2D optical microscopy of the surface of mild steel: (a) plain mild steel and (b) mild steel immersed in CH <sub>3</sub> COOH uninhibited	61

4.48	2D optical microscopy of the surface of MS immersed in CH <sub>3</sub> COOH in the presence of (a) 3CYC (b) 6MCH	61
4.49	2D optical microscopy of the surface of MS immersed in CH <sub>3</sub> COOH in the presence of 6MC2C	61
4.50	2D optical microscopy of the surface of mild steel: (a) plain mild steel and (b) mild steel immersed in H <sub>2</sub> SO <sub>4</sub> uninhibited	61
4.51	2D optical microscopy of the surface of MS immersed in H <sub>2</sub> SO <sub>4</sub> in the presence of (a) 3CYC (b) 6MCH	62
4.52	2D optical microscopy of the surface of MS immersed in H <sub>2</sub> SO <sub>4</sub> in the presence of 6MC2C	62
4.53	2D optical microscopy of the surface of zinc: (a) plain zinc and (b) zinc immersed in CH <sub>3</sub> COOH uninhibited	63
4.54	2D optical microscopy of the surface of zinc immersed in CH <sub>3</sub> COOH in the presence of (a) 3CYC (b) 6MCH	63
4.55	2D optical microscopy of the surface of zinc immersed in CH <sub>3</sub> COOH in the presence of 6MC2C	63
4.56	2D optical microscopy of the surface of zinc: (a) plain zinc and (b) zinc immersed in H <sub>2</sub> SO <sub>4</sub> uninhibited	64
4.57	2D optical microscopy of the surface of zinc immersed in H <sub>2</sub> SO <sub>4</sub> in the presence of (a) 3CYC (b) 6MCH	64
4.58	2D optical microscopy of the surface of zinc immersed in H <sub>2</sub> SO <sub>4</sub> in the presence of 6MC2C	64
4.59	2D optical microscopy of the surface of aluminium: (a) plain aluminium and (b) aluminium immersed in HNO <sub>3</sub> uninhibited	65
4.60	2D optical microscopy of the surface of aluminium immersed in HNO <sub>3</sub> in the presence of (a) 3CYC (b) 6MCH	65
4.61	2D optical microscopy of the surface of aluminium immersed in HNO <sub>3</sub> in the presence of 6MC2C	65
4.62	3D optical microscopy of the surface of mild steel: (a) plain mild steel and (b) mild steel immersed in CH <sub>3</sub> COOH uninhibited	65
4.63	3D optical microscopy of the surface of MS immersed in CH <sub>3</sub> COOH in the presence of (a) 3CYC (b) 6MCH	65
4.64	3D optical microscopy of the surface of MS immersed in CH <sub>3</sub> COOH in the presence of 6MC2C	65
4.65	3D optical microscopy of the surface of mild steel: (a) plain mild steel and (b) mild steel immersed in H <sub>2</sub> SO <sub>4</sub> uninhibited	66

4.66	3D optical microscopy of the surface of MS immersed in H <sub>2</sub> SO <sub>4</sub> in the presence of (a) 3CYC (b) 6MCH	66
4.67	3D optical microscopy of the surface of MS immersed in H <sub>2</sub> SO <sub>4</sub> in the presence of 6MC2C	66
4.68	3D optical microscopy of the surface of zinc: (a) plain zinc and (b) zinc immersed in CH <sub>3</sub> COOH uninhibited	67
4.69	3D optical microscopy of the surface of zinc immersed in CH <sub>3</sub> COOH in the presence of (a) 3CYC (b) 6MCH	67
4.70	3D optical microscopy of the surface of zinc immersed in CH <sub>3</sub> COOH in the presence of 6MC2C	67
4.71	3D optical microscopy of the surface of zinc: (a) plain zinc and (b) zinc immersed in H <sub>2</sub> SO <sub>4</sub> uninhibited	68
4.72	3D optical microscopy of the surface of zinc immersed in H <sub>2</sub> SO <sub>4</sub> in the presence of (a) 3CYC (b) 6MCH	68
4.73	3D optical microscopy of the surface of zinc immersed in H <sub>2</sub> SO <sub>4</sub> in the presence of 6MC2C	68
4.74	3D optical microscopy of the surface of aluminium: (a) plain aluminium and (b) aluminium immersed in HNO <sub>3</sub> uninhibited	69
4.75	3D optical microscopy of the surface of aluminium immersed in HNO <sub>3</sub> in the presence of (a) 3CYC (b) 6MCH	69
4.76	3D optical microscopy of the surface of aluminium immersed in HNO <sub>3</sub> in the presence of 6MC2C	69
4.77	Corrosion parameters obtained from atomic absorption spectroscopy of Al exposed in HNO <sub>3</sub>	73
4.78	Corrosion parameters obtained from atomic absorption spectroscopy of MS exposed in H <sub>2</sub> SO <sub>4</sub>	73
4.79	Corrosion parameters obtained from atomic absorption spectroscopy of MS exposed in CH <sub>3</sub> COOH	74
4.80	Corrosion parameters obtained from atomic absorption spectroscopy of Zn exposed in H <sub>2</sub> SO <sub>4</sub>	75
4.81	Corrosion parameters obtained from atomic absorption spectroscopy of Zn exposed in CH <sub>3</sub> COOH	75
4.82	FT-IR spectra for the studied corrosion inhibitors and adsorption films formed on Zn in 1.5 M H <sub>2</sub> SO <sub>4</sub> using 3CYC	76
4.83	FT-IR spectra for the studied corrosion inhibitors and adsorption films formed on MS in 1.5 M H <sub>2</sub> SO <sub>4</sub> using 3CYC	76



4.84	FT-IR spectra for the studied corrosion inhibitors and adsorption films formed on Zn in 1.5 M H <sub>2</sub> SO <sub>4</sub> using 6MC2C	77
4.85	FT-IR spectra for the studied corrosion inhibitors and adsorption films formed on MS in 1.5 M H <sub>2</sub> SO <sub>4</sub> using 6MC2C	77
4.86	FT-IR spectra for the studied corrosion inhibitors and adsorption films formed on Zn in 1.5 M H <sub>2</sub> SO <sub>4</sub> using 6MCH	78
4.87	FT-IR spectra for the studied corrosion inhibitors and adsorption films formed on MS in 1.5 M H <sub>2</sub> SO <sub>4</sub> using 6MCH	78
4.88	FT-IR spectra for the studied corrosion inhibitors and adsorption films formed on Al in 1.5 M HNO <sub>3</sub> using 3CYC	79
4.89	FT-IR spectra for the studied corrosion inhibitors and adsorption films formed on Al in 1.5 M HNO <sub>3</sub> using 6MC2C	79
4.90	FT-IR spectra for the studied corrosion inhibitors and adsorption films formed on Al in 1.5 M HNO <sub>3</sub> using 6MCH	80
4.91	FT-IR spectra for the studied corrosion inhibitors and adsorption films formed on Zn in 1.5 M CH <sub>3</sub> COOH using 3CYC	80
4.92	FT-IR spectra for the studied corrosion inhibitors and adsorption films formed on MS in 1.5 M CH <sub>3</sub> COOH using 3CYC	81
4.93	FT-IR spectra for the studied corrosion inhibitors and adsorption films formed on Zn in 1.5 M CH <sub>3</sub> COOH using 6MC2C	81
4.94	FT-IR spectra for the studied corrosion inhibitors and adsorption films formed on MS in 1.5 M CH <sub>3</sub> COOH using 6MC2C	82
4.95	FT-IR spectra for the studied corrosion inhibitors and adsorption films formed on Zn in 1.5 M CH <sub>3</sub> COOH using 6MCH	82
4.96	FT-IR spectra for the studied corrosion inhibitors and adsorption films formed on MS in 1.5 M CH <sub>3</sub> COOH using 6MCH	85
4.97	Weight loss measurements of mild steel in the presence of H <sub>2</sub> SO <sub>4</sub> at 300 K–333 K	87
4.98	Weight loss measurements of zinc in the presence of H <sub>2</sub> SO <sub>4</sub> at 300 K–333 K	87
4.99	Weight loss measurements of mild steel in the presence of CH <sub>3</sub> COOH at 300 K–333 K	88
4.100	Weight loss measurements of zinc in the presence of CH <sub>3</sub> COOH at 300 K–333 K	88

4.101	Weight loss measurements of aluminium in the presence of HNO <sub>3</sub> at 300 K–333 K	89
4.102	Weight loss measurements on mild steel exposed in 1.5 M H <sub>2</sub> SO <sub>4</sub> in the presence of 3CYC	92
4.103	Weight loss measurements on mild steel exposed in 1.5 M H <sub>2</sub> SO <sub>4</sub> in the presence of 6MCH	92
4.104	Weight loss measurements on mild steel exposed in 1.5 M H <sub>2</sub> SO <sub>4</sub> in the presence of 6MC2C	93
4.105	Weight loss measurements on mild steel exposed in 1.5 M CH <sub>3</sub> COOH in the presence of 3CYC	93
4.106	Weight loss measurements on mild steel exposed in 1.5 M CH <sub>3</sub> COOH in the presence of 6MCH	94
4.107	Weight loss measurements on mild steel exposed in 1.5 M CH <sub>3</sub> COOH in the presence of 6MC2C	94
4.108	Weight loss measurements on zinc exposed in 1.5 M H <sub>2</sub> SO <sub>4</sub> in the presence of 3CYC	96
4.109	Weight loss measurements on zinc exposed in 1.5 M H <sub>2</sub> SO <sub>4</sub> in the presence of 6MCH	97
4.110	Weight loss measurements on zinc exposed in 1.5 M H <sub>2</sub> SO <sub>4</sub> in the presence of 6MC2C	97
4.111	Weight loss measurements on zinc exposed in 1.5 M CH <sub>3</sub> COOH in the presence of 3CYC	97
4.112	Weight loss measurements on zinc exposed in 1.5 M CH <sub>3</sub> COOH in the presence of 6MCH	98
4.113	Weight loss measurements on zinc exposed in 1.5 M CH <sub>3</sub> COOH in the presence of 6MC2C	98
4.114	Weight loss measurements on aluminium exposed in 1.5 M HNO <sub>3</sub> in the presence of 3CYC	100
4.115	Weight loss measurements on aluminium exposed in 1.5 M HNO <sub>3</sub> in the presence of 6MC2C	100
4.116	Weight loss measurements on aluminium exposed in 1.5 M HNO <sub>3</sub> in the presence of 6MCH	100

4.117	Arrhenius plots for the corrosion of mild steel in 1.5 M H <sub>2</sub> SO <sub>4</sub> in the absence and presence of various concentrations of 3CYC	108
4.118	Arrhenius plots for the corrosion of mild steel in 1.5 M H <sub>2</sub> SO <sub>4</sub> in the absence and presence of various concentrations of 6MCH	109
4.119	Arrhenius plots for the corrosion of mild steel in 1.5 M H <sub>2</sub> SO <sub>4</sub> in the absence and presence of various concentrations of 6MC2C	109
4.120	Arrhenius plots for the corrosion of mild steel in 1.5 M CH <sub>3</sub> COOH in the absence and presence of various concentrations of 3CYC	110
4.121	Arrhenius plots for the corrosion of mild steel in 1.5 M CH <sub>3</sub> COOH in the absence and presence of various concentrations of 6MCH	110
4.122	Arrhenius plots for the corrosion of mild steel in 1.5 M CH <sub>3</sub> COOH in the absence and presence of various concentrations of 6MC2C	111
4.123	Arrhenius plots for the corrosion of zinc in 1.5 M H <sub>2</sub> SO <sub>4</sub> in the absence and presence of various concentrations of 3CYC	111
4.124	Arrhenius plots for the corrosion of zinc in 1.5 M H <sub>2</sub> SO <sub>4</sub> in the absence and presence of various concentrations of 6MCH	112
4.125	Arrhenius plots for the corrosion of zinc in 1.5 M H <sub>2</sub> SO <sub>4</sub> in the absence and presence of various concentrations of 6MC2C	112
4.126	Arrhenius plots for the corrosion of zinc in 1.5 M CH <sub>3</sub> COOH in the absence and presence of various concentrations of 3CYC	113
4.127	Arrhenius plots for the corrosion of zinc in 1.5 M CH <sub>3</sub> COOH in the absence and presence of various concentrations of 6MCH	113
4.128	Arrhenius plots for the corrosion of zinc in 1.5 M CH <sub>3</sub> COOH in the absence and presence of various concentrations of 6MC2C	114
4.129	Arrhenius plots for the corrosion of aluminium in 1.5 M HNO <sub>3</sub> in the absence and presence of various concentrations of 3CYC	114
4.130	Arrhenius plots for the corrosion of aluminium in 1.5 M HNO <sub>3</sub> in the absence and presence of various concentrations of 6MCH	115
4.131	Arrhenius plots for the corrosion of aluminium in 1.5 M HNO <sub>3</sub> in the absence and presence of various concentrations of 6MC2C	115
4.132	Transition state plots for the corrosion of mild steel in 1.5 M H <sub>2</sub> SO <sub>4</sub> in the absence and presence of various concentrations of 3CYC	118
4.133	Transition state plots for the corrosion of mild steel in 1.5 M H <sub>2</sub> SO <sub>4</sub> in the absence and presence of various concentrations of 6MCH	118
4.134	Transition state plots for the corrosion of mild steel in 1.5 M H <sub>2</sub> SO <sub>4</sub> in the absence and presence of various concentrations of 6MC2C	119

4.135	Transition state plots for the corrosion of mild steel in 1.5 M CH <sub>3</sub> COOH in the absence and presence of various concentrations of 3CYC	119
4.136	Transition state plots for the corrosion of mild steel in 1.5 M CH <sub>3</sub> COOH in the absence and presence of various concentrations of 6MCH	120
4.137	Transition state plots for the corrosion of mild steel in 1.5 M CH <sub>3</sub> COOH in the absence and presence of various concentrations of 6MC2C	120
4.138	Transition state plots for the corrosion of zinc in 1.5 M H <sub>2</sub> SO <sub>4</sub> in the absence and presence of various concentrations of 3CYC	121
4.139	Transition state plots for the corrosion of zinc in 1.5 M H <sub>2</sub> SO <sub>4</sub> in the absence and presence of various concentrations of 6MCH	121
4.140	Transition state plots for the corrosion of zinc in 1.5 M H <sub>2</sub> SO <sub>4</sub> in the absence and presence of various concentrations of 6MC2C	122
4.141	Transition state plots for the corrosion of zinc in 1.5 M CH <sub>3</sub> COOH in the absence and presence of various concentrations of 3CYC	122
4.142	Transition state plots for the corrosion of zinc in 1.5 M CH <sub>3</sub> COOH in the absence and presence of various concentrations of 6MCH	123
4.143	Transition state plots for the corrosion of zinc in 1.5 M CH <sub>3</sub> COOH in the absence and presence of various concentrations of 6MC2C	123
4.144	Transition state plots for the corrosion of aluminium in 1.5 M HNO <sub>3</sub> in the absence and presence of various concentrations of 3CYC	124
4.145	Transition state plots for the corrosion of aluminium in 1.5 M HNO <sub>3</sub> in the absence and presence of various concentrations of 6MCH	124
4.146	Transition state plots for the corrosion of aluminium in 1.5 M HNO <sub>3</sub> in the absence and presence of various concentrations of 6MC2C	125

### List of tables

No	Description	PAGE No
4.1	Potentiodynamic polarization (PDP) parameters such as corrosion potential ( $E_{\text{corr}}$ ), corrosion current density ( $i_{\text{corr}}$ ) and anodic and cathodic Tafel slopes ( $b_a$ and $b_c$ ) using different inhibitors on mild steel in $\text{H}_2\text{SO}_4$	37
4.2	Potentiodynamic polarization (PDP) parameters such as corrosion potential ( $E_{\text{corr}}$ ), corrosion current density ( $i_{\text{corr}}$ ) and anodic and cathodic Tafel slopes ( $b_a$ and $b_c$ ) using different inhibitors on zinc in $\text{H}_2\text{SO}_4$	37
4.3	Potentiodynamic polarization (PDP) parameters such as corrosion potential ( $E_{\text{corr}}$ ), corrosion current density ( $i_{\text{corr}}$ ) and anodic and cathodic Tafel slopes ( $b_a$ and $b_c$ ) using different inhibitors on mild steel in $\text{CH}_3\text{COOH}$	38
4.4	Potentiodynamic polarization (PDP) parameters such as corrosion potential ( $E_{\text{corr}}$ ), corrosion current density ( $i_{\text{corr}}$ ) and anodic and cathodic Tafel slopes ( $b_a$ and $b_c$ ) using different inhibitors on zinc in $\text{CH}_3\text{COOH}$	39
4.5	Potentiodynamic polarization (PDP) parameters such as corrosion potential ( $E_{\text{corr}}$ ), corrosion current density ( $i_{\text{corr}}$ ) and anodic and cathodic Tafel slopes ( $b_a$ and $b_c$ ) using different inhibitors on aluminium in $\text{HNO}_3$	40
4.6	Electrochemical impedance (EIS) parameters for MS corrosion in 1.5 M $\text{H}_2\text{SO}_4$	58
4.7	Electrochemical impedance (EIS) parameters for Al corrosion in 1.5 M nitric acid	58
4.8	Electrochemical impedance (EIS) parameters for Zn corrosion in 1.5 M $\text{H}_2\text{SO}_4$	59
4.9	Electrochemical impedance (EIS) parameters for MS corrosion in 1.5 M acetic acid	59
4.10	Electrochemical impedance (EIS) parameters for Zn corrosion in 1.5 M acetic acid.	60

4.11	Corrosion parameters obtained from atomic absorption spectroscopy of Aluminium exposed in HNO <sub>3</sub>	70
4.12	Corrosion parameters obtained from atomic absorption spectroscopy of mild steel exposed in H <sub>2</sub> SO <sub>4</sub>	70
4.13	Corrosion parameters obtained from atomic absorption spectroscopy of mild steel exposed in CH <sub>3</sub> COOH	71
4.14	Corrosion parameters obtained from atomic absorption spectroscopy of zinc exposed in H <sub>2</sub> SO <sub>4</sub>	71
4.15	Corrosion parameters obtained from atomic absorption spectroscopy of zinc exposed in CH <sub>3</sub> COOH	71
4.16	FTIR spectra indicating various functional group	84
4.17	Weight loss measurements of mild steel in H <sub>2</sub> SO <sub>4</sub> , in the absence of the corrosion inhibitors	85
4.18	Weight loss measurements of zinc in H <sub>2</sub> SO <sub>4</sub> , in the absence of the corrosion inhibitors	85
4.19	Weight loss measurements of mild steel in CH <sub>3</sub> COOH in the absence of the corrosion inhibitors	86
4.20	Weight loss measurements of zinc in CH <sub>3</sub> COOH in the absence of the corrosion inhibitors	86
4.21	Weight loss measurements of aluminium in HNO <sub>3</sub> in the absence of the corrosion inhibitors	87
4.22	Weight loss measurements on mild steel exposed in 1.5 M H <sub>2</sub> SO <sub>4</sub> in the presence of 3CYC	88
4.23	Weight loss measurements on mild steel exposed in 1.5 M H <sub>2</sub> SO <sub>4</sub> in the presence of 6MCH	89
4.24	Weight loss measurements on mild steel exposed in 1.5 M H <sub>2</sub> SO <sub>4</sub> in the presence of 6MC2C	89
4.25	Weight loss measurements on mild steel exposed in 1.5 M CH <sub>3</sub> COOH in the presence of 3CYC	89

4.26	Weight loss measurements on mild steel exposed in 1.5 M CH <sub>3</sub> COOH in the presence of 6MCH	90
4.27	Weight loss measurements on mild steel exposed in 1.5 M CH <sub>3</sub> COOH in the presence of 6MC2C	90
4.28	Weight loss measurements on zinc exposed in 1.5 M H <sub>2</sub> SO <sub>4</sub> in the presence of 3CYC	94
4.29	Weight loss measurements on zinc exposed in 1.5 M H <sub>2</sub> SO <sub>4</sub> in the presence of 6MCH	94
4.30	Weight loss measurements on zinc exposed in 1.5 M H <sub>2</sub> SO <sub>4</sub> in the presence of 6MC2C	94
4.31	Weight loss measurements on zinc exposed in 1.5 M CH <sub>3</sub> COOH in the presence of 3CYC	94
4.32	Weight loss measurements on zinc exposed in 1.5 M CH <sub>3</sub> COOH in the presence of 6MCH	95
4.33	Weight loss measurements on zinc exposed in 1.5 M CH <sub>3</sub> COOH in the presence of 6MC2C	95
4.34	Weight loss measurements on aluminium exposed in 1.5 M HNO <sub>3</sub> in the presence of 3CYC	99
4.35	Weight loss measurements on aluminium exposed in 1.5 M HNO <sub>3</sub> in the presence of 6MC2C	99
4.36	Weight loss measurements on aluminium exposed in 1.5 M HNO <sub>3</sub> in the presence of 6MCH	99
4.37	Surface coverage for mild steel exposed in H <sub>2</sub> SO <sub>4</sub>	101
4.38	Surface coverage for mild steel exposed in CH <sub>3</sub> COOH	102
4.39	Surface coverage for zinc exposed in H <sub>2</sub> SO <sub>4</sub>	102
4.40	Surface coverage for zinc exposed in CH <sub>3</sub> COOH	103
4.41	Surface coverage for aluminium exposed in HNO <sub>3</sub>	103
4.42	Inhibition efficiency for mild steel exposed in H <sub>2</sub> SO <sub>4</sub>	103
4.43	Inhibition efficiency for mild steel exposed in CH <sub>3</sub> COOH	104
4.44	Inhibition efficiency for zinc exposed in H <sub>2</sub> SO <sub>4</sub>	104

4.45	Inhibition efficiency for zinc exposed in $\text{CH}_3\text{COOH}$	105
4.46	Inhibition efficiency for aluminium exposed in $\text{HNO}_3$	105
4.47	Thermodynamic and adsorption parameters for mild steel in 1.5 M $\text{H}_2\text{SO}_4$ at various temperatures for the utilized corrosion inhibitors	115
4.48	Thermodynamic and adsorption parameters for mild steel in 1.5 M $\text{CH}_3\text{COOH}$ at various temperatures for the utilized corrosion inhibitors	115
4.49	Thermodynamic and adsorption parameters for zinc in 1.5 M $\text{H}_2\text{SO}_4$ at various temperatures for the utilized corrosion inhibitors	115
4.50	Thermodynamic and adsorption parameters for zinc in 1.5 M $\text{CH}_3\text{COOH}$ at various temperatures for the utilized corrosion inhibitors	116
4.51	Thermodynamic and adsorption parameters for aluminium in 1.5 M $\text{HNO}_3$ at various temperatures for the utilized corrosion inhibitors	116
4.52	Kinetic and activation parameters for mild steel in 1.5 M $\text{H}_2\text{SO}_4$ in the absence and presence of various concentrations of inhibitors	124
4.53	Kinetic and activation parameters for mild steel in 1.5 M $\text{CH}_3\text{COOH}$ in the absence and presence of various concentrations of inhibitors	125
4.54	Kinetic and activation parameters for zinc in 1.5 M $\text{H}_2\text{SO}_4$ in the absence and presence of various concentrations of inhibitors	125
4.55	Kinetic and activation parameters for mild steel in 1.5 M $\text{CH}_3\text{COOH}$ in the absence and presence of various concentrations of inhibitors	126
4.56	Kinetic and activation parameters for aluminium in 1.5 M $\text{HNO}_3$ in the absence and presence of various concentrations of inhibitors	126

...



### INTRODUCTION

#### 1. Introduction

Corrosion of materials and/or metals has been a serious problem for decades to various industries countrywide as a result of their consequences towards industrial equipment(s) including but not limited to packaging machineries, engineering structures, vehicles, reaction vessels and mining equipment (tools). Other major challenges of corrosion include contamination of products from industries such as oil, gas, water, liquid chemicals, etc. [1]. Metals are generated from stone/ore body; they usually convert their metal form back to their initial ore/stone state through corrosion process. Various metals such as iron (Fe) and zinc (Zn) usually undergo corrosion when exposed to acidic solution. These acidic media are useful in various laboratories and industries especially for processes such as acid cleaning, acid pickling, acid descaling and oil wet cleaning etc. [1, 3].

Mild steel which is ferrous metal made from iron (Fe) and carbon (C) has significant role and has been useful in gas and oil industries as sprawling pipelines and various equipment or tools. Mild steel is also used in various sectors including but not limited to construction, nuclear power, energy, food and medicine [1, 2]. As a result of its use, it is likely to be exposed to acidic medium which then results in the occurrence of corrosion. Zinc (Zn) metal is used to galvanise other metals, such as iron (Fe) to prevent rusting. Zinc, galvanised steel are mostly used for roofing purposes including various frames such as door frames, households tools such as dish washing sinks etc. Zinc galvanised used for roofing purpose usually becomes exposed to acid rain and extreme sunrays, thus leading to corrosion of unprotected steel. Zinc galvanised products used for household purposes normally becomes corroded when exposed to acidic water, food, etc. Aluminium metals are used in manufacturing frame structures such as window, and door frame. Atmospheric corrosion is common type of aluminium corrosion. It occurs because of the exposure to natural element. The atmospheric exposure of aluminium metallic structure to the environment contribute toward this form of corrosion [2, 3].

## 1.1 Definition of Corrosion

Corrosion of alloy materials or metals is a costly and harsh material scientific problem [3]. The term corrosion evolved from the Latin word “Corrosus” which means gnawed away. Corrosion can explicitly be defined as the gradual deterioration of material (usually metal) or its quantities due to chemical or electrochemical reaction between materials (usually metals) and environments of exposure. Destructive results of chemical reaction that occurs between material and surrounding environment is called corrosion. Most studies indicated that metals are not permanently stable and these contribute toward them reverting into more stable state through process called corrosion [3].

One may define corrosion as deterioration of intrinsic quantities and properties of material as a result of reactions with environment. It can also be referred to as the oxidation of metal(s) when reacting with either oxygen or water [4]. Corrosion can also be viewed as the reaction of a solid material with environment that results in solid material deteriorating.

Some researchers have defined corrosion of material as the gradual destruction of material through unintentional or electrochemical or unwanted chemical attack by its environment beginning at its surface [3, 4].

## 1.2 General Metallic Corrosion

Corrosion affects our daily existence since it can be found everywhere, including but not limited to metals of our motor vehicles, gates, fences, doors, dish washing machines, toilet seats, door lockers, wheel barrows, nails, window frames, door frames, the surface of pots or pans, chains, roof and also pipelines, consequently imposing damage on the metallic structures. Corrosion of metals is the progressively slow damage imposed on materials (usually metal) through interacting with their surrounding environment [5]. In Netherlands, almost 3.5% of Gross National Product (GDP), which corresponds to 1100 Euro inhabitant yearly is reserved for corrosion related problems [5, 6]. The cost of corrosion increase rapidly especially in industries as a result of high temperatures used in the proceedings, aggressive or corrosive chemicals and maintenance that has been overdue, thus, will contribute to extreme social problems including but not limited to loss of product, plant downtime and over-design. However, costs associated with corrosion can be reduced through the use of available knowledge [6].

Common forms of corrosion include but not limited to intergranular corrosion, uniform corrosion, crevice corrosion, galvanic corrosion, pitting, hydrogen damage, dealloying and erosion corrosion. These forms of corrosion are discussed as follows:

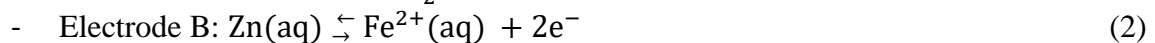
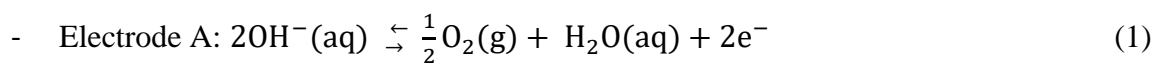
**Uniform Corrosion** is a common form of corrosion that continuously proceed at similar rate over the surface area of metal which then contribute towards rust appearance. Zinc metal corrode uniformly when exposed to aggressive environment such as open space (atmospheres), soils and also natural waters and thus contribute towards formation of rust as shown in Figure 1.1



Figure 1.1: Corroded hot-dip galvanised corrugated steel sheet used for roofing purpose.

This form of corrosion can be defined explicitly as the coupling (i.e, electrically) of two reversible electrodes that are infinitely-close. This explanation means that the occupying space proximity of these electrodes permit ohmic effects as a result of electrolyte resistance. Potential gradient could not exist within the space if there exist electrical resistance among cathodic and anodic site is not available. The potential of equilibrium of coupled system become uniform [7].

Zinc corrosion within concrete occurs as a consequence of joining two reversible electrodes together, the equilibrium equations below define electrolytic contact:



In this situation, the uniform character arises as a result of electrode A being present in dissolved form within the electrolytes in contact with the zinc [8].

**Galvanic Corrosion** usually occurs when metals of dissimilar characteristics are connected together for electrochemical reaction with the presence of electrolytes. In most cases, after occurrence of this kind of corrosion, rust is expected to be present within the joints connecting

these metals. It is an aggressive and localized type of corrosion that mostly occurs as a result of the electrochemical reaction that exists among two or more metals of dissimilar characters in electric conductive environment. This results from the occurrence of difference in potentials between metals, which contribute towards the current flow among them. In order to predict the behaviour or tendency of galvanic corrosion on various metals, the electromotive force (emf) series and the galvanic series is useful. Galvanic corrosion is usually experienced in marine industries and in joints pipes or metal structures [9, 10].

**Pitting Corrosion** usually occurs within the microscopic defects of surface of the metal and results in formation of small holes or tiny pits on the surface area of metal. It mostly attacks metals such as aluminium and magnesium. This form of corrosion may also be termed as “under deposit corrosion” [11]. Other than it being localized and characterised by severe penetration of general corrosion on the surface of the metal, it is considered as a dangerous form of corrosion. It is mostly characterised by pits throughout the whole surface area of the metal, producing rough or irregular surface profile. In some occurrences, pits could develop within a specific area and leave large portion of particular metal in new state or condition. It is one of the most a prevalent kind of corrosion that exist when a pipe surface is characterised by some of the following;

- Chemical protective film that is incomplete and/or insulating.
- Barrier deposit of dirt.
- Iron oxide.
- Organic and other foreign substances.

It commonly occurs within galvanic steel pipes, whereby failure associated with galvanizing causes pitting condition. This form of corrosion usually includes but not limited to erosion corrosion, under deposit attack, water-line attack and crevice corrosion attack [12].

**Fretting Corrosion (Friction Corrosion)** is the form of corrosion that attacks various metals and accelerates through relative motion of contacts with metal surface. It normally occurs when two heavily loaded metals that are not meant to vibrate against each other start moving and results in this form of corrosion within their interface [12].

**Corrosion Fatigue** is the process of reducing fatigue strength as a result of the existence of a corrosive environment. It is one of the common cases of normal fatigue having some modifying effects as a result of the presence of the environment. When various metals are attacked by corrosion during repeated cyclic loadings, specimen lifetime and the endurance limit are often reduced significantly. When the magnitude of applied stress is varied during service, the fatigue response of the metal usually becomes very complex. Cyclic stress in an environment, capable of causing corrosive attack must be avoided [13, 14].

**Crevice Corrosion** usually occurs when metal surface is shielded when oxygen exchange or open interaction between oxygen and metal surface is prevented. In most cases, it occurs in a space whereby there is a shortage or limited access of working fluid in the environment. However, spaces are normally called crevices. Examples include but not limited to contact areas or gaps between parts, underneath gaskets, within or inside cracks and seams, spaces filled with deposits are crevices. Sometimes, the factors such as surface deposit of corroded products and scratches within paint films create this form of corrosion [15].

**Intergranular Corrosion** usually occurs when there exist difference in potential among the grain boundary, these boundaries are either physically and chemically in various regions and in most cases, more reactive than grain matrix. In various application conditions, this has minor or less consequences, because grain boundaries are little bit more reactive when compared to the matrix obtained when uniform corrosion occurs on the metal surface. In most cases, grain boundaries can be very reactive. The localized attacks usually happen within the adjacent side towards the grain boundaries accompanied by corrosion of the matrix. These attacks mostly occur rapidly and penetrate deeply into the metal contributing toward the loss of quality or strength of metal and sometimes lead to catastrophic failures [16].

**Stress Corrosion (Cracking)** normally results from both crevice and pitting corrosion. Some of the common characteristics associated with this form of corrosion is brittle fracture which usually occurs in ductile materials [17].

**Dealloying** corrosion is a process characterized by the removal of one constituent of an alloy usually from an alloy and leaving altered residual structures. It commonly affects alloy elements that are more active, that is, negative electrochemically, in solvent components. This phenomenon is known as leaching which results from the selective corrosion of a

either phase or elements. Some familiar examples of this form of attacks include the removal of zinc metal from Cu-Zn alloy (dezincification) as well as the removal of ferrite from gray cast iron (graphitization) [18].

**Exfoliation** usually occurs when materials (metals) are lost in form of layers. It is mostly occurs within wrought products having elongated structures.

The familiar mechanism of this form of corrosion is the electrochemical oxidation of materials (metals) when reacting with oxidants like water and oxygen.

This chemical reaction or phenomenon is associated with a transfer of electrons. Corrosion phenomenon can be complicated because of various materials properties like composition and microstructure [19].

**Highly Temperature Corrosion** exists through chemical attacks especially from molten materials or molten salt, usually at temperature above 673K. Most, if not all materials and alloys useful for technological interest will undergo oxidization and then corrode usually when temperature is high. Depending on the temperature and environmental condition, the nature of corrosion products and the mechanism does vary. This form of corrosion is a serious problem industrially.

In a non-inert environment, any components exposed at high temperature are potentially at risk. This includes but not limited to the power generation such as fossil fuel and nuclear, the gas turbines and Aerospace, heat treatment, metallurgical and mineral processing, chemicals processing, petrochemical and refine, automotive, and waste incineration.

This form of corrosion is known as a scaling or dry corrosion.

Examples of this form of corrosion include carburization, chlorination, flue gas and deposit corrosion, nitridation, oxidation, and sulphidation.

### 1.3 Corrosion Problem Areas

Corrosion affects various areas in the industries. Below is a list of Identified problem areas in industries for the purpose of successful implementation of control measures. Corrosion problem areas in chemical and fertilizer industries can be broadly classified as follow:

- Storage area
- Transportation systems

- Pumps, compressors
- Special pressure vessels
- Tail pressure vessel
- Heat exchangers
- Steam generation systems
- Cooling waters
- Structural and civil structures

#### **1.4 Significance of the Study**

Corrosion study of metal is of paramount importance especially in industries and manufacturing companies. Metals usually corrode when exposed to either basic or acidic media. The increase in industrial metal application in acid solution caught researchers attention. Majority of frame structures, and machines are made up of metals. Crude oil refinery requires the use of various metal exposed in corrosive media. Studies indicated that refinery corrosion may be caused by either strong basic or acid attacks that occurs directly in the equipment [20].

Significance of this study may be classified into three main categories as briefly explained below;

##### **Conservation**

Corrosion results in the reduction of metal mass, this contributes towards metal and energy waste, and human efforts that were used in the production of those material. The wastage of metals due to corrosion has now become an important engineering problem [20, 21]. Non-corroded metals are required to replace corroded metals, this is a further costly investment that need to be avoided by conserving metals from corrosion. This study shall provide mechanism suitable to manage corrosion [21, 22].

##### **Safety**

Corrosion can cause failure in the operating equipments, which may lead to injuries and death of individuals surrounding the area. The purpose of this study is to eradicate risk associated with corrosion that may affect the safety of individuals.

##### **Economics**

Corrosion of materials affect the economy negatively; wide knowledge of corrosion will assist to reduce the economic impact of corrosion. This study aims to reduce material losses due to corrosion and associated economic loss that occurs from direct consequences of corrosion of materials such as machinery, bridges, marine structure, tanks(steel), vehicles metal components and so on [22].

### **1.5 Aim and Objectives**

The aim of this study is to investigate the inhibition potential of some chromones namely; 3-cyanochromones (3CYC), 6-methylchromone hydrate (6MCH), 6-methylchromone-2-carboxylic acid (6MC2C) on three different metals, namely; mild steel, aluminium and zinc in three corrosive environments i.e. acetic, nitric and sulphuric acids.

The research specific objectives are to;

- Apply kinetics, thermodynamics and adsorption principles in studying the inhibition potentials of chromone compounds, effect of chromone compounds concentration and temperature on the rate of corrosion.
- Determine the possible mechanism, type of adsorption and adsorption isotherm for the corrosion inhibition.
- Use the electrochemical techniques potentiodynamic polarization (PDP) and the electrochemical impedance spectroscopy (EIS) to study the corrosion behaviour of different metals and the influence of the corrosion inhibitors.
- Use 3D Optical Microscopic (3DOP) and Fourier Transform Infrared Spectrometry (FTIR) to study the surface morphology / interface interactions between the chromones compounds and the metal surfaces to determine the mode of interfacial reactions and to investigate the interaction between chromones compounds and metals to see the functional groups that have interacted.



---

LITERATURE SURVEY

## 2. Corrosion Protection

Studies indicate the existence of various chemicals that are utilized to metal to avoid harm or damage caused by corrosion. These anti-corrosion chemicals are applicable in various materials; this protection process is called corrosion protection. Some methods of corrosion protection are discussed in section 2.1

### 2.1 Methods of Corrosion Protection

There exist various methods useful when minimising or controlling corrosion. Various parameters are to be considered when monitoring and reducing corrosion. These include corrosion type, occurrence place, and practical use of metal to be protected and environmental location, amongst others. Below is a list of some of the methods that can be used to control damage associated with corrosion [23, 24].

#### 2.1.1 Selection of Materials

Selection of metals is achieved by choosing metals that are known to be resistant to corrosion. The choice of selection depends on many factors including but not limited to the mechanical and physical strength, chemical and cost of such material including the visual properties. Some examples of material resistant to corrosion include titanium which is one of material that are resistant to corrosion although it is expensive when compared with other metals such as steel. The material of choice when producing equipments in oil production is carbon steel. Carbon steel is useful in production of equipments such as pipes, vessels, and tanks due to low costs and good mechanical properties [25].

#### 2.1.2 Non-Metallic Piping, Coatings and Lining

Substances or chemical material that is applied to metal as either liquid or powder that become firm and attached to metal continuously during solidification is referred to as coating. When this metal protection is internal, this method can be called lining [26]. After materials undergone coating, it is important that the coated material is:

- Always resistive to chemical attacks.

- flexible
- have lower porosity and is stable at the temperature of exposure

### **2.1.3 Protecting through Cathodic**

Cathodic protection may be defined as a process whereby the corrosion potential is less negative when compared to potential of protected polarization structure, this is achieved by preventing anodic reaction from occurring thermodynamically. The external power generator is useful for this purpose. Sacrificial anode occurs when anode is composed of more active metals, this is another familiar way of protection through cathodic. It is mostly used when protecting underground structures including but not limited to water storage, marine facilities and ship hulls [27, 28].

### **2.1.4 Controlling through Inhibitors**

Compounds that reduce corrosion phenomenon when utilised to metal surface in small concentration to corrosive medium are referred to as corrosion inhibitors. They may either be organic or inorganic inhibitors. This method may be applicable within pipeline interior and vessels. The compounds (corrosion inhibitors) containing certain characteristics reduces corrosion effectively. These characteristics include heteroatoms like oxygen, sulphur, nitrogen. Studies also show that multiple bonds contribute towards the better inhibition efficiency because lone pairs in heteroatoms contribute towards electrons transfer, thus, leading to adsorption of these heteroatoms onto the surface of metal [26, 28].

## **2.2 Corrosion Inhibitors**

Any form of compound or chemicals reacting physically or chemically with the metal surface and environment of exposure by giving metal a maximum possible protection is referred to corrosion inhibitors. Inhibitors are categorised into different types.

### **2.2.1 The Anode Corrosion Inhibitors**

This kind of inhibitors is useful within solutions closer to neutrality, this result in the formation of soluble corrosion products such as hydroxides, oxides or salts. When in function, they shift the anode potential enabling passive films formation onto the metal surface by the inhibition of the anode metal dissolution reaction [29].

### **2.2.2 The Cathode Corrosion Inhibitors**

This kind of inhibitor inhibit corrosion by minimising cathode reaction itself (i.e., by minimising reaction rate). The efficiency of this inhibitor may also be achieved by selecting precipitates on the metal surface of cathode sites increasing the impedance of metal surface and limiting the diffusion of reducible species like the dissolved oxygen molecular. Selenides and sulphides has a tendency of adsorbing onto the surface and function as cathodic poisons [30].

### **2.2.3 Combined Type Corrosion Inhibitors**

This kind of inhibitor is also called mixed type corrosion inhibitors. In most cases, they are produced from organic compounds. They normally impact towards all electrochemical reactions (anode and cathode reaction). The advantage of mixed or combined type inhibitor is that they give protection to metal of interest due their high tendency of adsorbing onto metal surface. Physisorption and chemisorption are two common adsorptions obtained when using these inhibitors. Physisorption implies that the adsorption of inhibitor particles will occur physically (physical adsorption) and chemisorption simply mean that the adsorption or attachment of inhibitor particles onto the surface will happen chemically (chemical adsorption)

Sometimes both physisorption and chemisorption can contribute towards adsorption of inhibitor onto metal surface, however this process depend on the molecular structure of the inhibitor, physical and chemical properties or quantity of metal surface since this affect the chemical reactivity and also ability of charges to be wet and also the used electrolyte [31, 32].

### **2.2.4 Interface Corrosion Inhibitors**

Interface inhibitors work in similar manner as mixed type inhibitors discussed above. The particles of inhibitor adsorb onto the surface of metal, this lead to formation of film layer. The advantage of these kind of inhibitors is that it possible to transport them within closed environment and distribute to corrosion site through volatile from source. They belong to class of vapour phase and liquid inhibitors. They are also called volatile corrosion inhibitors (VCI). When they are in liquid phase, three reaction categories namely, cathodic, anodic or mixed type electrochemical reaction may occur [33].

### **2.2.5 Passivation Anodic Corrosion Inhibitors**

This form of inhibitor works in strange manner because if insufficient amount of concentration is used, it can contribute towards increment of corrosion rate instead of reducing it. Passivation anodic inhibitors are dangerous and may even cause pitting corrosion when unreasonable (small amount) concentration is used. It is associated with large shift of corrosion potential. Two common types of passivation anodic inhibitors include oxidizing anions and non-oxidizing ions whereby their examples are chromate and molybdate, respectively. Chromate and nitrite under oxidizing anions are capable of passivating steel in the absence of oxygen, however tungstate and molybdate under non oxidizing ions need oxygen for passivation of steel. The advantage of passivation inhibitor is that it works effectively in sufficient quantities, however it is difficult to maintain passivation using inhibitors under the following conditions:

- When temperature and salt concentration are high.
- When the pH value is lower.
- When the dissolved oxygen concentration is low.

Oxygen is essential to cause passivation in non-oxidizing passivation, thus, inhibition cannot happen in the absence of oxygen. These inhibitors are responsible for adsorption of oxygen to anodes; this is achieved by causing polarization towards the passive region. In non-oxidizing passivator, oxygen is essential for passivation because it is a best cathodic depolarizer [34, 35].

### **2.2.6 Precipitation Corrosion Inhibitors**

This form of inhibitor works in similar manner as interface inhibitors, particles of compound usually adsorb onto metal and lead to formation of film. It maintains this general action throughout the surface of the metal and interferes indirectly or directly with anode and cathode. Example of common class of precipitation inhibitors are silicates and phosphates. Oxygen is also essential for passivation to occur, when pH is seven and concentration of chloride is low then contribution toward passivation is high. They share common characteristics with interface inhibitors, this includes contributing towards pitting when insufficient amount of silicate or phosphate are used and they mostly behave like anodic inhibitor. Cathodic polarization may increase when silicates and phosphates form a deposit onto steel. They possess anodic and cathodic effect. The advantage of these inhibitors is that they possess a rare property of adsorbing and inhibiting corrosion on steel [36].

### 2.2.7 Adsorption Corrosion Inhibitors

Most if not all chemisorption inhibitors, reduce corrosion through adsorbing onto metal surface and react as cathodic, anodic or both. It is classified based on how they react with the metal surface and how potential is affected. Molecular or chemical structure of the inhibitor may be useful in determining whether the compound will adsorb onto the metal surface and inhibit effectively.

Factors that contribute toward the effectiveness of inhibitors include [37]:

- The molecule's size.
- The coupled bonding and aromaticity.
- The length of carbon chain.
- Toughness of bond to metal substrate.
- The kind of bonds and number of atoms bonded to molecule.
- Molecules ability to cover and protect metal area.

Studies indicate that corrosion rate may be reduced rapidly when using organic compounds that are capable to inhibit corrosion and adsorb onto the surface. The ability of a compound to adsorb on the metal depends upon the following [38]:

- The type of molecular structure.
- Solution's chemical composition.
- The essence of metal surface.
- Electrochemical potential within the metal or solution interface.

### 2.3 Factors affecting the characteristics of inhibitors

There are several factors that affect the potential of a corrosion inhibitor, such factors include but not limited to the following [39, 40]:

- Environmental condition
- Metal type and nature
- pH of the system
- Inhibitor concentration
- Temperature of the system
- Toxicity, disposal and effluent problems.

- Scale formation

## **2.4 Environmental Conditioners**

Effect of corrosive species in the electrolyte can be eradicated through environment conditioners. Scavenger inhibitors are capable of decreasing corrosivity, this lead towards decrease in corrosion rate and increase in inhibition efficiency [41].

### **2.4.1 Environment**

The environmental conditions play a significant role towards the corrosion of materials. Contributing factors towards pollution of air and water and most industrial by-products include but not limited to chlorine, ammonia, sulphur dioxide, and fuel gases. Some inorganic corrosive acids include hydrochloric, sulphuric, and nitric. Other harmful materials include steam, alkalis, solvents and organic acids [42, 43].

Sulphuric acid ( $H_2SO_4$ ) is one of corrosive agents that are mostly used country wide. It is mostly applicable in chemical processing. The consequences of stainless steels and zinc in sulphuric acid as a subject of this investigation, they pose some highly complex problems. In most cases, the acid is neither highly oxidizing nor highly reducing. The stainless steels may be either passivated or activated depending on the oxidizing or reducing agents present in the solution, also some impurities could affect the corrosion behaviour in some systems. These impurities come from the materials treated with the acid as well as being present in the manufactured acid [44].

### **2.4.2 Material Corrosion of Zinc**

Various metals are used numerous operation in the industry, zinc is one them. Other that being useful in industrial process, zinc may be used for roofing purposes and in iron galvanization process. It provides iron protection through cathodic protection because the electrochemical scale is high as compared to iron [45].

## **2.5 Corrosion Mechanisms in Acid Solutions**

Aqueous acid solutions contribute towards corrosion of metals and alloys. These forms of acids can cause severe corrosion, as a purpose of minimising corrosion, organic compounds can be used. Studies indicate that the best organic compounds should be characterized by the following family class [46]:

- triple-bonded hydrocarbons
- acetylenic alcohols
- sulfoxides
- sulphides
- mercaptans
- aliphatic
- aromatic
- heterocyclic compounds containing nitrogen

Various studies indicated how compounds adsorb onto the metal surface, sometimes electrostatic adsorption is responsible for inhibiting properties. Corrosion inhibitor interacts rapidly but weakly with the electrode surface, and thus, it can be easily removed. This adsorption phenomenon may be characterized by having a small value of activation energy, being temperature independent. However, some factors it depends upon include [47]:

- The inhibitors behaviour.
- Corrosion potential when compared to zero-charge potential.
- Kind of absorbable anions within aggressive solution medium.

## **2.6 Corrosion**

Studies indicate that the exist various factors that contribute toward corrosion rate, these session explains corrosion rate and conditions that affect it

### **2.6.1 Corrosion Rate and Conditions Affecting it**

Corrosion rate

When corrosion occurs, corroded metal usually experience a reduction in mass, this is commonly known as mass loss.

Rate of corrosion may be described as the speed in which material (metal) of interest deteriorates when exposed in corrosive environment. Depending upon individual preference,

one may express rate of corrosion in different way. One may also define it as the amount of mass loss by metal during corrosion per unit time. Corrosion rate is dependent towards exposure environmental conditions and the kind of metal used within the environment [48].

#### Influential condition affecting the rate of corrosion

There are several influential conditions affecting corrosion rate, such factors can slow down the rate of corrosion. Studies classified these influential conditions as primary factors and secondary factors whereby primary factor is associated with the metal itself while secondary factor is associated with environment that the metal is exposed within [49].

#### Primary factors

- The innate or nature of the metal.

Different metals experience unique corrosion attack, for example gold and silver are noble metals (i.e. they have fully filled d orbitals) thus make them less reactive as compared with zinc and mild steel.

- Metal surface appearance.

Uneven surfaces of metals play a major role in promoting corrosion speed in a sense that metals having uneven (rough) surfaces usually have higher rate compared to metals with flat surface.

#### Secondary factors

- Temperature.

The rate of corrosion increases when temperature of corrosive environment upsurge.

- Existence of agents that oxidizing.

Existence of oxidising agents increases corrosion rate.

- Existence of atmospheric impurities.

The existence of impurities tends to increase corrosion rate, for example impurities like sulphur dioxide ( $\text{SO}_2$ ) within acidic medium created by dissolution of the impurities.

### 2.6.2 Corrosion in Different Media



Corrosion exists naturally in aggressive conditions such as acidic and basic media. Studies show that material (such as metals) has been used for many years for many purposes in mining sectors and in industries for process like acid pickling where impurities in metals are being washed away. Acidic medium possesses low pH value while basic medium possesses high pH value. Studies have shown that the extent of corrosion in metal exposed to diluted acid is higher compared to the one exposed to concentrated acid. The best explanation could be that the diluted acid has large volume (amount) of water when compared to metals that are exposed to concentrated acid [50].

### **2.6.3 Importance of Corrosion**

Corrosion is an inherently difficult phenomenon and it required to be researched. It affects issue related to the human life and economic impact, safety, environmental pollution and conservation of metal and materials. The effects of corrosion are both direct and indirect.

Economic losses caused by corrosion can be categorised as indirect loss and direct loss.

Indirect economic losses caused by corrosion include but not limited to [51]:

- Loss of efficiency
- Shutdown losses
- Losses of production
- Contamination of the product
- Loss of valuable products

Indirect social loss includes but not limited to:

- Social Safety
- Fire
- Explosion or release of toxic products to the environment

Direct losses include but not limited to:

- Over - designing
- unable to re-use desirable materials
- Cost associated with replacing corroded materials

### **2.6.4 Consequences of Corrosion**

The consequences of corrosion subject human life at risk because corrosion is dangerous compared to loss of materials. The harmful effects of corrosion include [52, 53]:

- Decrease of metal thickness causing weakness towards metal's mechanical strength and result in structural collapse.
- Causing reduction of materials quality because of rust appearance.
- Causing cracks or aperture on pipes leading to leaking and environmental contamination.
- Contamination of fluids in vessels tubes and pipes. It may contaminate chemicals, pharmaceuticals, dyes, packed food and water etc.
- Damage of property and loss of life during structural failure or collapse.

## 2.7 Thermodynamics of Corrosion

The concept of thermodynamics play an important role in understanding the corrosion process. However, it is impossible to predict the rate of corrosion using thermodynamic calculations since it only helps when calculating the theoretical activity of a given metal when the composition of the environment is known. A reaction is alleged to be spontaneous when free energy of that specific reaction is of a negative value. The standard free energy of the cell reaction  $\Delta G^\circ$  under standard conditions can be calculated by the subsequent equation (3) [54];

$$\Delta G^\circ = -nF\Delta E^\circ \quad (3)$$

where  $\Delta G^\circ$  is the standard free energy change, n is the number of electrons exchanged, F is the Faraday constant and  $\Delta E^\circ$  is the standard electromotive force or potential difference in the reaction.

Studies distinguish physisorption from chemisorption as follows: physisorption values of  $\Delta G^\circ$  are around  $-20 \text{ kJ.mol}^{-1}$  or lower whereas chemisorption values are around  $-40 \text{ kJ.mol}^{-1}$  or higher. The other difference between these two is that chemisorption is irreversible while physisorption is reversible. Studies also indicate that chemisorption may be a process whereby the interactions involved are of covalent nature and the type of layer that results is monolayer whereas physisorption is a process that involves weak Van der Waals intermolecular interactions that result in multilayer products [55].

## 2.8 Electrochemical Approaches

This category involves chemical reactions that take place at the interface between an electronic conductor (the electrode / in this study mild steel or zinc) and an ionic conductor (the electrolyte), with electron transfer among the electrode and the electrolyte in solution. Most corrosion processes are of electrochemical nature and involve the reactions on the corroding metal surface. Electrochemical methods are useful in characterising corrosion phenomenon on the surface of interest. One amongst the benefit of these techniques is that it provides complex results in short periods of time providing useful information to elucidate mechanistic information about the processes studied [56]. Examples include but not limited to corrosion potential measurements (CPM), linear polarisation (LP), electrochemical impedance spectroscopy (EIS), potentiodynamic polarization (PDP), 2D and 3D microscopy.

These technique are briefly described below

### **2.8.1 Corrosion Potential Measurements (CPM)**

This is useful when monitoring corrosion of a complex situation. Measurements are achieved through voltage difference between the reference electrode and metal exposed to corrosive environment. Corrosion potential ( $E_{\text{corr}}$ ) measurements and open circuit potential (OCP) are associated with the recording of a corroding metal. At zero net current, the potential should be recorded, thus, may be a non – intrusive method for the studies of corrosion.  $E_{\text{corr}}$  should be measured immediately a specimen is placed in a cell. OCP is then measured using the potential difference between the material of study (working electrode, WE) and a reference electrode (RE) immersed in an electrolyte [56, 57].

The magnitude of the measured potential depends the following:

- The nature of the metallic layer or substrate stratum
- Chemical composition
- Temperature
- Hydrodynamic characteristics of the electrolyte

The application of this method is easy. Its application is doable even outside laboratory conditions, and it allows the differentiation between a passivation process or a localised corrosion process, that occur under the supply of some sorts of biofilms. However, separation contributions with  $E_{\text{corr}}$  are monitored together, such measurement does not provide

mechanistic information and it is advisable to use this method in parallel with other methods to work out the cathodic and anodic influences of the electrochemical processes [58].

### 2.8.2 Linear Polarisation (LP)

Linear polarisation may be a curve denoted in graphical form showing the link between the electrode current density ( $i$ ) expressed in logarithmic of this density,  $\log(i)$  and the potential of the electrode ( $E$ ). LP is related to measurements encompass changing the potential of the electrode linearly and records of the current as a function of the potential. Measurement of the polarisation curves happen within the three – electrode system. Anodic range is characterised by  $E > E_{\text{corr}}$ , thus registering polarisation curves here is feasible to work out the ranges related to active metal dissolution or deterioration (corrosion) or its passivation. When applying the cathodic potentials with  $E < E_{\text{corr}}$  it's possible to look at various reduction processes onto the metal surface. Both cathodic and anodic polarisation curves recorded around the corrosion potential display valuable and important information related to corrosion processes going down within the metal – solution system. While polarising the electrode is close to  $E_{\text{corr}}$ , a linear change of current density with various potential is observed within wide potential range then the Tafel relationship is additionally observed [59, 60]. Tafel equation can be written as equation (4)

$$\log(i) = \log(i_{\text{corr}}) + \frac{1}{b} (E - E_{\text{corr}}) \quad (4)$$

where  $i_{\text{corr}}$  is the corrosion current and  $b$  is the Tafel constant. This equation can be written using  $b_c$  and  $b_a$  resembling the cathodic and anodic Tafel constants, respectively. The above formula shows the linear dependence between  $\log(i)$  and  $E - E_{\text{corr}}$ , with slope denoted by  $1/b$ . This make it's possible to estimate directly the worth of  $i_{\text{corr}}$  by either reading it from the LP curve or calculate it indirectly using the Stern and Geary equation.

### 2.8.3 Electrochemical Impedance Spectroscopy (EIS)

This method is beneficial when approaching electrochemical systems by applying a minimal perturbation to the electrochemical cell by means of an alternate electrical signal of lower

amplitude; this enables observation of the behaviour of the system in an exceedingly pseudo – steady state. Ohm's law states that the current through a conductor between two points is directly proportional to the potential difference across the two points at a constant temperature [61, 62]. While considering the Ohm's law, the resistance  $R$  [ $\Omega$ ] can be described as:

$$I = \frac{E}{R} \quad (5)$$

where  $I$  is the current through the conductor in amperes (A) and  $E$  is the potential difference measured across the conductor in volts (V).

EIS is a technique within which the frequency response of the electrochemical system to the alternate signal is analysed in an exceedingly transfer function, between an signalling like voltage and therefore the resulting output signal like current processed by instrumentation to yield the frequency– depended transfer function. An experiment of impedance nature involves the conversion of the time–domain input and output signals into a complex quantity as a function of frequency. This technique is well established as a robust technique especially for investigating corrosion processes and other electrochemical systems. Recently it has also been successfully applied in studying the exopolysaccharide (EPS) influence on carbon steel [62, 63, 64].

Advantages of this technique include but not limited thereto being unintrusive, displaying big amount of mechanistic information, offering high precision on the measurements, and permit performing measurements in an exceedingly wide selection of frequencies. However, it has a disadvantage of having complex interpretation of the results.

This technique often uses the frequency range between  $10^{-4}$  to  $10^5$  Hz, thus permit identification of the elements comprising the electrochemical cell when the current is out of phase with the voltage [65].

#### **2.8.4 Potentiodynamic Polarization (PDP)**

These methods are useful for laboratory corrosion testing, and they include potentiodynamic polarization, cyclic voltammetry, and potentiostaircase. The advantage of these techniques is

that they display important useful data related to mechanism of corrosion and rate at which corrosion occurs. It involves the changing of potential of the working electrode and monitoring current produced as a function of time. The purpose of using this method is to get the relevant electrochemical parameters like the corrosion potential, corrosion density, anodic and cathodic Tafel slopes to calculate the inhibition efficiency, the measured corrosion current densities values are used according to equation (6) [66].

$$\%IE_{PDP} = \left[ \frac{i_{corr}^o - i_{corr}^i}{i_{corr}^o} \right] \times 100 \quad (6)$$

where  $i_{corr}^o$  and  $i_{corr}^i$  are values of corrosion current density in absence and in presence of inhibitor, respectively.

## 2.9 Chromones as Corrosion Inhibitors

Studies indicate that compounds characterised the presence of 5:6 benz -1:4-pyrone within their structures are classified as chromones. They are the heterocyclic compounds containing benzopyron having substituted keto group on pyron ring. It has same molecular formula but different structural formula with coumarin. Various studies show that most chromones as phenylpropanoids. Other names are 4-Chromone; 1,4-Benzopyrone; 4H-Chromen-4-one; Benzo-gamma-pyrone; 1-Benzopyran-4-one; 4H-Benzo(b)pyran-4-one [67].

### 2.9.1 Origin and Uses of Chromones

The journey in search of more secure anti-inflammatory drugs is still the centre of a few therapeutic chemistry programs. Chromone (4H-chromen-4-ones) is one of naturally occurring compounds omnipresent in plants and has demonstrated to be a favoured platform in therapeutic chemistry. Some of sources of chromone are plant genera including Aloe, Cassia, Aquilaria, and Hypericum. Bioactive chromones are produced by several genera of fungi like Penicillium, Mycoleptodiscus, and Aspergillus. Chromones derivatives contain enzymatic inhibition properties like kinase, cyclooxygenase, and oxidoreductase [68, 69].

The primary chromone in clinical use, called khellin, was obtained from plant called *Ammivisnaga* and had been useful for hundreds of years as a smooth muscle relaxant. These compounds had been reported to have variety of biological active molecules through synthetic or natural origin and most of them had been used for years in medicinal application. In 1947,

chromone had been reported to be useful in respiratory disorder such as bronchial asthma. Studies conducted in Bengers Laboratories in 1950s revealed the synthesis and production of khellin to treat asthma. Various compounds were subjected under screening using animal model to test the chances of the compounds being able to prevent the anaphylactic release of leukotrienes and histamine from lungs of pig and human model to test the chances of reduction of bronchoconstriction induced by inhaled bronchial challenge. Dr REC Altounyan, has undertaken the human initial screening. He suffered allergic bronchial asthma and by that time he was employed by bengers Laboratories. After 8 years, more than 600 challenges were encountered using over 200 compounds. In 1965, Dr REC Altounyan discovered that disodium cromoglycate (DSCG), the chromone effectively provide more than 6 hours protection. DSCG is still useful as a mast cell stabiliser. Hundreds of chromones derivatives were discovered and offer better mast cell stabiliser [70, 71, 72].

Several studies describe chromones as pharmacophores having variety of biological benefits like anticancer, antiviral, antifungal, and antimicrobial.

Chromones are useful as an alternative way in therapies to control early mild asthma nationally and internationally, however, inhaled glucocorticoid is preferred. Studies reveal that chromones are preferred by many patients, because of low side effects as compared with inhaled glucocorticoids. Chromone compounds are capable of preventing initial and late asthma to inhaled allergens because of their potent effects [73]. They offer better characteristics such as reducing airway reactivity to a range of inhaled irritants like sulphur dioxide and cold air, these characteristics contributed towards them being favoured by many patients

### **2.9.2 Mechanism Action in Pharmacotherapy**

The initial action of chromones is to inhibit a  $\text{Na}^+/\text{K}^+/\text{2Cl}^-$  and co-transporter occurs in the activation of all mast cells and sensory neurons. This is then shared among loop diuretics, frusemide (US furosemide) and bumetanide. Studies reveal the existence of two complementary mechanisms in which chromones effectively exert their beneficial characteristics against the initial phase asthma attacks [74].

### **Chromones Compounds Adopted in this Study**

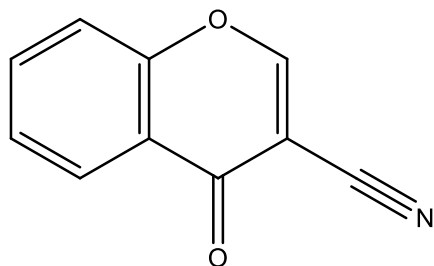


Figure 2.1: Structure of 3-Cyanochromones (3CYC)

### 2.9.3 Description and application of Structure of 3-cyanochromones (3CYC)

3-Cyanochromone has molecular formula  $C_{10}H_5NO_2$  and molecular weight of 171.15 g/mol. A synonym is 4-Oxo-4H-1-benzopyran-3-carbonitrile. It is characterised by a 3-substituted chromone. This substituent is a cyano (CN group) substituted to 1-benzopyran-4-one. As shown in figure above, it is an alpha, beta-unsaturated nitrile and also alpha, beta-unsaturated ketone.

3-Cyanochromones is useful in synthesizing various compounds. Some of 3cyanochromones derivatives include 3-(diaminomethylene)chroman-2,4-dione, 2-aminochromone-3-carboxamide, and 3-amino-4H-chromeno[3,4-d]isoxazol-4-one.

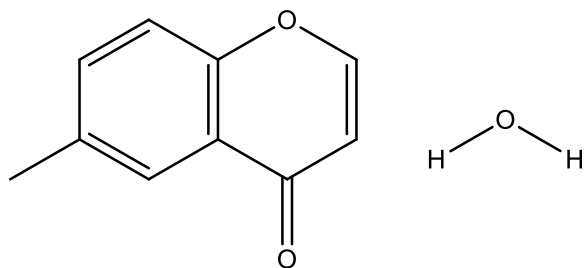


Figure 2.2: Structure of 6-Methylchromone hydrate (6MCH)

### 2.9.4 Description and Application of Structure of 6-Methylchromone hydrate (6MCH)

Other name is 6-methylchromen-4-one hydrate with molecular formula  $C_{10}H_{10}O_3$  and molecular weight of 178.18g/mol. It is a chromone derivative composed of cyclic compounds containing nine carbon atom that possess  $sp^2$  hybridization, The common names is 1,4-benzapyranes. It is useful as activated alkene in methanolic trimethylamine or sodium



methoxide catalysed Baylis-Hillman coupling reaction with aliphatic aldehydes and aromatic [75, 76].

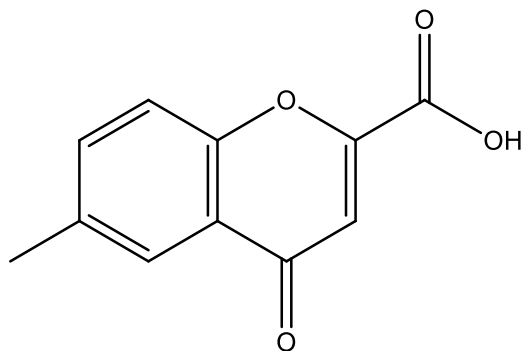


Figure 2.3: Structure of 6-methylchromone-2-carboxylic acid (6MC2C)

### 2.9.5 Description and Application of Structure of 6-methylchromone-2-carboxylic acid (6MC2C)

6-Methylchromone-2-carboxylic acid is also called 6-methyl-4-oxo-4H-chromene-2-carboxylic acid or 6-methyl-4-oxovhromene-2-carboxylic acid or 4h-1-benzopyran-2-carboxylic acid. It has a molecular formula  $C_{11}H_8O_4$  with molecular weight 204.18g/mol. It is a chromone derivative composed of cyclic compounds containing nine carbon atom that possess  $sp^2$  hybridization, The common names is 1,4-benzapyranes. They share common application with 6-methylchromone hydrate [77, 78].

---

## EXPERIMENTAL PROCEDURE

### 3.1 Metallic materials utilized

All gravimetric analysis experiments were performed using pure zinc (99.999%) and the mild steel with chemical composition: (Mn = 0.37 %), (Ni = 0.039%), (P = 0.02%), (S = 0.03%), (Mo = 0.01%), (C = 0.21%) and (Fe = 99.32%). A rectangle zinc sheet and mild steel with surface area of  $6\text{cm}^2$  were used for weight-loss measurements. Thermostat water-bath was used to maintain and control temperature. Sulphuric acid (98%), acetic acid (> 99%) and Dichloromethane were sourced from Sigma-Aldrich. Preparations of solution were done using various laboratory apparatus such as  $1\text{cm}^3$  volumetric flask,  $100\text{cm}^3$  beakers, and measuring cylinder. Heating mantle was also used to assist in dissolving compounds.

### 3.2 Solutions

Distilled water was useful in preparing all solutions. Various concentrations of acetic and sulphuric acid solutions were prepared by analytical dilution from stock solution.

### 3.3 Corrosion Inhibitors Utilized

Figure 3.1 shows a list of structures of chromones used as corrosion inhibitors

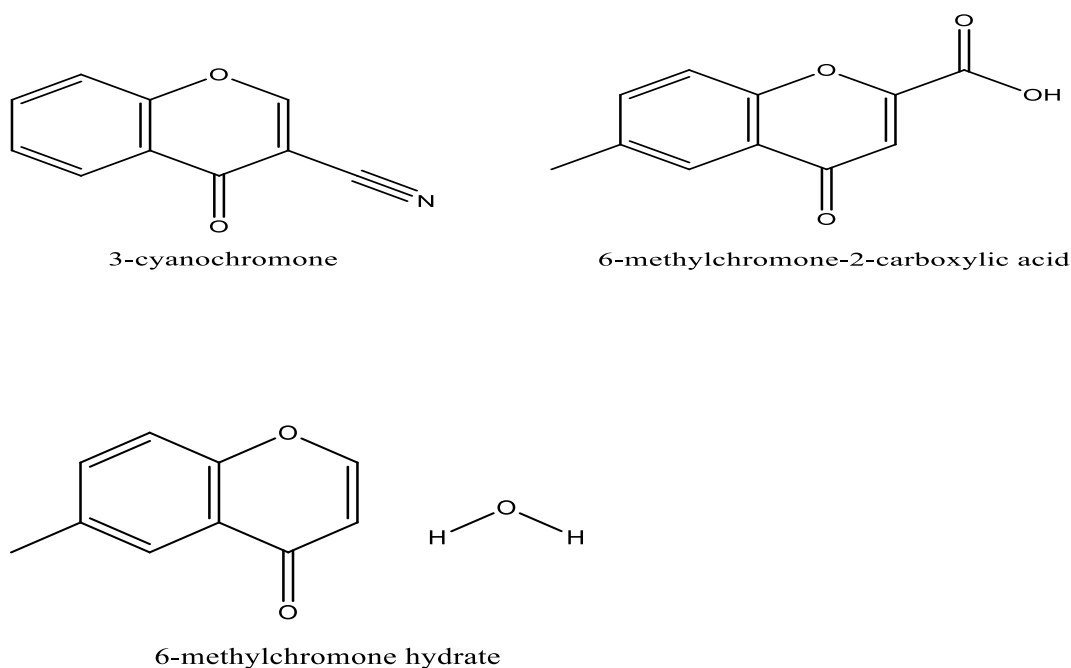


Figure 3.1: Structures of chromone used as corrosion inhibitors

The choice of choosing these compounds among others has been influenced by various characteristics that these compounds possess. These characteristics include the present of atoms such as oxygen and nitrogen, double bonds, triple bonds, and aromatic structure.

### 3.4 Electrochemical Measurements

In this study, the electrochemical techniques used were Potentiodynamic Polarization (PDP) and Electrochemical Impedance Spectroscopy (EIS).

#### 3.4.1 Potentiodynamic Polarization (PDP)

PDP analyses were performed using a Metrohm Autolab Potentiostat/Galvanostat having three-electrode cell, namely a platinum counter electrode (CE), with Ag/AgCl reference electrode (RE) and mild steel, zinc or aluminium working electrode (WE) so as to attain a stable value of  $E_{\text{corr}}$ . The stabilization period was 30 minutes to all electrochemical measurements. The obtained data were used to calculate inhibition efficiency and compared it with the inhibition efficiency from other techniques.

#### 3.4.2 Electrochemical Impedance Spectroscopy (EIS)

EIS (electrochemical impedance spectroscopy) is a technique for determining the resistive properties of materials at different frequencies. Because of the magnitude of polarization imposed on the sort of materials being described, EIS measurements for corrosion research are regarded to be non-destructive; typically, a signal of less than 30mV peak to peak is used.

Impedance is useful in determining the interaction between metal and inhibitor solution through model consisting of capacitance of double layer ( $C_{dl}$ ), Solution resistance ( $R_s$ ), and polarisation resistance ( $R_p$ ). The electrochemical parameters like the resistance of charge transfer, capacity of double layer, the constant phase element constant and exponents obtained are useful to calculate the inhibition efficiency from the equation (7):

$$\%IE_{IES} = \left(1 - \frac{R_{ct}^0}{R_{ct}}\right) \times 100 \quad (7)$$

where  $R_{ct}^0$  is the charge transfer resistance in the absence of the inhibitor and  $R_{ct}$  is the charge transfer resistance in the presence of the inhibitor.

The EIS approach, which is based on alternating currents, can be used to learn more about the corrosion mechanism and to determine how successful a certain corrosion-prevention strategy, such as inhibitors or coatings. In an alternating current circuit, impedance is used to estimate the amplitude of the current for a given voltage and is the proportionality factor between current and voltage. Direct currents are measured at zero frequency, and the capacitor's impedance reaches infinity. The smallest impedance circuits prevail in parallel electrical circuits, and the data acquired can be utilized to calculate the sum of  $R_s$  and  $R_p$  [80]. When compared to other methodologies for evaluating metal corrosion, EIS offers various advantages, which include:

- a) It gives mechanical data based on the use of an equivalent electrical circuit that responds similarly to the cells being studied.
- b) It provides greater information on the corrosion process' kinetic data.
- c) It provides information on the capacitance and resistance of coatings applied on metal.

### **3.5 3D Optical Microscopy (3DOP)**

This method was used to study surface of zinc, aluminium, and mild steel by acquisition the 3D data or information regarding their conditions. These metal specimens with a surface area of  $12 \text{ cm}^2$  were treated with  $1.5 \text{ M H}_2\text{SO}_4$ ,  $1.5\text{M HNO}_3$  and/or  $1.5 \text{ M CH}_3\text{COOH}$  in the absence and presence of all studied corrosion inhibitors.

### **3.6 Atomic Absorption Spectroscopy (AAS)**

This technique was useful in detecting aluminium, zinc, and mild steel in liquid sample using the wavelength of electromagnetic radiation from a light source. Liquid sample was obtained through immersing tested metals in various acidic media in the presence and absence of corrosion inhibitors namely; 3CYC, 6MCH, and 6MC2C. Metals such as zinc, aluminium, and mild steel absorb wavelengths differently, and this measured absorbance was used to calculate the concentration of each element on the liquid sample.

### **3.7 Fourier Transform Infrared Spectroscopy (FTIR)**

This analysis was done to check the functional groups on corroded zinc and mild steel in the absence and presence of all studied corrosion inhibitors at 303K. The corroded metal specimens were carefully scratched off the specimens surfaces with a pointy knife and the resultant powders were investigated using FTIR spectrometer.

### 3.8 Weight Loss Measurements

This method focuses on weight lost by metal during corrosive attack. Most studies indicate that this method is the most preferred method for the corrosion studies because it is easy to conduct, accurate, precise and reliable [81, 82]. Zinc and mild steel metals with surface area of  $12 \text{ cm}^2$  were immersed in corrosive medium (sulphuric and acetic acid) using glass rods and hooks for 4 hours. Five different concentrations of either sulphuric and/or acetic acid were used as the corrosive media in  $100 \text{ cm}^3$  beakers (0.2 M, 0.4 M, 0.6 M, 1.0 M, and 1.5 M) without the corrosion inhibitor for the blank test. Various concentrations of inhibitor molecules, that is,  $2 \times 10^{-4} \text{ M}$ ,  $4 \times 10^{-4} \text{ M}$ ,  $6 \times 10^{-4} \text{ M}$ ,  $8 \times 10^{-4} \text{ M}$ ,  $10 \times 10^{-4} \text{ M}$ , were added in  $100 \text{ cm}^3$  beakers with equal volumes of  $40 \text{ cm}^3$ . The weight loss of both experiments, with and without the inhibitor, were recorded and analysed.

---

RESULTS AND DISCUSSIONS

4.1 Potentiodynamic Polarization (PDP) results

Mild Steel and Zinc metal

The corrosion process occurred here was composed of the dissolution of mild steel anodic and reduction of hydrogen ions at the cathode. These anodic and cathodic reactions happen simultaneously. One of the best useful methods to understand this process is potentiodynamic polarization measurements; this was achieved by obtaining the current potential curve for metal of interest (mild steel, zinc) in various acid such as sulphuric and acetic acid solution with variation of concentration of inhibitor. These curves were obtain in the absence and presence of corrosion inhibitors such as 3CYC, 6MCH, 6MC2C as shown in Figures 4.1–4.15. The  $E_{corr}$  of the Blank, for all metals (less or more noble). This is due to the aggressiveness of the acid in the absence of inhibitor. The shift in the  $I_{corr}$  is influenced by the interaction between metal and the inhibitors. Low  $I_{corr}$  value in the presence of inhibitor is equivalent to maximum protection the inhibitor rendered to metal [79, 81].

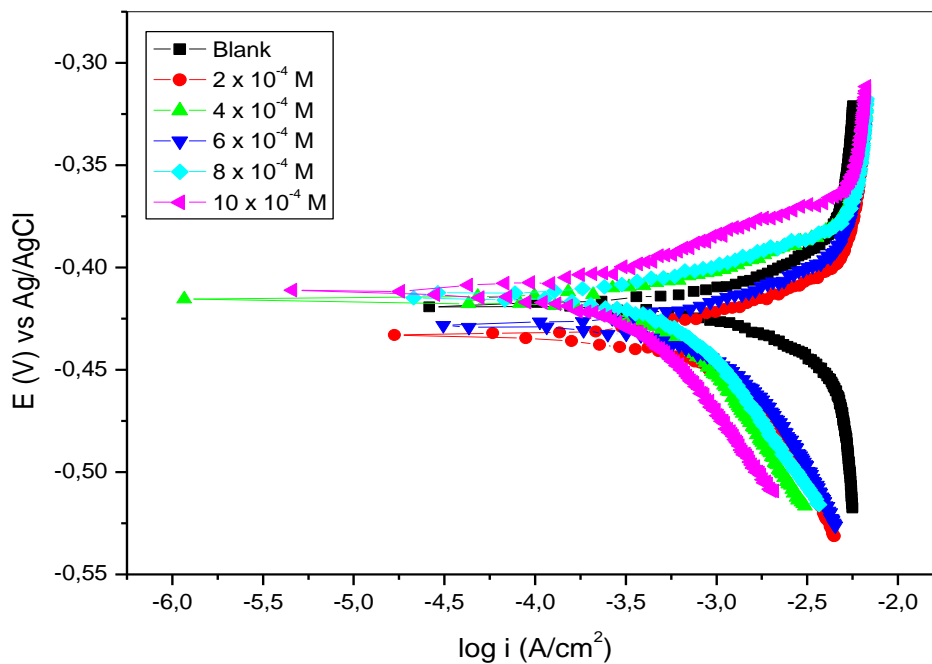


Figure 4.1: Tafel plots for mild steel in 1.5 M H<sub>2</sub>SO<sub>4</sub> in the absence and presence of different concentrations of 3CYC.

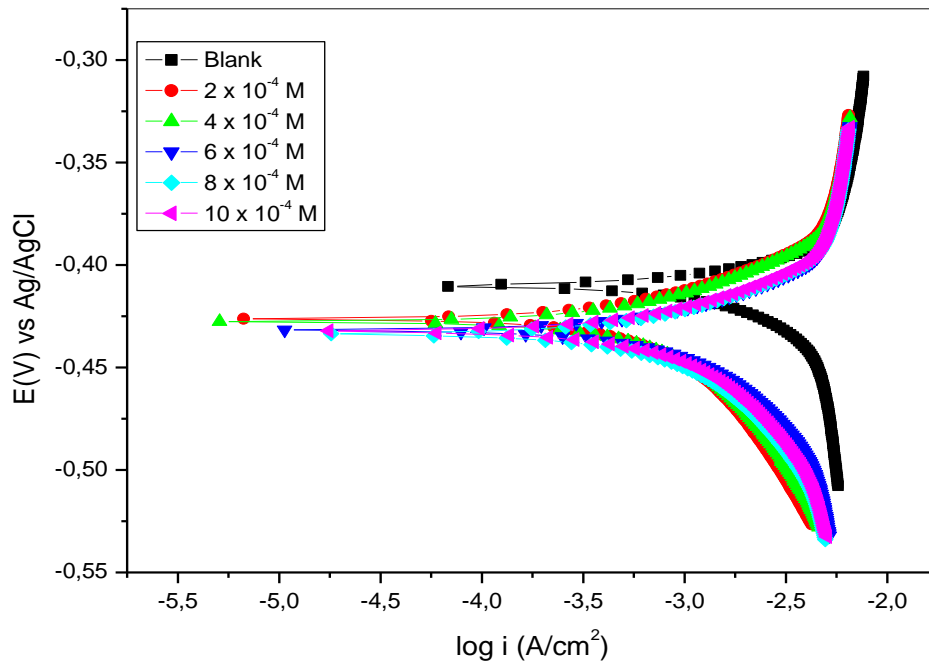


Figure 4.2: Tafel plots for mild steel in 1.5 M H<sub>2</sub>SO<sub>4</sub> in the absence and presence of different concentrations of 6MCH.

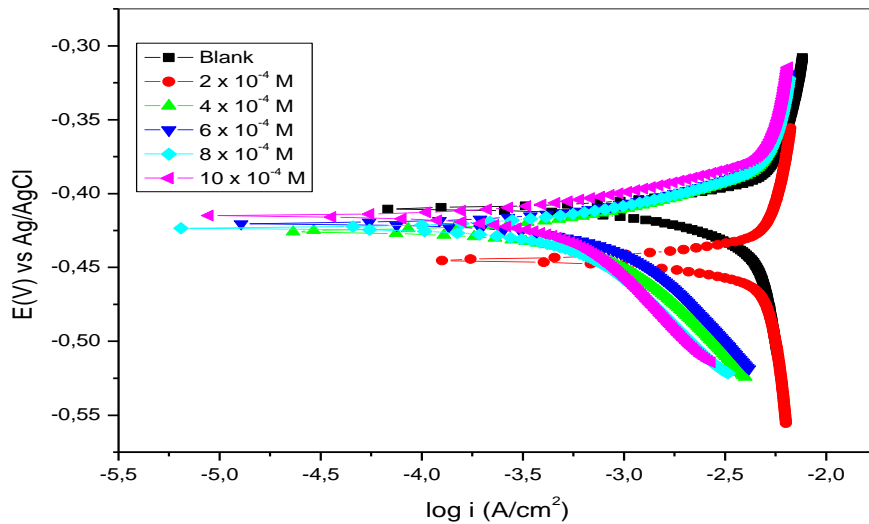


Figure 4.3: Tafel plots for mild steel in 1.5 M H<sub>2</sub>SO<sub>4</sub> in the absence and presence of different concentrations of 6MC2C.

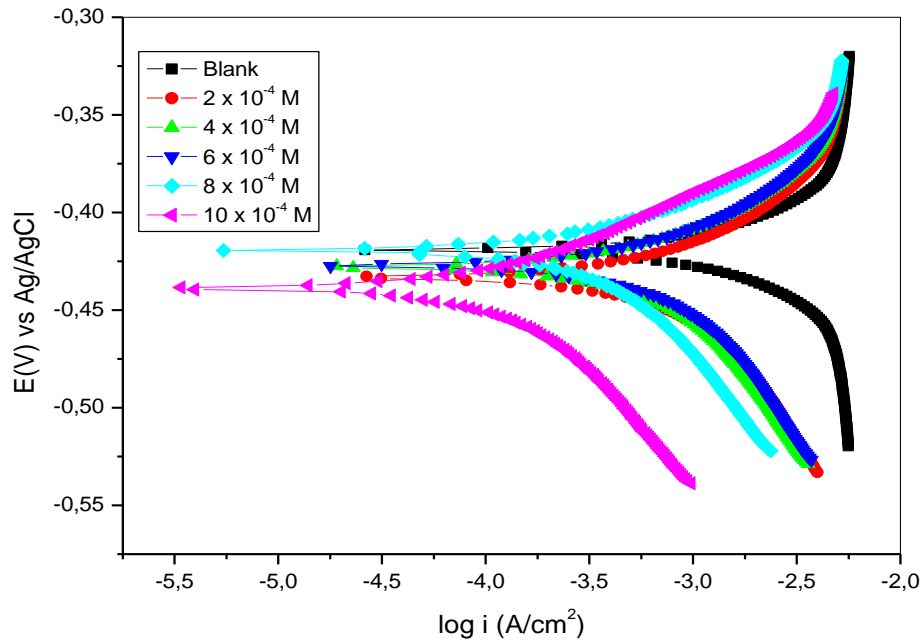


Figure 4.3: Tafel plots for zinc in 1.5 M H<sub>2</sub>SO<sub>4</sub> in the absence and presence of different concentrations of 3CYC.

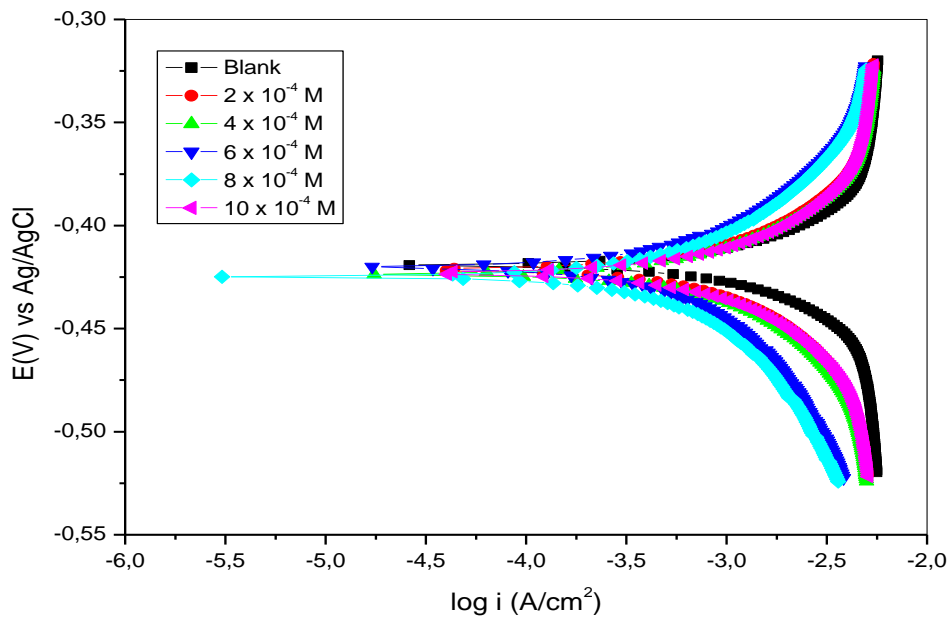


Figure 4.4: Tafel plots for zinc in 1.5 M H<sub>2</sub>SO<sub>4</sub> in the absence and presence of different concentrations of 6MCH.



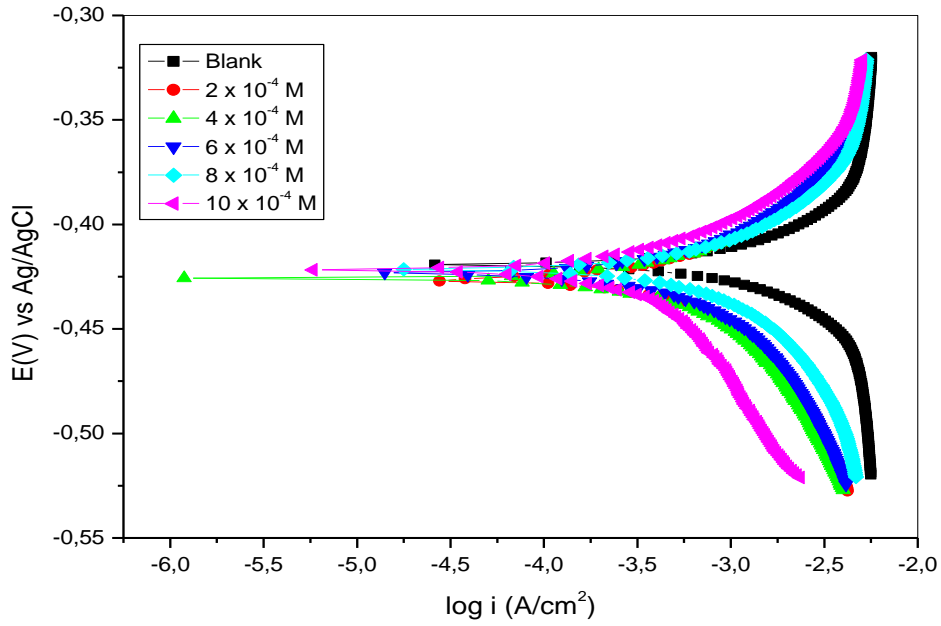


Figure 4.5: Tafel plots for zinc in 1.5 M H<sub>2</sub>SO<sub>4</sub> in the absence and presence of different concentrations of 6MC2C.

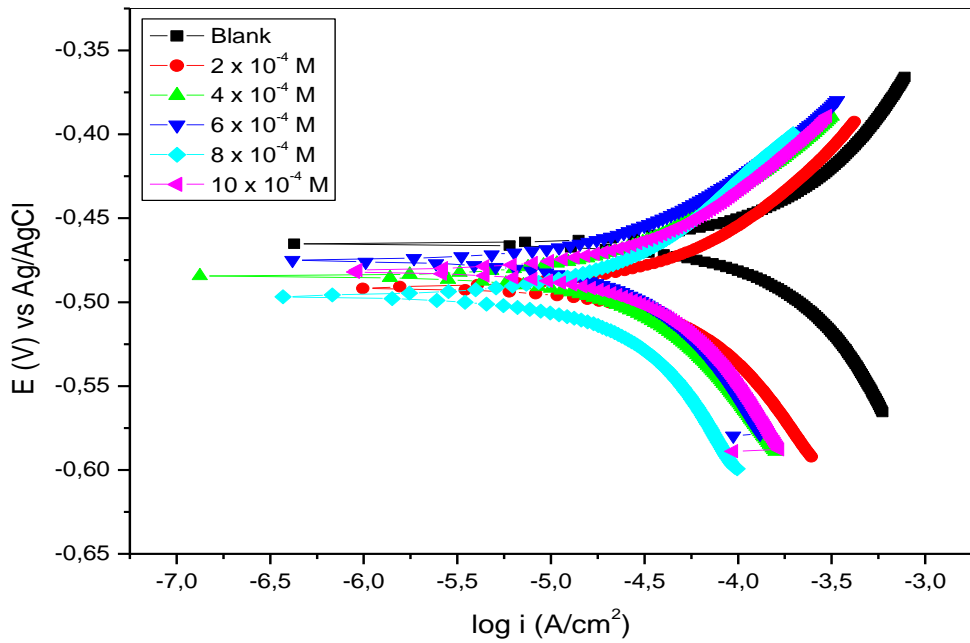


Figure 4.6: Tafel plots for mild steel in 1.5 M acetic acid in the absence and presence of different concentrations of 3CYC.

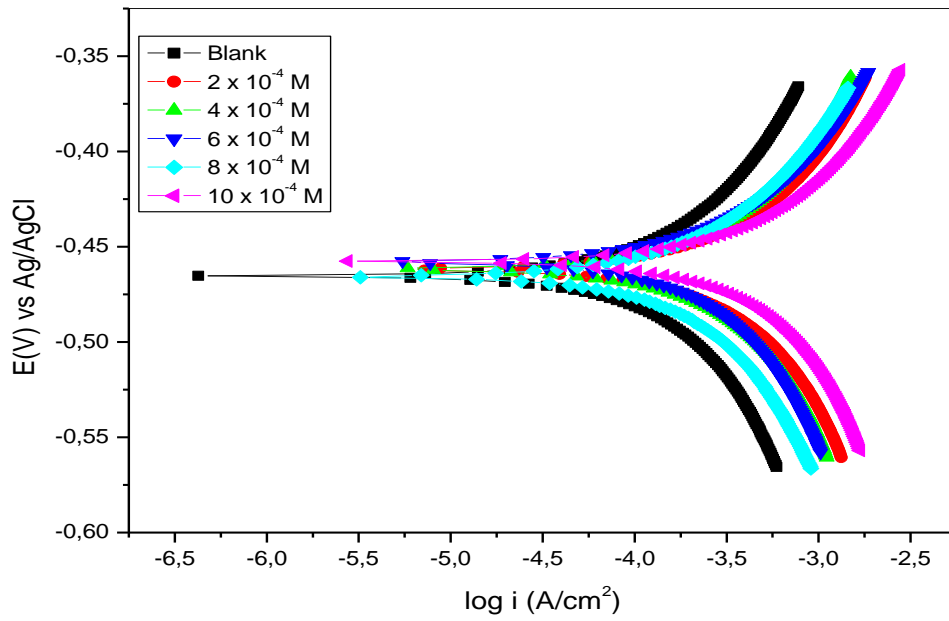


Figure 4.7: Tafel plots for mild steel in 1.5 M  $\text{CH}_3\text{COOH}$  in the absence and presence of different concentrations of 6MCH.

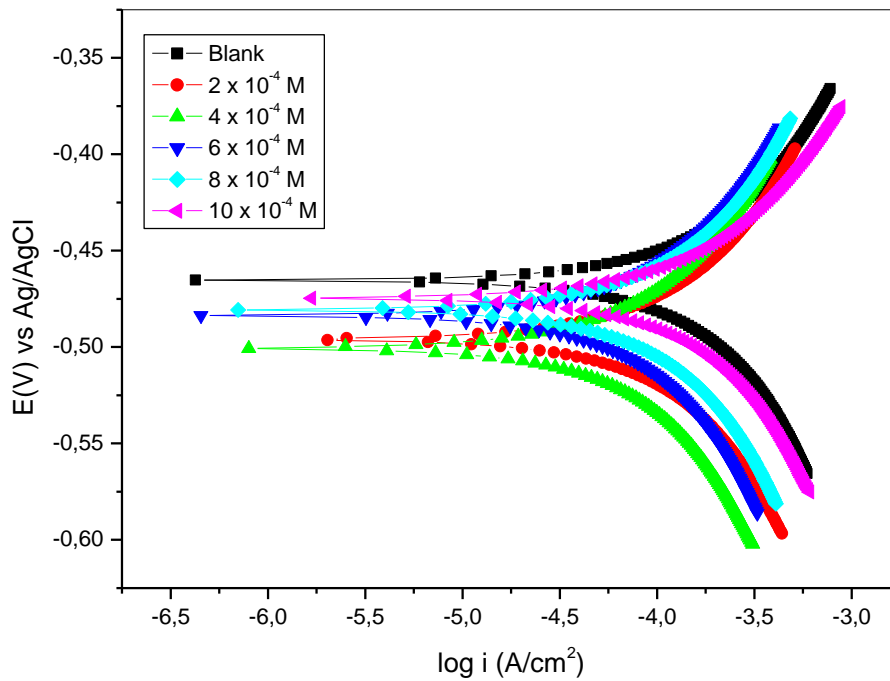


Figure 4.8: Tafel plots for mild steel in 1.5 M  $\text{CH}_3\text{COOH}$  in the absence and presence of different concentrations of 6MC2C.

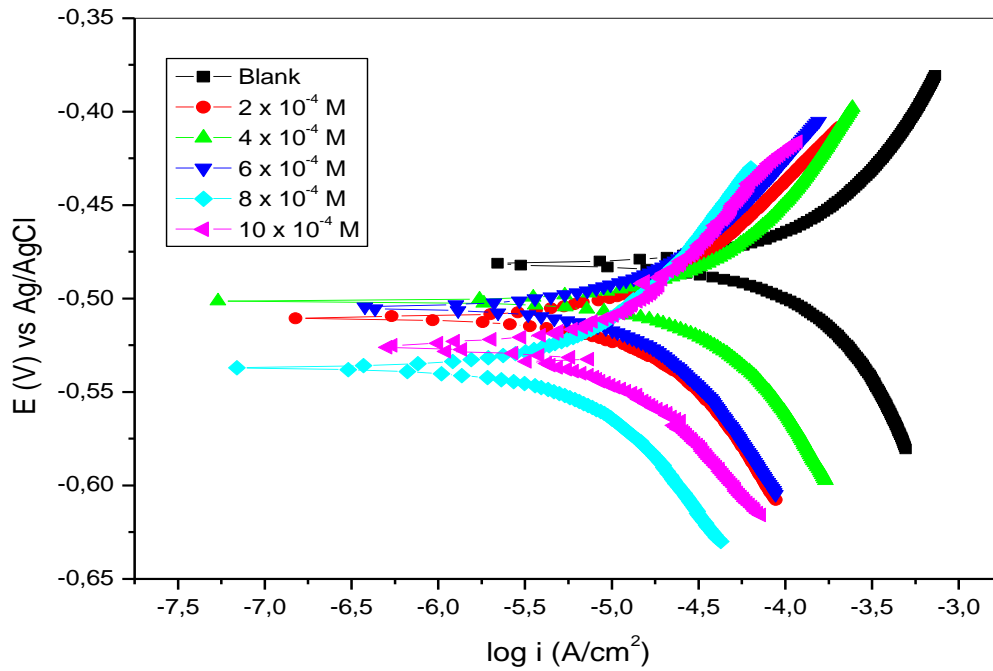


Figure 4.10: Tafel plots for zinc in 1.5 M  $\text{CH}_3\text{COOH}$  in the absence and presence of different concentrations of 3CYC.

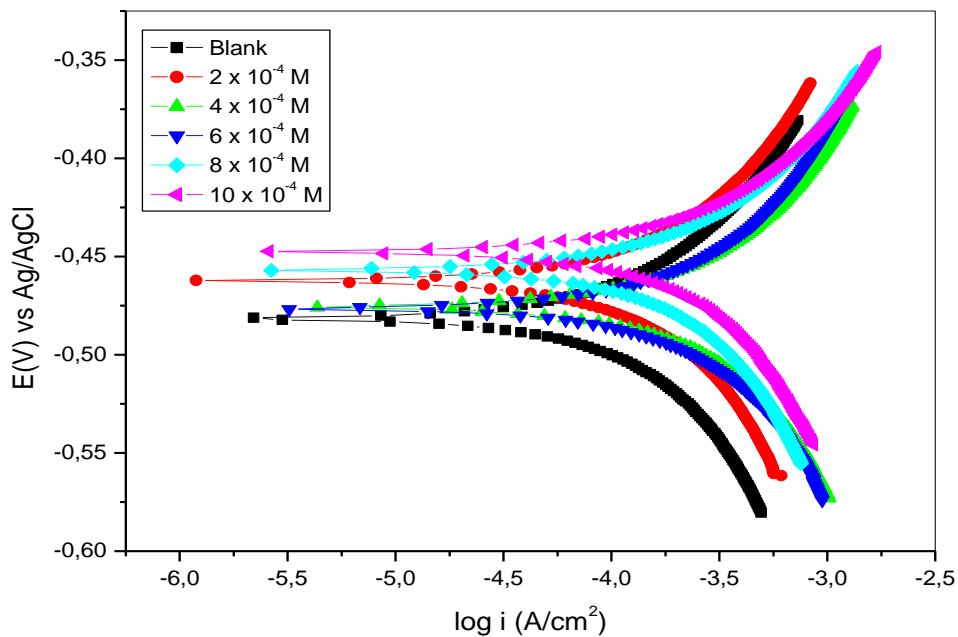


Figure 4.11: Tafel plots for zinc in 1.5 M  $\text{CH}_3\text{COOH}$  in the absence and presence of different concentrations of 6MCH.

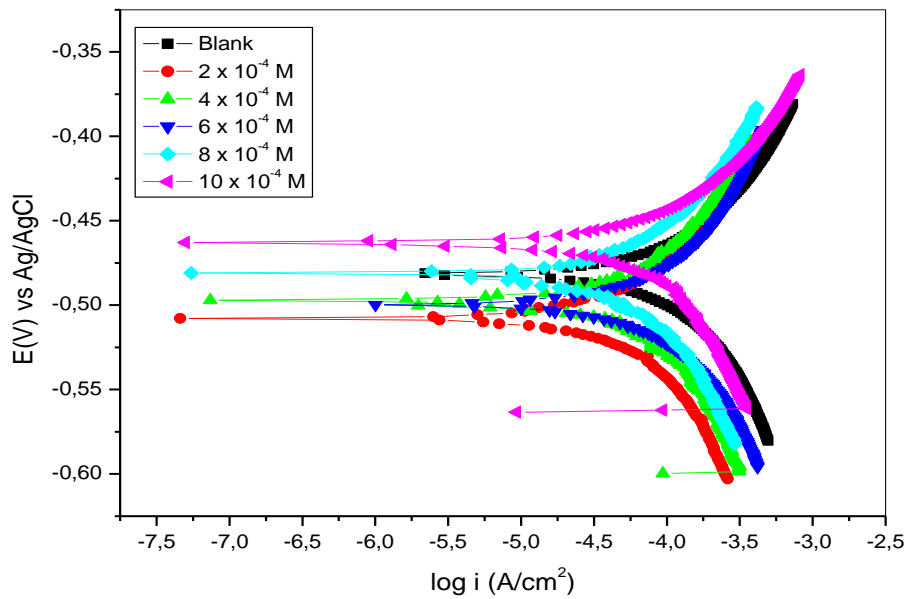


Figure 4.12: Tafel plots for zinc in 1.5 M  $\text{CH}_3\text{COOH}$  in the absence and presence of different concentrations of 6MC2C.

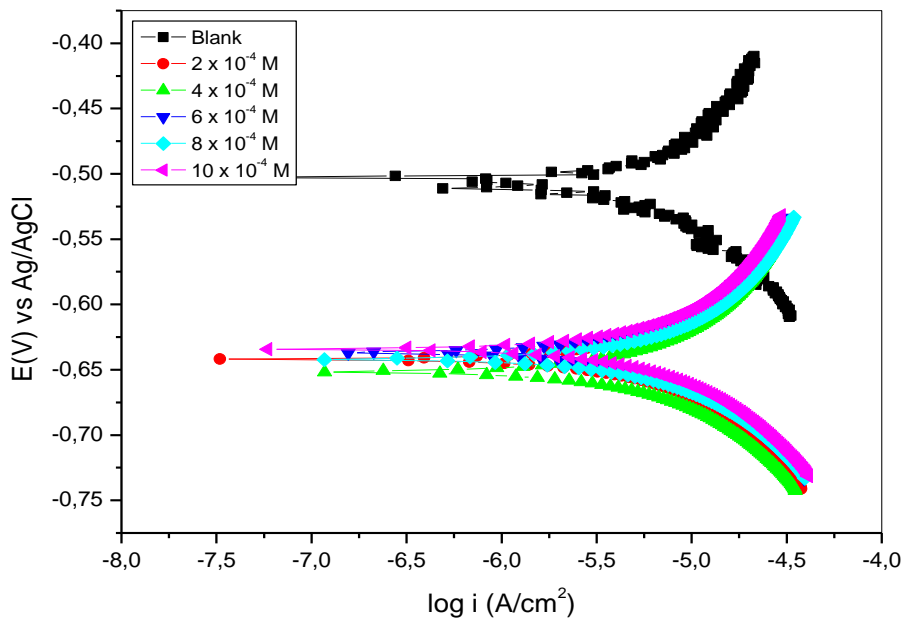


Figure 4.13: Tafel plots for aluminium in 1.5 M  $\text{HNO}_3$  in the absence and presence of different concentrations of 3CYC.

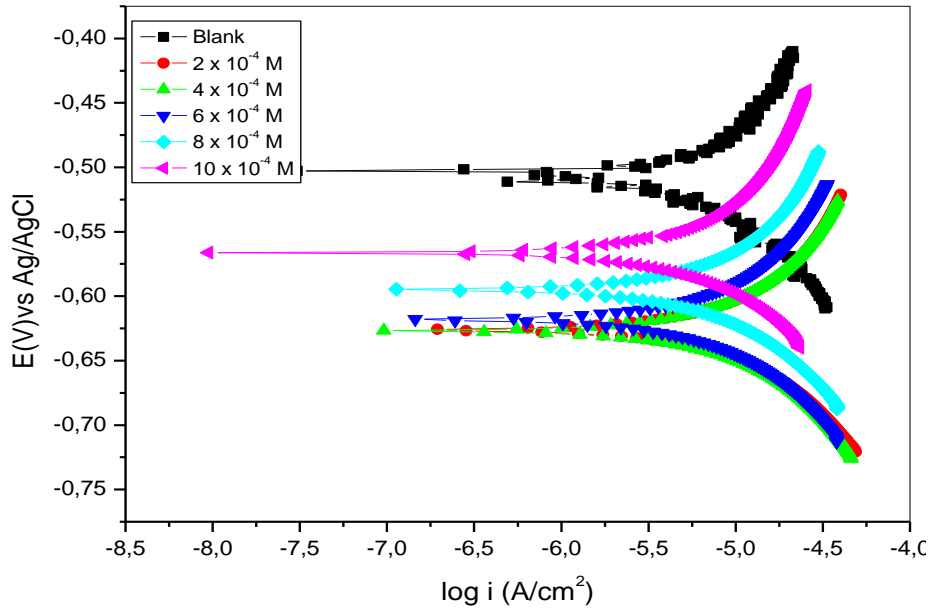


Figure 4.14: Tafel plots for aluminium in 1.5 M  $HNO_3$  in the absence and presence of different concentrations of 6MC2C.

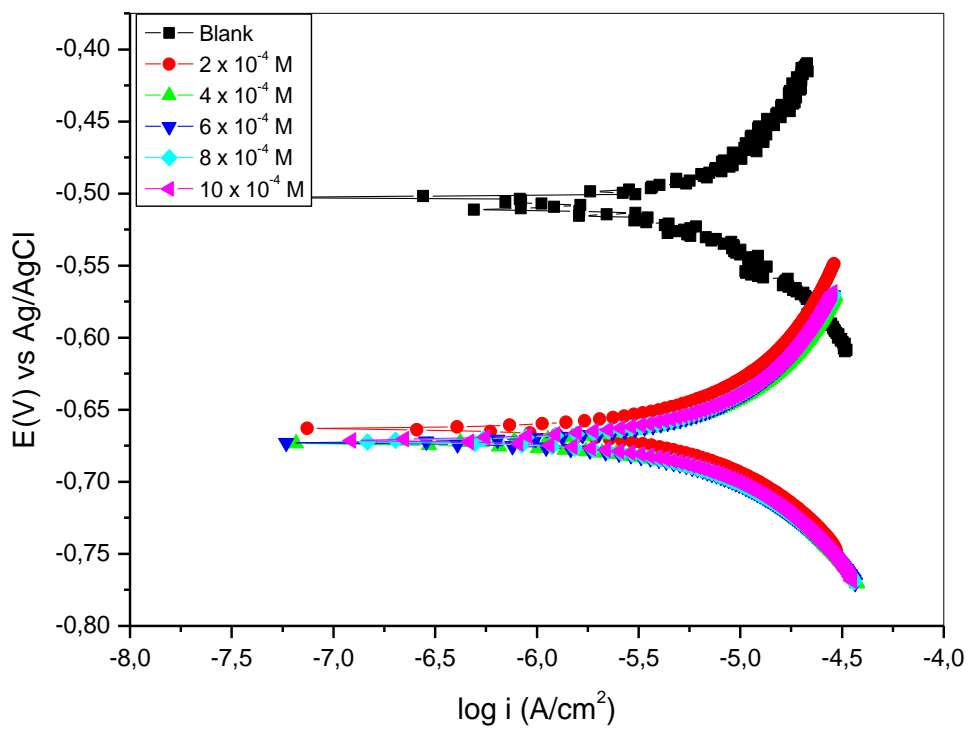


Figure 4.15: Tafel plots for aluminium in 1.5 M  $HNO_3$  in the absence and presence of different concentrations of 6MCH.

Tables 4.1 – 4.4 and figures 4.1 – 4.15 show the effect of introduction of three inhibitors 3CYC, 6MCH, and 6MC2C. These tables clearly show rapid decrease of corrosion current densities of anodic and cathodic half-reaction. The current density before introduction of inhibitors for anodic and cathodic half-reaction were  $0.081\text{mV}\cdot\text{dec}^{-1}$  and  $0.093\text{mV}\cdot\text{dec}^{-1}$  for zinc in acetic acid,  $0.175\text{ mV}\cdot\text{dec}^{-1}$  and  $0.225\text{mV}\cdot\text{dec}^{-1}$ , respectively for mild steel in acetic acid,  $0.131\text{ mV}\cdot\text{dec}^{-1}$  and  $0.131\text{mV}\cdot\text{dec}^{-1}$ , respectively for zinc in sulphuric acid and  $0.052\text{ mV}\cdot\text{dec}^{-1}$  and  $0.093\text{mV}\cdot\text{dec}^{-1}$ , respectively for mild steel in sulphuric acid. The introduction of three studied inhibitors namely, 3CYC, 6MCH, and 6MC2C yield corrosion current densities ranging between  $0.006\text{ mV}\cdot\text{dec}^{-1}$  to  $0.123\text{mV}\cdot\text{dec}^{-1}$ , respectively for anodic and cathodic half-reaction. This trend suggests the anodic dissolution of zinc and mild steel and also the cathodic reduction of hydrogen ion being inhibited. The anodic and cathodic half-reaction were affected by the presence of studies inhibitors, these can be confirmed by variation of Tafel plots when compared with those of uninhibited process. Tables 4.1–4.4 also shows that the inhibition efficiency increase when concentration of studied inhibitors increases. It can be suggested from PDP inhibition efficiency results that all three studied inhibitor where able to adsorb and form thin film layer protecting mild steel and zinc from dissolution when exposed to acetic and sulphuric acid [82]. The inhibition efficiency obtained from weight loss measurement were correlate with the inhibition efficiency from PDP. For example inhibition efficiency for zinc in 3CYC (0.0008M) exposed in acetic acid for PDP and weight loss method were 83.33% and 83.06%, respectively

Table 4.1: Potentiodynamic polarization (PDP) parameters such as corrosion potential ( $E_{\text{corr}}$ ), corrosion current density ( $i_{\text{corr}}$ ) and anodic and cathodic Tafel slopes ( $b_a$  and  $b_c$ ) using different inhibitors on mild steel in  $\text{H}_2\text{SO}_4$

Inhibitor	Inhibitor conc (M)	$-E_{\text{corr}}$ (mV) with Ag/AgCl	$i_{\text{corr}}$ ( $\text{mA}\cdot\text{cm}^{-2}$ )	$R_p$ ( $10^{-1}$ ) ( $\Omega$ )	$b_a$ ( $\text{V}\cdot\text{dec}^{-1}$ )	$b_c$ ( $\text{V}\cdot\text{dec}^{-1}$ )	%IE PDP	%IEW <sub>L</sub>
<b>Blank</b>	0.000	410.08	1.671	0.870	0.052	0.093	-	-
3CYC	$2 \times 10^{-4}$	434.48	0.546	1.686	0.028	0.084	67.07	85.84
	$4 \times 10^{-4}$	417.20	0.345	2.311	0.023	0.089	79.64	93.51
	$6 \times 10^{-4}$	429.22	0.295	2.181	0.027	0.033	82.35	94.71
	$8 \times 10^{-4}$	414.59	0.091	3.009	0.011	0.015	94.55	96.17
	$10 \times 10^{-4}$	412.84	0.053	6.173	0.013	0.019	96.83	97.96
6MC2C	$2 \times 10^{-4}$	444.96	0.198	0.524	0.005	0.005	88.15	83.13
	$4 \times 10^{-4}$	425.55	0.117	2.589	0.012	0.017	93.00	84.22
	$6 \times 10^{-4}$	420.18	0.083	2.231	0.008	0.009	95.03	97.53
	$8 \times 10^{-4}$	423.30	0.065	2.836	0.008	0.010	96.11	99.10
	$10 \times 10^{-4}$	415.10	0.041	3.229	0.006	0.006	97.55	99.22
6MCH	$2 \times 10^{-4}$	426.29	0.621	2.222	0.047	0.098	62.84	68.49
	$4 \times 10^{-4}$	427.64	0.570	2.290	0.047	0.082	65.89	69.25
	$6 \times 10^{-4}$	431.80	0.443	1.547	0.026	0.040	73.49	70.57
	$8 \times 10^{-4}$	433.76	0.360	1.823	0.024	0.041	78.46	72.88
	$10 \times 10^{-4}$	432.37	0.193	1.995	0.016	0.020	88.45	84.12

Table 4.2: Potentiodynamic polarization (PDP) parameters such as corrosion potential ( $E_{\text{corr}}$ ), corrosion current density ( $i_{\text{corr}}$ ) and anodic and cathodic Tafel slopes ( $b_a$  and  $b_c$ ) using different inhibitors on zinc in  $\text{H}_2\text{SO}_4$

Inhibitor	Inhibitor conc (M)	$-E_{\text{corr}}$ (mV) with Ag/AgCl	$i_{\text{corr}}$ ( $\text{mA}\cdot\text{cm}^{-2}$ )	$R_p$ ( $10^{-1}$ ) ( $\Omega$ )	$b_a$ ( $\text{V}\cdot\text{dec}^{-1}$ )	$b_c$ ( $\text{V}\cdot\text{dec}^{-1}$ )	%IE PDP	%IEW <sub>L</sub>
<b>Blank</b>	0.000	419.09	1.589	1.793	0.131	0.131	-	-
3CYC	$2 \times 10^{-4}$	433.23	0.484	2.607	0.045	0.082	69.54	72.52
	$4 \times 10^{-4}$	427.88	0.431	3.025	0.046	0.086	72.88	72.97
	$6 \times 10^{-4}$	427.01	0.406	3.605	0.058	0.081	74.45	74.36
	$8 \times 10^{-4}$	419.28	0.326	4.817	0.054	0.111	79.48	75.87
	$10 \times 10^{-4}$	418.14	0.300	4.231	0.048	0.076	81.12	76.46
6MC2C	$2 \times 10^{-4}$	426.64	1.057	2.801	0.122	0.154	33.48	34.48
	$4 \times 10^{-4}$	425.70	1.034	2.857	0.122	0.154	34.93	34.54
	$6 \times 10^{-4}$	423.26	0.934	2.650	0.110	0.118	41.22	39.15
	$8 \times 10^{-4}$	421.23	0.415	2.102	0.036	0.045	73.88	40.74
	$10 \times 10^{-4}$	421.57	0.311	4.444	0.047	0.100	80.43	69.82
6MCH	$2 \times 10^{-4}$	421.40	0.577	1.897	0.049	0.052	63.69	64.28
	$4 \times 10^{-4}$	423.51	0.564	1.863	0.045	0.052	64.51	66.45
	$6 \times 10^{-4}$	420.28	0.556	3.072	0.070	0.090	65.01	67.07
	$8 \times 10^{-4}$	424.73	0.555	3.183	0.067	0.104	65.07	67.17
	$10 \times 10^{-4}$	423.07	0.468	1.734	0.038	0.037	70.55	69.21

Table 4.3: Potentiodynamic polarization (PDP) parameters such as corrosion potential ( $E_{\text{corr}}$ ), corrosion current density ( $i_{\text{corr}}$ ) and anodic and cathodic Tafel slopes ( $b_a$  and  $b_c$ ) using different inhibitors on mild steel in  $\text{CH}_3\text{COOH}$

Inhibitor	Inhibitor conc (M)	$-E_{\text{corr}}$ (mV) with Ag/AgCl	$i_{\text{corr}}$ (mA.c $\text{m}^{-2}$ )	$R_p$ ( $10^{-1}$ ) ( $\Omega$ )	$b_a$ (V.dec $^{-1}$ )	$b_c$ (V.dec $^{-1}$ )	%IE PDP	%IE WL
Blank		465.31	0.212	20.210	0.175	0.225	-	-
3CYC	$2 \times 10^{-4}$	491.38	0.038	54.380	0.085	0.105	82.08	73.40
	$4 \times 10^{-4}$	484.56	0.032	79.000	0.095	0.151	84.91	77.40
	$6 \times 10^{-4}$	475.16	0.025	89.980	0.082	0.138	88.21	79.20
	$8 \times 10^{-4}$	496.45	0.016	124.55	0.084	0.109	92.45	86.60
	$10 \times 10^{-4}$	481.50	0.006	89.964	0.032	0.035	97.17	90.00
6MC2C	$2 \times 10^{-4}$	495.89	0.041	31.874	0.056	0.066	80.66	75.00
	$4 \times 10^{-4}$	500.54	0.038	49.159	0.081	0.090	82.08	77.50
	$6 \times 10^{-4}$	483.68	0.029	39.461	0.049	0.056	86.32	80.00
	$8 \times 10^{-4}$	480.64	0.023	32.989	0.034	0.035	89.15	82.50
	$10 \times 10^{-4}$	474.44	0.021	22.329	0.021	0.023	90.09	85.83
6MCH	$2 \times 10^{-4}$	461.86	0.035	09.591	0.015	0.016	83.49	52.50
	$4 \times 10^{-4}$	461.72	0.034	10.941	0.016	0.018	83.96	58.33
	$6 \times 10^{-4}$	458.05	0.028	11.225	0.014	0.015	86.79	60.00
	$8 \times 10^{-4}$	465.66	0.024	14.346	0.016	0.017	88.68	77.50
	$10 \times 10^{-4}$	457.75	0.023	06.637	0.006	0.008	89.15	81.67

Table 4.4: Potentiodynamic polarization (PDP) parameters such as corrosion potential ( $E_{\text{corr}}$ ), corrosion current density ( $i_{\text{corr}}$ ) and anodic and cathodic Tafel slopes ( $b_a$  and  $b_c$ ) using different inhibitors on zinc in  $\text{CH}_3\text{COOH}$

Inhibitor	Inhibitor conc (M)	$-E_{\text{corr}}$ (mV) with Ag/AgCl	$i_{\text{corr}}$ (mA. $\text{cm}^{-2}$ )	$R_p$ ( $10^{-1}$ ) ( $\Omega$ )	$b_a$ (V.dec $^{-1}$ )	$b_c$ (V.dec $^{-1}$ )	%IE PDP	%IE WL
Blank	0.000	481.56	0.060	31.356	0.081	0.093	-	-
3CYC	$2 \times 10^{-4}$	510.33	0.016	144.17	0.090	0.123	73.33	76.32
	$4 \times 10^{-4}$	501.37	0.015	87.388	0.059	0.061	75.00	81.25
	$6 \times 10^{-4}$	504.80	0.014	161.07	0.090	0.117	76.67	82.57
	$8 \times 10^{-4}$	525.61	0.010	235.14	0.105	0.105	83.33	83.06
	$10 \times 10^{-4}$	537.15	0.007	344.98	0.119	0.116	88.33	83.22
6MC2C	$2 \times 10^{-4}$	507.83	0.023	50.080	0.053	0.052	61.67	74.67
	$4 \times 10^{-4}$	495.83	0.017	51.423	0.036	0.044	71.67	75.49
	$6 \times 10^{-4}$	499.91	0.006	33.760	0.010	0.009	90.00	76.15
	$8 \times 10^{-4}$	480.97	0.004	39.020	0.005	0.016	93.33	77.80
	$10 \times 10^{-4}$	464.34	0.002	51.218	0.005	0.005	96.67	86.35
6MCH	$2 \times 10^{-4}$	462.36	0.020	20.768	0.019	0.020	66.67	76.48
	$4 \times 10^{-4}$	475.56	0.017	12.728	0.011	0.009	71.67	77.30
	$6 \times 10^{-4}$	476.50	0.014	13.621	0.009	0.008	76.67	77.80
	$8 \times 10^{-4}$	456.88	0.013	14.576	0.008	0.009	78.33	79.44
	$10 \times 10^{-4}$	447.63	0.012	13.346	0.007	0.007	80.00	83.22



It's clear as denoted in Table 4.5 that these three corrosion inhibitor, namely, 3CYC, 6MCH, and 6MC2C effectively minimise corrosion. Corrosion current ( $i_{\text{corr}}$ ) values are useful in understanding the effectiveness of the corrosion inhibitors, thus implies that the higher the corrosion current ( $i_{\text{corr}}$ ) values the more corrosive the exposure environment become. In the absence of three inhibitors, namely 3CYC, 6MCH, and 6MC2C the current value was  $1.816 \times 10^6 \text{ A/cm}^2$ , this value rapidly drop down when corrosion inhibitors were utilised. It is clear from Table 4.5 that when the concentration of inhibitors increases the current values ( $i_{\text{corr}}$ ) decreases.

These currents ( $i_{\text{corr}}$ ) values are useful in calculating the inhibition efficiency and comparing the inhibition efficiency obtained from weight loss method and PDP it was found that these values correlate with each other.

Table 4.5: Potentiodynamic polarization (PDP) parameters such as corrosion potential ( $E_{\text{corr}}$ ), corrosion current density ( $i_{\text{corr}}$ ) and anodic and cathodic Tafel slopes ( $b_a$  and  $b_c$ ) using different inhibitors on aluminium in  $\text{HNO}_3$

Inhibitor	Inhibitor conc (M)	$-E_{\text{corr}}$ (mV) with Ag/AgCl	$i_{\text{corr}}$ ( $10^6$ ) ( $\text{A.cm}^{-2}$ )	$R_p$ ( $10^{-3}$ ) ( $\Omega$ )	$b_a$ ( $\text{V.dec}^{-1}$ )	$b_c$ ( $\text{V.dec}^{-1}$ )	%IE PDP	%IE WL
Blank	0.000	509.55	1.816	4.824	0.045	0.037	-	-
3CYC	$2 \times 10^{-4}$	642.14	0.499	4.177	0.010	0.009	72.52	54.08
	$4 \times 10^{-4}$	651.68	0.434	4.192	0.009	0.008	76.10	65.31
	$6 \times 10^{-4}$	636.83	0.399	4.022	0.008	0.007	78.03	75.51
	$8 \times 10^{-4}$	642.17	0.281	3.667	0.005	0.004	84.53	79.59
	$10 \times 10^{-4}$	633.97	0.188	4.091	0.003	0.004	89.65	90.82
6MC2C	$2 \times 10^{-4}$	626.00	0.509	3.083	0.007	0.008	71.97	86.73
	$4 \times 10^{-4}$	627.16	0.407	3.198	0.007	0.005	77.59	89.80
	$6 \times 10^{-4}$	618.09	0.269	3.844	0.004	0.005	85.19	92.86
	$8 \times 10^{-4}$	594.70	0.265	3.903	0.004	0.005	85.41	97.96
	$10 \times 10^{-4}$	566.33	0.145	5.231	0.004	0.003	92.02	98.98
6MCH	$2 \times 10^{-4}$	663.52	0.381	4.599	0.009	0.007	79.02	79.59
	$4 \times 10^{-4}$	673.89	0.315	4.116	0.006	0.006	82.65	81.63
	$6 \times 10^{-4}$	672.55	0.312	4.206	0.006	0.006	82.82	83.67
	$8 \times 10^{-4}$	671.95	0.244	4.318	0.005	0.005	86.56	84.69
	$10 \times 10^{-4}$	671.17	0.237	4.348	0.005	0.004	86.95	94.90

## 4.2 Electrochemical Impedance Spectroscopy (EIS)

EIS is a useful technique to monitor corrosion processes in aggressive environments such as acidic medium [84]. In this study, the behaviour of 1,5M of  $\text{CH}_3\text{COOH}$ ,  $\text{H}_2\text{SO}_4$ , and  $\text{HNO}_3$  with and without corrosion inhibitors namely, 3CYC, 6MC2C, and 6MCH were studied. The experimental data obtain from EIS was fitted with an equivalent circuit to study their electrochemical properties. Figures 4.16 – 4.45 show the Nyquist plots with capacitive loops for Zn, Al, and MS in 1.5 M of  $\text{H}_2\text{SO}_4$ ,  $\text{CH}_3\text{COOH}$ , and  $\text{HNO}_3$  solution in the absence and presence of various concentrations of 3CYC, 6MCH, and 6MC2C at 303K. The capacitive loops observed were semicircles. This is due to frequency dispersion that normally comes from the inhomogenities of the surface of electrode [85, 86, 87]. When concentration of inhibitors increases the capacitive loop increases. Figure below shows impedance diagram characterised by large capacitive loop with lower inductive arc and the bode plots acquired in the absence and presence of inhibitor. These plots contain single time constant indicating the formation of film on MS, Al, and Zn surface. Figures 4.16–4.45 shows Nyquist and bode plots obtained in this study

The impedance spectra gotten are displayed as Nyquist and Bode plots, as appeared in Figures 4.16–4.45. The obtained shape appear to be similar regardless of the present of inhibitor or not, implying that the presence of inhibitors does not change the anodic and cathodic process. The radius of blank is noticeably smaller as indicated in Nyquist plots. There was a shift in Nyquist plots as the concentration of the inhibitors increased. This conduct was due to the arrangement of the adsorption film layer on the surface of MS, Zn, and Al as the concentration of the inhibitors atoms were able to supply higher scope of the metal surface [88, 89, 90]. The `shift within the semicircle loops with an increment in inhibitors concentration could be a result of the stabilization of the adsorption phenomenon. The semicircles gotten are not culminate, and a littler curve for the blank shows that the corrosion of MS, Zn and Al is controlled basically by charge exchange/transfer process. The inhibitors don't alter the electrochemical process of corrosion but anticipate it by adsorbing on the metal surface. The advantage of this plot is that all information is clearly self-evident [89, 90, 91, 92].

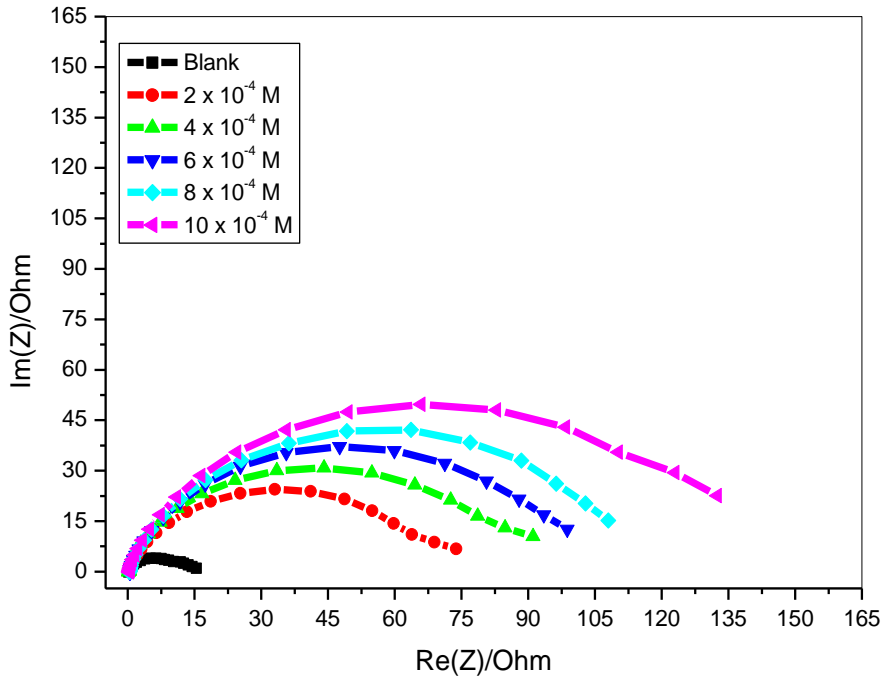


Figure 4.16: Nyquist plot of mild steel metal in sulphuric acid in the presence of various concentrations of 3CYC

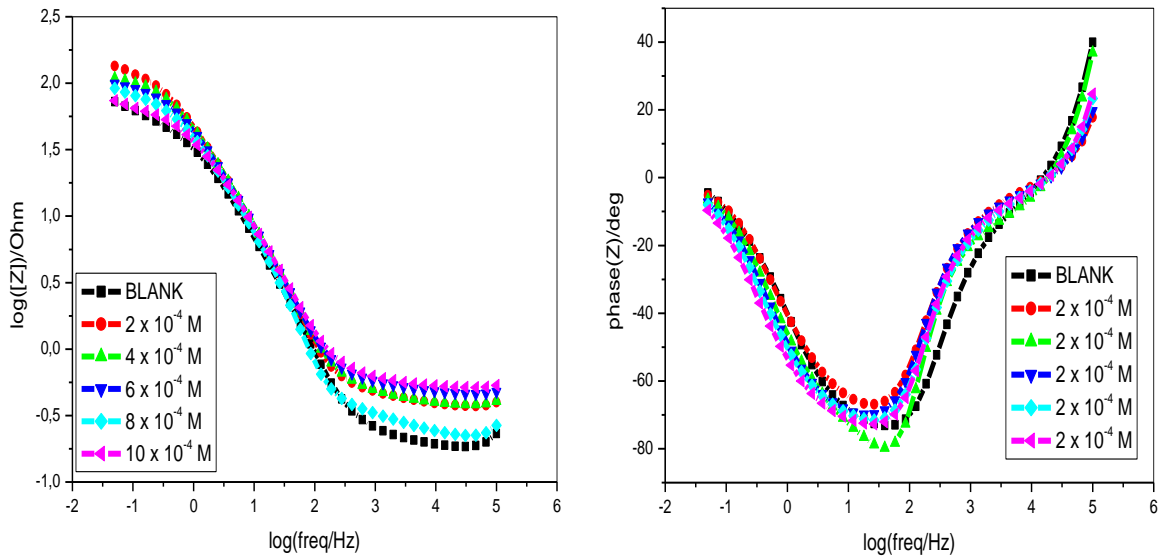


Figure 4.17: Bode diagrams of the impedance for MS in 1.5 M sulphuric acid without and with different concentration of 3CYC.

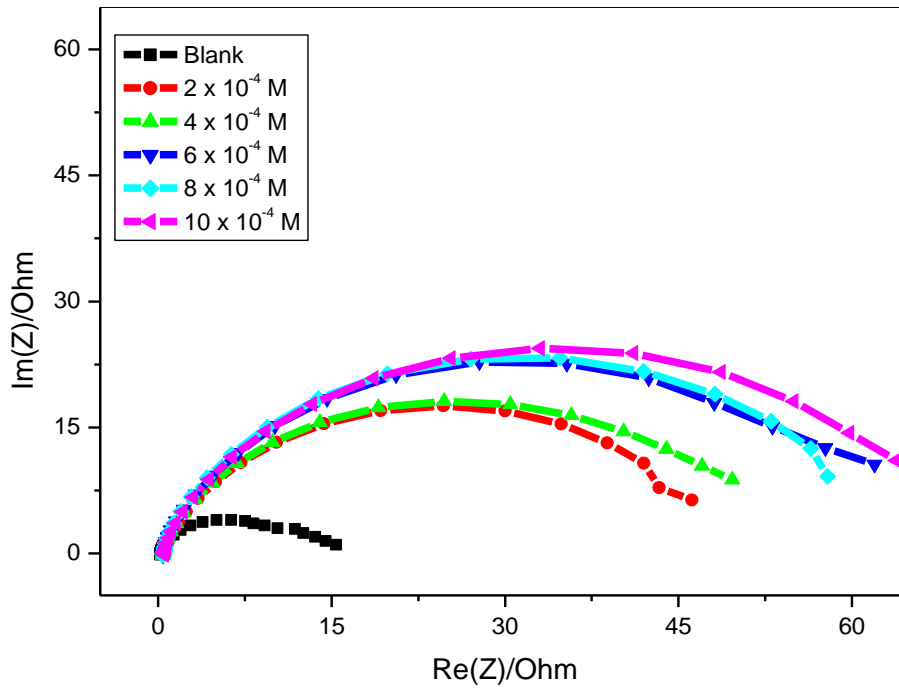


Figure 4.18: Nyquist plot of mild steel metal in sulphuric acid in the presence of various concentrations of 6MC2C

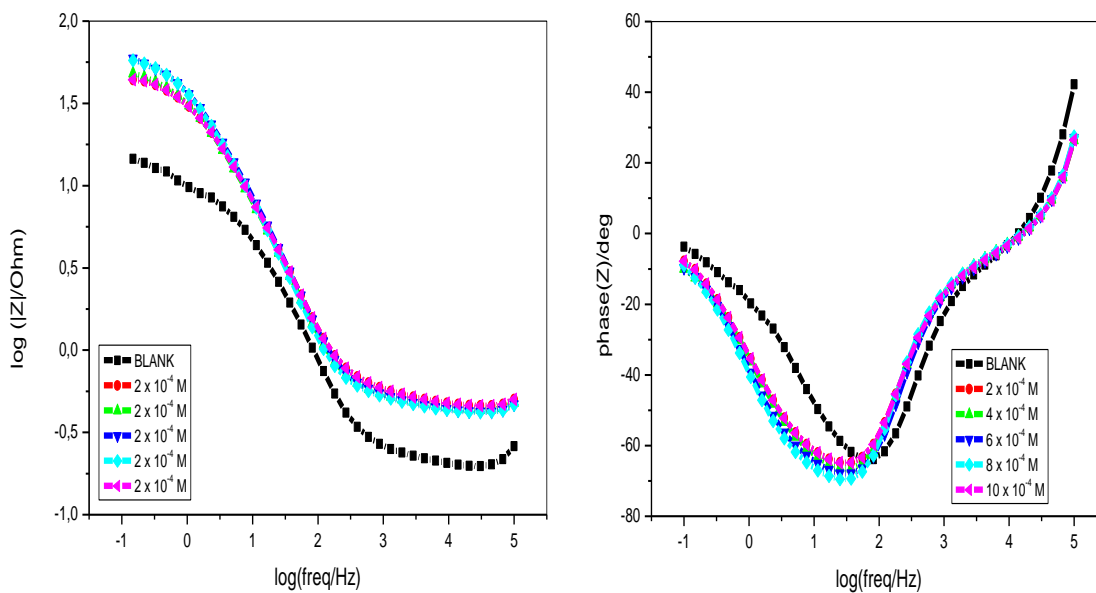


Figure 4.19: Bode diagrams of the impedance for MS in 1.5 M sulphuric acid without and with different concentration of 6MC2C.

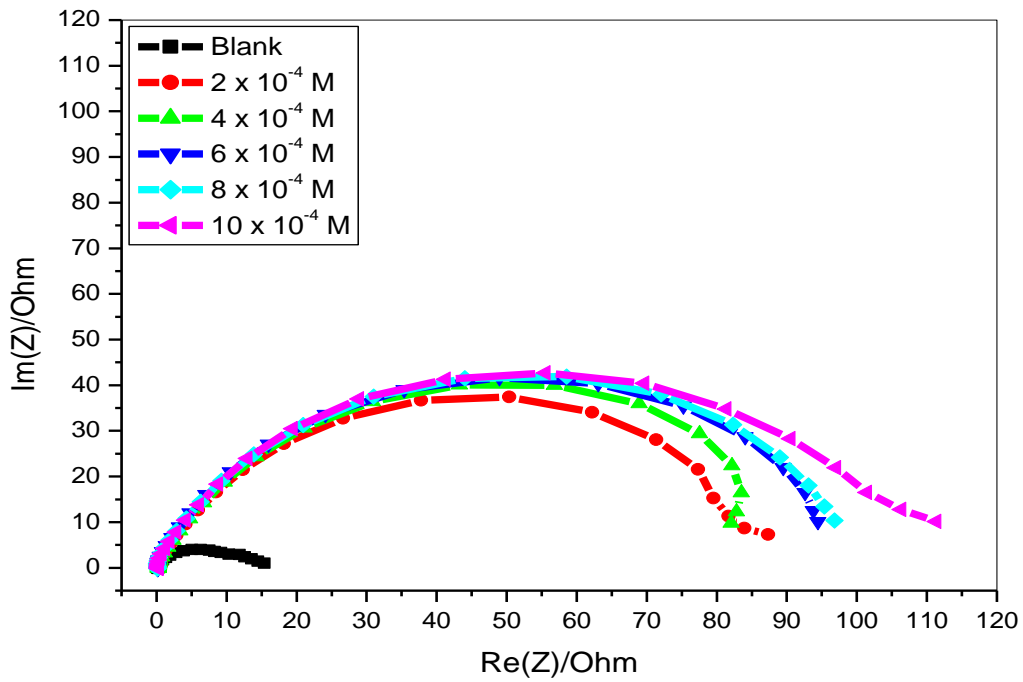


Figure 4.20: Nyquist plot of mild steel metal in sulphuric acid in the presence of various concentrations of 6MCH

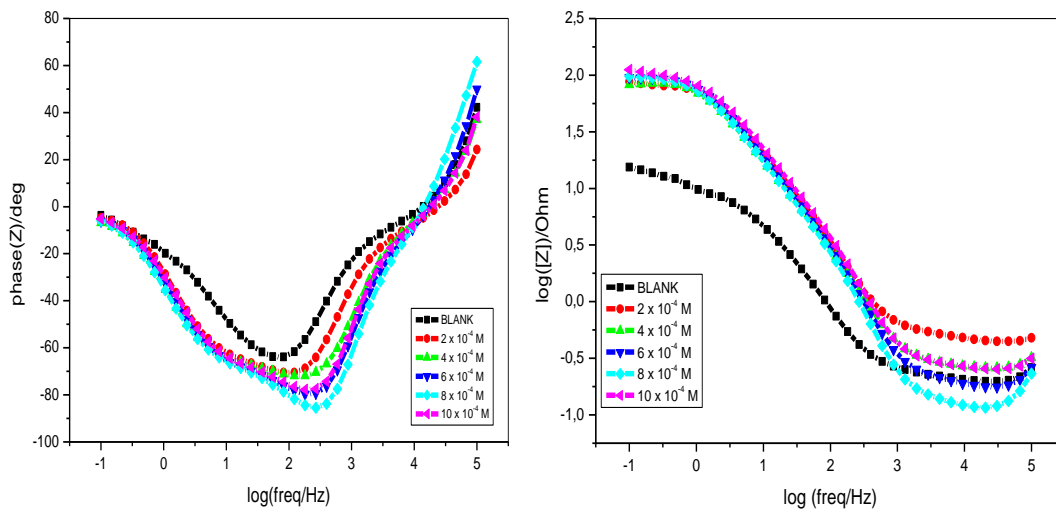


Figure 4.21: Bode diagrams of the impedance for MS in 1.5 M sulphuric acid without and with different concentration of 6MCH.

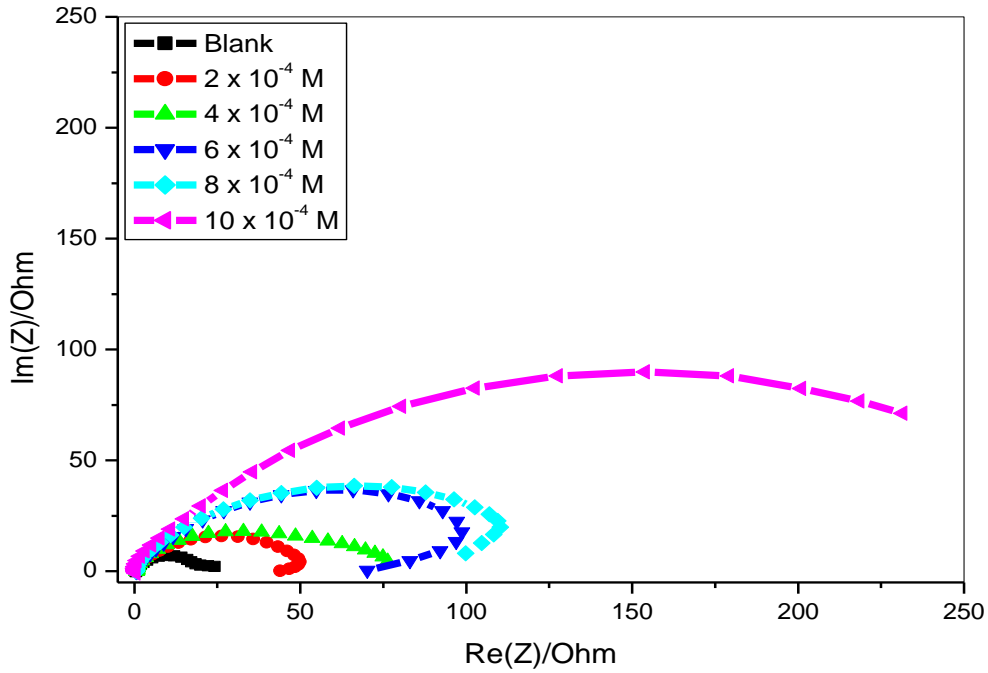


Figure 4.22: Nyquist plot of Aluminium metal in nitric acid in the presence of various concentrations of 3CYC

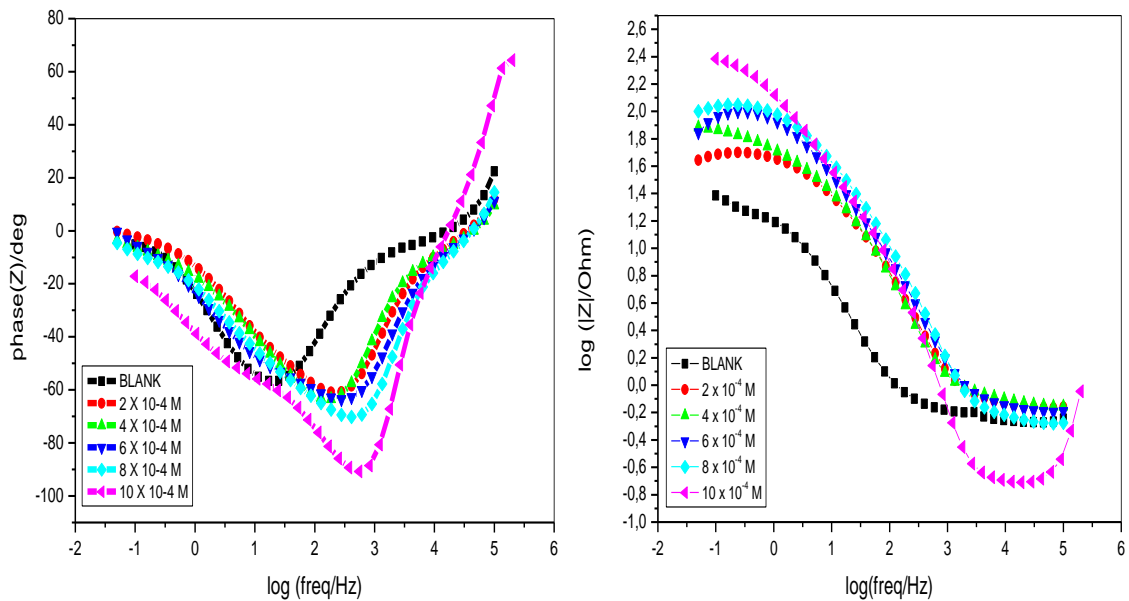


Figure 4.23: Bode diagrams of the impedance for Al in 1.5 M nitric acid without and with different concentration of 3CYC.

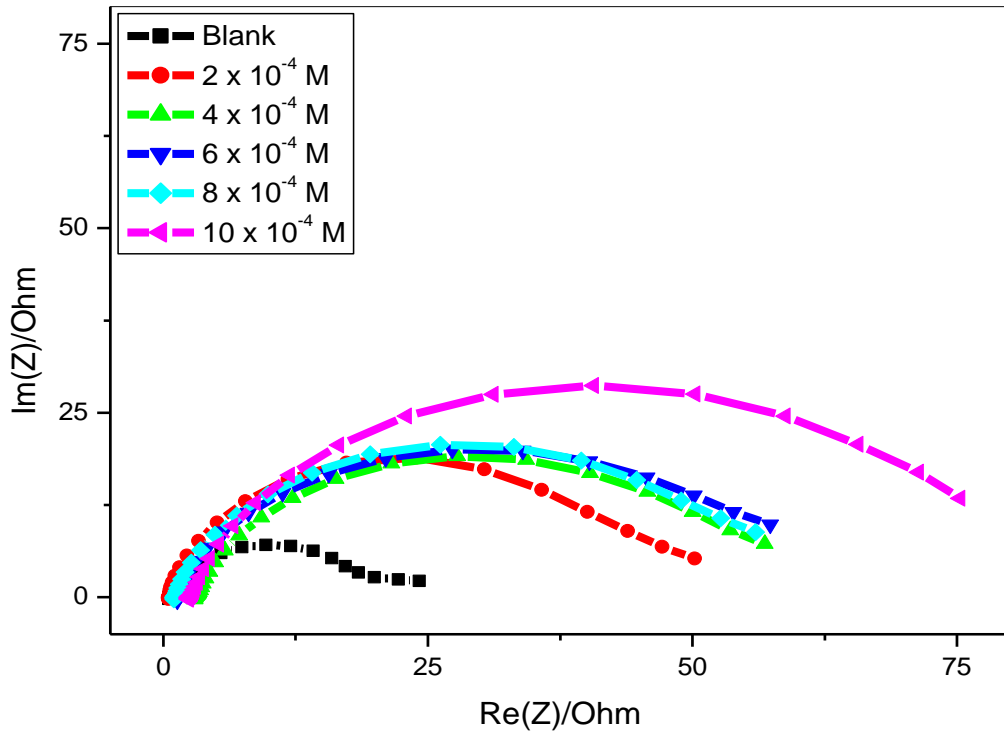


Figure 4.24: Nyquist plot of Aluminium metal in nitric acid in the presence of various concentrations of 6MC2C

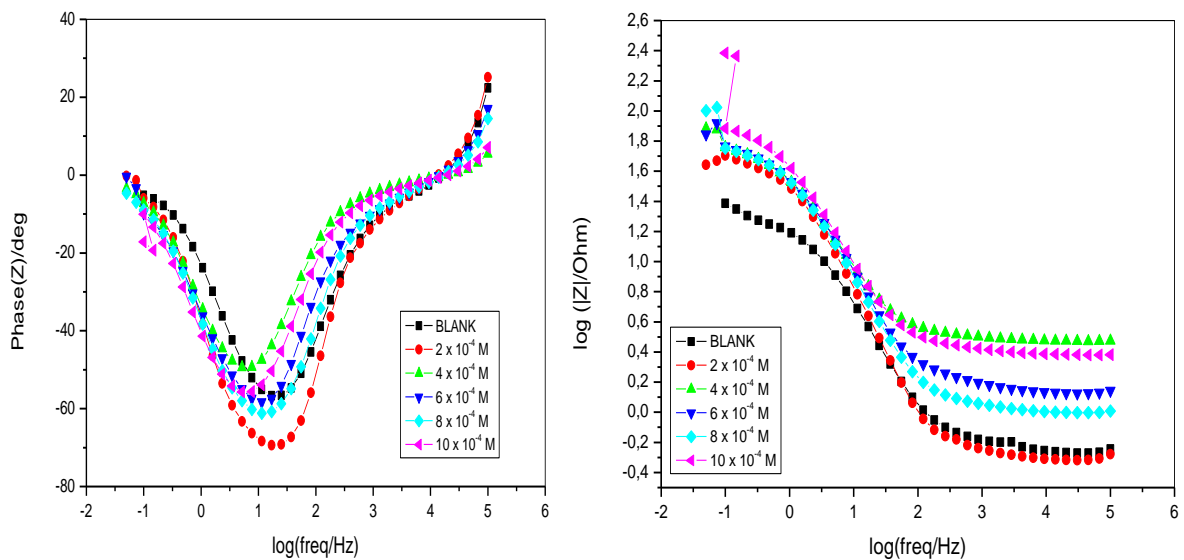


Figure 4.25: Bode diagrams of the impedance for Al in 1.5 M nitric acid without and with different concentration of 6MC2C.

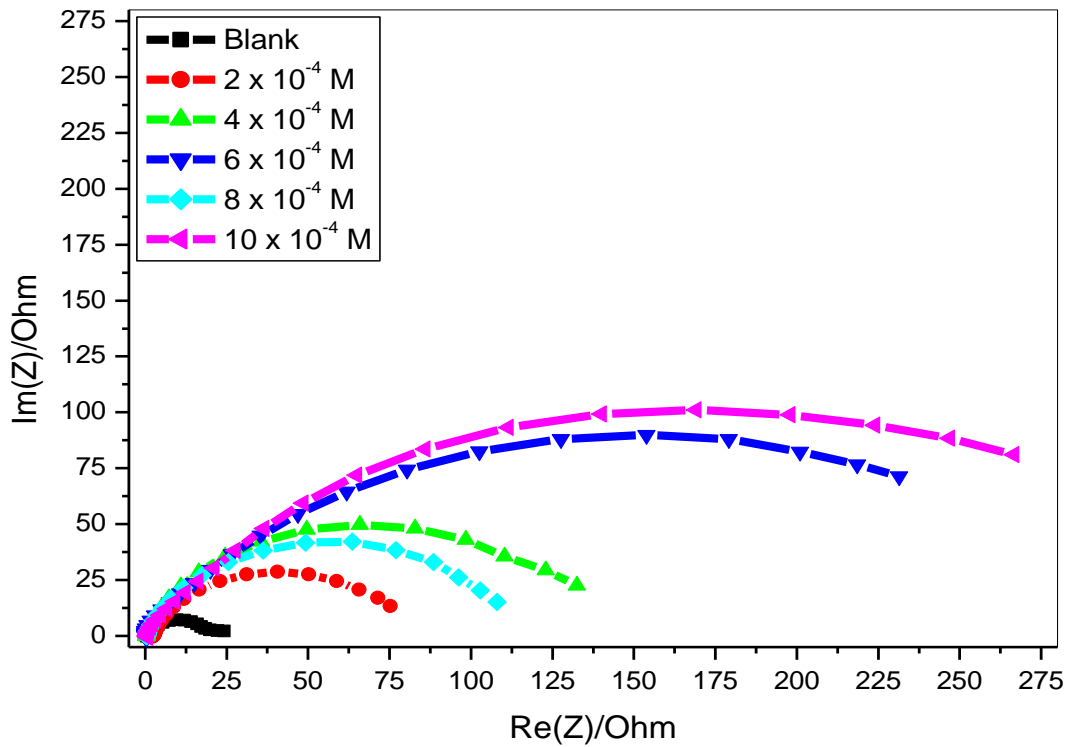


Figure 4.26: Nyquist plot of Aluminium metal in nitric acid in the presence of various concentrations of 6MCH

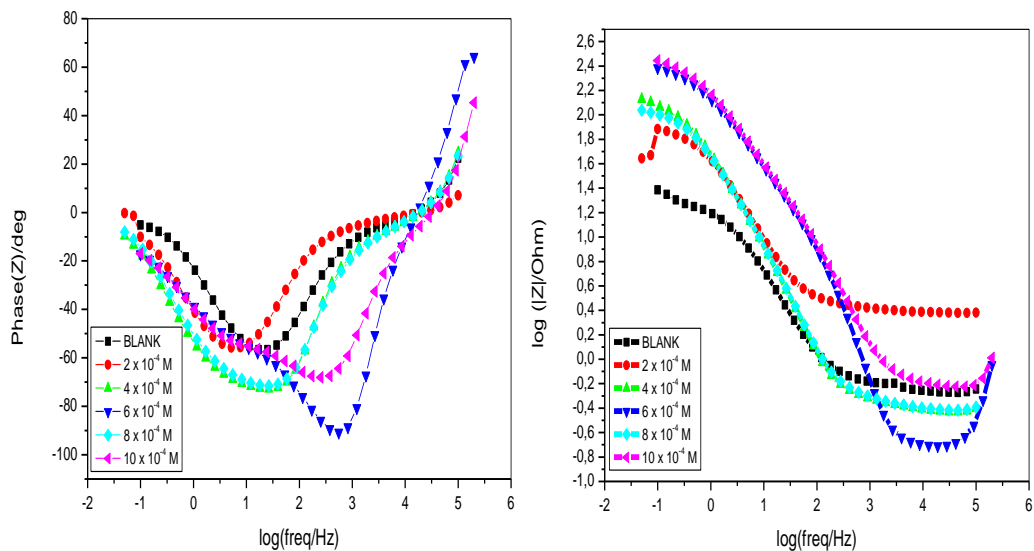


Figure 4.27: Bode diagrams of the impedance for Al in 1.5 M nitric acid without and with different concentration of 6MCH.



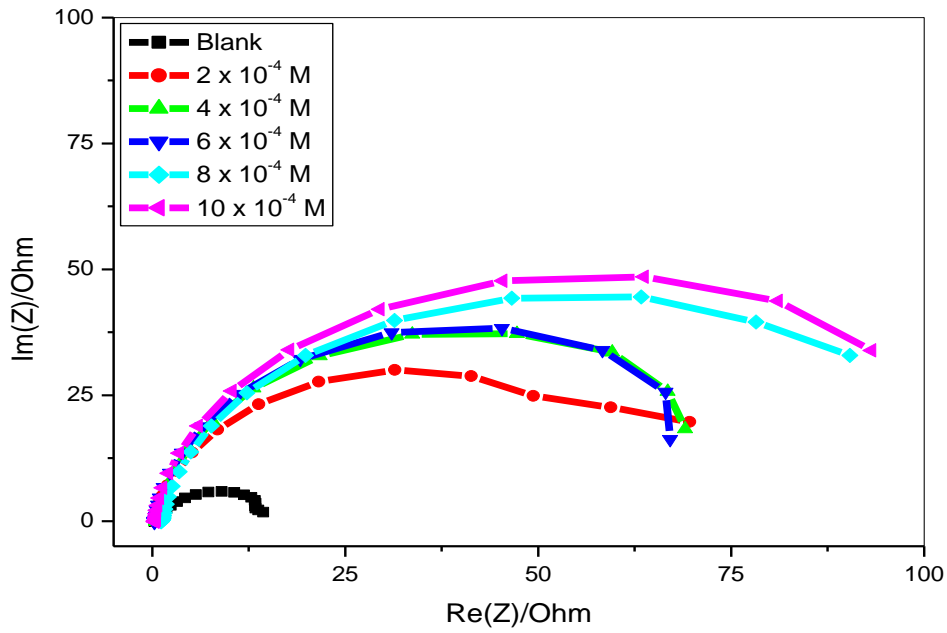


Figure 4.28: Nyquist plot of zinc metal in sulphuric acid in the presence of various concentrations of 3CYC

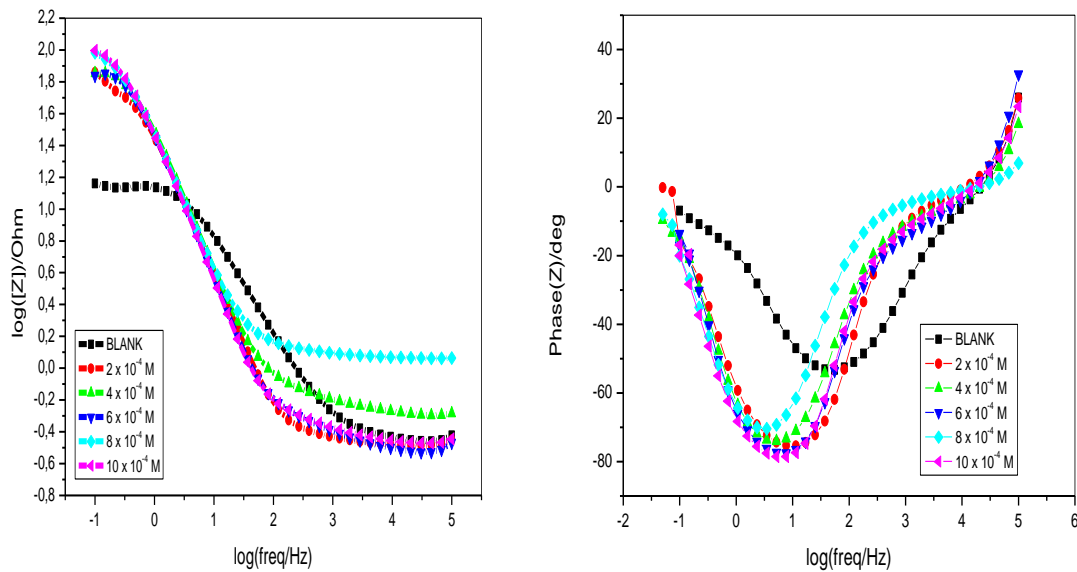


Figure 4.29: Bode diagrams of the impedance for Zn in 1.5 M sulphuric acid without and with different concentration of 3CYC.

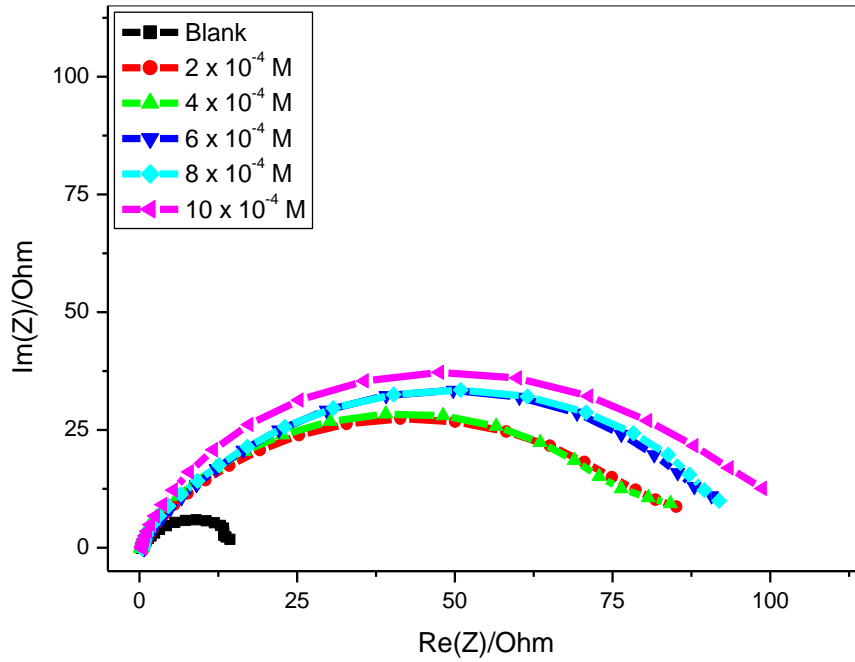


Figure 4.30: Nyquist plot of zinc metal in sulphuric acid in the presence of various concentrations of 6MC2C

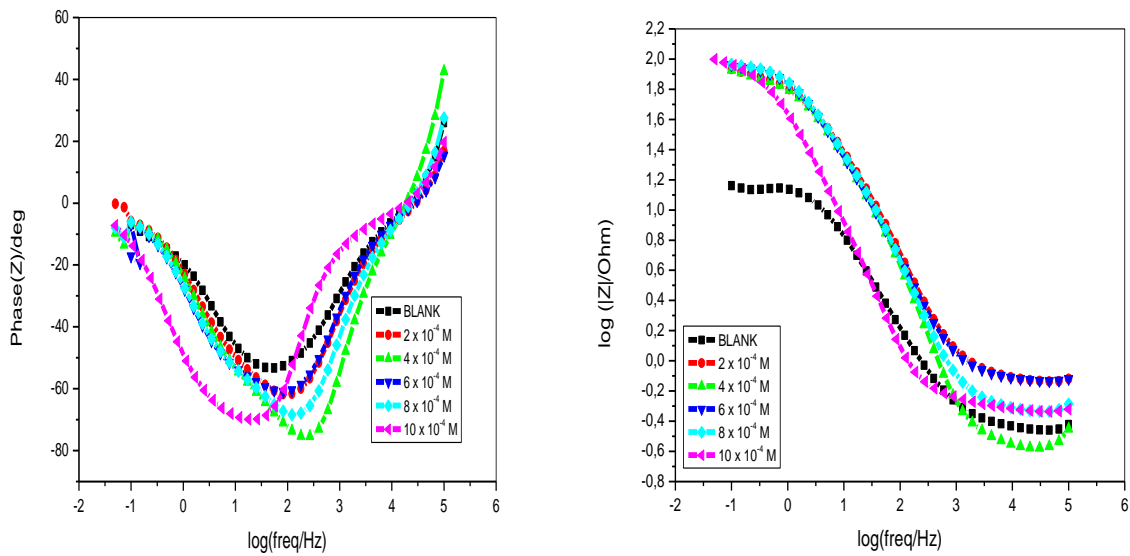


Figure 4.31: Bode diagrams of the impedance for Zn in 1.5 M sulphuric acid without and with different concentration of 6MC2C.

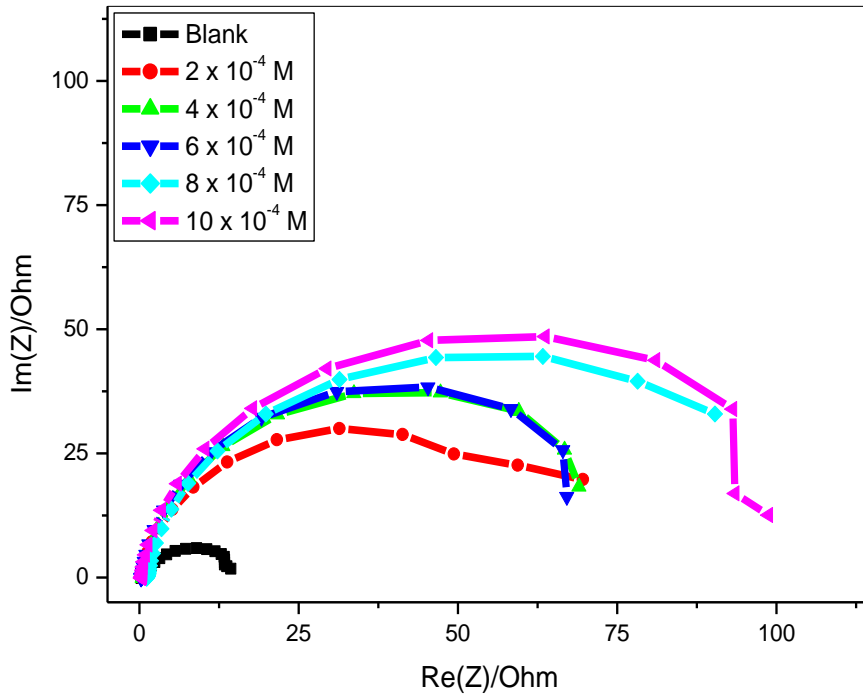


Figure 4.32: Nyquist plot of zinc metal in sulphuric acid in the presence of various concentrations of 6MCH

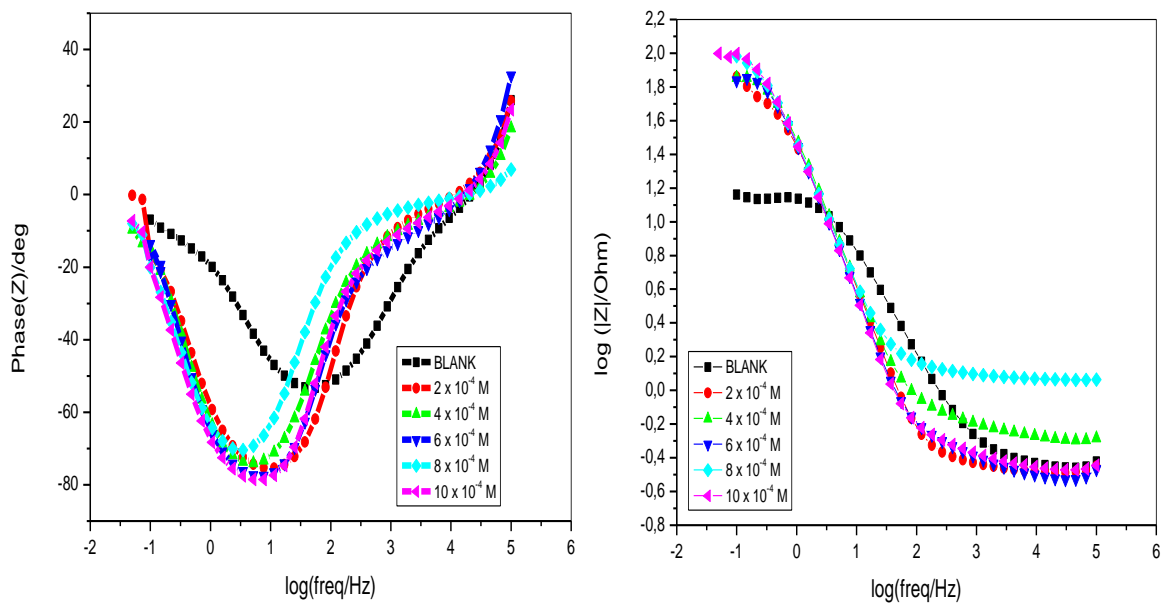


Figure 4.33: Bode diagrams of the impedance for Zn in 1.5 M sulphuric acid without and with different concentration of 6MCH.

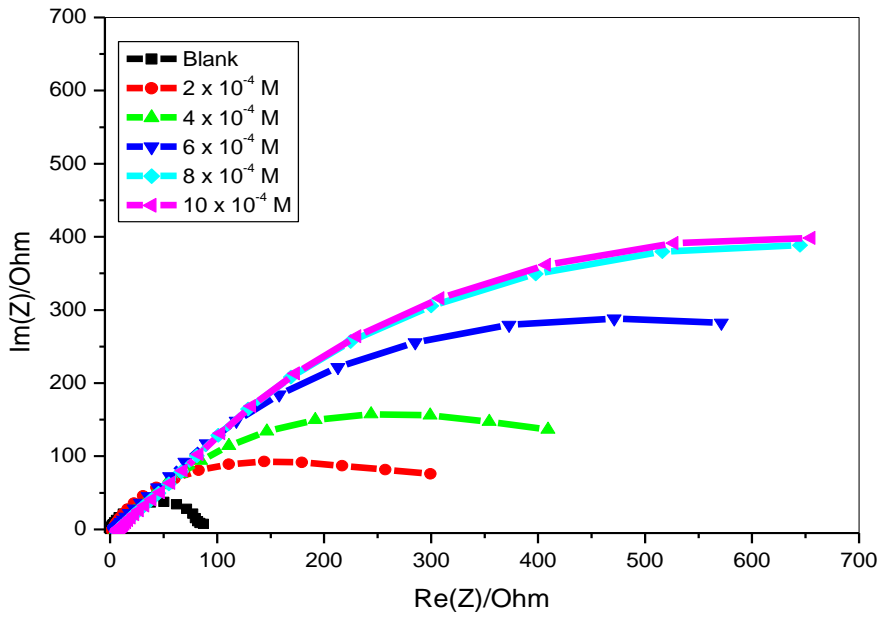


Figure 4.34: Nyquist plot of mild steel metal in acetic acid in the presence of various concentrations of 6MCH

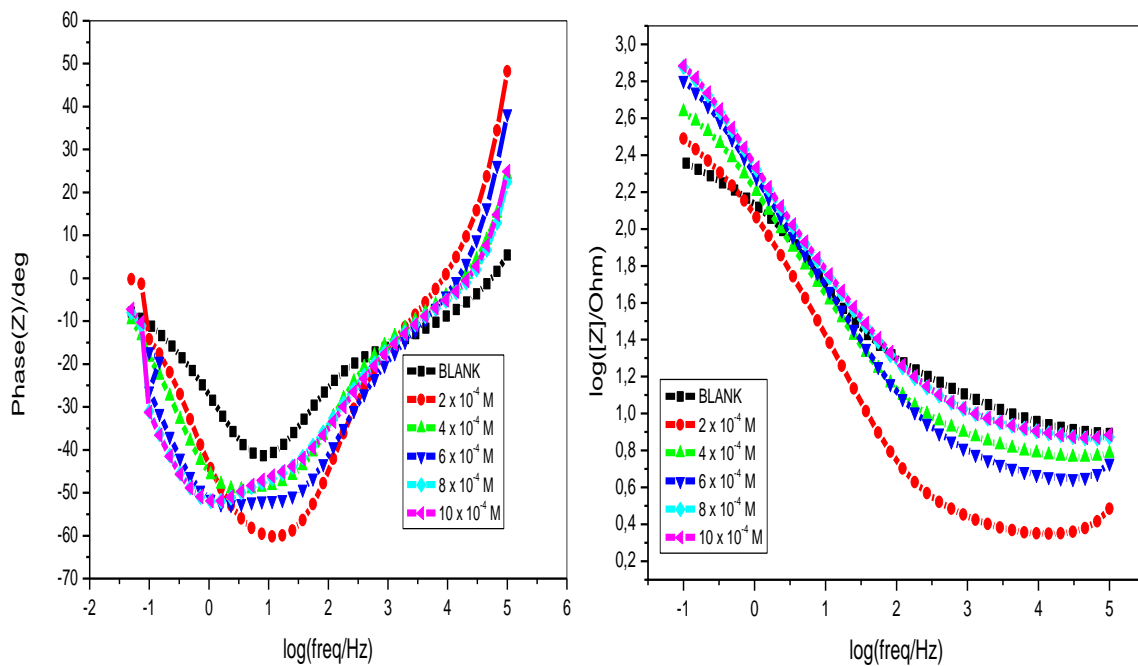


Figure 4.35: Bode diagrams of the impedance for MS in 1.5 M sulphuric acid without and with different concentration of 6MCH.

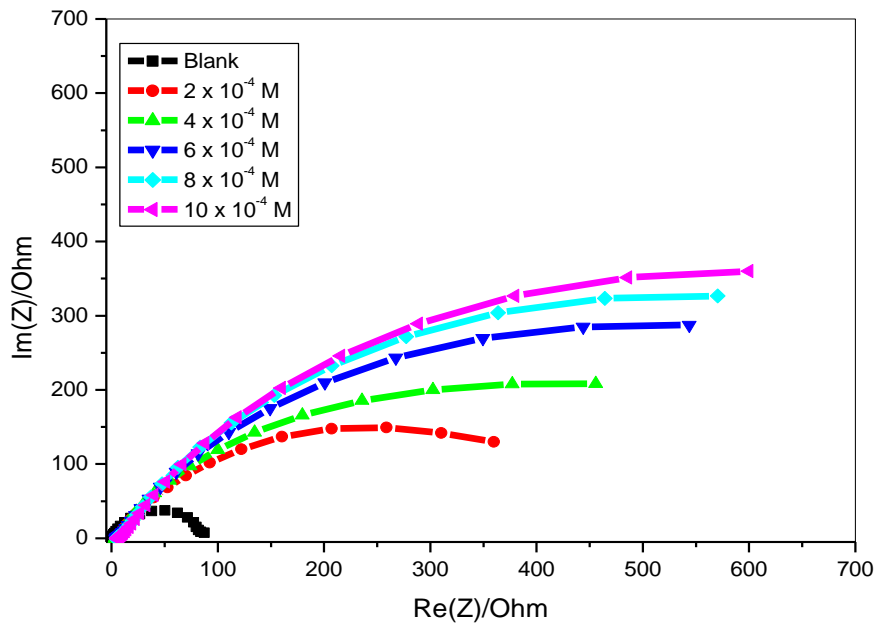


Figure 4.36: Nyquist plot of mild steel metal in acetic acid in the presence of various concentrations of 6MC2C

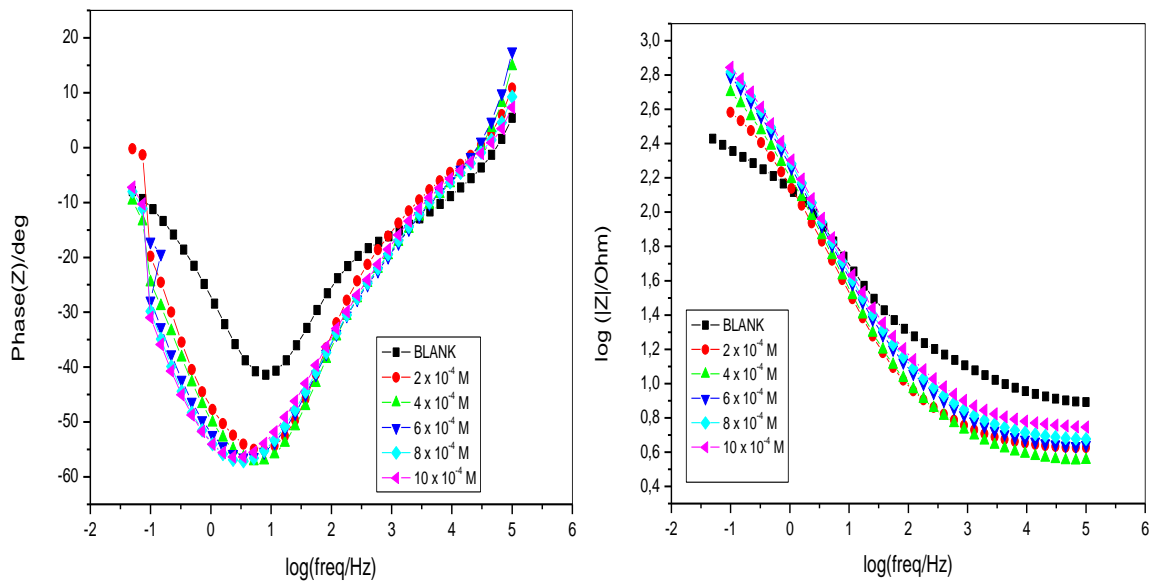


Figure 4.37: Bode diagrams of the impedance for MS in 1.5 M sulphuric acid without and with different concentration of 6MC2C.

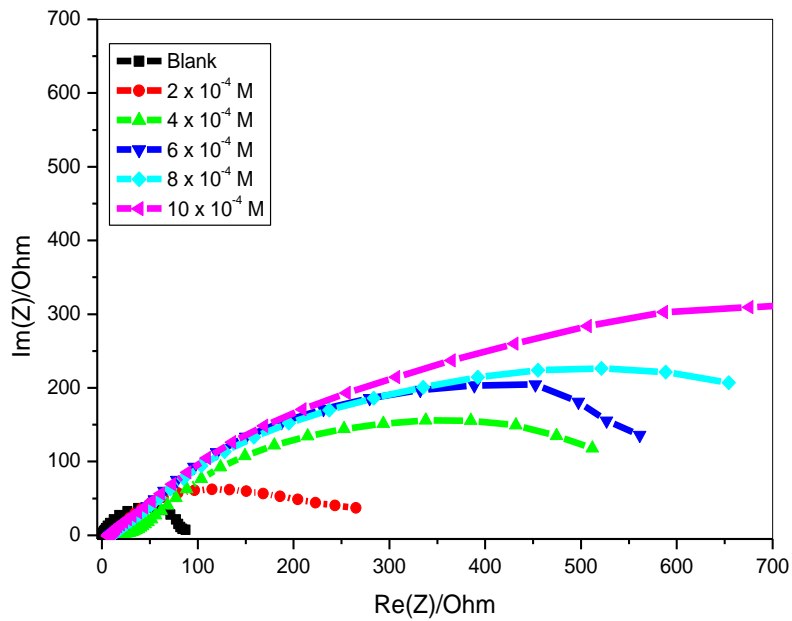


Figure 4.38: Nyquist plot of mild steel metal in acetic acid in the presence of various concentrations of 3CYC

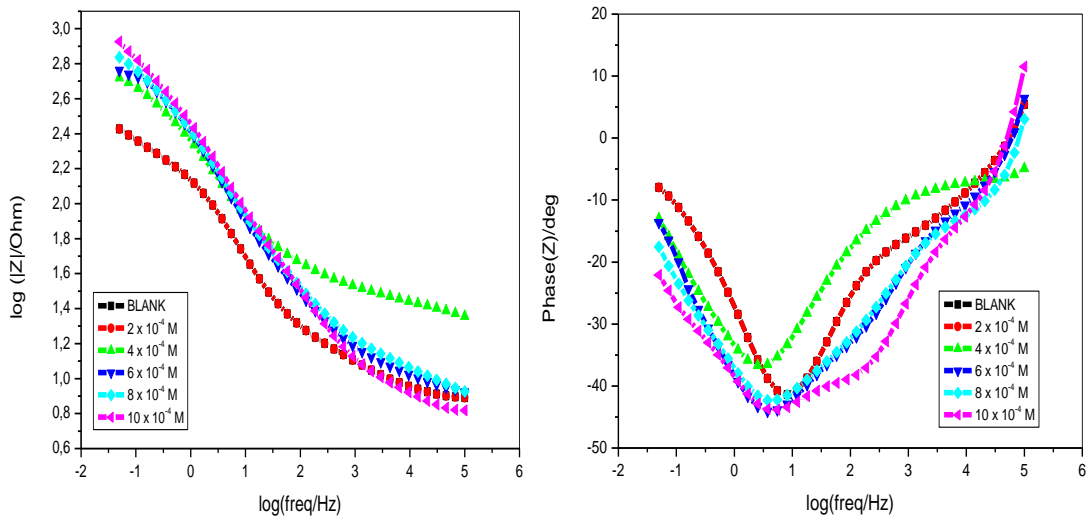


Figure 4.39: Bode diagrams of the impedance for MS in 1.5 M acetic acid without and with different concentration of 3CYC.

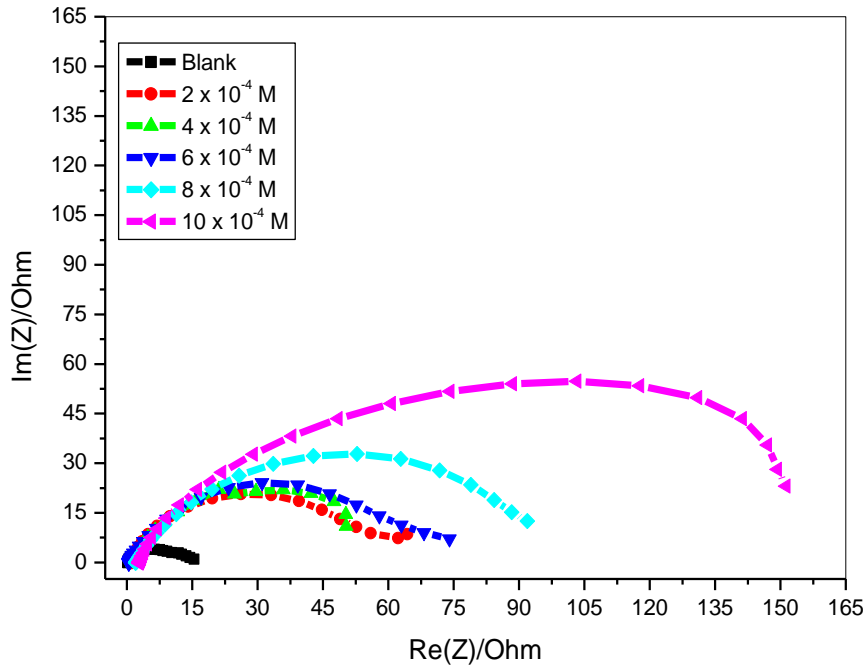


Figure 4.40: Nyquist plot of zinc metal in acetic acid in the presence of various concentrations of 3CYC

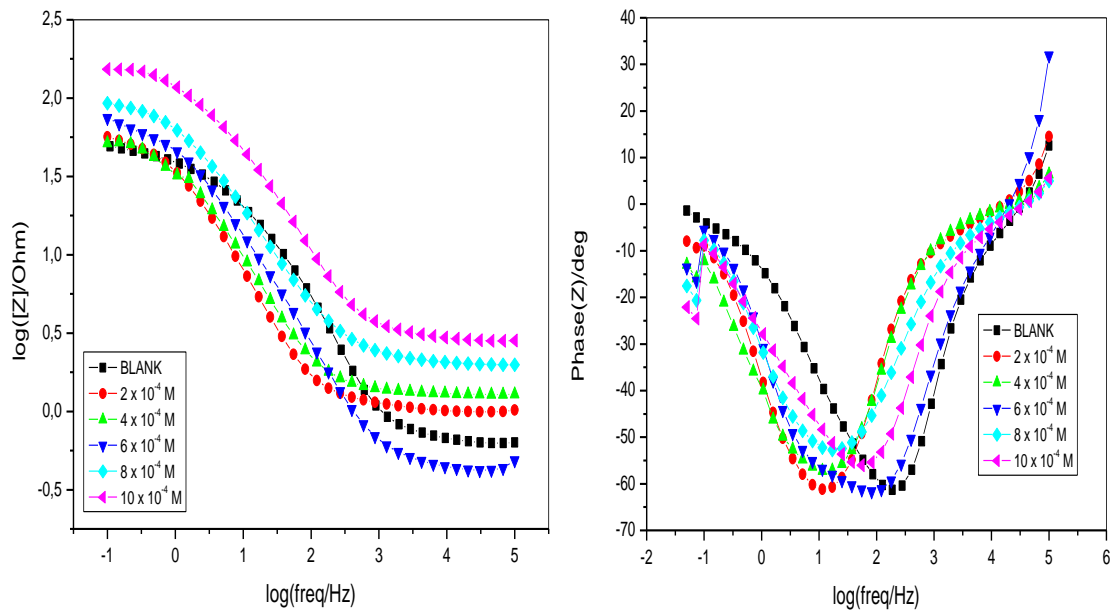


Figure 4.41: Bode diagrams of the impedance for Zn in 1.5 M acetic acid without and with different concentration of 3CYC.

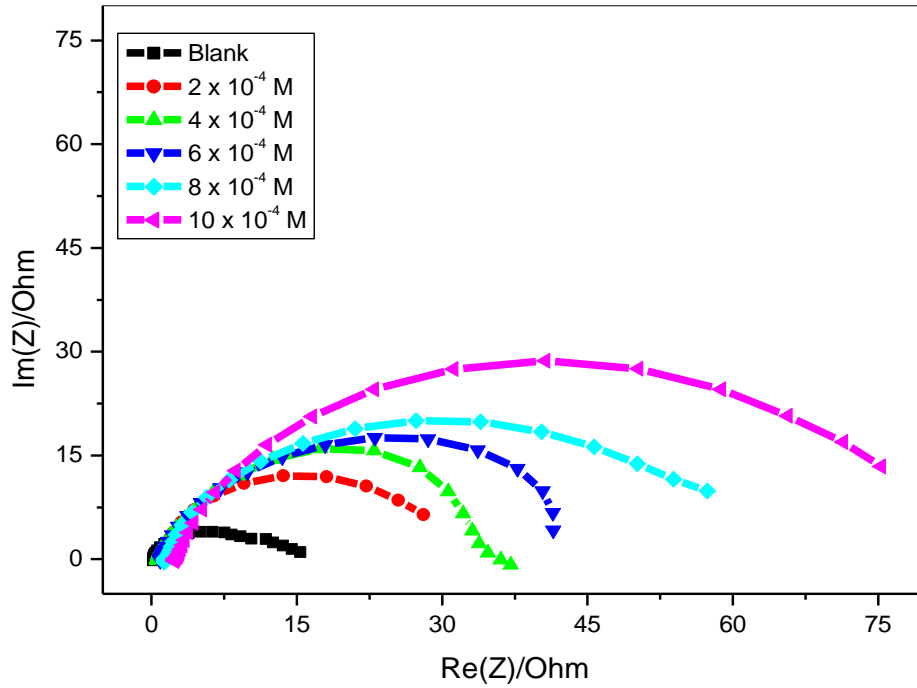


Figure 4.42: Nyquist plot of zinc metal in acetic acid in the presence of various concentrations of 6MCH

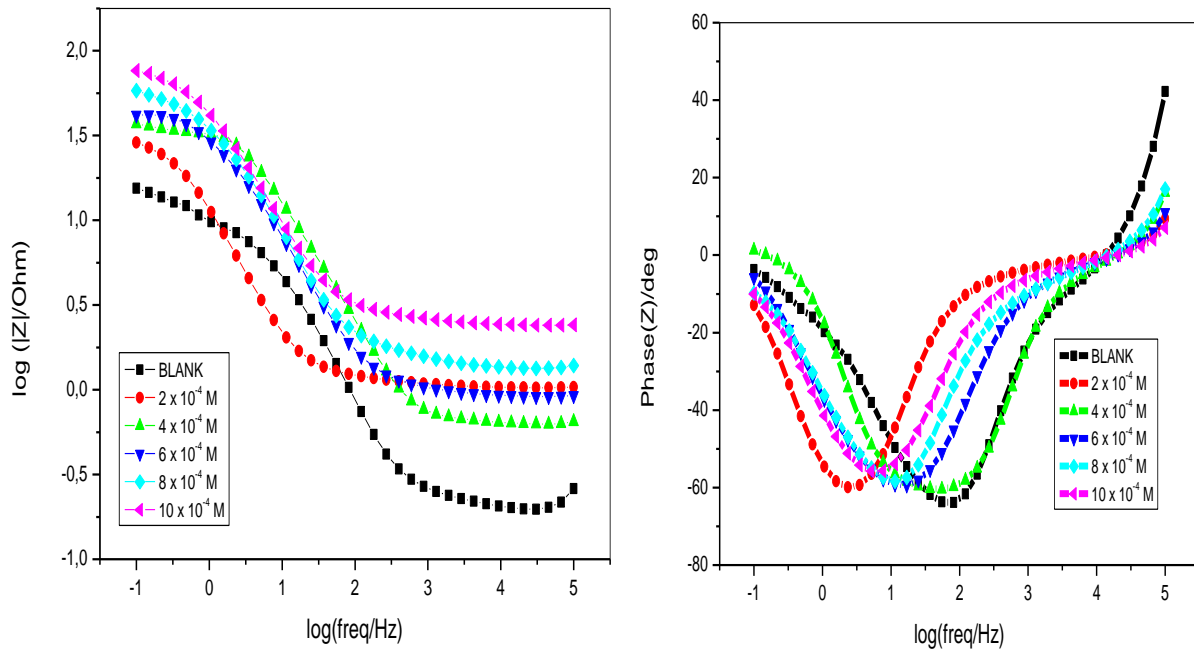


Figure 4.43: Bode diagrams of the impedance for Zn in 1.5 M acetic acid without and with different concentration of 6MCH.



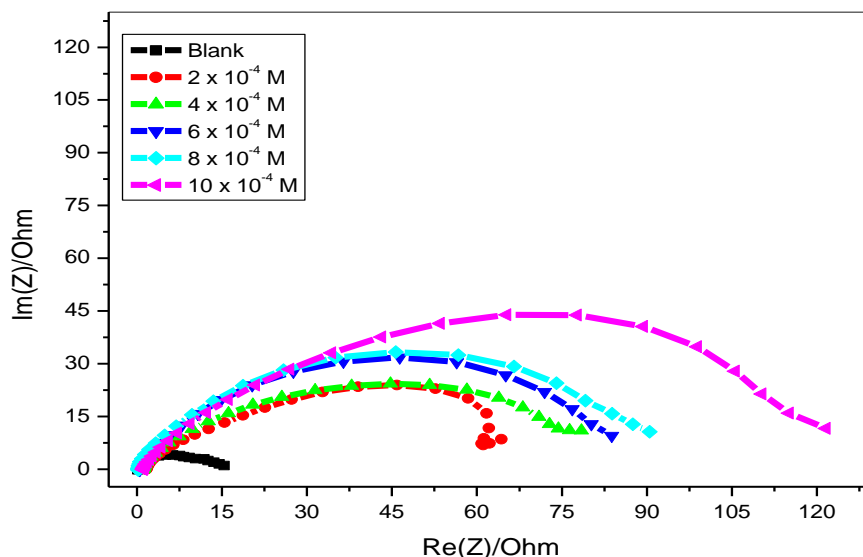


Figure 4.44: Nyquist plot of zinc metal in acetic acid in the presence of various concentrations of 6MC2C

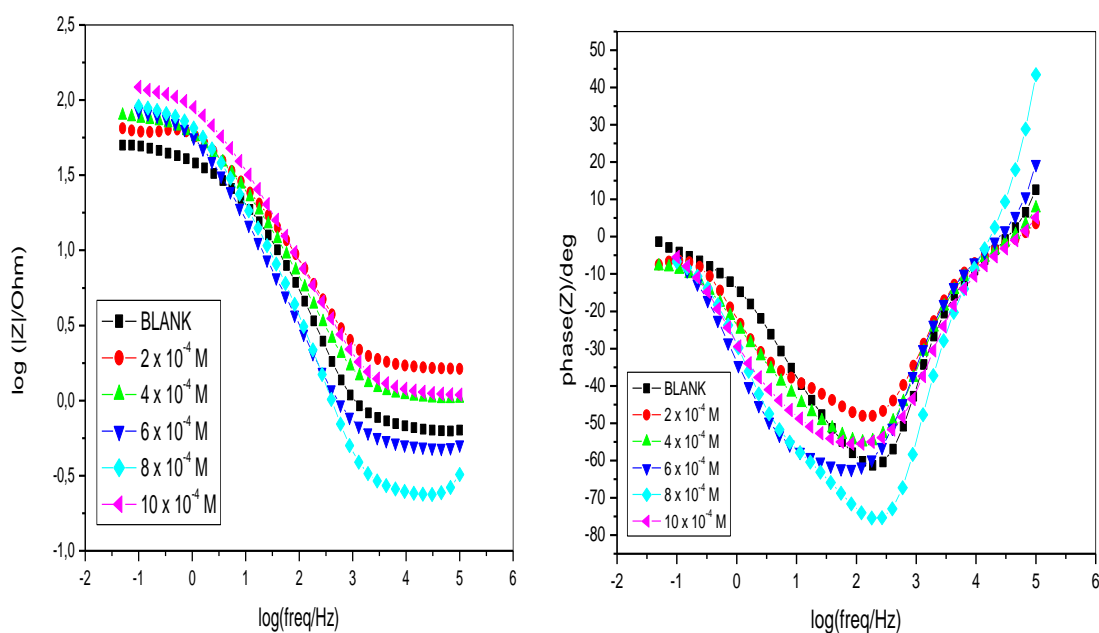


Figure 4.45: Bode diagrams of the impedance for Zn in 1.5 M acetic acid without and with different concentration of 6MC2C.

The EIS adopted in the present study best fit the circuit in Figure 4.46. The circuit is composed of elements represented by symbols such as R for the resistor of the circuit, L4 for the inductor, C for the capacitor. The electrode equivalent circuit (EEC) were useful when interpreting EIS measurements. The experimental best fit impedance data of 3CYC, 6MC2C, and 6MCH in

acetic, sulphuric and nitric acid comprised of elements R1 up to R5, Q1, C2 and C5 as shown in Figure 4.46

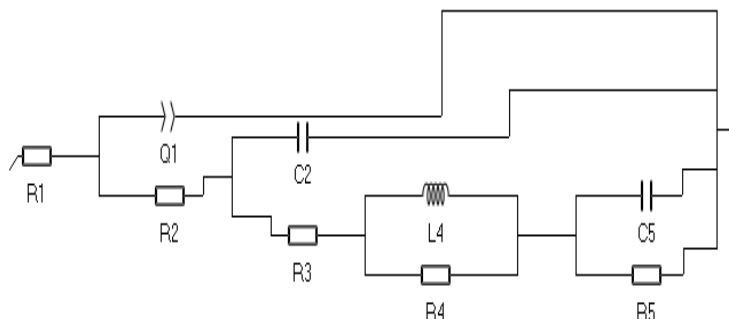


Figure 4.46: Equivalent circuit used to fit the impedance spectra

Elements, R1 and R2 represent solution resistance ( $R_s$ ) and charge transfer resistance ( $R_{ct}$ ) whereby the charge transfer resistance is useful when calculating inhibition efficiency. The EIS parameters inferred from these information are displayed in Tables 4.6–4.10.

Table 4.6: Electrochemical impedance (EIS) parameters for MS corrosion in 1.5 M  $H_2SO_4$

Inhibitor	Conc (M)	$R_1$ /Ohm	N	$R_{ct}$ /Ohm	$\theta$	$IE_{EIS}\%$	$IE_{WL}\%$
BLANK	0	0.2071	0.567	0.00193	0	0	0
6MC2C	$2 \times 10^{-4}$	0.4334	0.8161	0.0055	0.6490	64.90	83.13
	$4 \times 10^{-4}$	0.4303	0.0128	0.0128	0.8487	84.87	84.22
	$6 \times 10^{-4}$	0.4181	0.5194	0.0147	0.8687	86.87	97.53
	$8 \times 10^{-4}$	0.4337	0.8601	0.0334	0.9423	94.23	99.10
	$10 \times 10^{-4}$	0.4470	0.8274	0.3811	0.9949	99.49	99.22
3CYC	$2 \times 10^{-4}$	0.5304	0.7736	0.0040	0.5175	51.75	85.84
	$4 \times 10^{-4}$	0.2252	0.4410	0.0054	0.6426	64.26	93.51
	$6 \times 10^{-4}$	0.4795	0.7077	0.0063	0.6937	69.37	94.71
	$8 \times 10^{-4}$	0.4013	0.8808	0.0114	0.8307	83.07	96.17
	$10 \times 10^{-4}$	0.3701	0.8079	0.2533	0.9924	99.24	97.96
6MCH	$2 \times 10^{-4}$	0.4616	0.9001	0.0060	0.6783	67.83	68.49
	$4 \times 10^{-4}$	0.1765	0.6345	0.0061	0.6836	68.36	69.25
	$6 \times 10^{-4}$	0.2580	0.5182	0.0070	0.7243	72.43	70.57
	$8 \times 10^{-4}$	0.1084	0.0871	0.0092	0.7902	79.02	72.88
	$10 \times 10^{-4}$	0.2494	0.3160	0.0115	0.8322	83.22	84.12

Table 4.7: Electrochemical impedance (EIS) parameters for Al corrosion in 1.5 M nitric acid

Inhibitor	Conc (M)	R <sub>i</sub> /Ohm	N	R <sub>ct</sub> /Ohm	θ	IE <sub>EIS</sub> %	IE <sub>WL</sub> %
BLANK	0	0.5423	0.7593	0.5824	0	0	0
6MC2C	2 x 10 <sup>-4</sup>	1.0210	0.8288	1.6530	0.6477	64.77	86.73
	4 x 10 <sup>-4</sup>	2.974	0.7551	1.6750	0.6523	65.23	89.80
	6 x 10 <sup>-4</sup>	1.3430	0.7424	1.8720	0.6889	68.89	92.86
	8 x 10 <sup>-4</sup>	0.4996	0.8778	3.5830	0.8375	83.75	97.96
	10 x 10 <sup>-4</sup>	2.4800	0.8122	3.6380	0.8399	83.99	98.98
3CYC	2 x 10 <sup>-4</sup>	0.6879	0.8670	1.0150	0.4262	42.62	54.08
	4 x 10 <sup>-4</sup>	0.7153	0.8423	1.7780	0.6724	67.24	65.31
	6 x 10 <sup>-4</sup>	0.6423	0.8672	2.0340	0.7134	71.34	75.51
	8 x 10 <sup>-4</sup>	0.1886	1.0000	2.1120	0.7242	72.42	79.59
	10 x 10 <sup>-4</sup>	0.5320	0.9078	2.8630	0.7966	79.66	90.82
6MCH	2 x 10 <sup>-4</sup>	2.416	0.7614	1.8580	0.6865	68.65	79.59
	4 x 10 <sup>-4</sup>	0.4003	0.8706	2.1500	0.7291	72.91	81.63
	6 x 10 <sup>-4</sup>	0.5530	0.7644	3.2800	0.8224	82.24	83.67
	8 x 10 <sup>-4</sup>	0.3778	0.8701	5.357	0.8913	89.13	84.69
	10 x 10 <sup>-4</sup>	0.1883	0.9974	9.9390	0.9414	94.14	94.90

Table 4.8: Electrochemical impedance (EIS) parameters for Zn corrosion in 1.5 M H<sub>2</sub>SO<sub>4</sub>

Inhibitor	Conc (M)	R <sub>i</sub> /Ohm	N	R <sub>ct</sub> /Ohm	θ	IE <sub>EIS</sub> %	IE <sub>WL</sub> %
BLANK	0	0.3502	0.7067	0.0057	0	0	0
6MC2C	2 x 10 <sup>-4</sup>	0.7316	0.6103	0.0159	0.6415	64.15	34.48
	4 x 10 <sup>-4</sup>	0.6959	0.4187	0.0857	0.9335	93.35	34.54
	6 x 10 <sup>-4</sup>	0.2701	0.9574	0.1130	0.9496	94.96	39.15
	8 x 10 <sup>-4</sup>	0.4596	0.8025	0.3109	0.9817	98.17	40.74
	10 x 10 <sup>-4</sup>	0.4676	0.8104	0.4466	0.9872	98.72	69.82
3CYC	2 x 10 <sup>-4</sup>	0.3274	0.8885	0.0252	0.7738	77.38	72.52
	4 x 10 <sup>-4</sup>	0.5200	0.8383	0.0306	0.8137	81.37	72.97
	6 x 10 <sup>-4</sup>	0.3044	0.8790	0.0429	0.8671	86.71	74.36
	8 x 10 <sup>-4</sup>	1.0640	0.3018	0.1485	0.9616	96.16	75.87
	10 x 10 <sup>-4</sup>	0.0073	0.1496	0.3446	0.9835	98.35	76.46
6MCH	2 x 10 <sup>-4</sup>	0.3263	0.0516	0.0261	0.7816	78.16	64.28
	4 x 10 <sup>-4</sup>	0.0238	1.0000	0.2959	0.8074	80.74	66.45
	6 x 10 <sup>-4</sup>	0.4664	0.3550	0.0633	0.9099	90.99	67.07
	8 x 10 <sup>-4</sup>	1.1640	0.8019	0.0795	0.9283	92.83	67.17
	10 x 10 <sup>-4</sup>	0.0560	0.0000	0.0938	0.9393	93.93	69.21

Table 4.9: Electrochemical impedance (EIS) parameters for MS corrosion in 1.5 M acetic acid

Inhibitor	Conc (M)	R <sub>i</sub> /Ohm	N	R <sub>ct</sub> /Ohm	θ	IE <sub>EIS</sub> %	IE <sub>WL</sub> %
BLANK	0	0.3151	0.8502	0.0035	0	0	0
6MC2C	2 x 10 <sup>-4</sup>	5.0270	0.6666	0.0184	0.8098	80.98	75.00
	4 x 10 <sup>-4</sup>	4.5200	0.5878	0.0216	0.8380	83.80	77.50
	6 x 10 <sup>-4</sup>	3.6980	0.6514	0.0336	0.8959	89.59	80.00
	8 x 10 <sup>-4</sup>	5.6420	0.6518	0.0346	0.8988	89.88	82.50
	10 x 10 <sup>-4</sup>	4.2490	0.6664	0.0485	0.9278	92.78	85.83
3CYC	2 x 10 <sup>-4</sup>	7.6130	0.5281	0.0071	0.5070	50.70	73.40
	4 x 10 <sup>-4</sup>	8.5990	0.5497	0.0341	0.8973	89.73	77.40
	6 x 10 <sup>-4</sup>	8.6470	0.4801	0.1266	0.9724	97.24	79.20
	8 x 10 <sup>-4</sup>	22.82	0.4495	0.0514	0.9319	93.19	86.60
	10 x 10 <sup>-4</sup>	6.7160	0.5310	0.4341	0.9919	99.19	90.00
6MCH	2 x 10 <sup>-4</sup>	2.2640	0.7589	0.0324	0.8920	89.20	52.50
	4 x 10 <sup>-4</sup>	5.8940	0.6379	0.0511	0.9315	93.15	58.33
	6 x 10 <sup>-4</sup>	4.5270	0.6055	0.0681	0.9486	94.86	60.00
	8 x 10 <sup>-4</sup>	7.5490	0.5632	0.0914	0.9617	96.17	77.50
	10 x 10 <sup>-4</sup>	7.5740	0.6316	0.4749	0.9926	99.26	81.67

Table 4.10: Electrochemical impedance (EIS) parameters for Zn corrosion in 1.5 M acetic acid.

Inhibitor	Conc (M)	R <sub>i</sub> /Ohm	N	R <sub>ct</sub> /Ohm	θ	IE <sub>EIS</sub> %	IE <sub>WL</sub> %
BLANK	0	0.1958	0.8041	0.1889	0	0	0
6MC2C	2 x 10 <sup>-4</sup>	0.0580	0.2534	0.4796	0.6061	60.61	74.67
	4 x 10 <sup>-4</sup>	0.2397	0.9682	0.6657	0.7162	71.62	75.49
	6 x 10 <sup>-4</sup>	0.9229	0.6719	0.9844	0.8081	80.81	76.15
	8 x 10 <sup>-4</sup>	2.3e-156	0.2926	1.3450	0.8596	85.96	77.80
	10 x 10 <sup>-4</sup>	1.4880	0.6805	8.4470	0.9776	97.76	86.35
3CYC	2 x 10 <sup>-4</sup>	0.4495	0.1847	0.9857	0.8084	80.84	76.32
	4 x 10 <sup>-4</sup>	0.9972	0.7847	1.0420	0.8187	81.87	81.25
	6 x 10 <sup>-4</sup>	0.4222	0.8229	1.7700	0.8933	89.33	82.57
	8 x 10 <sup>-4</sup>	2.7890	0.7639	2.7940	0.9324	93.24	83.06
	10 x 10 <sup>-4</sup>	1.9870	0.7220	5.5040	0.9657	96.57	83.22
6MCH	2 x 10 <sup>-4</sup>	1.0380	0.7567	0.6107	0.6903	69.03	76.48
	4 x 10 <sup>-4</sup>	0.0015	0.0036	0.6473	0.7082	70.82	77.30
	6 x 10 <sup>-4</sup>	0.4483	0.1275	1.0140	0.8137	81.37	77.80
	8 x 10 <sup>-4</sup>	0.9257	0.7989	1.6990	0.8888	88.88	79.44
	10 x 10 <sup>-4</sup>	2.4140	0.7587	1.7900	0.8945	89.45	83.22

### 4.3 Optical Microscopy –2D and 3D

Two-dimensional (2D) microstructure of samples in this study are in Figures 4.47 –4.61. 3D optical microscopy results in a three-dimensional are shown in Figures 4.62– 4.76 and has awesome advantage since it rejects the light that does not come from the central plane, empowering one to perform optical cutting and development of three-dimensional (3D) pictures [93, 94]. It helps with the information regarding the metal through high quality image. 3DOP is presently finding more extensive applications within materials. This paper surveys the surface morphology of mild steel, zinc, and aluminium exposed in acidic medium.

The results obtained from this technique show the effectiveness of the three tested inhibitors. The surface morphology on each metal was captured before corrosion and also after corrosion in the presence of 3CYC, 6MCH, and 6MC2C. The surface area of metal exposed in acidic medium was rough when compared to the surface area of metal exposed in acid in the presence of corrosion inhibitor. This could be due to adsorption of inhibitor onto the metal forming thin protective layer. Surface area of metal exposed in acidic medium in the presence of inhibitor looks less rough when compared to that of blank. This happen because the corrosion process or rate of corrosion is lowered. The microstructures shown in Figures 4.47–4.76 demonstrate that the presence of inhibitor reduce the aggressiveness of acidic medium. This is clearly shown by the surface of metal exposed in nitric, sulphuric, and acetic acid. The damage done on metal immersed in acidic medium in the absence of inhibitors was severe when compared to damage done in the presence of inhibitors.

The surface morphology of Zn, Al, and MS exposed in acetic, sulphuric and nitric acid in the absence and presence of 3CYC, 6MCH, and 6MC2C are as follow

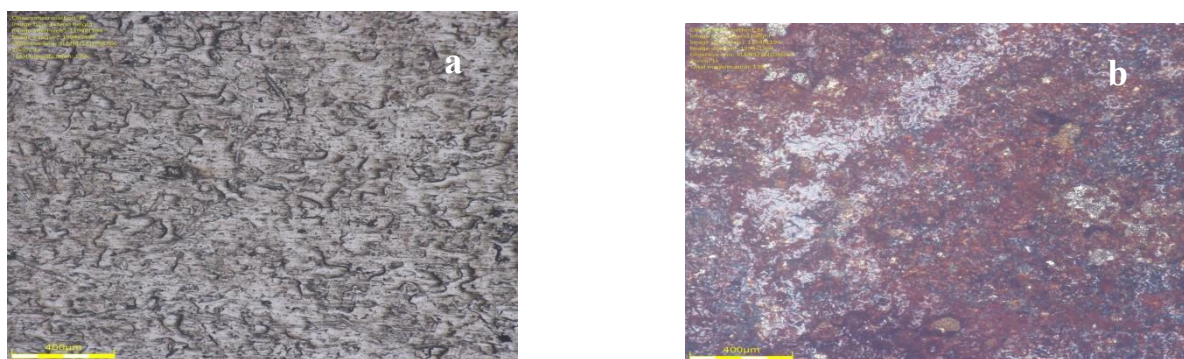


Figure 4.47: 2D optical microscopy of the surface of mild steel: (a) plain mild steel and (b) mild steel immersed in  $\text{CH}_3\text{COOH}$  uninhibited.



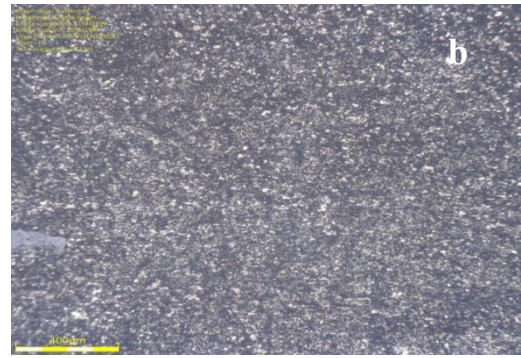
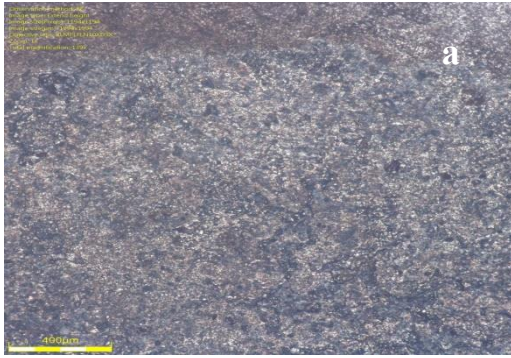


Figure 4.48: 2D optical microscopy of the surface of MS immersed in  $\text{CH}_3\text{COOH}$  in the presence of (a) 3CYC (b) 6MCH



Figure 4.49: 2D optical microscopy of the surface of MS immersed in  $\text{CH}_3\text{COOH}$  in the presence of 6MC2C

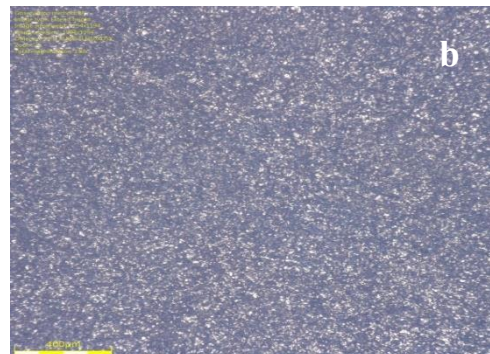


Figure 4.50: 2D optical microscopy of the surface of mild steel: (a) plain mild steel and (b) mild steel immersed in  $\text{H}_2\text{SO}_4$  uninhibited.

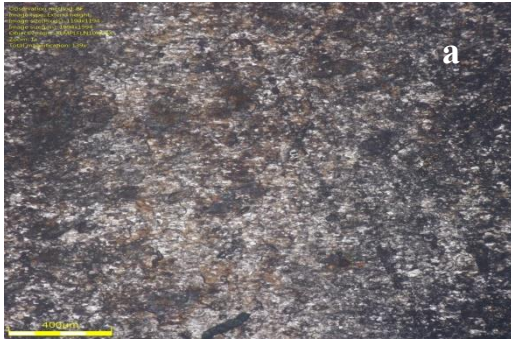


Figure 4.51: 2D optical microscopy of the surface of MS immersed in  $H_2SO_4$  in the presence of (a) 3CYC (b) 6MCH

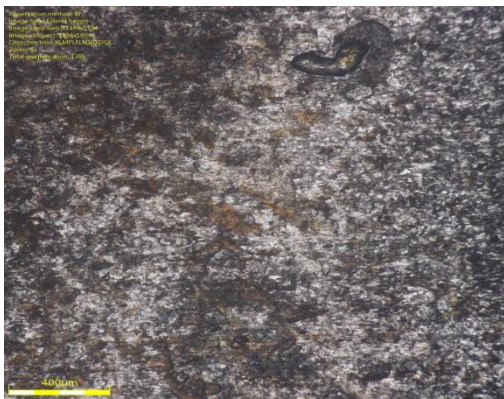


Figure 4.52: 2D optical microscopy of the surface of MS immersed in  $H_2SO_4$  in the presence of 6MC2C

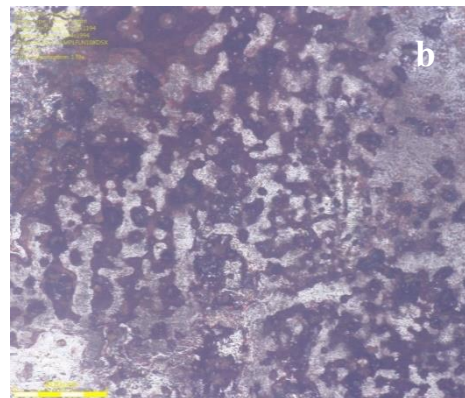
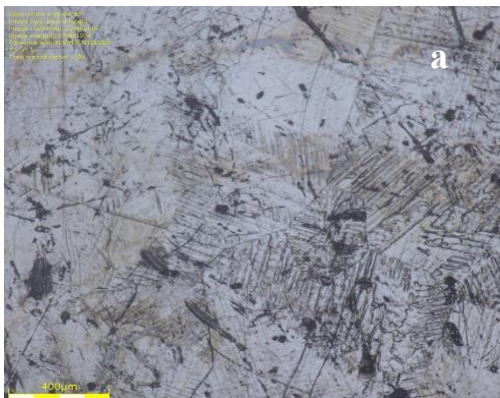


Figure 4.53: 2D optical microscopy of the surface of zinc: (a) plain zinc and (b) zinc immersed in  $CH_3COOH$  uninhibited.



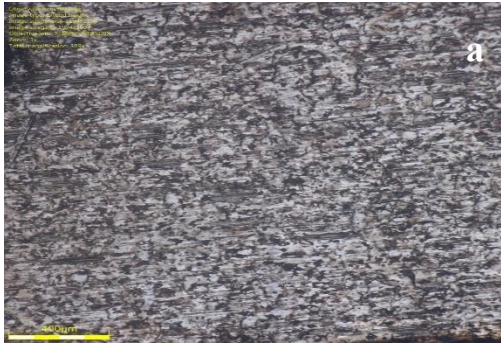


Figure 4.54: 2D optical microscopy of the surface of zinc immersed in  $\text{CH}_3\text{COOH}$  in the presence of (a) 3CYC (b) 6MCH

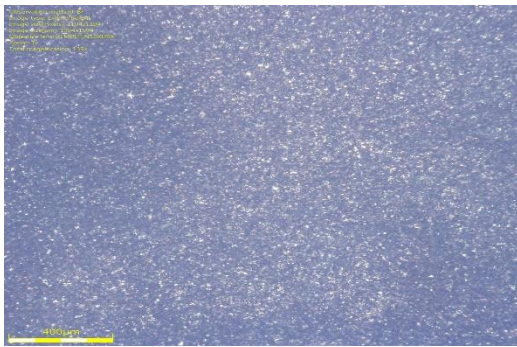


Figure 4.55: 2D optical microscopy of the surface of zinc immersed in  $\text{CH}_3\text{COOH}$  in the presence of 6MC2C

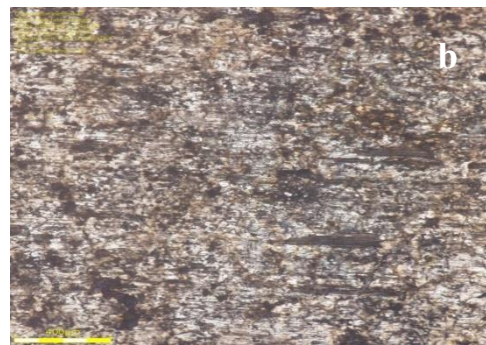
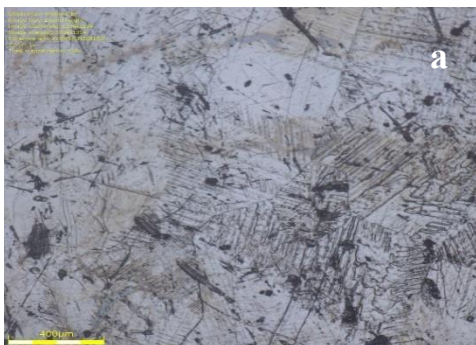


Figure 4.56: 2D optical microscopy of the surface of zinc: (a) plain zinc and (b) zinc immersed in  $\text{H}_2\text{SO}_4$  uninhibited.



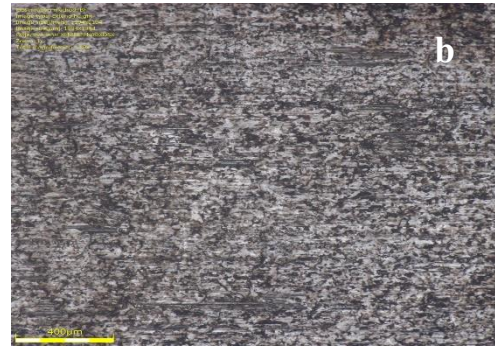
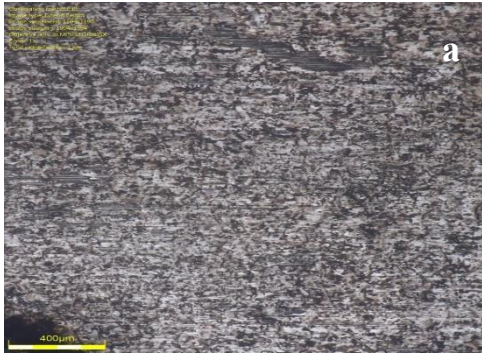


Figure 4.57: 2D optical microscopy of the surface of zinc immersed in  $H_2SO_4$  in the presence of (a) 3CYC (b) 6MCH



Figure 4.58: 2D optical microscopy of the surface of zinc immersed in  $H_2SO_4$  in the presence of 6MC2C

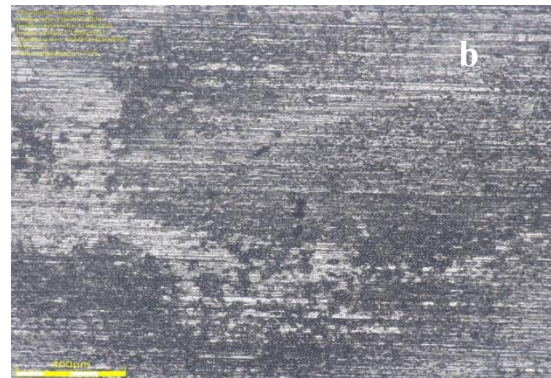


Figure 4.59: 2D optical microscopy of the surface of aluminium: (a) plain aluminium and (b) aluminium immersed in  $HNO_3$  uninhibited.

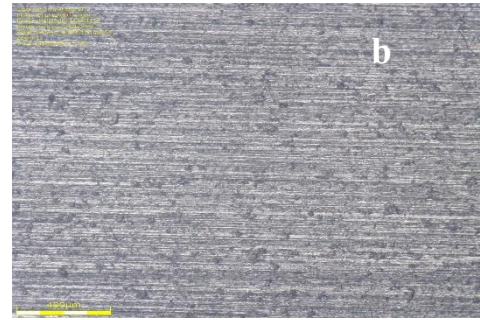
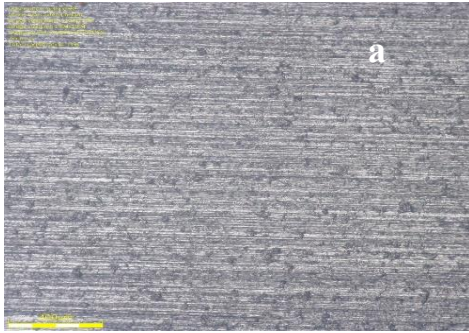


Figure 4.60: 2D optical microscopy of the surface of aluminium immersed in  $\text{HNO}_3$  in the presence of (a) 3CYC (b) 6MCH

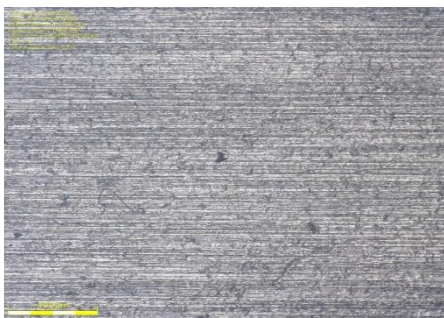


Figure 4.61: 2D optical microscopy of the surface of aluminium immersed in  $\text{HNO}_3$  in the presence of 6MC2C

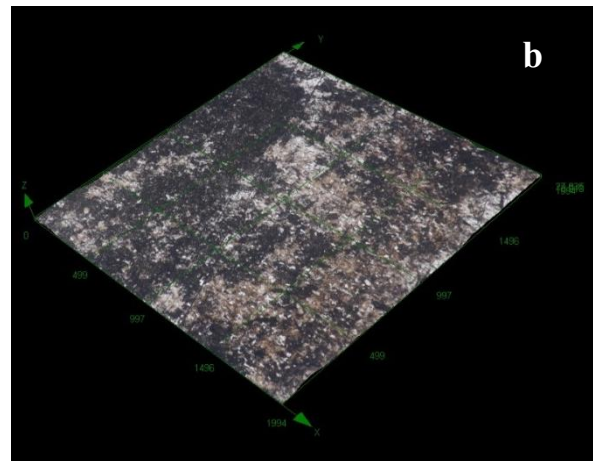
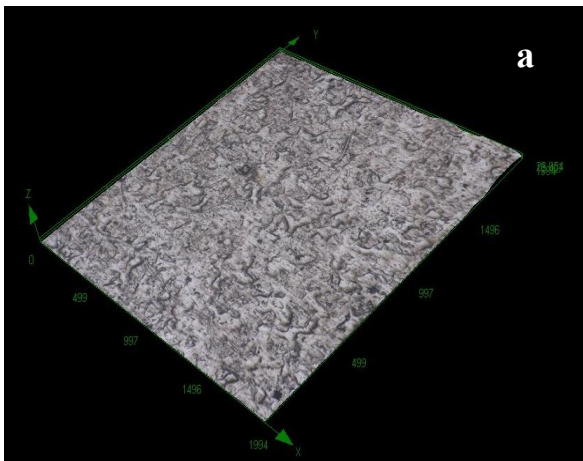


Figure 4.62: 3D optical microscopy of the surface of mild steel: (a) plain mild steel and (b) mild steel immersed in  $\text{CH}_3\text{COOH}$  uninhibited.



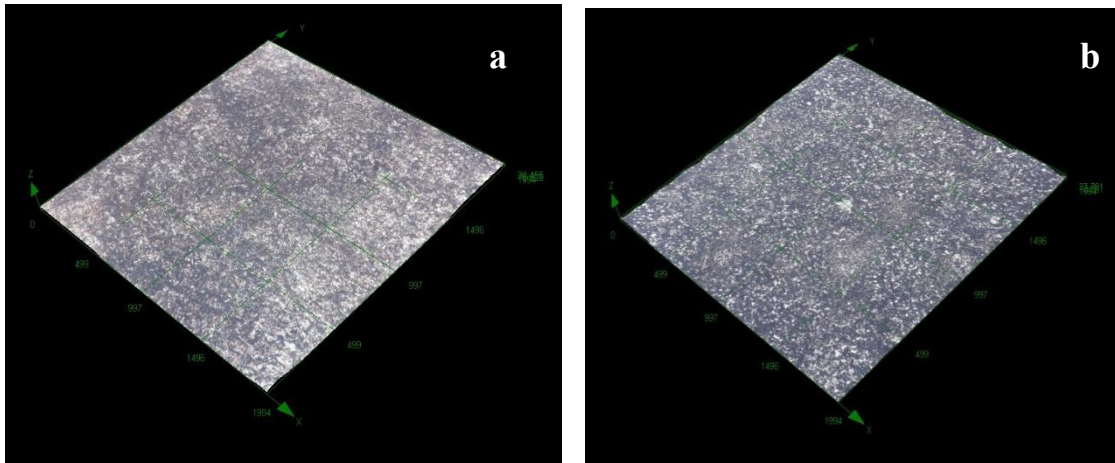


Figure 4.63: 3D optical microscopy of the surface of MS immersed in  $\text{CH}_3\text{COOH}$  in the presence of (a) 3CYC (b) 6MCH

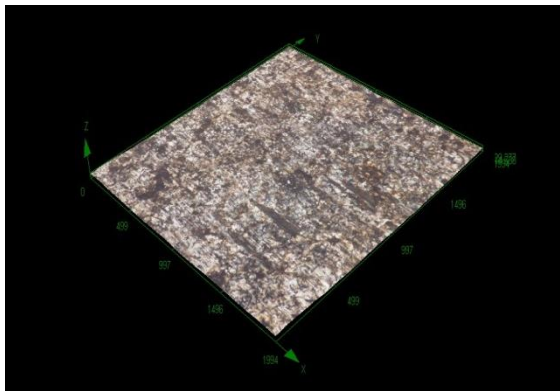


Figure 4.64: 3D optical microscopy of the surface of MS immersed in  $\text{CH}_3\text{COOH}$  in the presence of 6MC2C

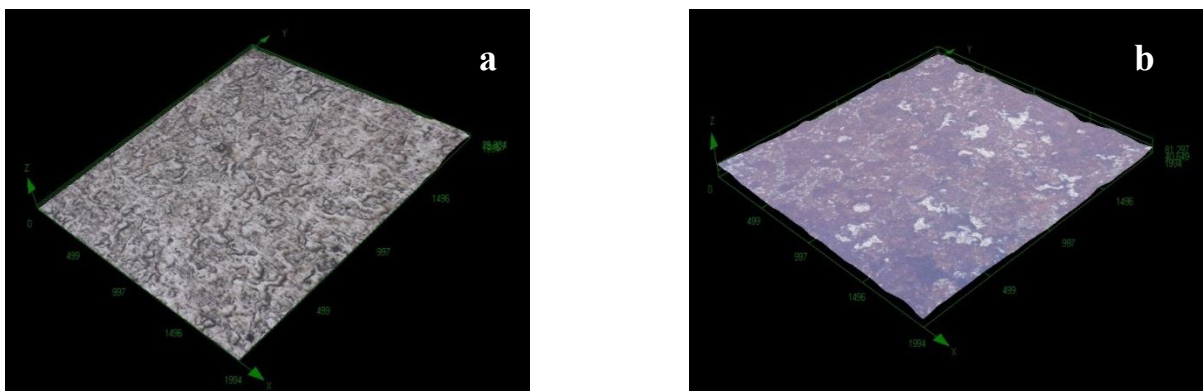


Figure 4.65: 3D optical microscopy of the surface of mild steel: (a) plain mild steel and (b) mild steel immersed in  $\text{H}_2\text{SO}_4$  uninhibited.

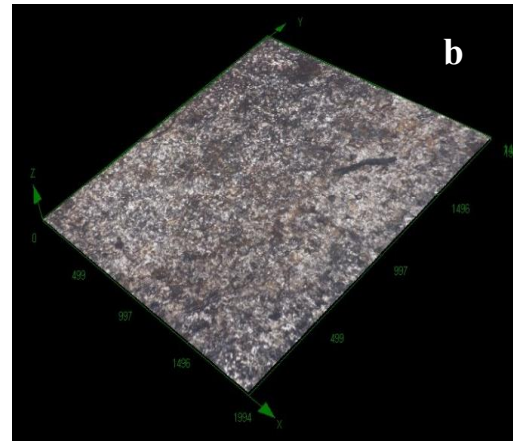
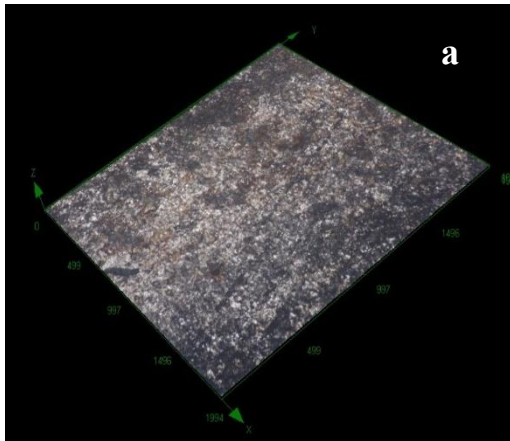


Figure 4.66: 3D optical microscopy of the surface of MS immersed in  $H_2SO_4$  in the presence of (a) 3CYC (b) 6MCH

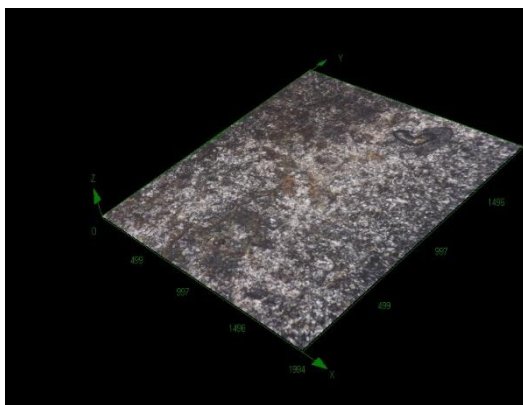


Figure 4.67: 3D optical microscopy of the surface of MS immersed in  $H_2SO_4$  in the presence of 6MC2C

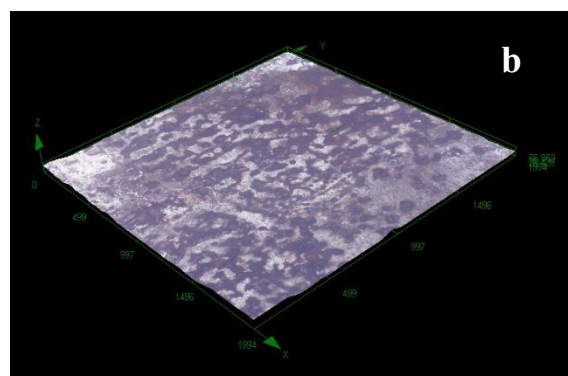
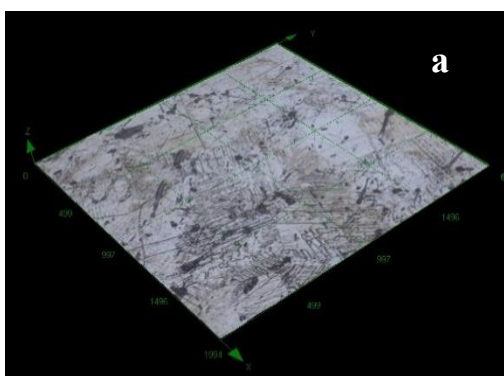


Figure: 4.68 3D optical microscopy of the surface of zinc: (a) plain zinc and (b) zinc immersed in  $CH_3COOH$  uninhibited.

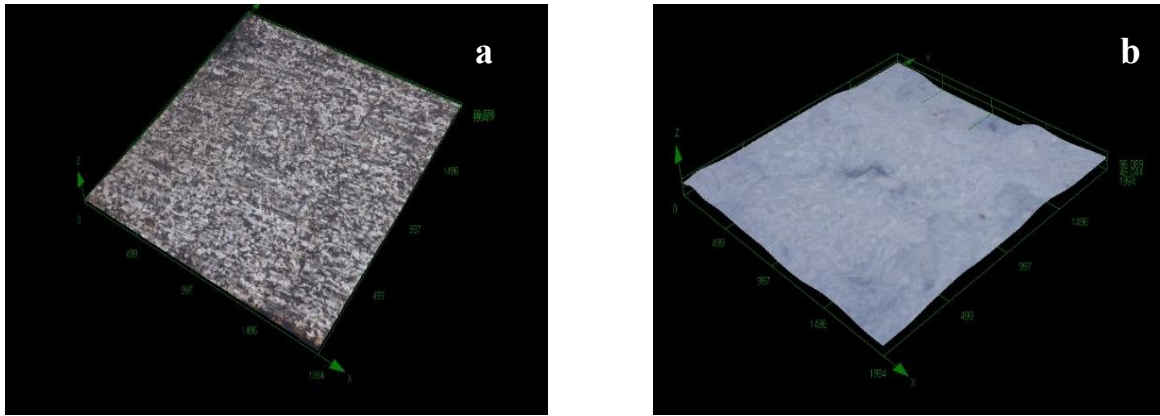


Figure 4.69: 3D optical microscopy of the surface of zinc immersed in  $\text{CH}_3\text{COOH}$  in the presence of (a) 3CYC (b) 6MCH

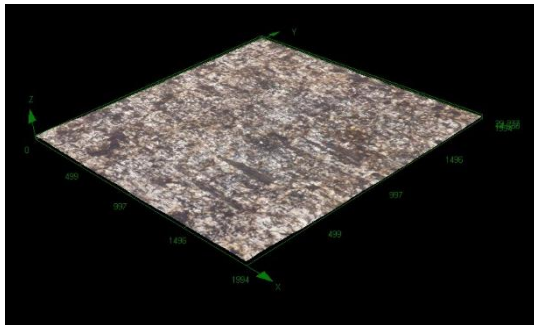


Figure 4.70: 3D optical microscopy of the surface of zinc immersed in  $\text{CH}_3\text{COOH}$  in the presence of 6MC2C

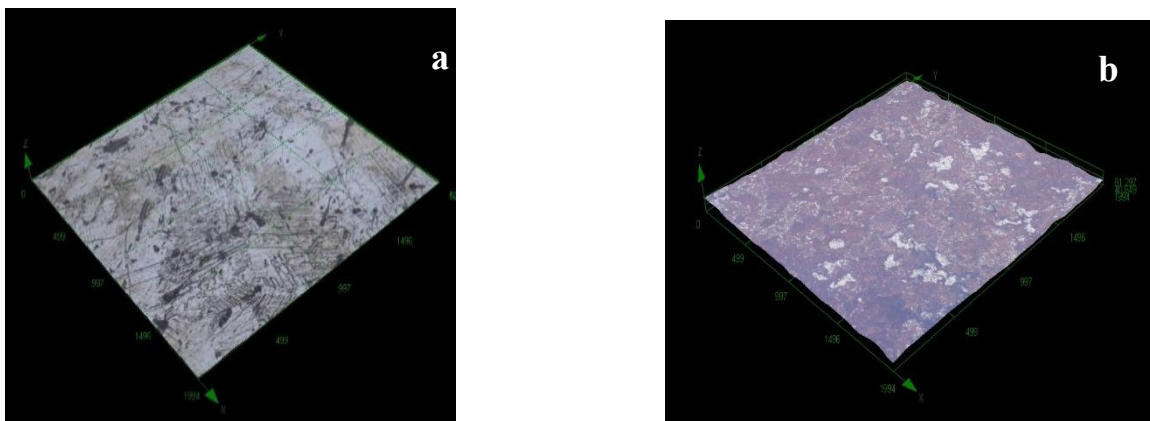


Figure 4.71: 3D optical microscopy of the surface of zinc: (a) plain zinc and (b) zinc immersed in  $\text{H}_2\text{SO}_4$  uninhibited.

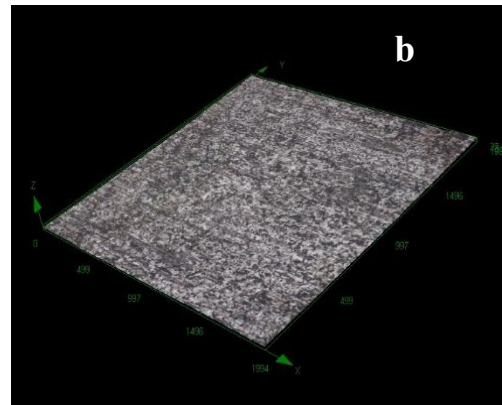
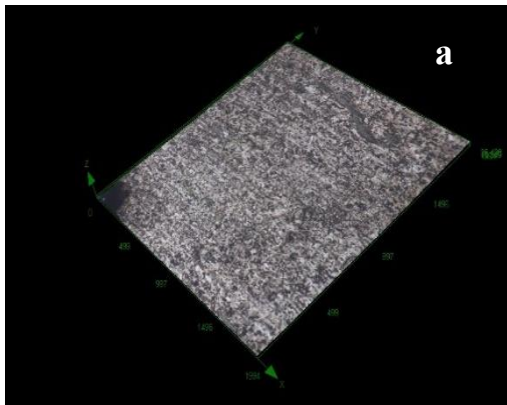


Figure 4.72: 3D optical microscopy of the surface of zinc immersed in  $H_2SO_4$  in the presence of (a) 3CYC (b) 6MCH

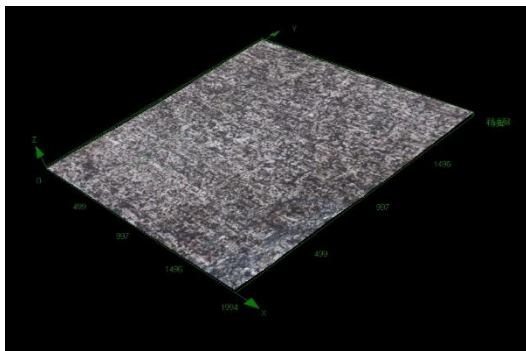


Figure 4.73: 3D optical microscopy of the surface of zinc immersed in  $H_2SO_4$  in the presence of 6MC2C

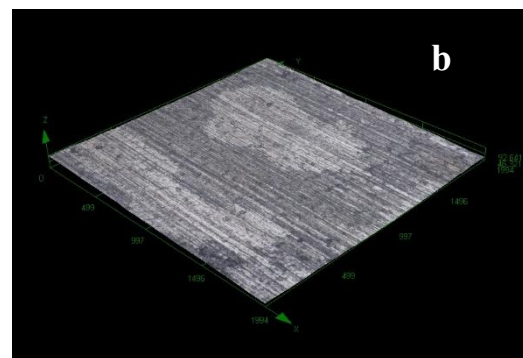
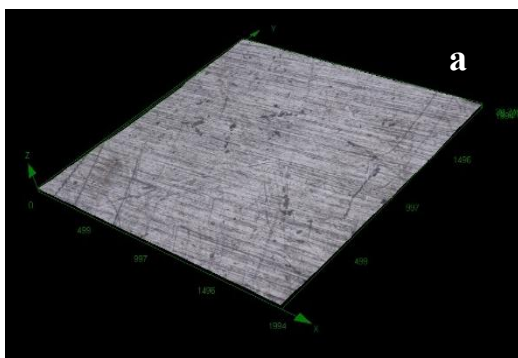


Figure 4.74: 3D optical microscopy of the surface of aluminium: (a) plain aluminium and (b) aluminium immersed in  $HNO_3$  uninhibited.



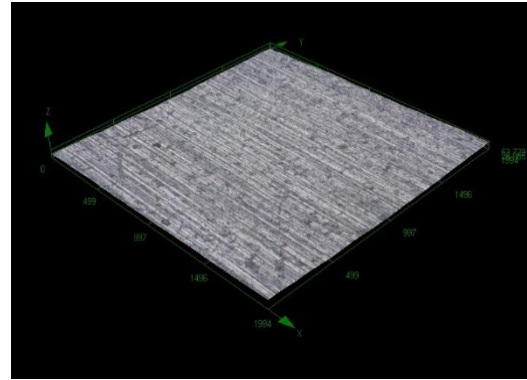
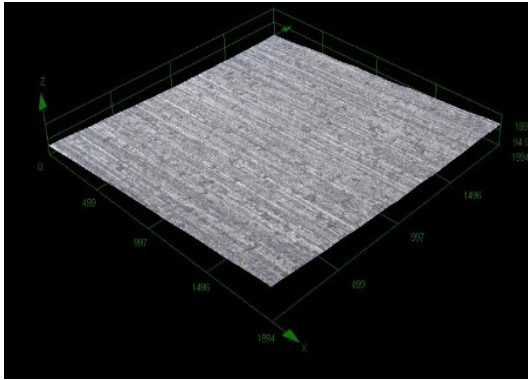


Figure 4.75: 3D optical microscopy of the surface of aluminium immersed in  $\text{HNO}_3$  in the presence of (a) 3CYC (b) 6MCH

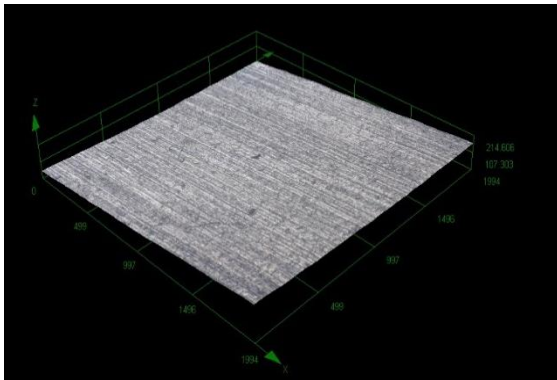


Figure 4.76: 3D optical microscopy of the surface of aluminium immersed in  $\text{HNO}_3$  in the presence of 6MC2C

#### 4.4 Atomic Absorption Spectroscopy (AAS)

One of the useful outputs data obtained from Atomic absorption spectroscopy (AAS) was absorbance. The relationship between absorbance and concentrations were denoted by equation (8), (9), and (10) below for zinc, mild steel, and aluminium respectively,

Equation for zinc

$$Y = 1.1565x + 0.0958 \quad (8)$$

Y = Abs and x = concentration (mg/L)

Equation for mild steel

$$Y = 0.7193x + 0.0724 \quad (9)$$

Y = Abs and x = concentration (mg/L)

Equation for Al

$$Y = 0.4404x + 0.2945 \quad (10)$$

Y = Abs and x = concentration (mg/L)

Equations (8), (9), and (10) were useful in calculating concentrations, surface coverage, and inhibition efficiency represented in tables 4.11–4.15. The experiment was conducted in triplicate resulting in three mean absorbance values for each trial. Mean absorbance recorded in Tables 4.11–4.15 was calculated by adding three absorbance values divide by three. High mean absorbance is equivalent to high concentration of metal dissolve during corrosion. Blank possess high mean absorbance when compared with other mean absorbance in the presence of inhibitors.

Table 4.11 Corrosion parameters obtained from atomic absorption spectroscopy of Aluminium exposed in HNO<sub>3</sub>

Corrosion Inhibitor	Mean absorbance	Concentration (M)	Surface coverage	Inhibition efficiency (%)
Blank	5.5593	11.9546	-	-
3CYC	1.2840	2.2468	0.81206	81.21
6MCH	1.4504	2.6247	0.78044	78.04
6MC2C	0.4839	0.4301	0.96402	96.40

Table 4.12 Corrosion parameters obtained from atomic absorption spectroscopy of mild steel exposed in H<sub>2</sub>SO<sub>4</sub>

Corrosion Inhibitor	Mean absorbance	Concentration (M)	Surface coverage	Inhibition efficiency (%)
Blank	7.2807	10.0213	-	-
3CYC	2.2185	02.9836	0.70227	70.23
6MCH	2.2905	03.0837	0.69229	69.23
6MC2C	2.1774	02.9265	0.70797	70.80

Table 4.13 Corrosion parameters obtained from atomic absorption spectroscopy of mild steel exposed in CH<sub>3</sub>COOH

Corrosion Inhibitor	Mean absorbance	Concentration (M)	Surface coverage	Inhibition efficiency (%)
Blank	6.0181	08.2660	-	-
3CYC	1.0000	01.2896	0.84399	84.40
6MCH	2.3264	03.1336	0.6209	62.09
6MC2C	1.1062	01.4372	0.8261	82.61



Table 4.14 Corrosion parameters obtained from atomic absorption spectroscopy of zinc exposed in H<sub>2</sub>SO<sub>4</sub>

Corrosion Inhibitor	Mean absorbance	Concentration (M)	Surface coverage	Inhibition efficiency (%)
Blank	1.0739	0.8457	-	-
3CYC	0.1095	0.0118	0.9860	98.60
6MCH	0.1423	0.0402	0.9525	95.25
6MC2C	0.1350	0.0339	0.9599	95.99

Table 4.15 Corrosion parameters obtained from atomic absorption spectroscopy of zinc exposed in CH<sub>3</sub>COOH

Corrosion Inhibitor	Mean absorbance	Concentration (M)	Surface coverage	Inhibition efficiency (%)
Blank	1.2998	1.0411	-	-
3CYC	0.1569	0.0528	0.94928	94.93
6MCH	0.1793	0.0722	0.93065	93.07
6MC2C	0.6475	0.4770	0.54183	54.18

Figure 4.77-4.81 shows the concentration of various metals, namely aluminium, zinc, and mild steel in the presence and absence of corrosion inhibitors exposed in acidic medium such as nitric acid, sulphuric acid and acetic acid.

Minimum concentrations of metals in the presence of corrosion inhibitors, namely, 3CYC, 6MCH, and 6MC2C imply that the dissolution of metal or metal weight loss was lower [95, 96]. Effective corrosion inhibitor must minimise dissolution of metal by adsorbing onto the metal surface and form thin protective layer [97]. Lower concentrations of metals (Al, Fe, and Zn) within the solution in the presence of corrosion inhibitors imply higher surface coverage. Effective corrosion inhibitor is expected to protect metal from dissolution as a results of acid attack so higher metal concentration indicate that metal weight loss were higher [97].

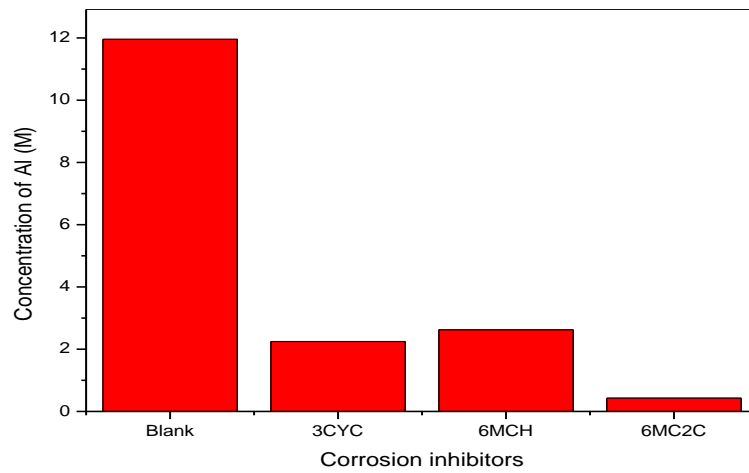


Figure 4.77: Corrosion parameters obtained from atomic absorption spectroscopy of Al exposed in  $\text{HNO}_3$

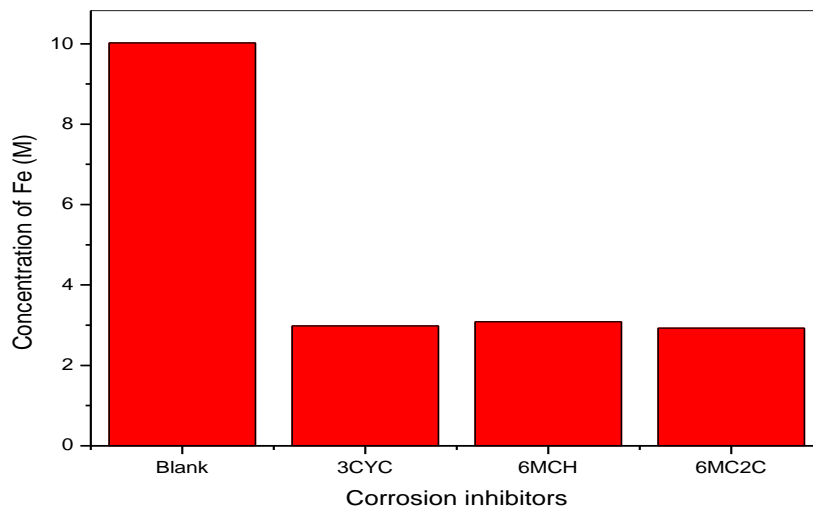


Figure 4.78: Corrosion parameters obtained from atomic absorption spectroscopy of MS exposed in  $\text{H}_2\text{SO}_4$

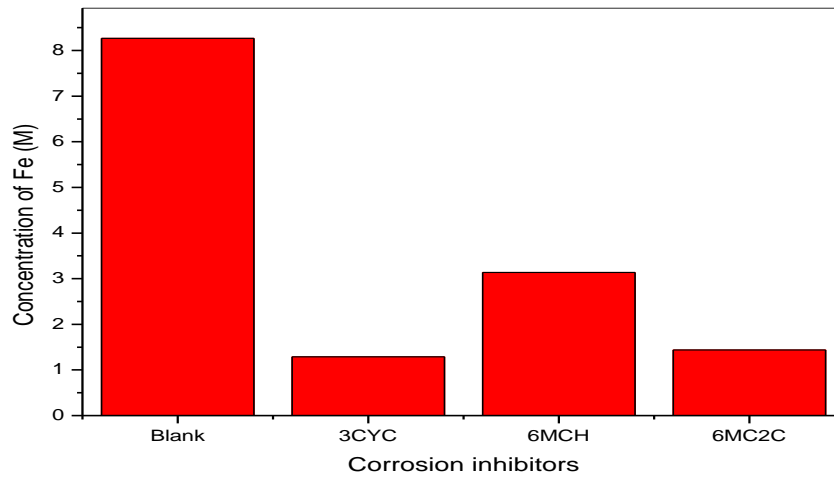


Figure 4.79: Corrosion parameters obtained from atomic absorption spectroscopy of MS exposed in  $\text{CH}_3\text{COOH}$

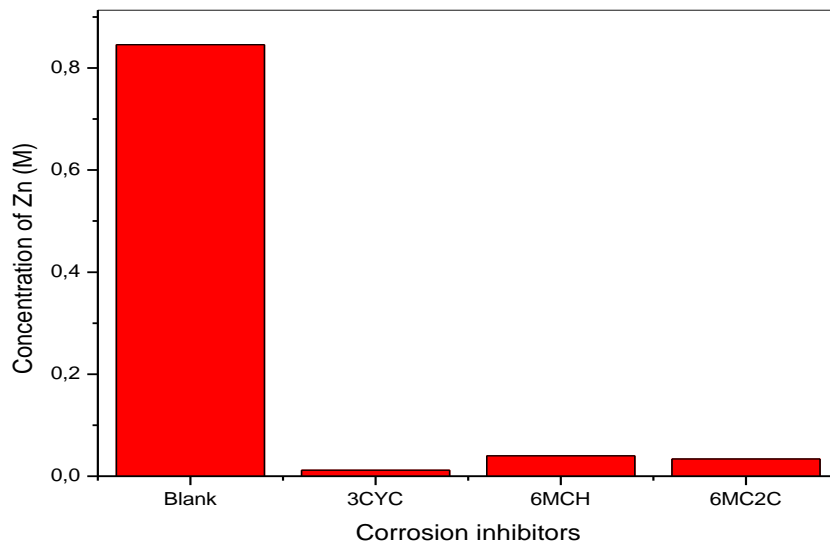


Figure 4.80: Corrosion parameters obtained from atomic absorption spectroscopy of Zn exposed in  $\text{H}_2\text{SO}_4$

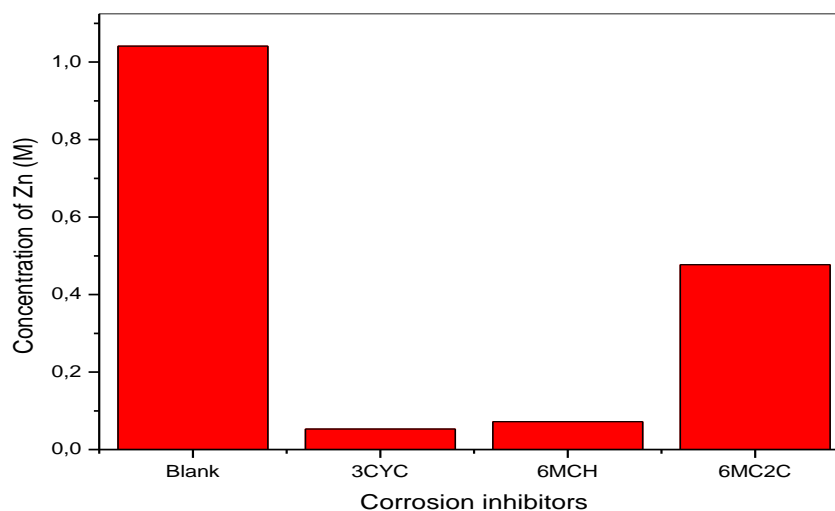


Figure 4.81: Corrosion parameters obtained from atomic absorption spectroscopy of Zn exposed in  $\text{CH}_3\text{COOH}$

#### 4.5 Fourier Transform Infrared Spectroscopy (FTIR)

This technique is primarily useful in characterizing 3CYC, 6MCH, and 6MC2C spectra of adsorption to a mild steel, zinc, and aluminium metal. Figures 4.82–4.96 show the adsorption of these inhibitors.

It is clear from Figures 4.82–4.96 that adsorption of 3CYC, 6MCH, and 6MC2C on mild steel, zinc, and aluminium occurs. This adsorption contributed towards the protection of metal from corrosive attack by reducing corrosion rate and increasing inhibition efficiency. These adsorptions of inhibitor form thin layers that protect metal from corrosion attack. The spectrum of 3CYC-MS resemble spectrum of 3CYC, these confirm that the 3CYC molecules was present in the rust formed onto the mild steel metal [100, 102]. Same explanation applies to other inhibitors (6MCH and 6MC2C). Figure 4.82 successful shows the adsorption of 3CYC onto zinc metal surface. This observation is attributed to the formation and disappearance of peaks. Figures 4.82–4.96 show similar trends.

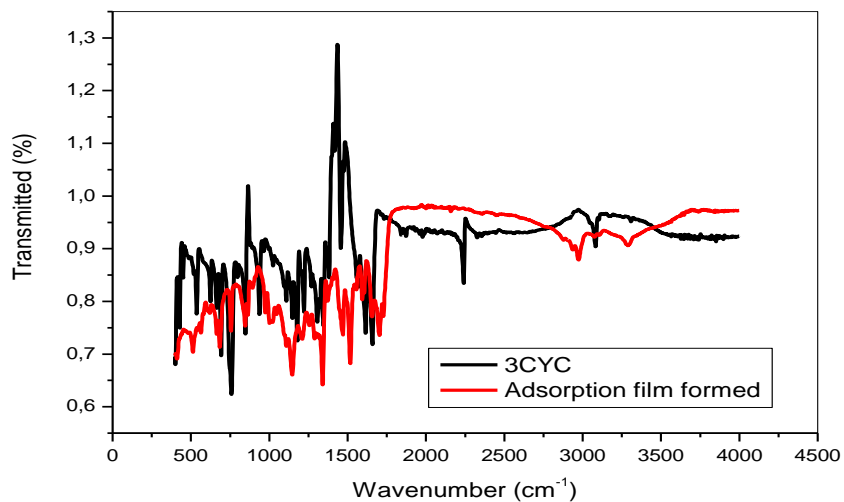


Figure 4.82: FT-IR spectra for the studied corrosion inhibitors and adsorption films formed on Zn in 1.5 M H<sub>2</sub>SO<sub>4</sub> using 3CYC

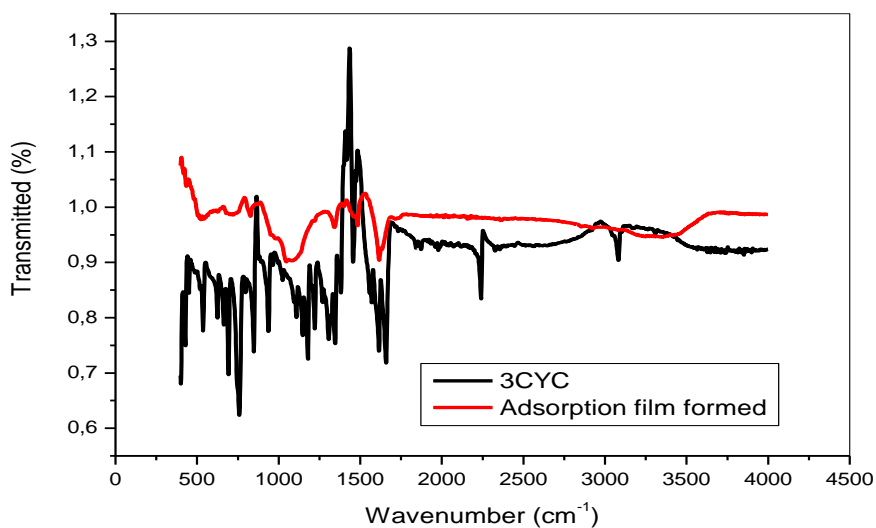


Figure 4.83: FT-IR spectra for the studied corrosion inhibitors and adsorption films formed on MS in 1.5 M H<sub>2</sub>SO<sub>4</sub> using 3CYC

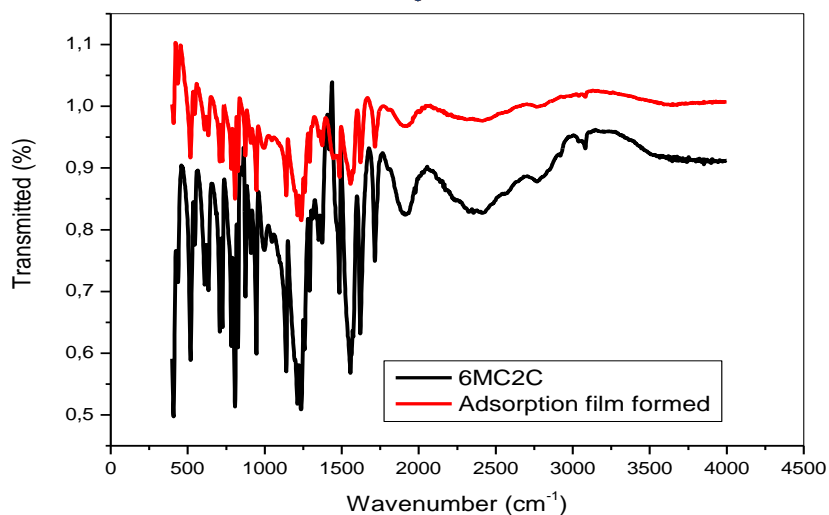


Figure 4.84: FT-IR spectra for the studied corrosion inhibitors and adsorption films formed on Zn in 1.5 M H<sub>2</sub>SO<sub>4</sub> using 6MC2C

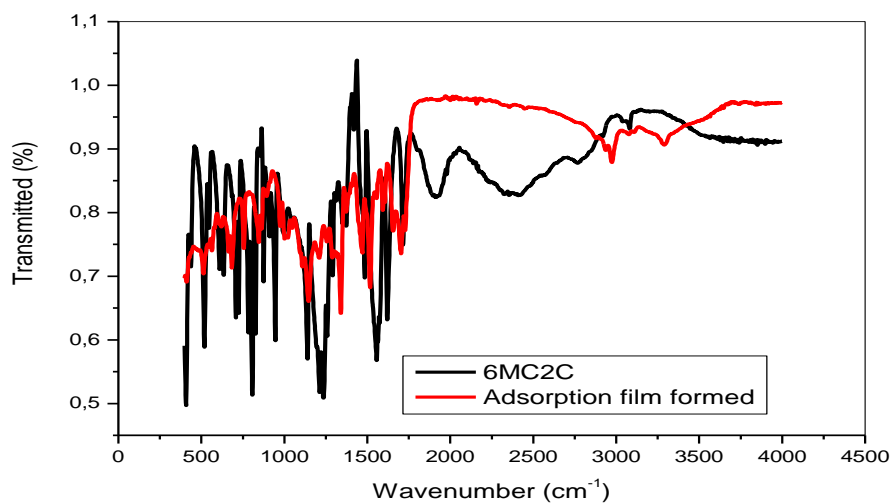


Figure 4.85: FT-IR spectra for the studied corrosion inhibitors and adsorption films formed on MS in 1.5 M H<sub>2</sub>SO<sub>4</sub> using 6MC2C

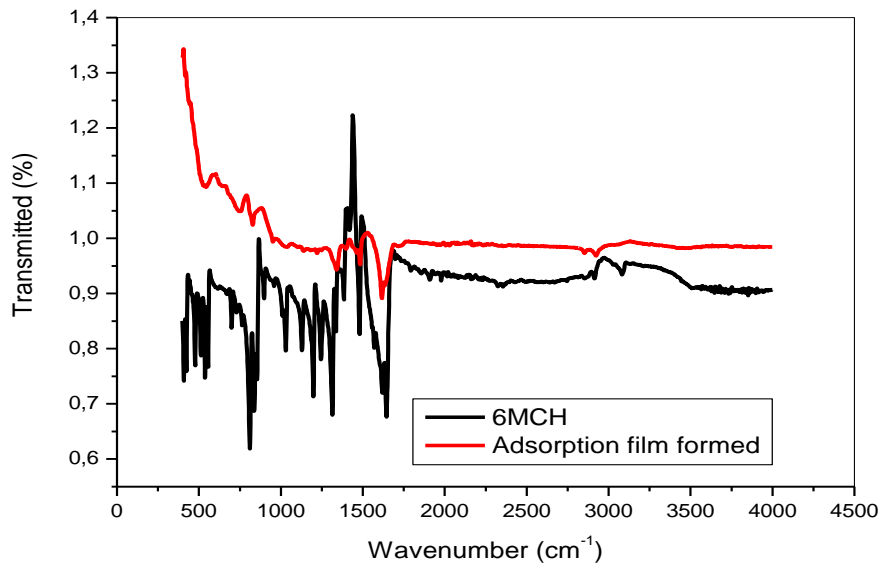


Figure 4.86: FT-IR spectra for the studied corrosion inhibitors and adsorption films formed on Zn in 1.5 M H<sub>2</sub>SO<sub>4</sub> using 6MCH

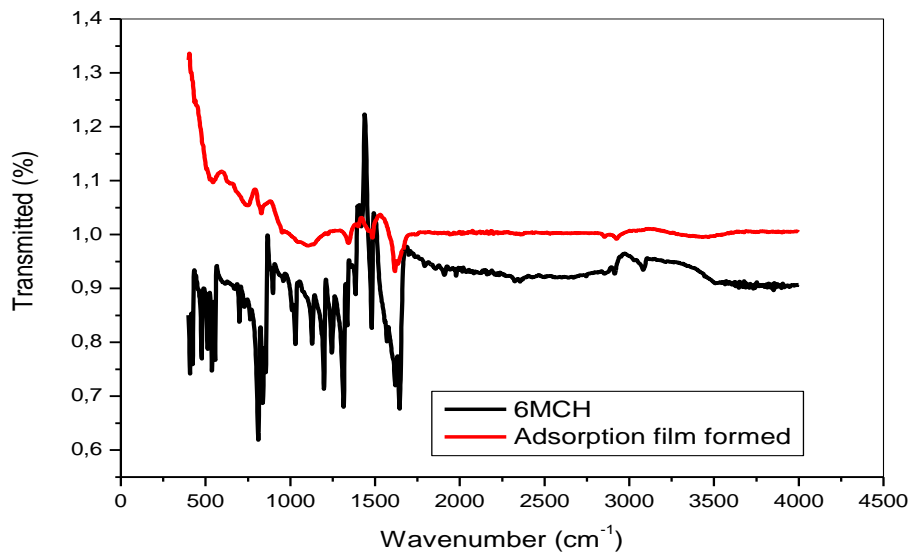


Figure 4.87: FT-IR spectra for the studied corrosion inhibitors and adsorption films formed on MS in 1.5 M H<sub>2</sub>SO<sub>4</sub> using 6MCH

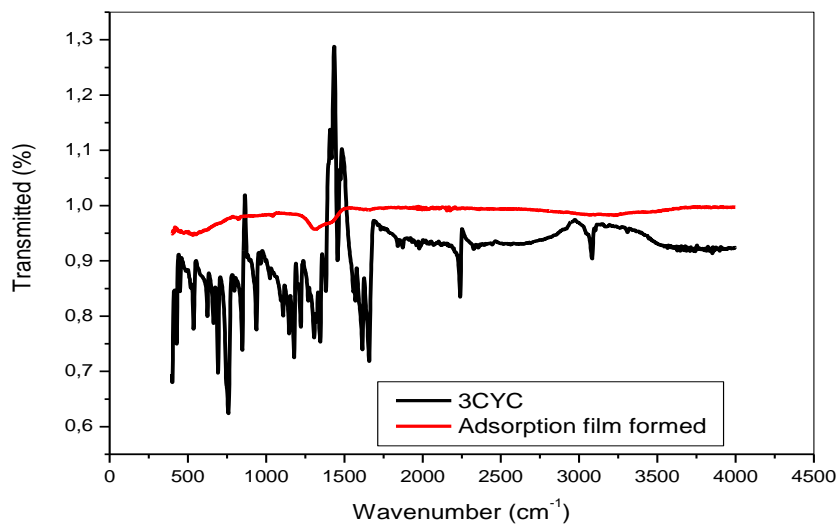


Figure 4.88: FT-IR spectra for the studied corrosion inhibitors and adsorption films formed on Al in 1.5 M HNO<sub>3</sub> using 3CYC

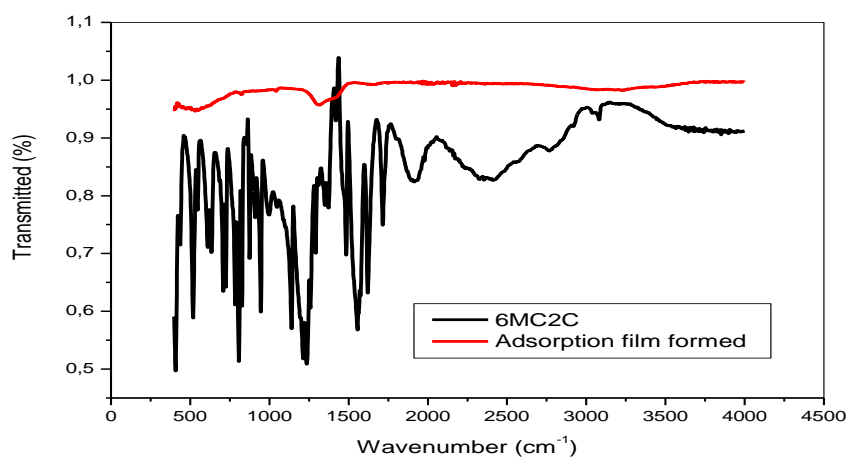


Figure 4.89: FT-IR spectra for the studied corrosion inhibitors and adsorption films formed on Al in 1.5 M HNO<sub>3</sub> using 6MC2C



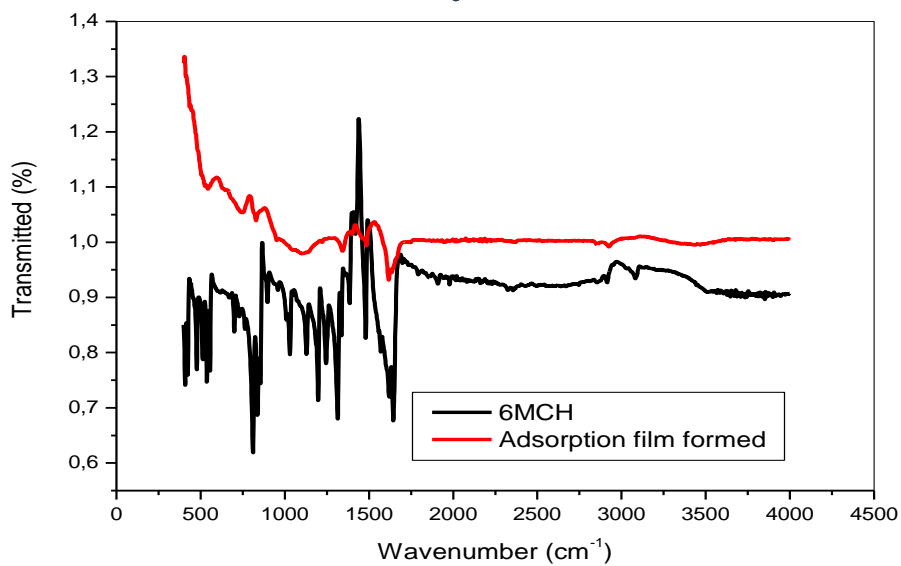


Figure 4.90: FT-IR spectra for the studied corrosion inhibitors and adsorption films formed on Al in 1.5 M HNO<sub>3</sub> using 6MCH

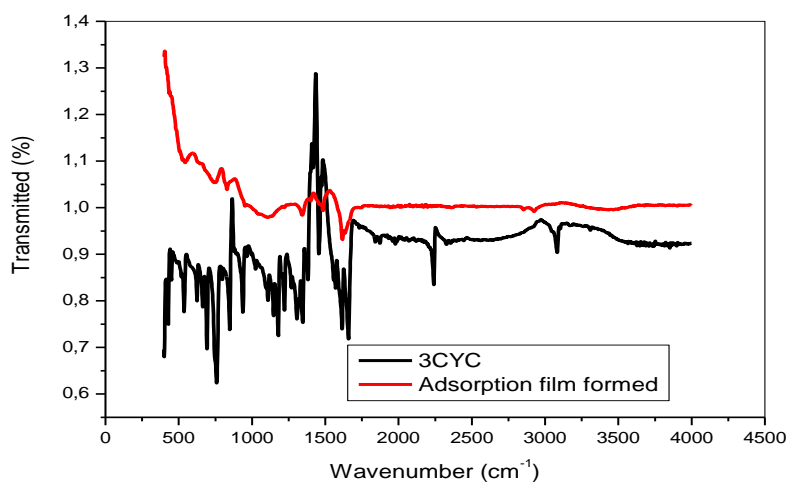


Figure 4.91: FT-IR spectra for the studied corrosion inhibitors and adsorption films formed on Zn in 1.5 M CH<sub>3</sub>COOH using 3CYC

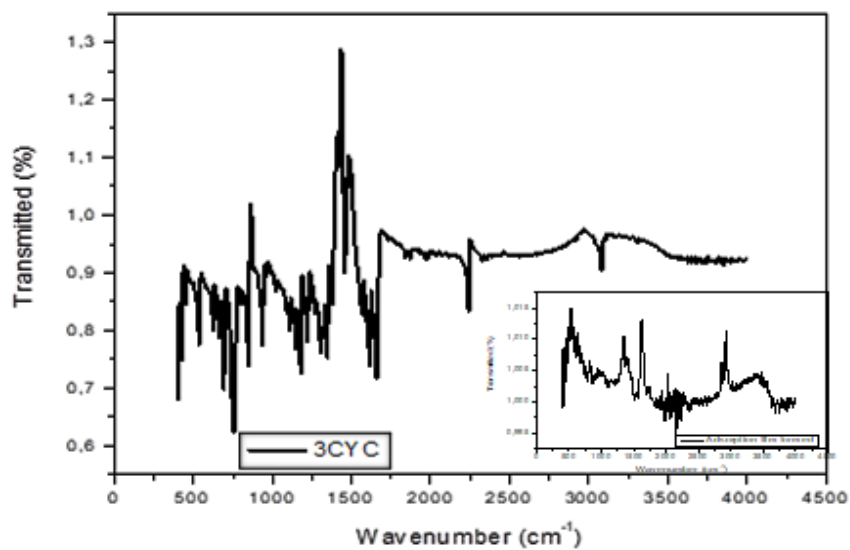


Figure 4.92: FT-IR spectra for the studied corrosion inhibitors and adsorption films formed on MS in 1.5 M CH<sub>3</sub>COOH using 3CYC

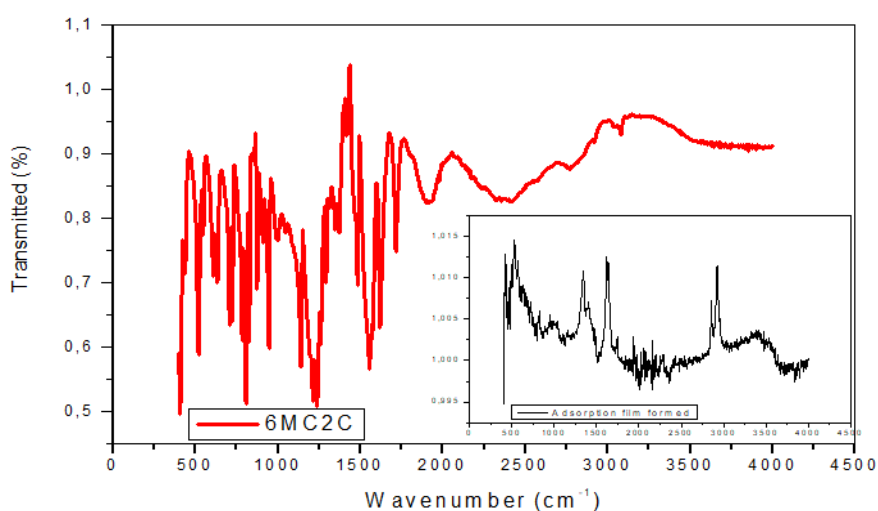


Figure 4.93: FT-IR spectra for the studied corrosion inhibitors and adsorption films formed on Zn in 1.5 M CH<sub>3</sub>COOH using 6MC2C

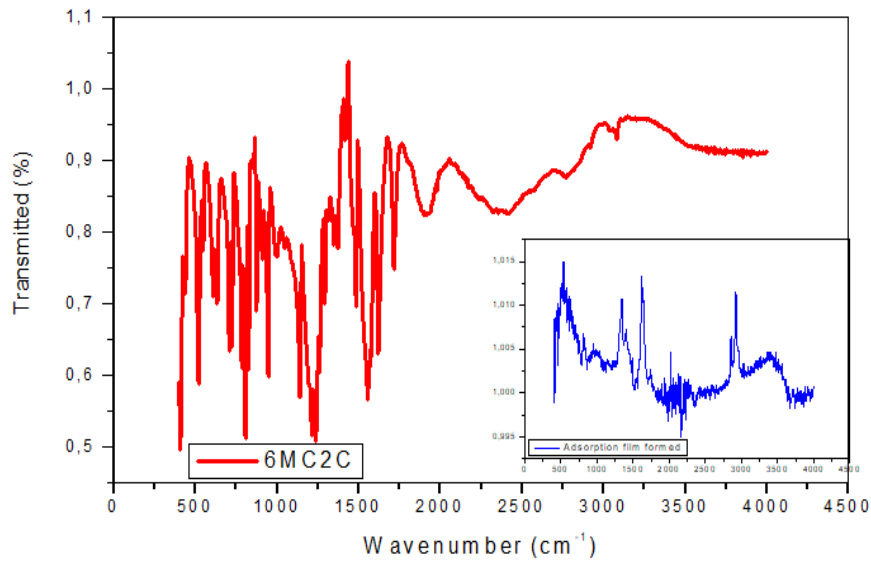


Figure 4.94: FT-IR spectra for the studied corrosion inhibitors and adsorption films formed on MS in 1.5 M CH<sub>3</sub>COOH using 6MC2C

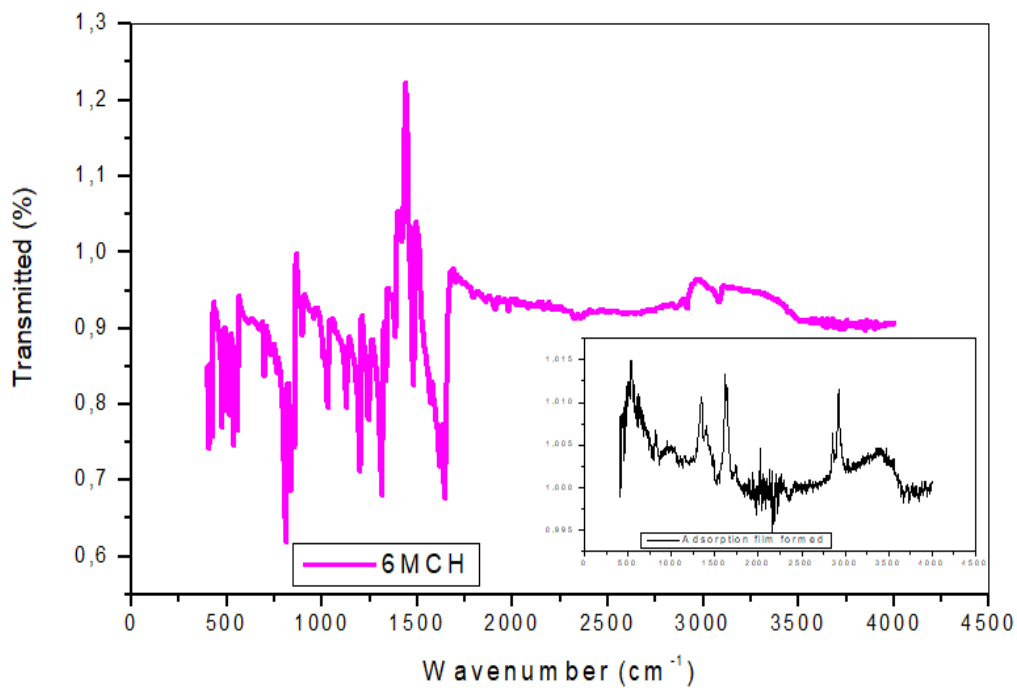


Figure 4.95: FT-IR spectra for the studied corrosion inhibitors and adsorption films formed on Zn in 1.5 M CH<sub>3</sub>COOH using 6MCH

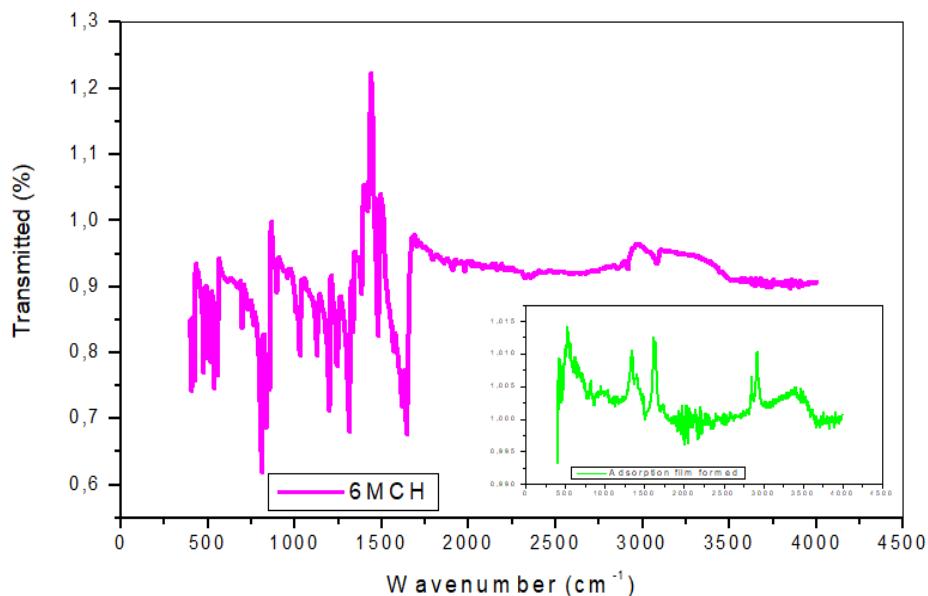


Figure 4.96: FT-IR spectra for the studied corrosion inhibitors and adsorption films formed on MS in 1.5 M CH<sub>3</sub>COOH using 6MCH

Table 4.16 indicated that the inhibitor 3CYC, 6MCH, 6MC2C possesses quality of being a good corrosion inhibitor. The FTIR spectra indicated various bonds that disappeared and formed when the inhibitor interact with the metal surface, this implies that the tested inhibitor adsorb onto metal and form thin protective layer [98, 99]. The wavenumber between 2250-2256cm<sup>-1</sup> indicated the presence of primary amine, (CN group) of 3CYC as indicated in figure 4.82 in Table 4.16. This peak disappeared and formation of new bond occurs at wavenumber 1590-1620cm<sup>-1</sup> when 3CYC-Zn is utilised. The CO<sub>2</sub>H peak corresponding to 6MC2C at wavenumber 1580-1690cm<sup>-1</sup> seems to disappear and formation of new bond occurs at wavenumber 1498cm<sup>-1</sup> for same inhibitor 6MC2C in mild steel.

Table 4.16: FTIR spectra indicating various functional group

Figure	Inhibitor-Metal	Functional Groups Peaks obtained from FT-IR Spectra (cm <sup>-1</sup> )				
		=C-H	-CN	Ar(C=C)	CO <sub>2</sub> H	C <sub>6</sub> H <sub>6</sub> Y
4.82	3CYC	3210	2260	-	-	750
	3CYC-Zn	3000	-	1590	-	-
4.83	3CYC-MS	-	-	1620	-	-
4.84	6MC2C	-	-	1580	1556	753
	6MC2C-Zn	-	-	1580	-	751
4.85	6MC2C-MS	3100	-	1579	1498	-

4.86	6MCH	-	-	1643	1458	760
	6MCH-Zn	-	-	1622	-	-
4.87	6MCH-MS	-	-	1621	-	-
4.88	3CYC-Al	-	-	1388	-	-
4.89	6MC2C-Al	-	-	1344	-	-
4.90	6MCH-Al	-	-	1642	-	-
4.91	3CYC-Zn	-	-	1644	-	-
4.92	3CYC-MS	-	2100	-	-	746
4.93	6MC2C-Zn	-	-	-	-	744
4.94	6MC2C-MS	-	-	-	-	798
4.95	6MCH-Zn	-	-	-	-	788
4.96	6MCH-MS	-	-	-	-	778

#### 4.6 Weight loss measurements results

Mild steel and zinc were exposed in different concentrations of sulphuric acid and different temperatures in the absence of corrosion inhibitors. Metals were fully immersed for 4 hours maintaining at 303K–333K using thermostat water bath. The weight loss are shown in Tables 4.17–4.18

Table 4.17: Weight loss measurements of mild steel in H<sub>2</sub>SO<sub>4</sub>, in the absence of the corrosion inhibitors

Concentration (M)	Weight loss (g)			
	303K	313K	323K	333K
0.2	0.0911	0.2603	0.3870	0.6289
0.4	0.2037	0.4634	0.6900	0.9869
0.6	0.3371	0.5676	0.8400	1.2313
1.0	0.4625	0.7317	1.1043	1.5933
1.5	0.5535	0.9009	1.3950	1.9320

Table 4.18: Weight loss measurements of zinc in H<sub>2</sub>SO<sub>4</sub>, in the absence of the corrosion inhibitors

Concentration (M)	Weight loss (g)			
	303K	313K	323K	333K
0.2	0.2545	0.3607	0.4801	0.7017
0.4	0.3063	0.4541	0.6641	1.0000
0.6	0.3697	0.5673	0.7893	1.2122
1.0	0.4506	0.6728	1.0011	1.4673
1.5	0.5272	0.7677	1.1651	1.8519

Both Tables 4.17 and 4.18 indicate rapid increase in weight loss as the temperature increases. This trend implies that there higher the temperature, the more aggressive the environment becomes. Minimum weight loss was obtained at 303K for zinc and mild steel. When comparing Table 4.17 and 4.18 it is clear that sulphuric acid was more aggressive towards mild steel than zinc because maximum weight loss was 1.9320g and 1.8519 g at 333K, respectively.

Mild steel and zinc were exposed to different concentrations of acetic acid at at 303K – 333K in the absence of corrosion. Tables 4.19–4.20 indicate rapid increase in weight loss as the temperature increases. This trend implies that there higher, the temperature the more aggressive the environment become [102, 104]. Minimum weight loss was obtained at 303K for zinc and mild steel. When comparing Tables 4.19–4.20 with Tables 4.17–4.18 it is clear that sulphuric acid is more corrosive than acetic acid. This can specifically be seen when zinc is exposed to 1.5 M sulphuric acid at 333K and when exposed to also show concentration of acetic acid that the values of weight loss are 1.8519g and 1.1483g, respectively.

Table 4.19: Weight loss measurements of mild steel in  $\text{CH}_3\text{COOH}$  in the absence of the corrosion inhibitors

Concentration (M)	Weight loss (g)			
	303K	313K	323K	333K
0.2	0.0063	0.0071	0.0101	0.0223
0.4	0.0081	0.0084	0.0141	0.0310
0.6	0.0092	0.0098	0.0152	0.0389
1.0	0.0100	0.0112	0.0198	0.0410
1.5	0.0120	0.0134	0.0228	0.0430

Table 1.20: Weight loss measurements of zinc in  $\text{CH}_3\text{COOH}$  in the absence of the corrosion inhibitors

Concentration (M)	Weight loss (g)			
	303K	313K	323K	333K
0.2	0.0125	0.0367	0.0410	0.0775
0.4	0.0230	0.0413	0.0488	0.0980
0.6	0.0369	0.0497	0.0679	0.1087
1.0	0.0492	0.0549	0.0782	0.1208
1.5	0.0608	0.0648	0.0922	0.1483

Table 4.21: Weight loss measurements of aluminium in  $\text{HNO}_3$  in the absence of the corrosion inhibitors

Concentration (M)	Weight loss (g)			
	303K	313K	323K	333K
0.2	0.0009	0.0006	0.0034	0.0209
0.4	0.0013	0.0301	0.0054	0.0170
0.6	0.0012	0.0062	0.0041	0.0151
1.0	0.0015	0.0088	0.0066	0.0167
1.5	0.0098	0.0190	0.0230	0.0419

Table 4.21 clearly shows similar trend as observed in Tables 4.17 – 4.20, it can be observed that when concentration of nitric acid decreases, weight loss also decreases. This implies that there more aluminium metal is exposed to a minimal concentration the lesser the dissolution of the metal. The trend above also shows that the higher the concentration of nitric acid, the more corrosive it become. Temperature seems to have contributed toward weight loss, this can be supported by the trend observed when temperature increase from 303K–333K. Weight loss increased when temperature increases, this may be due to the fact that temperature is one of factors that affect the rate of reaction. In this study, higher temperature contributed toward faster dissolution of aluminium. The overall trend obtained from tables 4.17–4.20 indicated that nitric acid, sulphuric acid and acetic acid are corrosive. This is due to weight lost by metal when each metal were exposed in acid for four hours. It is also clear that if concentration of nitric, sulphuric or acetic acid increased the rate of metal dissolution occurs faster and mass lost become higher.

It is clear from these graphs that the corrosion occurred because metal loses weight when exposed to acidic medium. The extent of mass loss seems to depend on factors such as temperature, concentration of acid and type of acid [104, 105]. When temperature increases, weight loss also increases and when concentration of each acid decreases the mass loss also decreases. In order to minimise corrosion rate, chromone compounds where used as corrosion inhibitors aiming to reduce weight loss to the extent of having reducing it to zero weight loss.

The data on Table 4.17–4.21 can be represented graphically as in figures 4.97 – 4.101

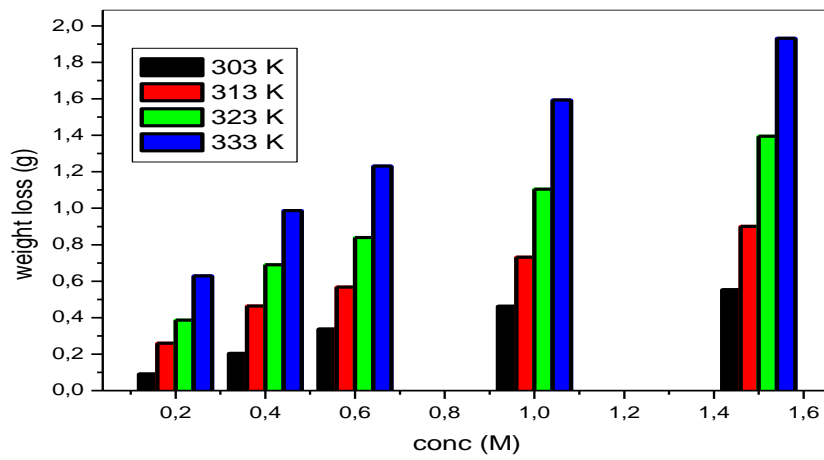


Figure 4.97: Weight loss measurements of mild steel in the presence of  $H_2SO_4$  at 300 K–333K

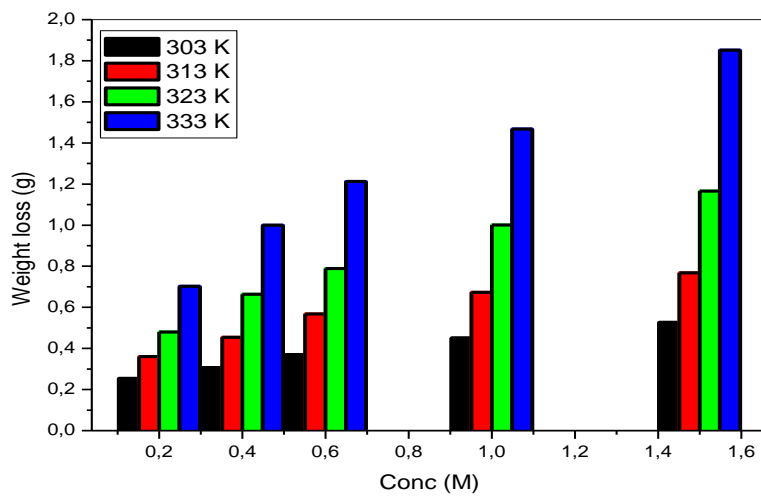


Figure 4.98: Weight loss measurements of zinc in the presence of  $H_2SO_4$  at 300 K–333 K



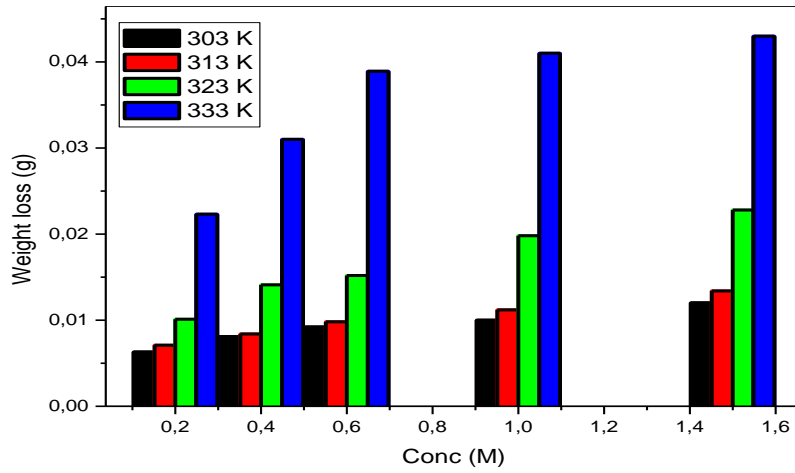


Figure 4.99: Weight loss measurements of mild steel in the presence of CH<sub>3</sub>COOH at 300 K–333 K

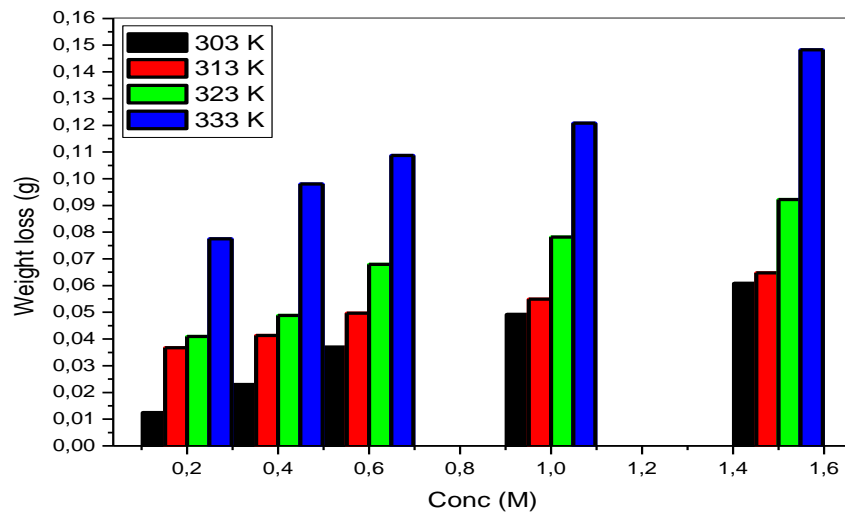


Figure 4.100: Weight loss measurements of zinc in the presence of CH<sub>3</sub>COOH at 300 K–333 K

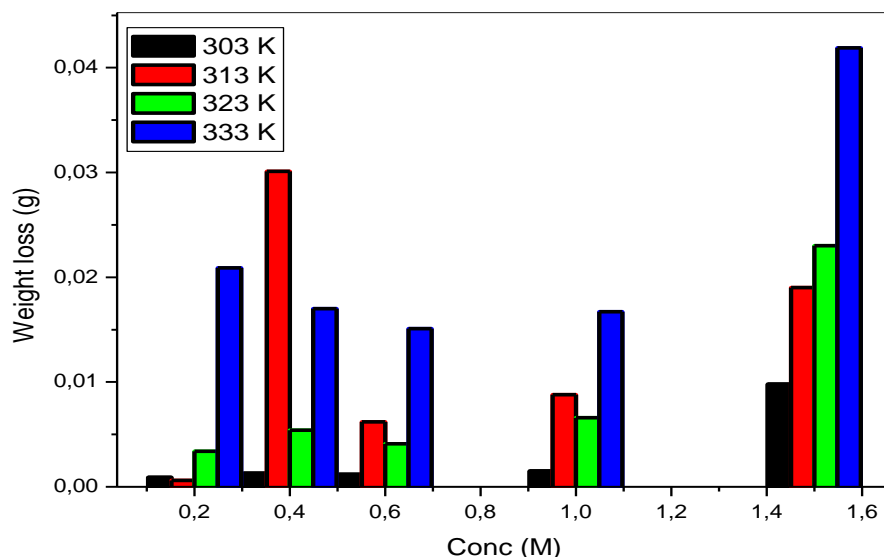


Figure 4.101: Weight loss measurements of aluminium in the presence of  $\text{HNO}_3$  at 300 K–333 K

Three organic compounds namely 3CYC, 6MCH and 6MCC were used as corrosion inhibitor to conduct corrosion test using weight loss method. Metals were exposed to various concentrations of inhibitors at different temperature. Weight loss was calculated and recorded on the Tables 4.22–4.27. The weight loss in the presence of each corrosion inhibitor is less when compared to weight loss in the absence of corrosion inhibitors. This shows that 3CYC, 6MCH, and 6MC2C are good corrosion inhibitors. The extents of weight loss were observed to be reduced rapidly when concentrations of 3CYC, 6MCH and 6MC2C were increased. When temperature increased, the weight loss also seems to increase regardless of increasing the concentration of inhibitors, however the overall weight loss was less compared to mass lost in the absence of corrosion inhibitors. Minimum weight loss was obtained at 303K using 3CYC as corrosion inhibitor exposed in acetic acid with a weight loss value of 0.0012 g. It is also clear from the Tables 4.22–4.27 that sulphuric acid is more corrosive when compared to acetic acid, these can be explicitly seen from Table 4.26 that maximum weight loss was 0.0254 g for acetic acid at 333 K and for sulphuric acid Table 4.23 indicate maximum weight loss of 0.8857 g obtain at 333 K.

It is clear from Table 4.26 at 303 K that when concentration of 6MC2C increases the weight loss rapidly decreases to the extent that it can be assumed that if concentration keep increasing in the same manner then weight loss might likely be reduced to almost zero but not necessarily zero.

Table 4.22: Weight loss measurements on mild steel exposed in 1.5 M H<sub>2</sub>SO<sub>4</sub> in the presence of 3CYC

Concentration of inhibitor (M)	Weight loss (g)			
	303K	313K	323K	333K
0.000	0.5535	0.9009	1.3950	1.9320
2x10 <sup>-4</sup>	0.0784	0.1463	0.3760	0.6802
4x10 <sup>-4</sup>	0.0359	0.0976	0.2455	0.5896
6x10 <sup>-4</sup>	0.0293	0.0635	0.1809	0.4215
8x10 <sup>-4</sup>	0.0212	0.0476	0.1435	0.3789
10x10 <sup>-4</sup>	0.0113	0.0386	0.0862	0.2605

Table 4.23: Weight loss measurements on mild steel exposed in 1.5 M H<sub>2</sub>SO<sub>4</sub> in the presence of 6MCH

Concentration of inhibitor (M)	Weight loss (g)			
	303K	313K	323K	333K
0.000	0.5535	0.9009	1.3950	1.9320
2x10 <sup>-4</sup>	0.1744	0.2994	0.5064	0.8857
4x10 <sup>-4</sup>	0.1702	0.2881	0.4954	0.7891
6x10 <sup>-4</sup>	0.1629	0.2848	0.4858	0.7693
8x10 <sup>-4</sup>	0.1501	0.2802	0.4693	0.7680
10x10 <sup>-4</sup>	0.0879	0.2655	0.4058	0.7273

Table 4.24: Weight loss measurements on mild steel exposed in 1.5 M H<sub>2</sub>SO<sub>4</sub> in the presence of 6MC2C

Concentration of inhibitor (M)	Weight loss (g)			
	303K	313K	323K	333K
0.000	0.5535	0.9009	1.3950	1.9320
2x10 <sup>-4</sup>	0.0933	0.1939	0.4441	0.7968
4x10 <sup>-4</sup>	0.0873	0.1525	0.3798	0.7531
6x10 <sup>-4</sup>	0.0137	0.1085	0.3541	0.7271
8x10 <sup>-4</sup>	0.0050	0.0536	0.3000	0.6985
10x10 <sup>-4</sup>	0.0043	0.0102	0.1481	0.6616

Table 4.25: Weight loss measurements on mild steel exposed in 1.5 M CH<sub>3</sub>COOH in the presence of 3CYC

Concentration of inhibitor (M)	Weight loss (g)			
	303K	313K	323K	333K
0.000	0.0120	0.0134	0.0228	0.0430
2x10 <sup>-4</sup>	0.0032	0.0068	0.0115	0.0234
4x10 <sup>-4</sup>	0.0027	0.0055	0.0108	0.0182
6x10 <sup>-4</sup>	0.0025	0.0045	0.0089	0.0178
8x10 <sup>-4</sup>	0.0016	0.0042	0.0056	0.0147
10x10 <sup>-4</sup>	0.0012	0.0040	0.0054	0.0143

Table 4.26: Weight loss measurements on mild steel exposed in 1.5 M CH<sub>3</sub>COOH in the presence of 6MCH

Concentration of inhibitor (M)	Weight loss (g)			
	303K	313K	323K	333K
0.000	0.0120	0.0134	0.0228	0.0430
2x10 <sup>-4</sup>	0.0057	0.0098	0.0158	0.0254
4x10 <sup>-4</sup>	0.0050	0.0090	0.0151	0.0253
6x10 <sup>-4</sup>	0.0048	0.0081	0.0144	0.0233
8x10 <sup>-4</sup>	0.0027	0.0080	0.0140	0.0222
10x10 <sup>-4</sup>	0.0022	0.0070	0.0093	0.0221

Table 4.27: Weight loss measurements on mild steel exposed in 1.5 M CH<sub>3</sub>COOH in the presence of 6MC2C

Concentration of inhibitor (M)	Weight loss (g)			
	303K	313K	323K	333K
0.000	0.0120	0.0134	0.0228	0.0430
2x10 <sup>-4</sup>	0.0030	0.0061	0.0164	0.0209
4x10 <sup>-4</sup>	0.0027	0.0057	0.0121	0.0201
6x10 <sup>-4</sup>	0.0024	0.0053	0.0098	0.0165
8x10 <sup>-4</sup>	0.0021	0.0047	0.0097	0.0152
10x10 <sup>-4</sup>	0.0017	0.0043	0.0093	0.0111

The results on Tables 4.22–4.27 are graphically represented in Figure 4.102–4.107 showing that when concentration of corrosion inhibitors increases, the weight loss decreases. This simply means that the higher the concentration of the corrosion inhibitors, the lower the weight loss. The first four bars on each of Figure 4.102–4.107 represent blank trials. It is clear that the blank results are taller compared to other bars when corrosion inhibitors were present.

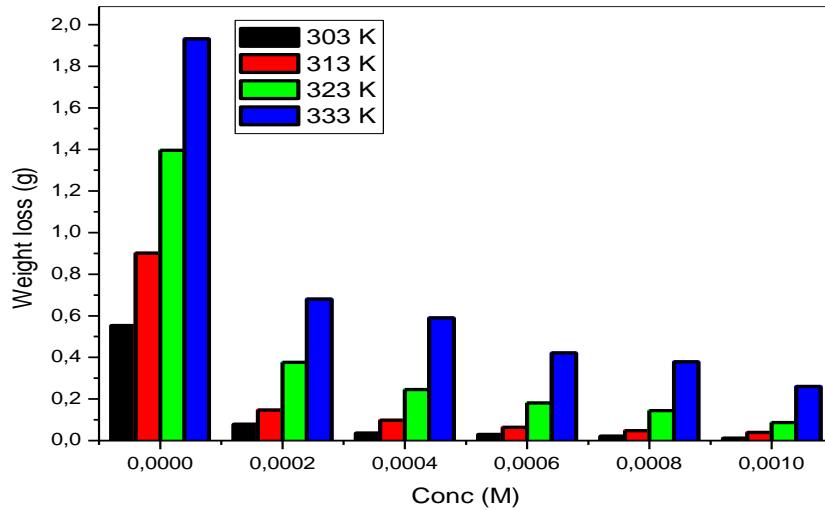


Figure 4.102: Weight loss measurements on mild steel exposed in 1.5 M H<sub>2</sub>SO<sub>4</sub> in the presence of 3CYC

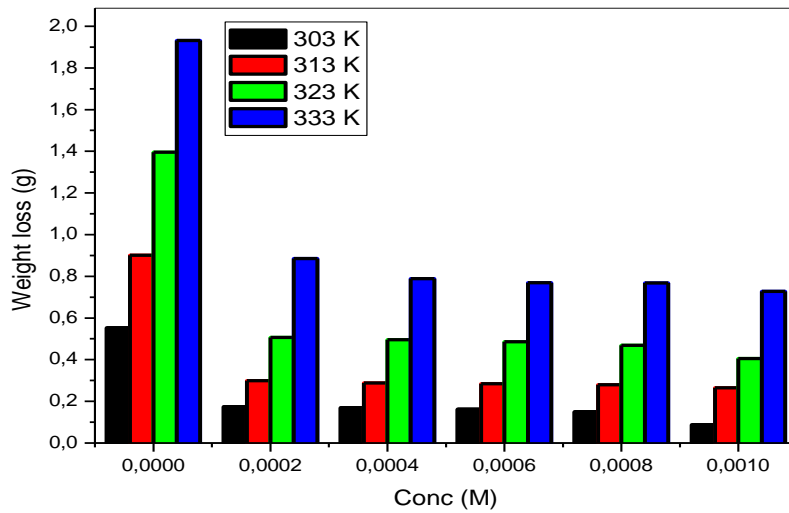


Figure 4.103: Weight loss measurements on mild steel exposed in 1.5 M H<sub>2</sub>SO<sub>4</sub> in the presence of 6MCH

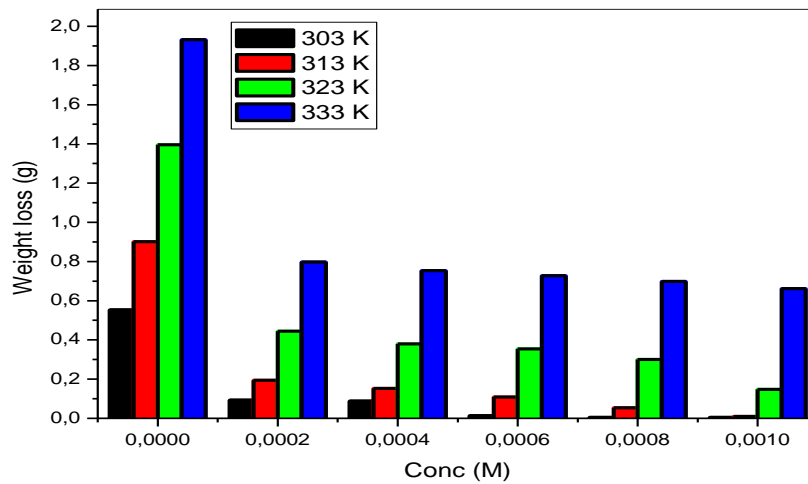


Figure 4.104: Weight loss measurements on mild steel exposed in 1.5 M H<sub>2</sub>SO<sub>4</sub> in the presence of 6MC2C

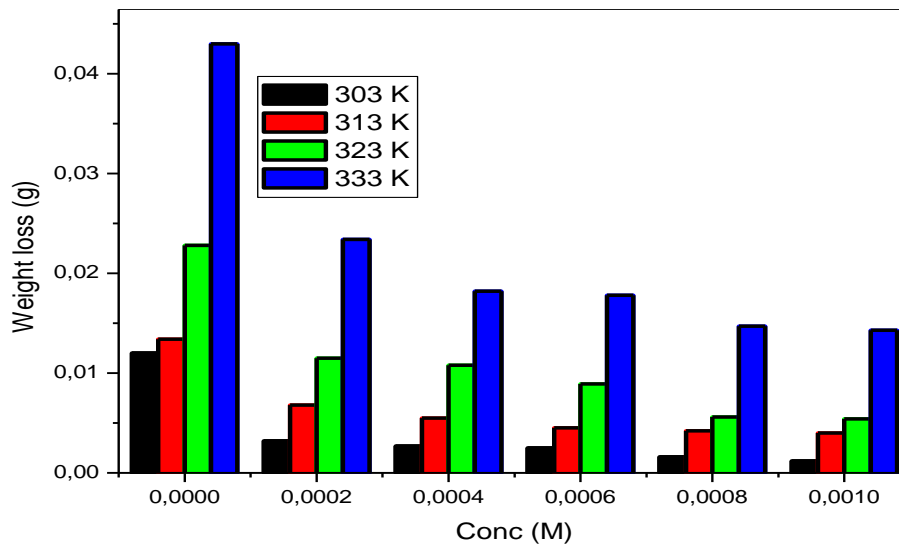


Figure 4.105: Weight loss measurements on mild steel exposed in 1.5 M CH<sub>3</sub>COOH in the presence of 3CYC

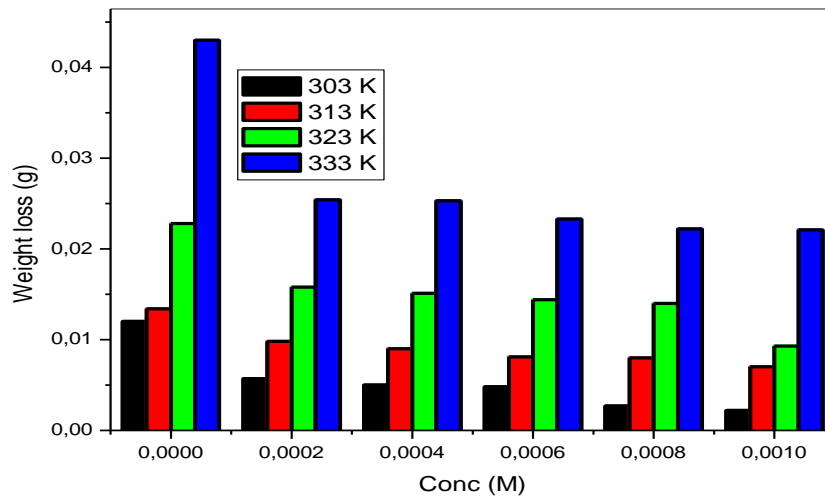


Figure 4.16: Weight loss measurements on mild steel exposed in 1.5 M CH<sub>3</sub>COOH in the presence of 6MCH

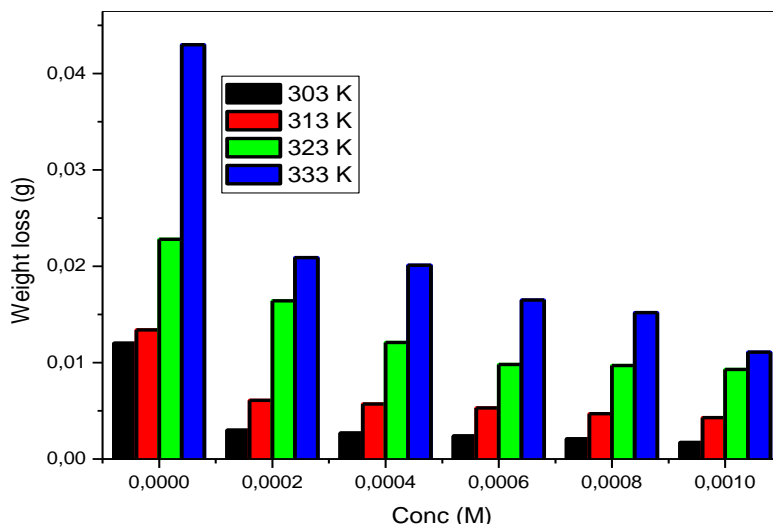


Figure 4.107: Weight loss measurements on mild steel exposed in 1.5 M CH<sub>3</sub>COOH in the presence of 6MC2C

The data on Tables 4.28–4.33 denote similar trends as discussed in Tables 4.22–4.27, Therefore, Tables 4.22–4.33 indicate that the presence of 3CYC, 6MCH and 6MC2C minimise weight loss thus corrosion rate were reduced. It is clear without any doubt that the present of corrosion inhibitors reduce weight loss.

Table 4.28: Weight loss measurements on zinc exposed in 1.5 M H<sub>2</sub>SO<sub>4</sub> in the presence of 3CYC

Concentration of inhibitor (M)	Weight loss (g)			
	303K	313K	323K	333K
0.000	0.5272	0.7677	1.1651	1.8519
2x10 <sup>-4</sup>	0.1449	0.1933	0.3058	0.6067
4x10 <sup>-4</sup>	0.1425	0.1589	0.2561	0.4934
6x10 <sup>-4</sup>	0.1352	0.1565	0.2154	0.4428
8x10 <sup>-4</sup>	0.1272	0.1477	0.2135	0.3617
10x10 <sup>-4</sup>	0.1241	0.1422	0.1784	0.3285

Table 4.29: Weight loss measurements on zinc exposed in 1.5 M H<sub>2</sub>SO<sub>4</sub> in the presence of 6MCH

Concentration of inhibitor (M)	Weight loss (g)			
	303K	313K	323K	333K
0.000	0.5272	0.7677	1.1651	1.8519
2x10 <sup>-4</sup>	0.1883	0.2816	0.4426	0.6802
4x10 <sup>-4</sup>	0.1769	0.2707	0.4209	0.6641
6x10 <sup>-4</sup>	0.1736	0.2602	0.4003	0.6444
8x10 <sup>-4</sup>	0.1731	0.2525	0.3862	0.6044
10x10 <sup>-4</sup>	0.1623	0.2477	0.3742	0.5593

Table 4.30: Weight loss measurements on zinc exposed in 1.5 M H<sub>2</sub>SO<sub>4</sub> in the presence of 6MC2C

Concentration of inhibitor (M)	Weight loss (g)			
	303K	313K	323K	333K
0.000	0.5272	0.7677	1.1651	1.8519
2x10 <sup>-4</sup>	0.3454	0.4966	0.7399	1.1073
4x10 <sup>-4</sup>	0.3451	0.4964	0.7286	1.0659
6x10 <sup>-4</sup>	0.3208	0.4764	0.7095	1.0592
8x10 <sup>-4</sup>	0.3124	0.4702	0.7057	1.0154
10x10 <sup>-4</sup>	0.1591	0.2078	0.6090	1.0053

 Table 4.31: Weight loss measurements on zinc exposed in 1.5 M CH<sub>3</sub>COOH in the presence of 3CYC

Concentration of inhibitor (M)	Weight loss (g)			
	303K	313K	323K	333K
0.000	0.0608	0.0648	0.0922	0.1483
2x10 <sup>-4</sup>	0.0144	0.0281	0.0557	0.1165
4x10 <sup>-4</sup>	0.0114	0.0266	0.0352	0.0814
6x10 <sup>-4</sup>	0.0106	0.0192	0.0346	0.0676
8x10 <sup>-4</sup>	0.0103	0.0179	0.0278	0.0461
10x10 <sup>-4</sup>	0.0102	0.0130	0.0262	0.0436

 Table 4.32: Weight loss measurements on zinc exposed in 1.5 M CH<sub>3</sub>COOH in the presence of 6MCH

Concentration of inhibitor (M)	Weight loss (g)			
	303K	313K	323K	333K
0.000	0.0608	0.0648	0.0922	0.1483
2x10 <sup>-4</sup>	0.0154	0.0618	0.0858	0.1033
4x10 <sup>-4</sup>	0.0149	0.0467	0.0642	0.0895
6x10 <sup>-4</sup>	0.0145	0.0319	0.0569	0.0888
8x10 <sup>-4</sup>	0.0135	0.0217	0.0539	0.0765
10x10 <sup>-4</sup>	0.0083	0.0212	0.0224	0.0598

 Table 4.33: Weight loss measurements on zinc exposed in 1.5 M CH<sub>3</sub>COOH in the presence of 6MC2C

Concentration of inhibitor (M)	Weight loss (g)			
	303K	313K	323K	333K
0.000	0.0608	0.0648	0.0922	0.1483
2x10 <sup>-4</sup>	0.0143	0.0417	0.0651	0.1103
4x10 <sup>-4</sup>	0.0138	0.0348	0.0602	0.0615
6x10 <sup>-4</sup>	0.0135	0.0286	0.0597	0.0608
8x10 <sup>-4</sup>	0.0125	0.0218	0.0519	0.0565
10x10 <sup>-4</sup>	0.0102	0.0213	0.0394	0.0481



Graphs in Figures 4.108–4.113 confirm that 3CYC, 6MCH and 6MC2C are good corrosion inhibitors. This can be seen clearly when comparing weight loss before introducing corrosion inhibitor with weight lost in the present of corrosion inhibitor. As indicated by graphs in Figures 4.108–4.113. The longer the bar on the bar graphs above imply more mass loss, that mean if the bar is shorter then mass loss was small. For example, yellow bar in Figure 4.113 is shorter compared to other within same graph. This implies that mass loss at 303K were lower when compared to mass loss at 333K. This shows that when temperature increases the mass loss also increases.

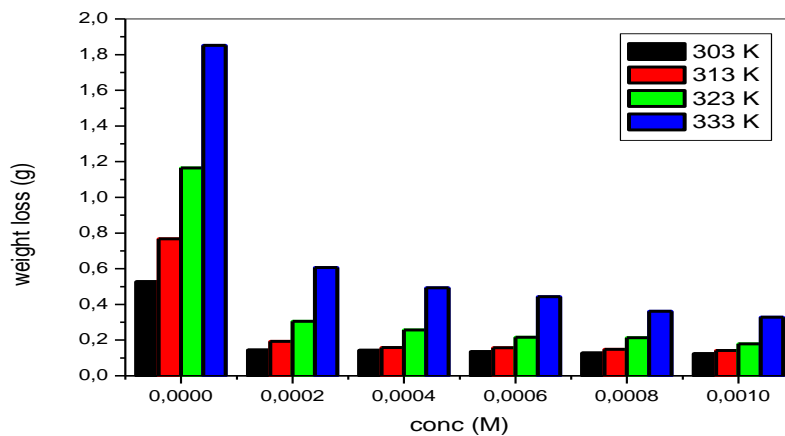


Figure 4.108: Weight loss measurements on zinc exposed in 1.5 M H<sub>2</sub>SO<sub>4</sub> in the presence of 3CYC

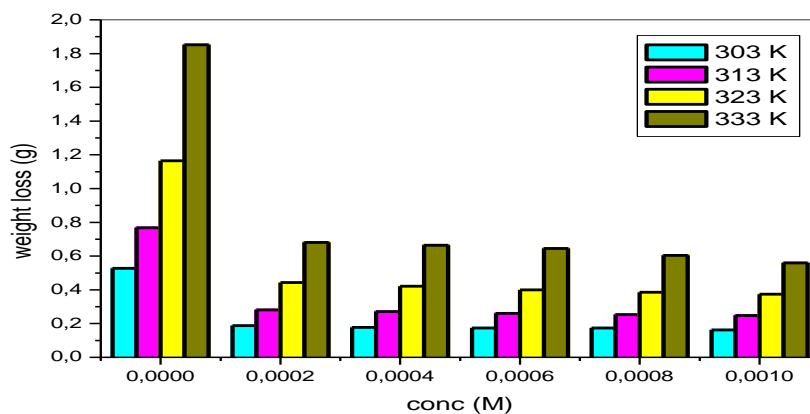


Figure 4.109: Weight loss measurements on zinc exposed in 1.5 M H<sub>2</sub>SO<sub>4</sub> in the presence of 6MCH

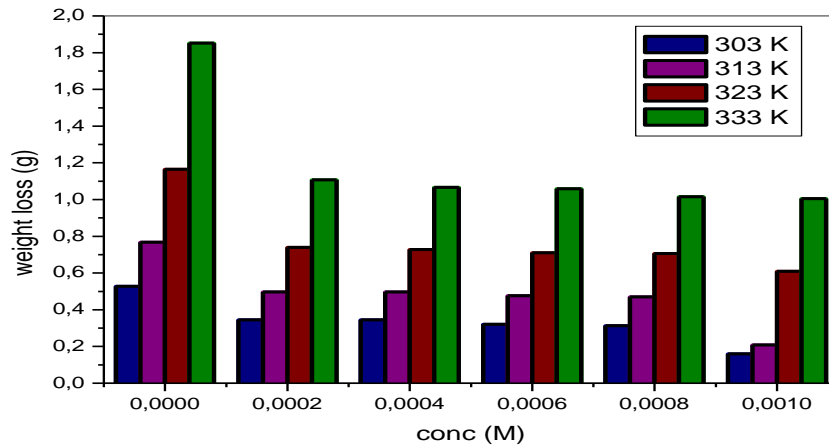


Figure 4.110: Weight loss measurements on zinc exposed in 1.5 M H<sub>2</sub>SO<sub>4</sub> in the presence of 6MC2C

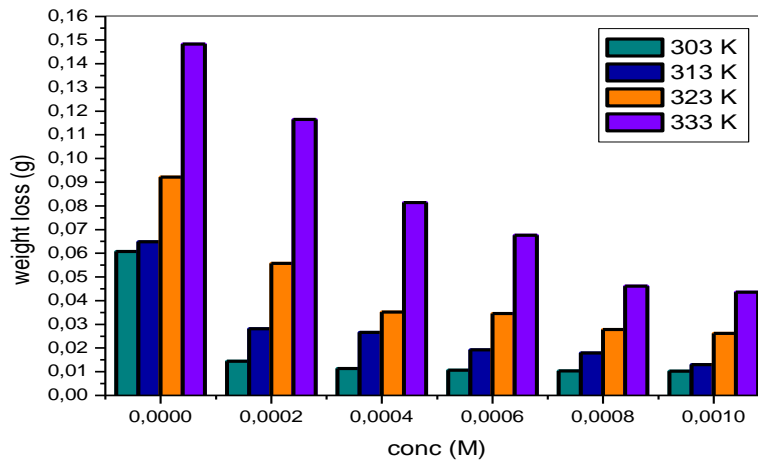


Figure 4.111: Weight loss measurements on zinc exposed in 1.5 M CH<sub>3</sub>COOH in the presence of 3CYC

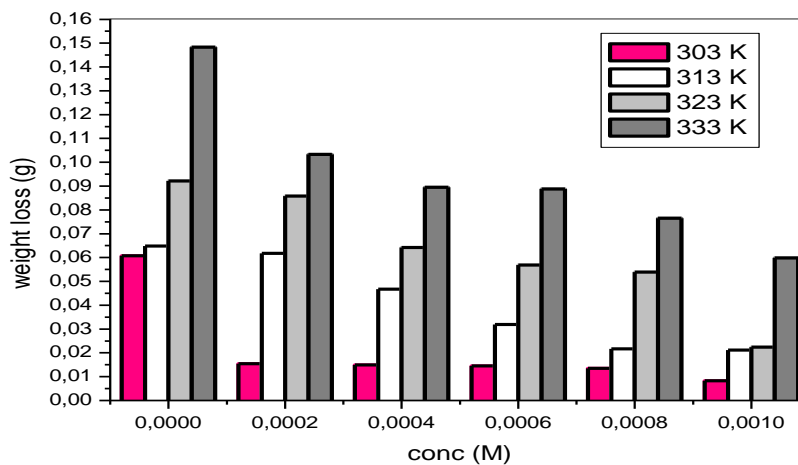


Figure 4.112: Weight loss measurements on zinc exposed in 1.5 M CH<sub>3</sub>COOH in the presence of 6MCH

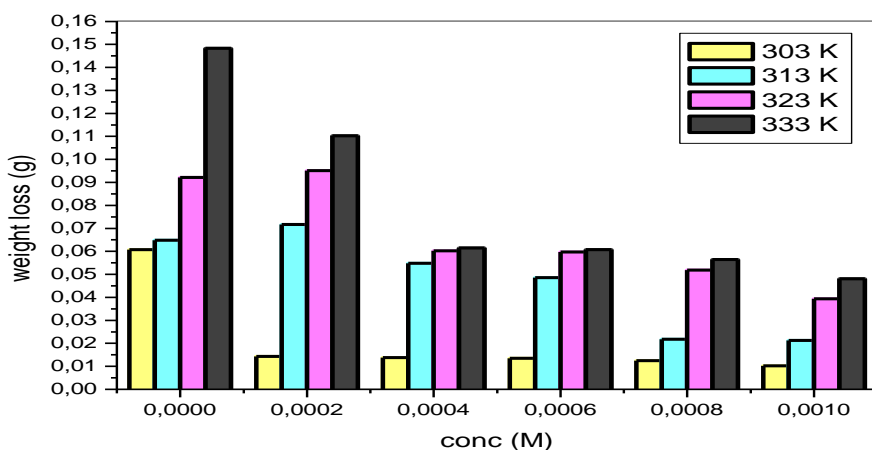


Figure 4.113: Weight loss measurements on zinc exposed in 1.5 M  $\text{CH}_3\text{COOH}$  in the presence of 6MC2C

Table 4.34: Weight loss measurements on aluminium exposed in 1.5 M  $\text{HNO}_3$  in the presence of 3CYC

Concentration Of inhibitor (M)	Weight loss (g)			
	303K	313K	323K	333K
$2 \times 10^{-4}$	0.0045	0.0081	0.0137	0.0231
$4 \times 10^{-4}$	0.0034	0.0063	0.0126	0.0209
$6 \times 10^{-4}$	0.0024	0.0048	0.0112	0.0170
$8 \times 10^{-4}$	0.0020	0.0029	0.0109	0.0167
$10 \times 10^{-4}$	0.0009	0.0018	0.0101	0.0151

Table 4.35: Weight loss measurements on aluminium exposed in 1.5 M  $\text{HNO}_3$  in the presence of 6MC2C

Concentration Of inhibitor (M)	Weight loss (g)			
	303K	313K	323K	333K
$2 \times 10^{-4}$	0.0013	0.0046	0.0049	0.0146
$4 \times 10^{-4}$	0.0010	0.0029	0.0043	0.0106
$6 \times 10^{-4}$	0.0007	0.0027	0.0034	0.0104
$8 \times 10^{-4}$	0.0002	0.0026	0.0029	0.0102
$10 \times 10^{-4}$	0.0001	0.0017	0.0023	0.0085

Table 4.36: Weight loss measurements on aluminium exposed in 1.5 M HNO<sub>3</sub> in the presence of 6MCH

Concentration Of inhibitor (M)	Weight loss (g)			
	303K	313K	323K	333K
$2 \times 10^{-4}$	0.0020	0.0057	0.0088	0.0156
$4 \times 10^{-4}$	0.0018	0.0039	0.0077	0.0131
$6 \times 10^{-4}$	0.0016	0.0031	0.0062	0.0125
$8 \times 10^{-4}$	0.0015	0.0025	0.0055	0.0121
$10 \times 10^{-4}$	0.0005	0.0019	0.0041	0.0110

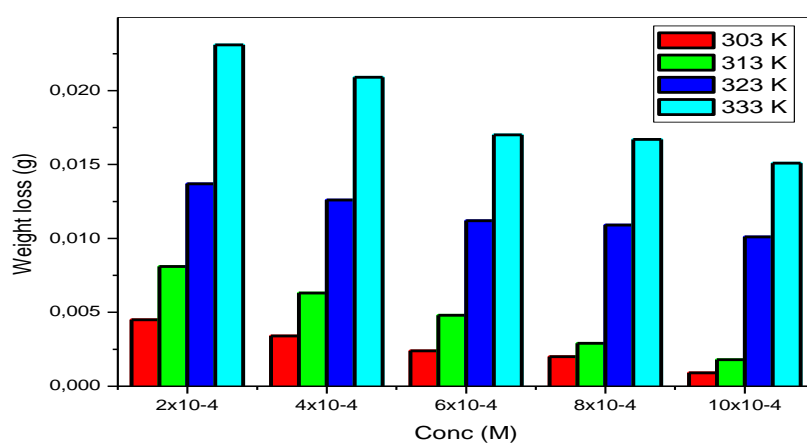


Figure 4.114: Weight loss measurements on aluminium exposed in 1.5 M HNO<sub>3</sub> in the presence of 3CYC

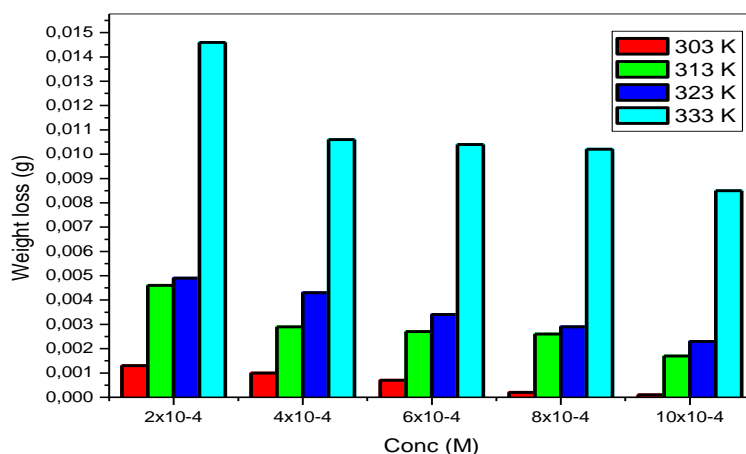


Figure 4.2: Weight loss measurements on aluminium exposed in 1.5 M HNO<sub>3</sub> in the presence of 6MC2C

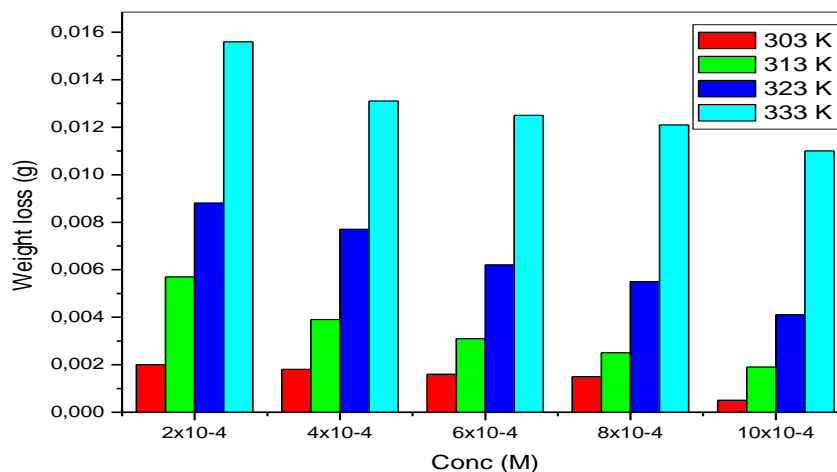


Figure 4.116: Weight loss measurements on aluminium exposed in 1.5 M HNO<sub>3</sub> in the presence of 6MCH

#### 4.1 The adsorption isotherms

The adsorption isotherms display information about the interaction of adsorbed molecules with a metal surface [106]. Studies show that good corrosion inhibitors adsorb onto metal and form thin layer that will protect metal from corrosive attack. The extents at which 3CYC, 6MCH and 6MC2C covered and protect metal from corrosive attack were studied. The primary step in the action of inhibitors in acid solution is generally agreed to be the adsorption on the metal surface. This is based on the assumption that the corrosion reactions are prevented from proceeding over the area (or active sites) of the metal surface covered by adsorbed inhibitor species, whereas these corrosion reactions occur normally on the inhibitor-free area. The surface coverage,  $\theta$ , is useful in discussing the adsorption characteristics. The value of surface coverage of good corrosion inhibitor should be closer to unity but not necessarily equals to 1. This is due to the assumption that adsorbed species cannot proceed beyond the actual surface of the metal. Adsorption isotherm studies provide information describing mechanism on how the organic inhibitor adsorb to the metal surface. There are numerous factors that govern this process, thus include the nature and charge of the metal surface, adsorption of solvent and other ionic species, electronic characteristics of the metal surface, a temperature of corrosion reactants, and electronic potential of metal-solution interface. Tables 4.37–4.41 show the surface coverage of different metals exposed to acidic medium.

It is clear from Tables 4.37–4.41 that the surface coverage especially at 303K is higher when compared to other temperatures. This shows that 3CYC, 6MCH and 6MC2C work efficiently at 303K. This implies that the more temperature increases, the more corrosive the acid become. Table 4.37 indicate maximum surface coverage of 0.9922 at highest concentration of 6MC2C, this implies that when the concentration of 6MC2C increase the extent at which 6MC2C adsorb and covers the surface area of mild steel metal also increases. Table 4.40 shows a minimum surface coverage value of 0.2144 for compound 3CYC exposed to acetic acid at 333K. This shows that 3CYC were failing to cover the zinc metal. The general trend observed shows that when temperature increases the surface coverage decrease. This might be caused by molecules of 3CYC, 6MCH and 6MC2C failing to adsorb onto surface area of metal.

Table 4.37: Surface coverage for mild steel exposed in H<sub>2</sub>SO<sub>4</sub>

Corrosion inhibitor	Concentration (M)	Surface coverage( $\theta$ )			
		303K	313K	323K	333K
	0.00	-	-	-	-
3CYC	2x10 <sup>-4</sup>	0.8584	0.8376	0.7305	0.6479
	4x10 <sup>-4</sup>	0.9351	0.8917	0.8240	0.6948
	6x10 <sup>-4</sup>	0.9471	0.9295	0.8703	0.7818
	8x10 <sup>-4</sup>	0.9617	0.9472	0.8971	0.8039
	10x10 <sup>-4</sup>	0.9796	0.9572	0.9382	0.8653
6MCH	2x10 <sup>-4</sup>	0.6849	0.6677	0.6370	0.5416
	4x10 <sup>-4</sup>	0.6925	0.6802	0.6449	0.5916
	6x10 <sup>-4</sup>	0.7057	0.6839	0.6518	0.6018
	8x10 <sup>-4</sup>	0.7288	0.6890	0.6636	0.6025
	10x10 <sup>-4</sup>	0.8412	0.7053	0.7091	0.6236
6MC2C	2x10 <sup>-4</sup>	0.8313	0.7848	0.6817	0.5876
	4x10 <sup>-4</sup>	0.8422	0.8308	0.7277	0.6102
	6x10 <sup>-4</sup>	0.9753	0.8796	0.7463	0.6236
	8x10 <sup>-4</sup>	0.9910	0.9406	0.7850	0.6385
	10x10 <sup>-4</sup>	0.9922	0.9885	0.8939	0.6575

Table 4.38: Surface coverage for mild steel exposed in CH<sub>3</sub>COOH

Corrosion inhibitor	Concentration (M)	Surface coverage			
		303K	313K	323K	333K
	0.00	-	-	-	-
3CYC	$2 \times 10^{-4}$	0.7340	0.4928	0.4958	0.4559
	$4 \times 10^{-4}$	0.7740	0.5896	0.5263	0.5770
	$6 \times 10^{-4}$	0.7920	0.6631	0.6095	0.5859
	$8 \times 10^{-4}$	0.8660	0.6864	0.7547	0.6579
	$10 \times 10^{-4}$	0.9000	0.7007	0.7632	0.6674
6MCH	$2 \times 10^{-4}$	0.5250	0.2687	0.3070	0.4093
	$4 \times 10^{-4}$	0.5833	0.3284	0.3377	0.4116
	$6 \times 10^{-4}$	0.6000	0.3955	0.3684	0.4581
	$8 \times 10^{-4}$	0.7750	0.4030	0.3860	0.4837
	$10 \times 10^{-4}$	0.8167	0.4776	0.5921	0.4860
6MC2C	$2 \times 10^{-4}$	0.7500	0.5448	0.2807	0.5140
	$4 \times 10^{-4}$	0.7750	0.5746	0.4693	0.5326
	$6 \times 10^{-4}$	0.8000	0.6045	0.5702	0.6163
	$8 \times 10^{-4}$	0.8250	0.6493	0.5746	0.6465
	$10 \times 10^{-4}$	0.8583	0.6791	0.5921	0.7419

Table 4.39: Surface coverage for zinc exposed in  $H_2SO_4$

Corrosion inhibitor	Concentration (M)	Surface coverage			
		303K	313K	323K	333K
	0.00	-	-	-	-
3CYC	$2 \times 10^{-4}$	0.7252	0.7482	0.7375	0.6724
	$4 \times 10^{-4}$	0.7297	0.7930	0.7802	0.7336
	$6 \times 10^{-4}$	0.7436	0.7961	0.8151	0.7609
	$8 \times 10^{-4}$	0.7587	0.8076	0.8168	0.8047
	$10 \times 10^{-4}$	0.7646	0.8148	0.8469	0.8226
6MCH	$2 \times 10^{-4}$	0.6428	0.6332	0.6201	0.6327
	$4 \times 10^{-4}$	0.6645	0.6474	0.6387	0.6414
	$6 \times 10^{-4}$	0.6707	0.6611	0.6564	0.6520
	$8 \times 10^{-4}$	0.6717	0.6711	0.6685	0.6736
	$10 \times 10^{-4}$	0.6921	0.6773	0.6788	0.6980
6MC2C	$2 \times 10^{-4}$	0.3448	0.3531	0.3649	0.4021
	$4 \times 10^{-4}$	0.3454	0.3534	0.3746	0.4244
	$6 \times 10^{-4}$	0.3915	0.3794	0.3910	0.4280
	$8 \times 10^{-4}$	0.4074	0.3875	0.3943	0.4517
	$10 \times 10^{-4}$	0.6982	0.7293	0.4773	0.4572

Table 4.40: Surface coverage for zinc exposed in  $CH_3COOH$

Corrosion inhibitor	Concentration (M)	Surface coverage			
		303K	313K	323K	333K
	0.00	-	-	-	-
3CYC	$2 \times 10^{-4}$	0.7632	0.5664	0.3959	0.2144
	$4 \times 10^{-4}$	0.8125	0.5895	0.6182	0.4511
	$6 \times 10^{-4}$	0.8257	0.7037	0.6247	0.5442
	$8 \times 10^{-4}$	0.8306	0.7238	0.6985	0.6891
	$10 \times 10^{-4}$	0.8322	0.7994	0.7158	0.7060
6MCH	$2 \times 10^{-4}$	0.7467	0.0463	0.0694	0.3034
	$4 \times 10^{-4}$	0.7549	0.2793	0.3037	0.3965
	$6 \times 10^{-4}$	0.7615	0.5077	0.3829	0.4012
	$8 \times 10^{-4}$	0.7780	0.6651	0.4154	0.4842
	$10 \times 10^{-4}$	0.8635	0.6728	0.7570	0.5968
6MC2C	$2 \times 10^{-4}$	0.7648	0.3565	0.2939	0.2562
	$4 \times 10^{-4}$	0.7730	0.4630	0.3471	0.5853
	$6 \times 10^{-4}$	0.7780	0.5586	0.3525	0.5900
	$8 \times 10^{-4}$	0.7944	0.6636	0.4371	0.6190
	$10 \times 10^{-4}$	0.8322	0.6713	0.5727	0.6757

Table 4.41: Surface coverage for aluminium exposed in  $\text{HNO}_3$

Corrosion inhibitor	Concentration (M)	Surface coverage			
		303K	313K	323K	333K
	0.00	-	-	-	-
3CYC	$2 \times 10^{-4}$	0.5408	0.5737	0.4043	0.4487
	$4 \times 10^{-4}$	0.6531	0.6684	0.4522	0.5012
	$6 \times 10^{-4}$	0.7551	0.7474	0.5130	0.5943
	$8 \times 10^{-4}$	0.7959	0.8474	0.5261	0.6014
	$10 \times 10^{-4}$	0.9082	0.9053	0.5609	0.6396
6MCH	$2 \times 10^{-4}$	0.7959	0.7000	0.6174	0.6277
	$4 \times 10^{-4}$	0.8163	0.7947	0.6652	0.6874
	$6 \times 10^{-4}$	0.8367	0.8368	0.7304	0.7017
	$8 \times 10^{-4}$	0.8469	0.8684	0.7609	0.7111
	$10 \times 10^{-4}$	0.9490	0.9000	0.8217	0.7375
6MC2C	$2 \times 10^{-4}$	0.8673	0.7579	0.7870	0.6516
	$4 \times 10^{-4}$	0.8980	0.8474	0.8130	0.7470
	$6 \times 10^{-4}$	0.9286	0.8579	0.8522	0.7518
	$8 \times 10^{-4}$	0.9796	0.8632	0.8739	0.7566
	$10 \times 10^{-4}$	0.9898	0.9105	0.9000	0.7971

The extent at which corrosion inhibitor covers metal expressed in percentage is called inhibition efficiency. Tables 4.42–4.46 show the inhibition efficiency. General trend observed



in the Tables 4.42–4.46 was that as the temperature increases, the inhibition efficiency decreases due to an increase in rate of the dissolution process of mild steel and zinc metal and partial desorption of the inhibitor from the metal surface when temperature increase. High temperature causes to vigorous reaction which affects the inhibition power of compounds.

The maximum percentage inhibition efficiency of 6MCH in acetic acid medium is 86.35% at 303K temperature which decreases to 59.68% as the temperature increases up to 333K with 0.0010M Concentration of inhibitor. On other hand, 6MCH in sulphuric acid medium shows 69.21% inhibition efficiency at 303K of 0.0010M concentration of inhibitor and this IE increases to 69.80% as the temperature increases up to 333K. This implies that there were partial adsorptions of the inhibitor to the metal surface when temperature increases.

The maximum percentage inhibition efficiency of 6MC2C in acetic acid medium is 83.22% at 303K which decreases to 57.27 % as the temperature increases up to 323K and then increases to 67.57% when temperature raise to 333K with 0.0010M concentration of inhibitor. On other hand, 6MC2C in sulphuric acid medium shows 69.82%inhibition efficiency at 303K of 0.0010M concentration of inhibitor and this IE decreases to 45.72% as the temperature increases up to 333K. Experimental results reveal that % IE decreases with increasing temperature of both media. When temperature increases the surrounding environment contribute to an increase in mild steel and zinc corrosion rate.

Table 4.42: Inhibition efficiency for mild steel exposed in H<sub>2</sub>SO<sub>4</sub>

Corrosion inhibitor	Concentration (M)	Inhibition efficiency (IE%)			
		303K	313K	323K	333K
	0.00	-	-	-	-
3CYC	2x10 <sup>-4</sup>	85.84	83.76	73.05	64.79
	4x10 <sup>-4</sup>	93.51	89.17	82.40	69.48
	6x10 <sup>-4</sup>	94.71	92.95	87.03	78.18
	8x10 <sup>-4</sup>	96.17	94.72	89.71	80.39
	10x10 <sup>-4</sup>	97.96	95.72	93.82	86.53
6MCH	2x10 <sup>-4</sup>	68.49	66.77	63.70	54.16
	4x10 <sup>-4</sup>	69.25	68.02	64.49	59.16
	6x10 <sup>-4</sup>	70.57	68.39	65.18	60.18
	8x10 <sup>-4</sup>	72.88	68.90	66.36	60.25
	10x10 <sup>-4</sup>	84.12	70.53	70.91	62.36
6MC2C	2x10 <sup>-4</sup>	83.13	78.48	68.17	58.76
	4x10 <sup>-4</sup>	84.22	83.08	72.77	61.02
	6x10 <sup>-4</sup>	97.53	87.96	74.63	62.36
	8x10 <sup>-4</sup>	99.10	94.06	78.50	63.85

	$10 \times 10^{-4}$	99.22	98.85	89.39	65.75
--	---------------------	-------	-------	-------	-------

Table 4.43: Inhibition efficiency for mild steel exposed in  $\text{CH}_3\text{COOH}$

Corrosion inhibitor	Concentration (M)	Inhibition efficiency (IE%)			
		303K	313K	323K	333K
	0.00	-	-	-	-
3CYC	$2 \times 10^{-4}$	73.40	49.28	49.58	45.59
	$4 \times 10^{-4}$	77.40	58.96	52.63	57.70
	$6 \times 10^{-4}$	79.20	66.31	60.95	58.59
	$8 \times 10^{-4}$	86.60	68.64	75.47	65.79
	$10 \times 10^{-4}$	90.00	70.07	76.32	66.74
6MCH	$2 \times 10^{-4}$	52.50	26.87	30.70	40.93
	$4 \times 10^{-4}$	58.33	32.84	33.77	41.16
	$6 \times 10^{-4}$	60.00	39.55	36.84	45.81
	$8 \times 10^{-4}$	77.50	40.30	38.60	48.37
	$10 \times 10^{-4}$	81.67	47.76	59.21	48.60
6MC2C	$2 \times 10^{-4}$	75.00	54.48	28.07	51.40
	$4 \times 10^{-4}$	77.50	57.46	46.93	53.26
	$6 \times 10^{-4}$	80.00	60.45	57.02	61.63
	$8 \times 10^{-4}$	82.50	64.93	57.46	64.65
	$10 \times 10^{-4}$	85.83	67.91	59.21	74.19

Table 4.44: Inhibition efficiency for zinc exposed in  $\text{H}_2\text{SO}_4$

Corrosion inhibitor	Concentration (M)	Inhibition efficiency (IE%)			
		303K	313K	323K	333K
	0.00	-	-	-	-
3CYC	$2 \times 10^{-4}$	72.52	74.82	73.75	67.24
	$4 \times 10^{-4}$	72.97	79.30	78.02	73.36
	$6 \times 10^{-4}$	74.36	79.61	81.51	76.09
	$8 \times 10^{-4}$	75.87	80.76	81.68	80.47
	$10 \times 10^{-4}$	76.46	81.48	84.69	82.26
6MCH	$2 \times 10^{-4}$	64.28	63.32	62.01	63.27
	$4 \times 10^{-4}$	66.45	64.74	63.87	64.14
	$6 \times 10^{-4}$	67.07	66.11	65.64	65.20
	$8 \times 10^{-4}$	67.17	67.11	66.85	67.36
	$10 \times 10^{-4}$	69.21	67.73	67.88	69.80
6MC2C	$2 \times 10^{-4}$	34.48	35.31	36.49	40.21
	$4 \times 10^{-4}$	34.54	35.34	37.46	42.44
	$6 \times 10^{-4}$	39.15	37.94	39.10	42.80
	$8 \times 10^{-4}$	40.74	38.75	39.43	45.17
	$10 \times 10^{-4}$	69.82	72.93	47.73	45.72

Table 4.45: Inhibition efficiency for zinc exposed in  $\text{CH}_3\text{COOH}$

Corrosion inhibitor	Concentration (M)	Inhibition efficiency (IE%)			
		303K	313K	323K	333K

	0.00	-	-	-	-
3CYC	$2 \times 10^{-4}$	76.32	56.64	39.59	21.44
	$4 \times 10^{-4}$	81.25	58.95	61.82	45.11
	$6 \times 10^{-4}$	82.57	70.37	62.47	54.42
	$8 \times 10^{-4}$	83.06	72.38	69.85	68.91
	$10 \times 10^{-4}$	83.22	79.94	71.58	70.60
6MCH	$2 \times 10^{-4}$	74.67	04.63	06.94	30.34
	$4 \times 10^{-4}$	75.49	27.93	30.37	39.65
	$6 \times 10^{-4}$	76.15	50.77	38.29	40.12
	$8 \times 10^{-4}$	77.80	66.51	41.54	48.42
	$10 \times 10^{-4}$	86.35	67.28	75.70	59.68
6MC2C	$2 \times 10^{-4}$	76.48	35.65	29.39	25.62
	$4 \times 10^{-4}$	77.30	46.30	34.71	58.53
	$6 \times 10^{-4}$	77.80	55.86	35.25	59.00
	$8 \times 10^{-4}$	79.44	66.36	43.71	61.90
	$10 \times 10^{-4}$	83.22	67.13	57.27	67.57

 Table 4.46: Inhibition efficiency for aluminium exposed in  $\text{HNO}_3$ 

Corrosion inhibitor	Concentration (M)	Inhibition efficiency (IE%)			
		303K	313K	323K	333K
	0.00	-	-	-	-
3CYC	$2 \times 10^{-4}$	54.08	57.37	40.43	44.87
	$4 \times 10^{-4}$	65.31	66.84	45.22	50.12
	$6 \times 10^{-4}$	75.51	74.74	51.30	59.43
	$8 \times 10^{-4}$	79.59	84.74	52.61	60.14
	$10 \times 10^{-4}$	90.82	90.53	56.09	63.96
6MCH	$2 \times 10^{-4}$	79.59	70.00	61.74	62.77
	$4 \times 10^{-4}$	81.63	79.47	66.52	68.74
	$6 \times 10^{-4}$	83.67	83.68	73.04	70.17
	$8 \times 10^{-4}$	84.69	86.84	76.09	71.11
	$10 \times 10^{-4}$	94.90	90.00	82.17	73.75
6MC2C	$2 \times 10^{-4}$	86.73	75.79	78.70	65.16
	$4 \times 10^{-4}$	89.80	84.74	81.30	74.70
	$6 \times 10^{-4}$	92.86	85.79	85.22	75.18
	$8 \times 10^{-4}$	97.96	86.32	87.39	75.66
	$10 \times 10^{-4}$	98.98	91.05	90.00	79.71

There exist several parameters that are directly or indirectly related to this behaviour, thus include the activation energy. The activation energy ( $E_a$ ) of either mild steel or zinc corrosion is the minimum amount of energy that mild steel or zinc components would require in order to produce the corrosion products, such as rust. High activation values are associated lower

dissolution of either zinc or mild steel metal whereas low values of activation energy are associated with high dissolution of mild steel or zinc metal.

The tendency of adsorption of 3CYC, 6MCH and 6MC2C onto surface of either zinc or mild steel and activation energy can be calculated using Arrhenius equation.

Equation (11) shows the type of Arrhenius equation to calculate  $E_a$  for mild steel and zinc corrosion

$$\log(C_R) = \log A - \left( \frac{E_a}{2.303R} \right) \left( \frac{1}{T} \right) \quad (11)$$

where  $C_R$  is the corrosion rate in  $\text{g}\cdot\text{cm}^{-2}\cdot\text{h}^{-1}$ ,  $A$  is the Arrhenius pre-exponential factor,  $R$  is the gas constant and  $T$  is the absolute temperature. The Arrhenius plots are shown in Figures 4.117–4.131

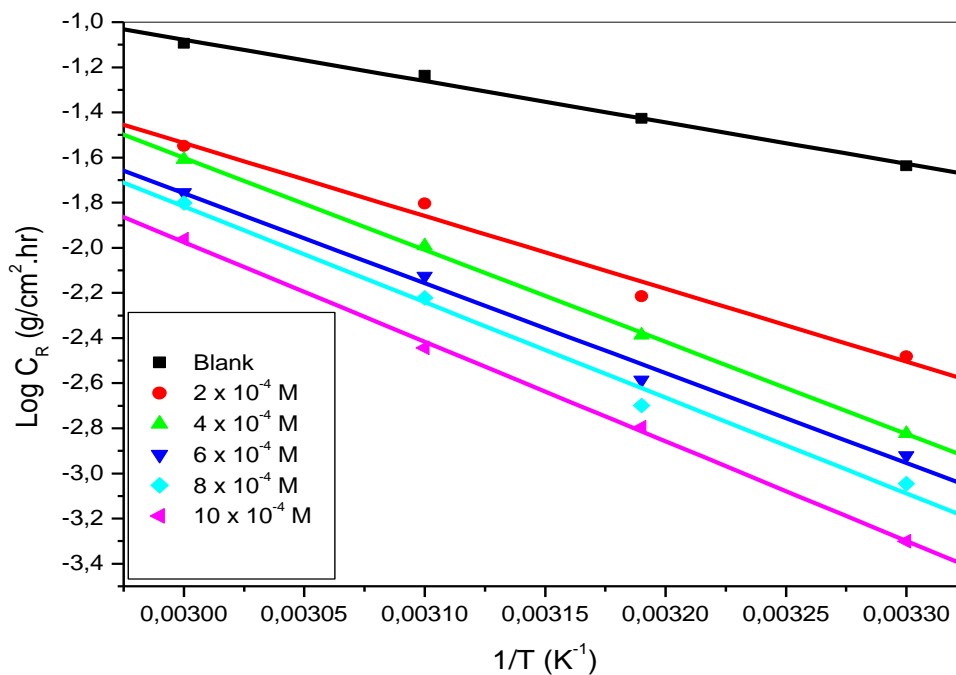


Figure 4.37: Arrhenius plots for the corrosion of mild steel in 1.5 M  $\text{H}_2\text{SO}_4$  in the absence and presence of various concentrations of 3CYC.

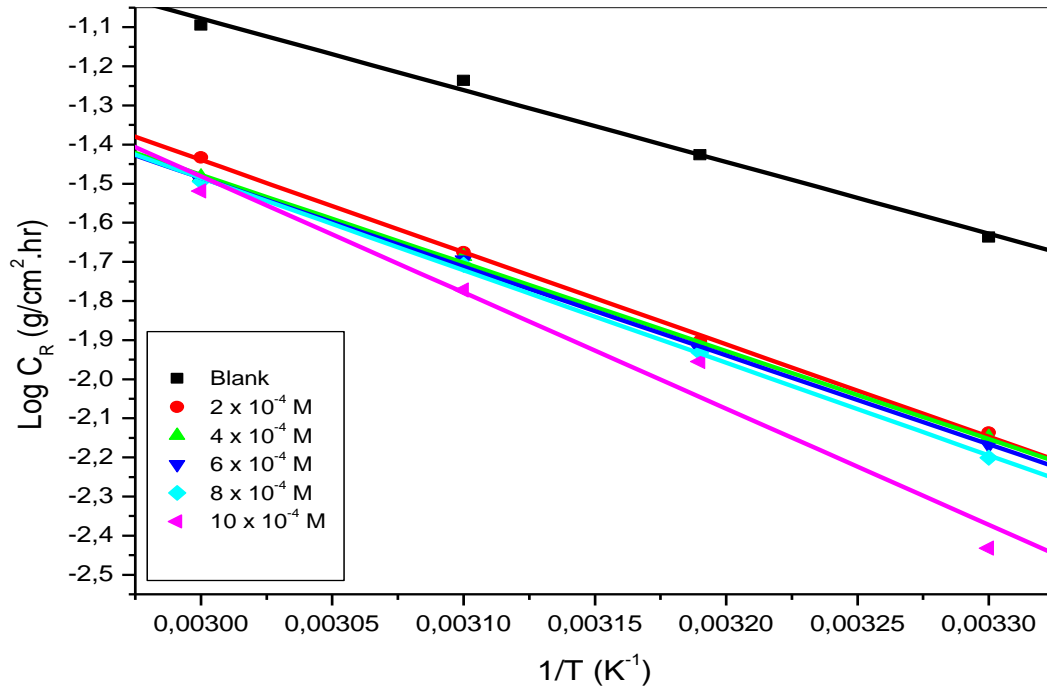


Figure 4.118: Arrhenius plots for the corrosion of mild steel in 1.5 M H<sub>2</sub>SO<sub>4</sub> in the absence and presence of various concentrations of 6MCH.

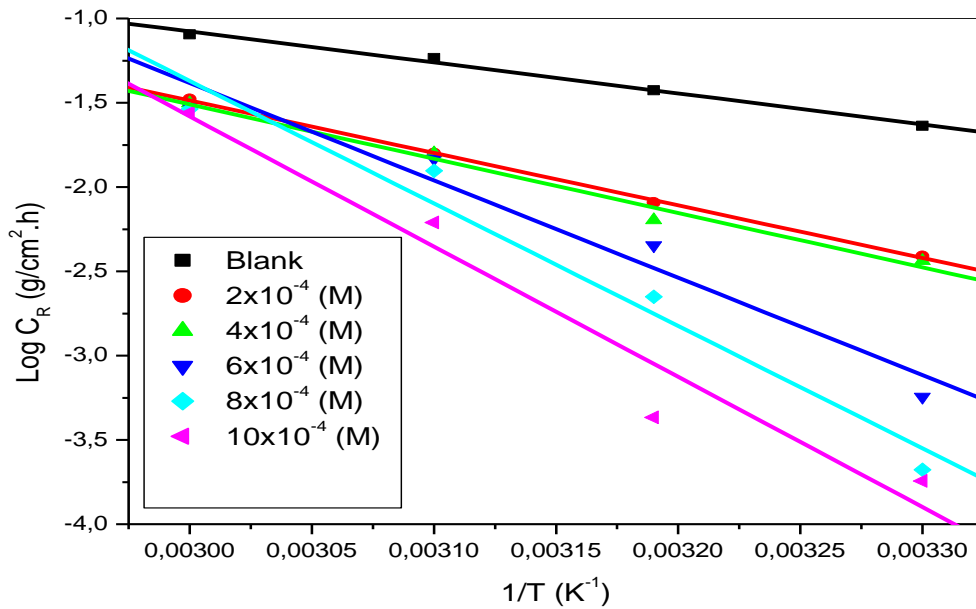


Figure 4.119: Arrhenius plots for the corrosion of mild steel in 1.5 M H<sub>2</sub>SO<sub>4</sub> in the absence and presence of various concentrations of 6MC2C.

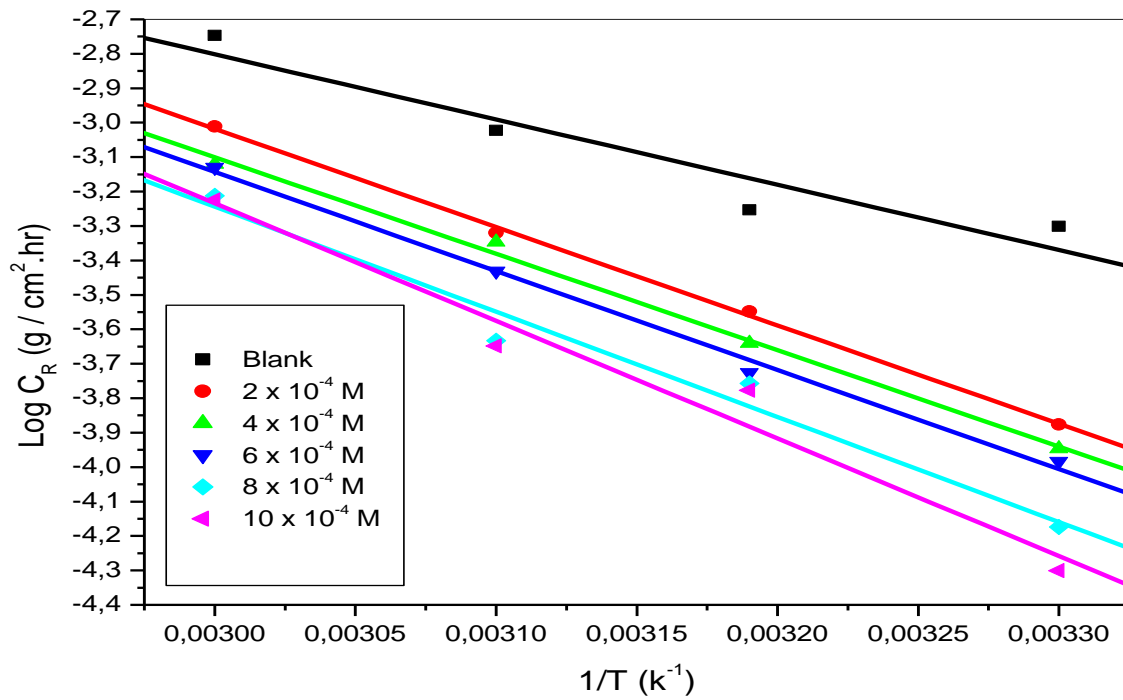


Figure 4.120: Arrhenius plots for the corrosion of mild steel in 1.5 M  $\text{CH}_3\text{COOH}$  in the absence and presence of various concentrations of 3CYC.

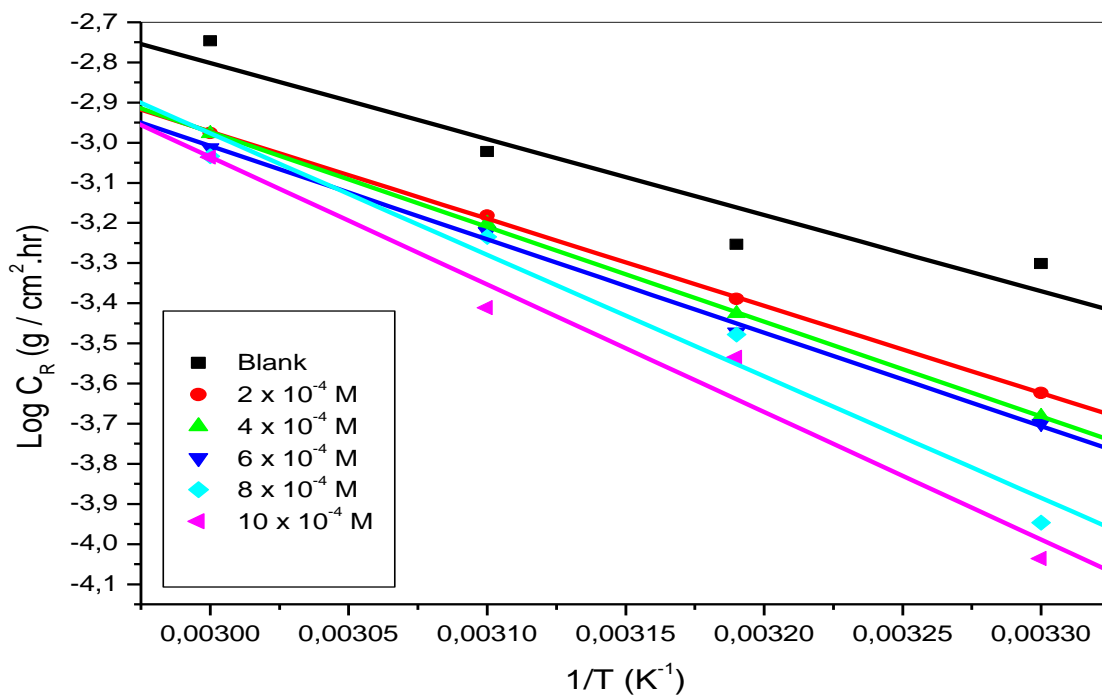


Figure 4.121: Arrhenius plots for the corrosion of mild steel in 1.5 M  $\text{CH}_3\text{COOH}$  in the absence and presence of various concentrations of 6MCH.

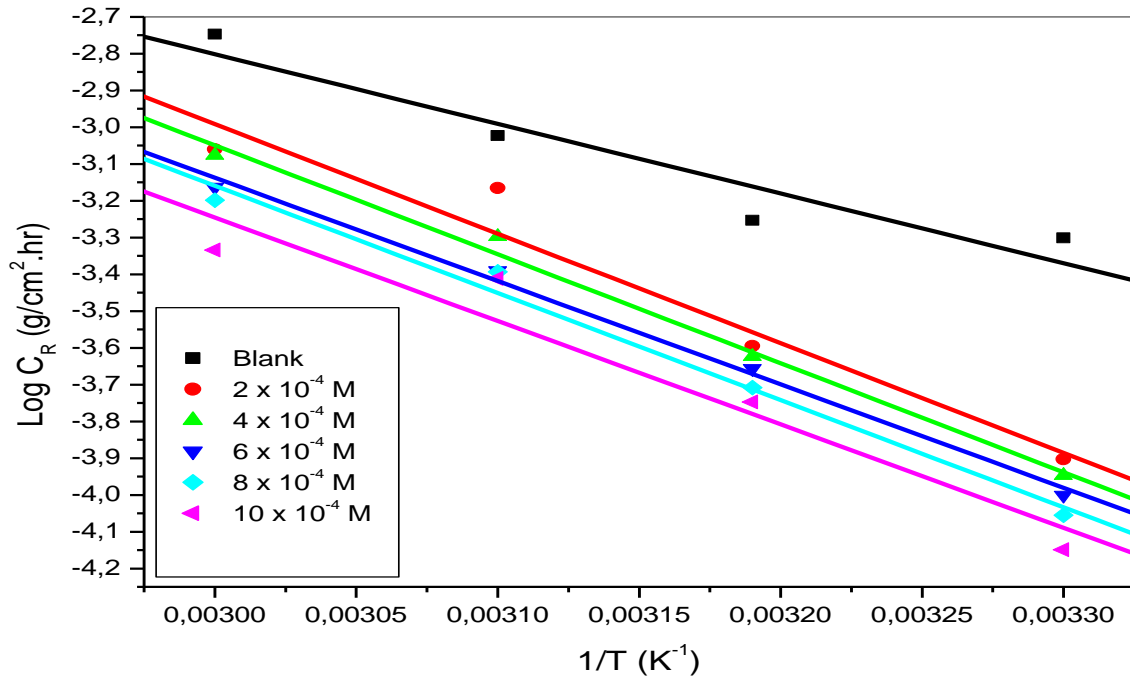


Figure 4.122: Arrhenius plots for the corrosion of mild steel in 1.5 M  $\text{CH}_3\text{COOH}$  in the absence and presence of various concentrations of 6MC2C.

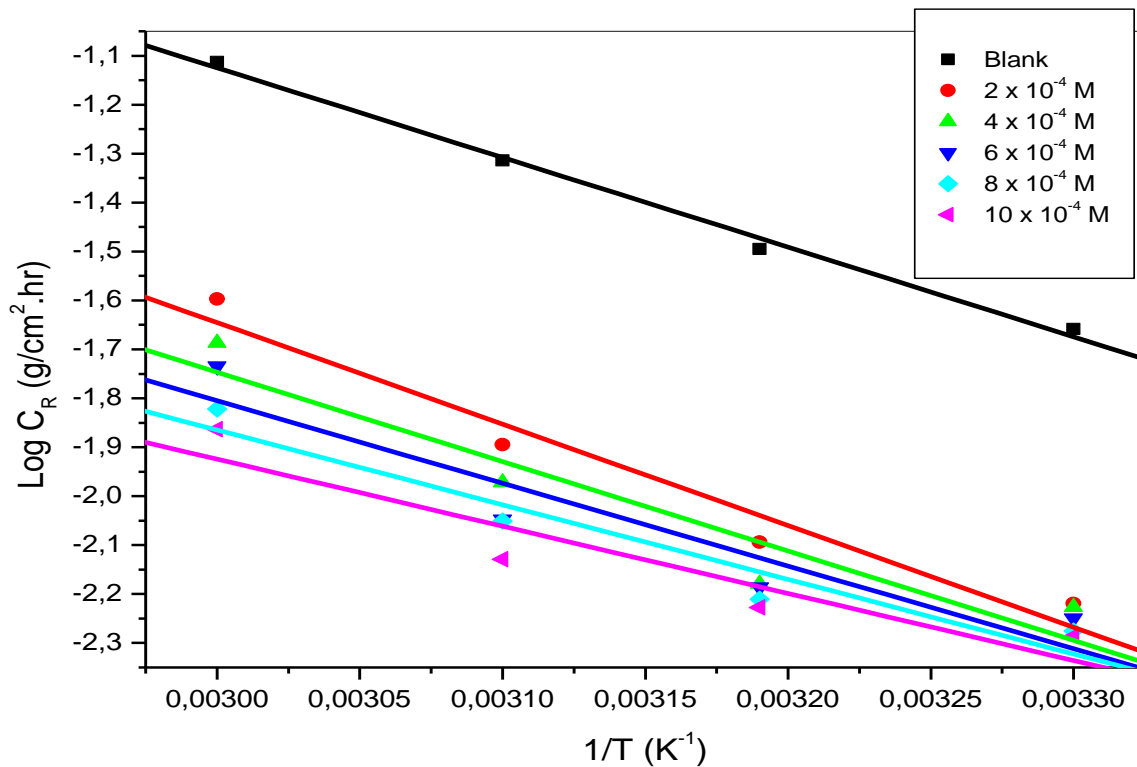


Figure 4.123: Arrhenius plots for the corrosion of zinc in 1.5 M  $\text{H}_2\text{SO}_4$  in the absence and presence of various concentrations of 3CYC.

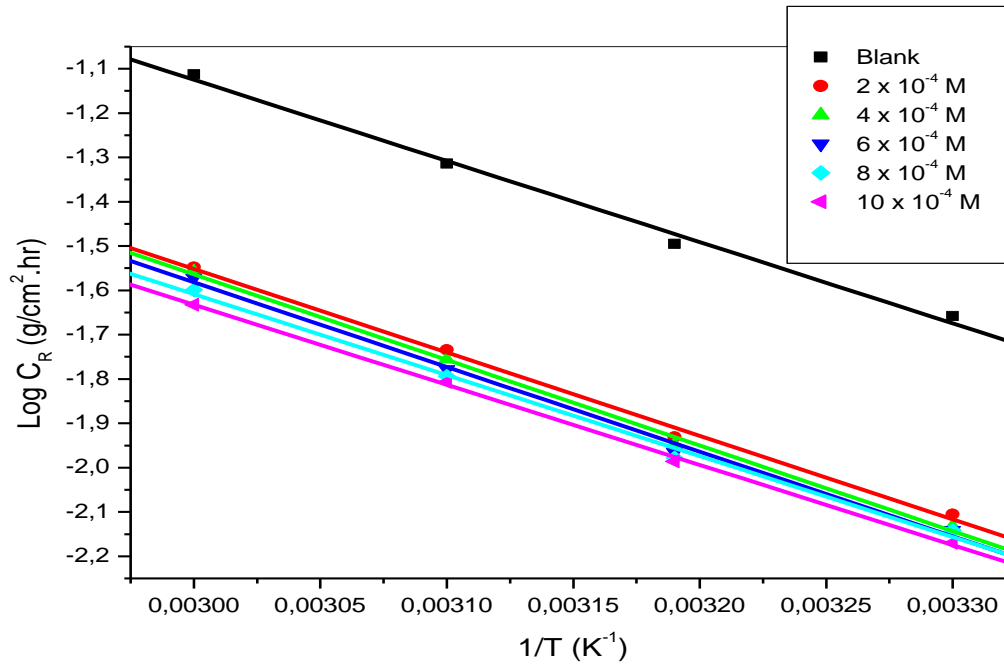


Figure 4.124: Arrhenius plots for the corrosion of zinc in 1.5 M H<sub>2</sub>SO<sub>4</sub> in the absence and presence of various concentrations of 6MCH.

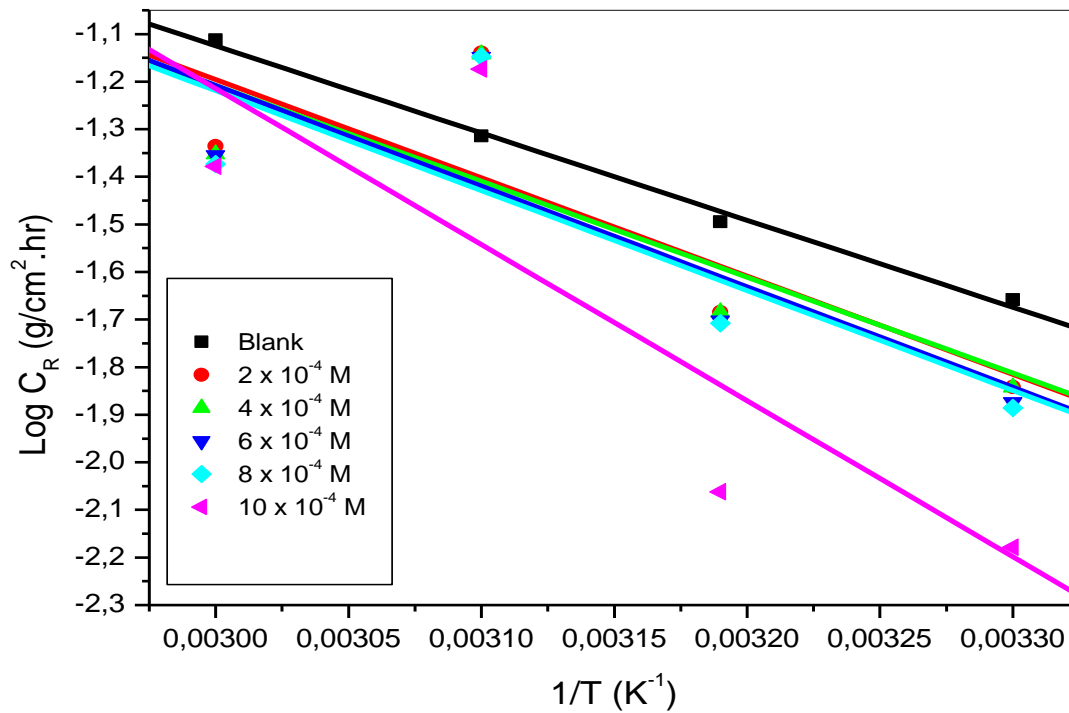


Figure 4.125: Arrhenius plots for the corrosion of zinc in 1.5 M H<sub>2</sub>SO<sub>4</sub> in the absence and presence of various concentrations of 6MC2C.



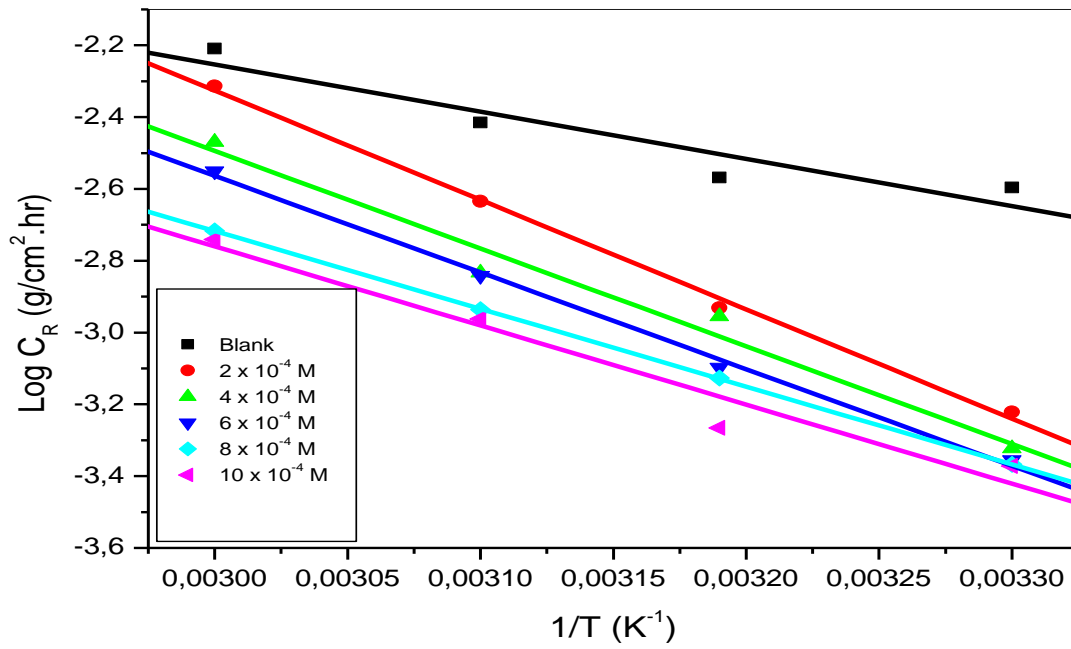


Figure 4.126: Arrhenius plots for the corrosion of zinc in 1.5 M CH<sub>3</sub>COOH in the absence and presence of various concentrations of 3CYC.

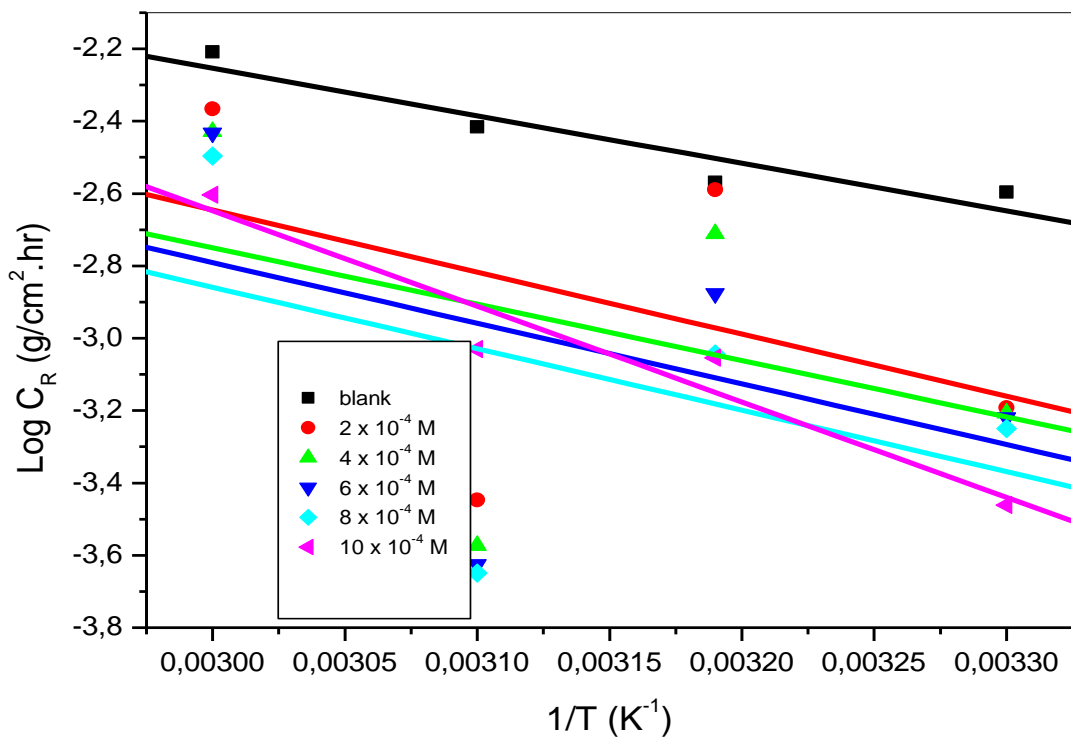


Figure 4.127: Arrhenius plots for the corrosion of zinc in 1.5 M CH<sub>3</sub>COOH in the absence and presence of various concentrations of 6MCH.

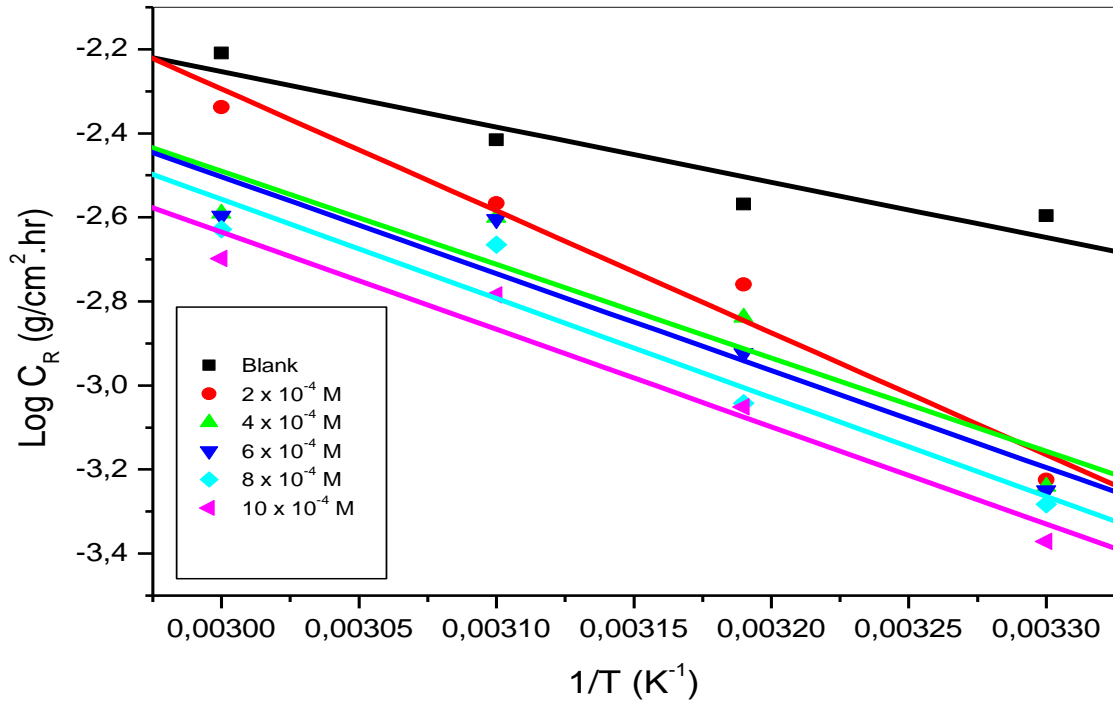


Figure 4.128: Arrhenius plots for the corrosion of zinc in 1.5 M  $\text{CH}_3\text{COOH}$  in the absence and presence of various concentrations of 6MC2C.

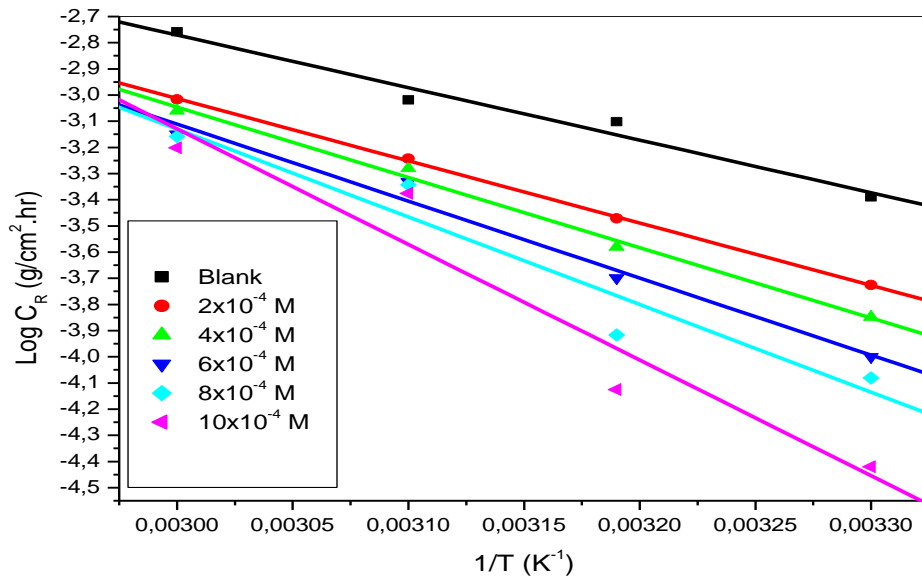


Figure 4.129: Arrhenius plots for the corrosion of aluminium in 1.5 M  $\text{HNO}_3$  in the absence and presence of various concentrations of 3CYC.

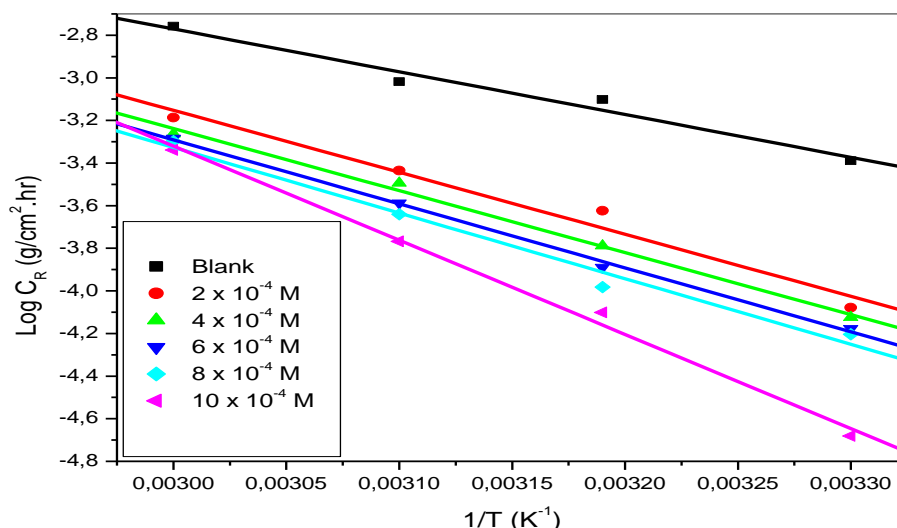


Figure 4.130: Arrhenius plots for the corrosion of aluminium in 1.5 M HNO<sub>3</sub> in the absence and presence of various concentrations of 6MCH.

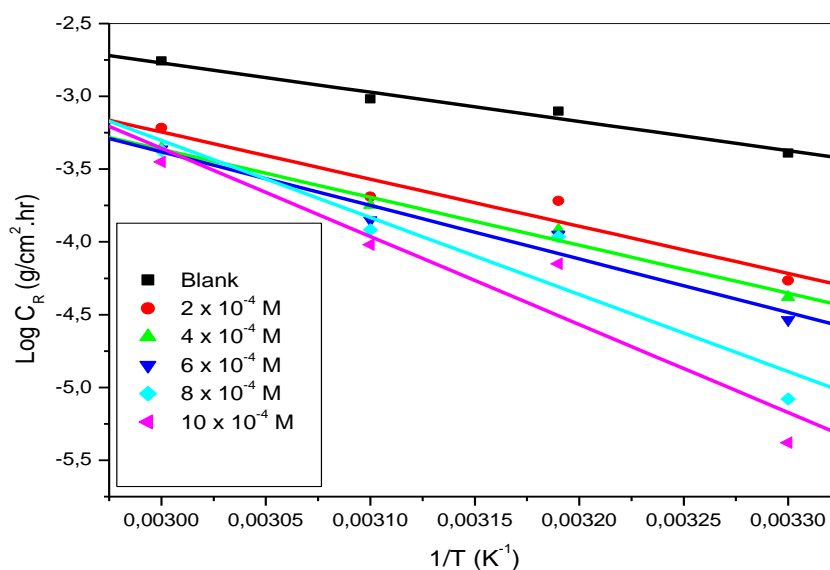


Figure 4.131: Arrhenius plots for the corrosion of aluminium in 1.5 M HNO<sub>3</sub> in the absence and presence of various concentrations of 6MC2C.

The Arrhenius plots above were useful in calculating the activation energy. Studies indicate that the activation energy values of effective inhibitor increase with the increase in the concentrations of inhibitor molecules. Thus implies that the activation energy corresponding to the uninhibited mild steel and zinc corrosion is always less than that of the inhibited process [40]. Tables 4.47–4.51 show corrosion parameters such as adsorption and gibbs.

Table 4.47: Thermodynamic and adsorption parameters for mild steel in 1.5 M H<sub>2</sub>SO<sub>4</sub> at various temperatures for the utilized corrosion inhibitors.

Inhibitor	Temperature(K)	K <sub>ads</sub> (M <sup>-1</sup> )	ΔG <sub>ads</sub> <sup>o</sup> (kJ/mol)
3CYC	303	28.20	-18.53
	313	23.76	-18.70
	323	11.88	-17.44
	333	07.90	-16.85
6MCH	303	09.33	-15.75
	313	38.63	-19.96
	323	16.45	-18.31
	333	17.04	-18.97
6MC2C	303	14.41	-16.84
	313	10.99	-16.69
	323	08.29	-16.47
	333	17.04	-18.97

Table 4.48: Thermodynamic and adsorption parameters for mild steel in 1.5 M CH<sub>3</sub>COOH at various temperatures for the utilized corrosion inhibitors.

Inhibitor	Temperature(K)	K <sub>ads</sub> (M <sup>-1</sup> )	ΔG <sub>ads</sub> <sup>o</sup> (kJ/mol)
3CYC	303	11.00	-16.16
	313	06.35	-15.27
	323	03.71	-14.31
	333	05.50	-15.84
6MCH	303	03.92	-13.56
	313	02.12	-12.41
	323	01.79	-12.35
	333	06.64	-16.36
6MC2C	303	17.06	-17.27
	313	07.82	-15.81
	323	02.55	-13.30
	333	04.57	-15.33

Table 4.49: Thermodynamic and adsorption parameters for zinc in 1.5 M H<sub>2</sub>SO<sub>4</sub> at various temperatures for the utilized corrosion inhibitors.

Inhibitor	Temperature(K)	K <sub>ads</sub> (M <sup>-1</sup> )	ΔG <sub>ads</sub> <sup>o</sup> (kJ/mol)
3CYC	303	36.76	-19.21
	313	39.52	-20.02
	323	19.76	-18.80
	333	12.18	-18.04
6MCH	303	31.54	-18.82
	313	29.58	-19.27
	323	22.07	-19.10
	333	17.60	-19.06

6MC2C	303	01.72	-11.49
	313	01.72	-11.49
	323	04.27	-14.69
	333	10.29	-17.58

Table 4.50: Thermodynamic and adsorption parameters for zinc in 1.5 M CH<sub>3</sub>COOH at various temperatures for the utilized corrosion inhibitors.

Inhibitor	Temperature(K)	K <sub>ads</sub>	$\Delta G_{ads}^{\circ}$ (kJ/mol)
3CYC	303	41.84	-19.53
	313	09.00	-16.17
	323	04.06	-14.55
	333	01.37	-11.99
6MCH	303	14.08	-16.78
	313	01.18	-10.89
	323	00.74	-09.98
	333	02.02	-13.07
6MC2C	303	24.39	-18.17
	313	02.64	-12.98
	323	01.72	-12.25
	333	02.23	-13.34

Table 4.51: Thermodynamic and adsorption parameters for aluminium in 1.5 M HNO<sub>3</sub> at various temperatures for the utilized corrosion inhibitors.

Inhibitor	Temperature(K)	K <sub>ads</sub>	$\Delta G_{ads}^{\circ}$ (kJ/mol)
3CYC	303	04.54	-45.93
	313	04.94	-51.63
	323	04.84	-52.20
	333	05.02	-55.82
6MCH	303	13.61	-137.70
	313	11.48	-119.99
	323	07.57	-81.65
	333	16.13	-179.36
6MC2C	303	19.75	-199.83
	313	18.18	-190.01
	323	18.47	-199.21
	333	15.30	-170.13

Figure 4.132 – 4.146 shows the transition state plots in the presence and absence of various concentration of the inhibitor. The black plot representing blank seems to be upper than other plots. The plots seem to shift down when the concentration of inhibitor increases. Figure 4.136 plots contain one point that deviate from other points within the same line, however, the best fit obtained yield straight line plot. These plots were used to calculating the activation energy, entropy, and change in enthalpy that was recorded in Table 4.52 – 4.56.

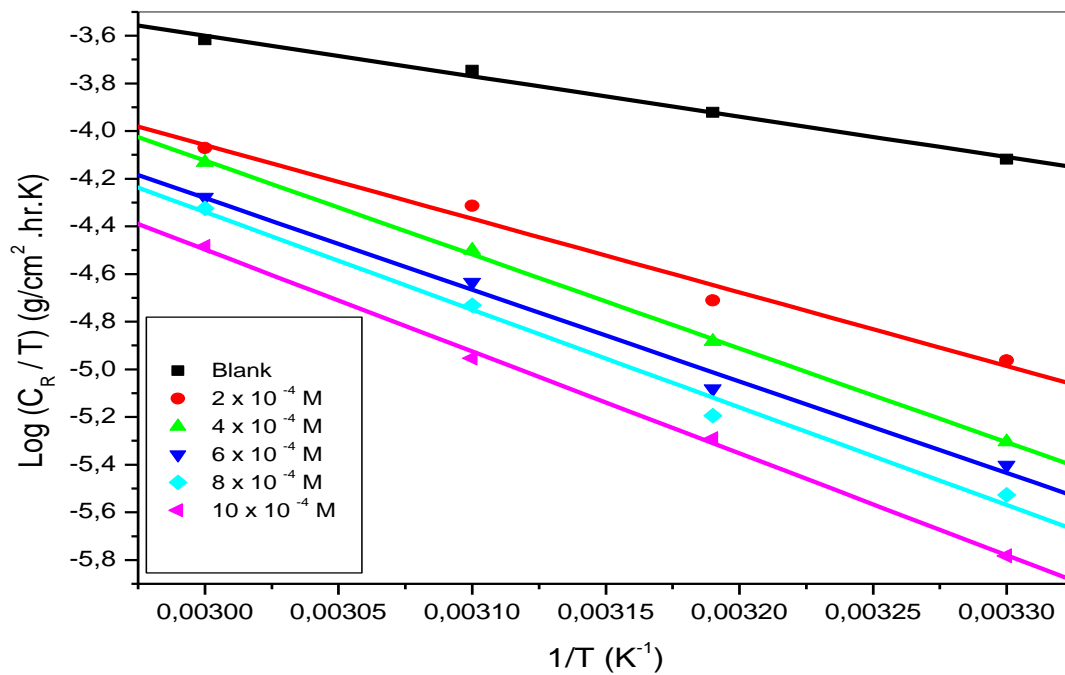


Figure 4.132: Transition state plots for the corrosion of mild steel in 1.5 M H<sub>2</sub>SO<sub>4</sub> in the absence and presence of various concentrations of 3CYC.

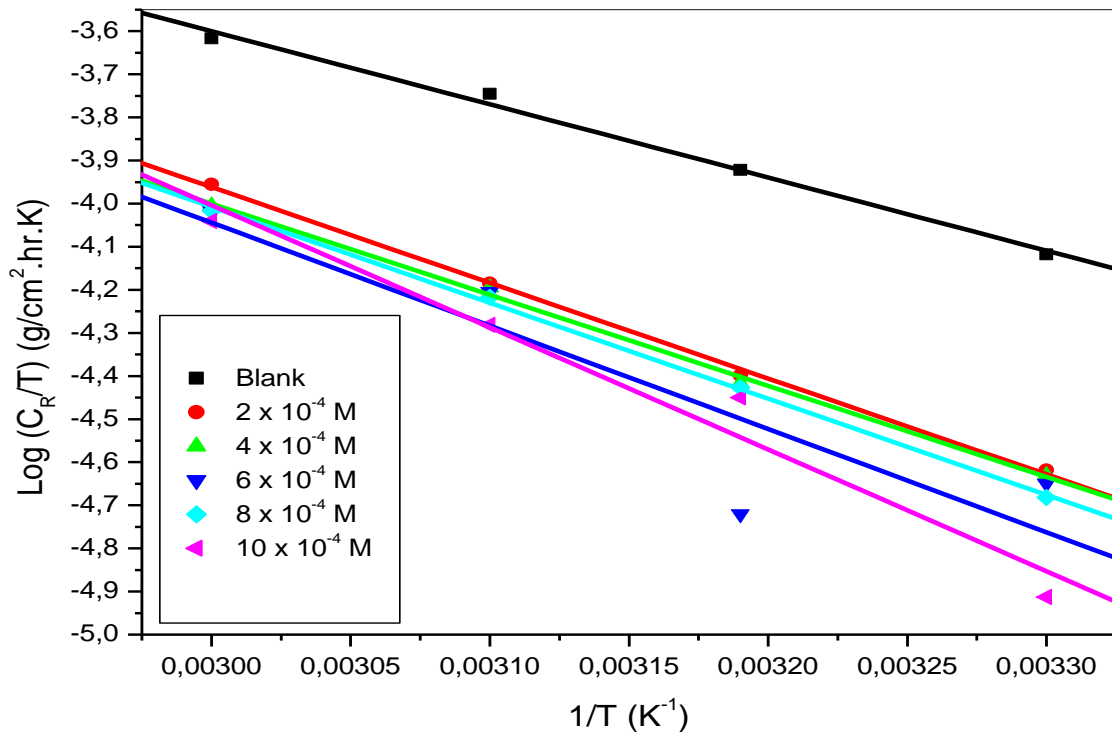


Figure 4.133: Transition state plots for the corrosion of mild steel in 1.5 M H<sub>2</sub>SO<sub>4</sub> in the absence and presence of various concentrations of 6MCH.

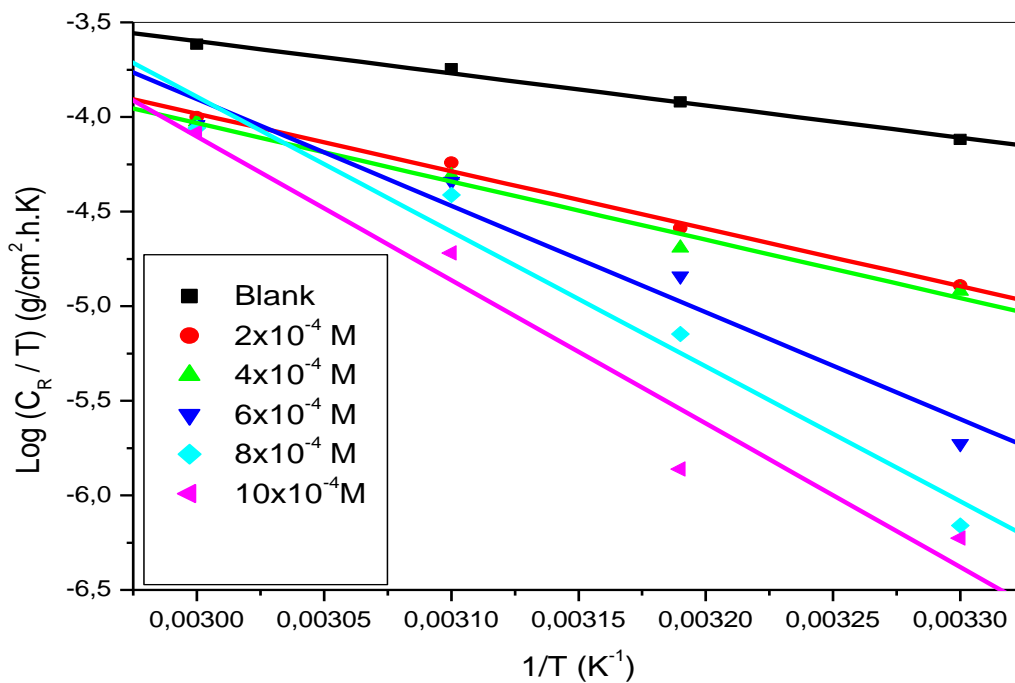


Figure 4.134: Transition state plots for the corrosion of mild steel in 1.5 M H<sub>2</sub>SO<sub>4</sub> in the absence and presence of various concentrations of 6MC2C.

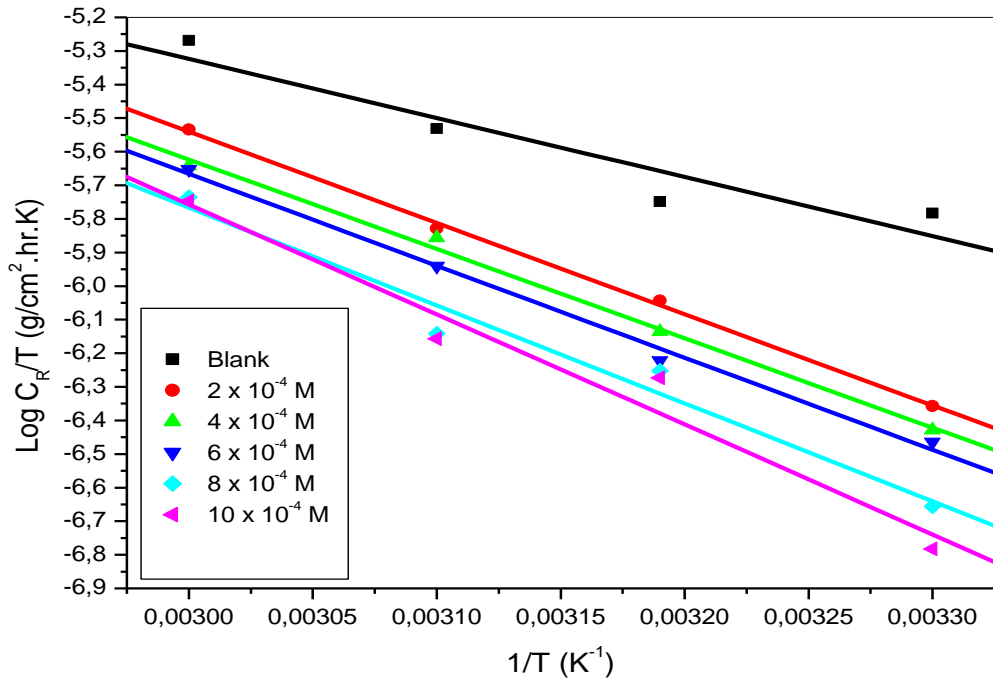


Figure 4.135: Transition state plots for the corrosion of mild steel in 1.5 M  $\text{CH}_3\text{COOH}$  in the absence and presence of various concentrations of 3CYC.

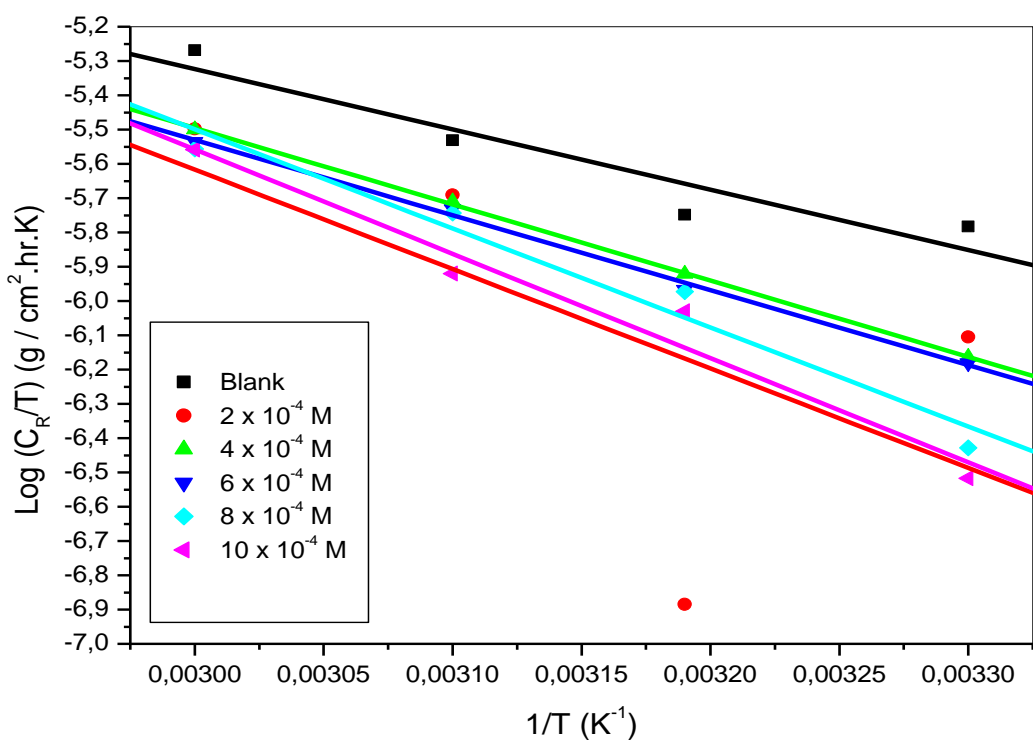


Figure 4.136: Transition state plots for the corrosion of mild steel in 1.5 M  $\text{CH}_3\text{COOH}$  in the absence and presence of various concentrations of 6MCH.



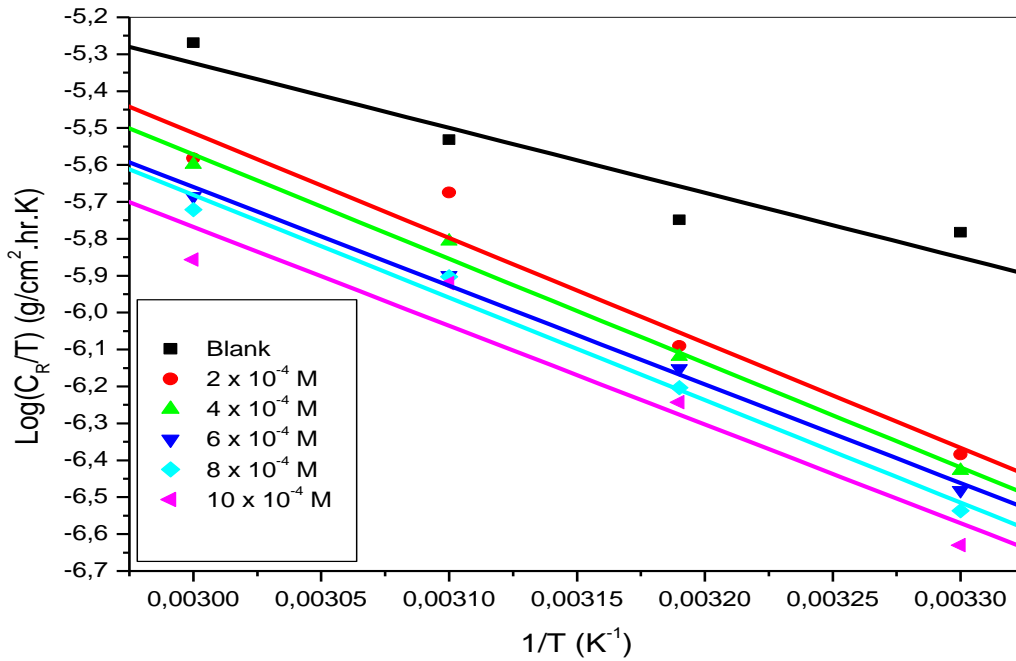


Figure 4.137: Transition state plots for the corrosion of mild steel in 1.5 M  $\text{CH}_3\text{COOH}$  in the absence and presence of various concentrations of 6MC2C.

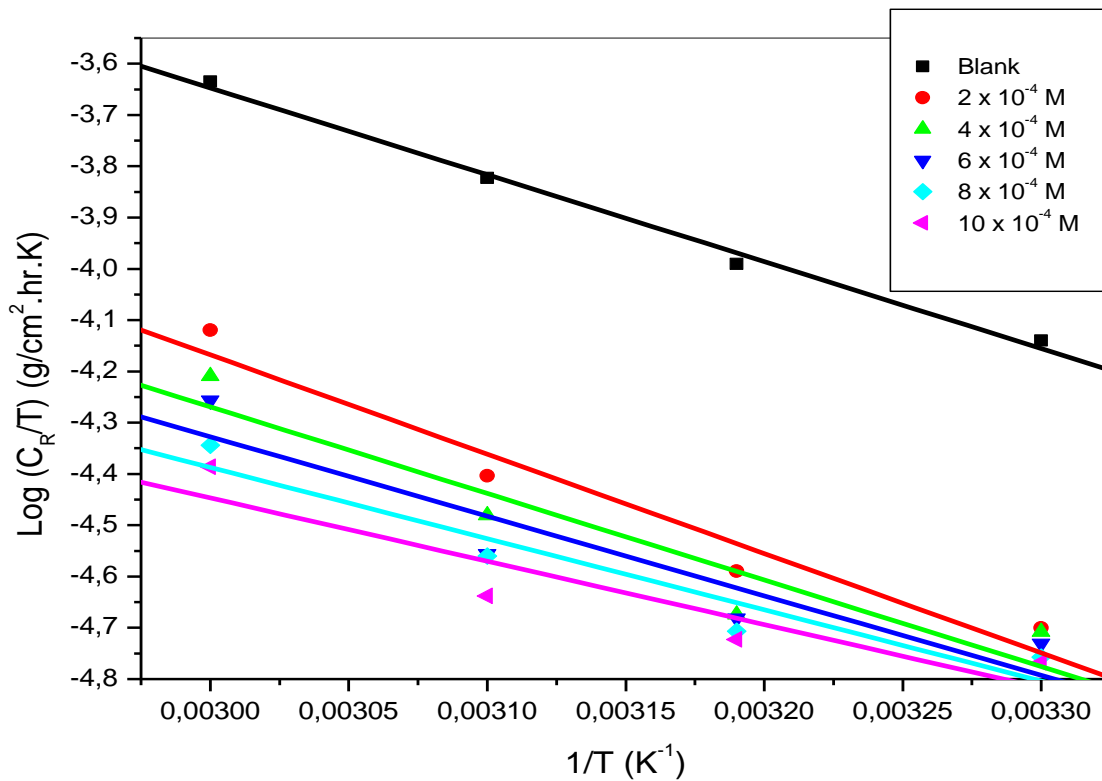


Figure 4.138: Transition state plots for the corrosion of zinc in 1.5 M  $\text{H}_2\text{SO}_4$  in the absence and presence of various concentrations of 3CYC.

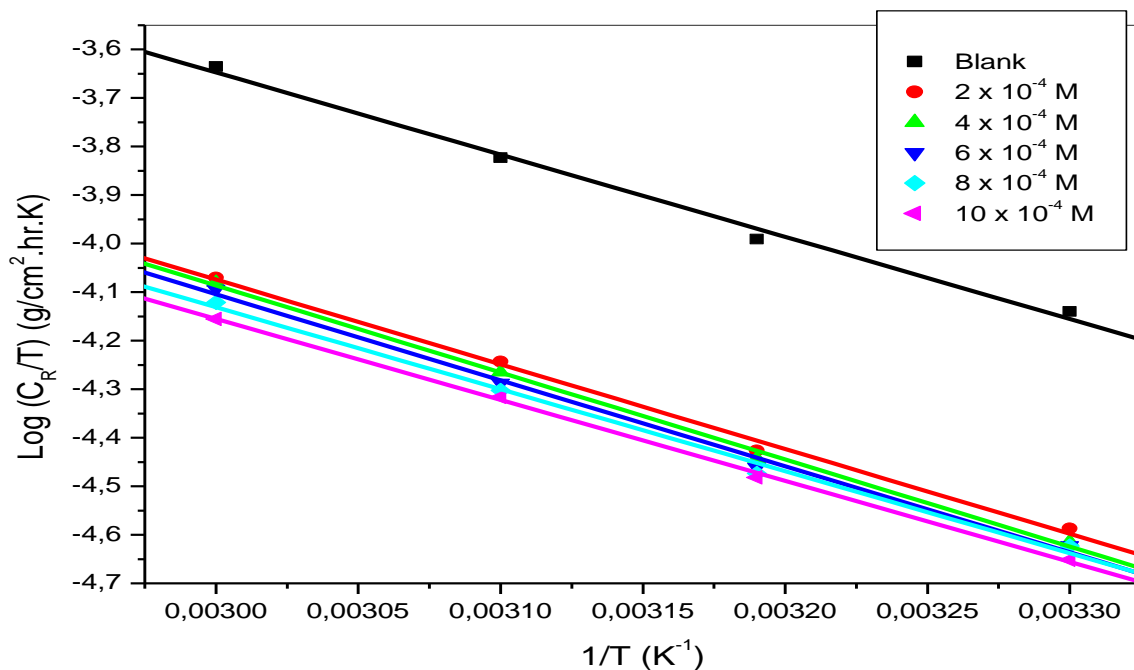


Figure 4.139: Transition state plots for the corrosion of zinc in 1.5 M H<sub>2</sub>SO<sub>4</sub> in the absence and presence of various concentrations of 6MCH.

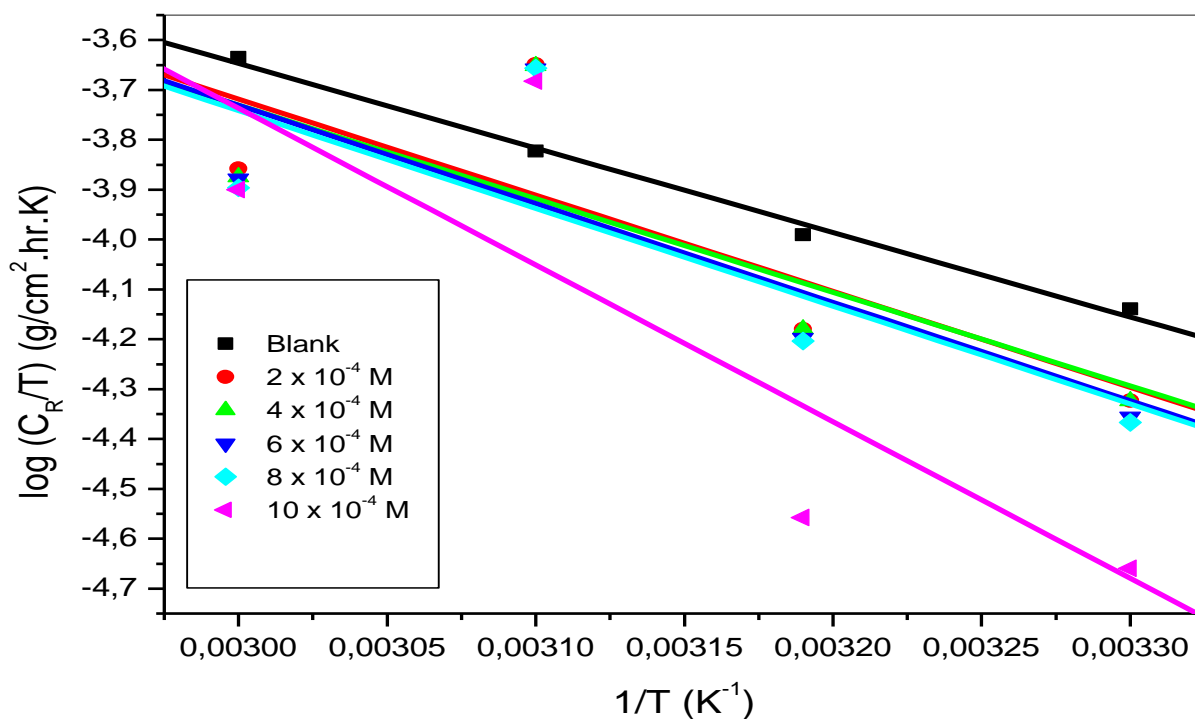


Figure 4.140: Transition state plots for the corrosion of zinc in 1.5 M H<sub>2</sub>SO<sub>4</sub> in the absence and presence of various concentrations of 6MC2C.

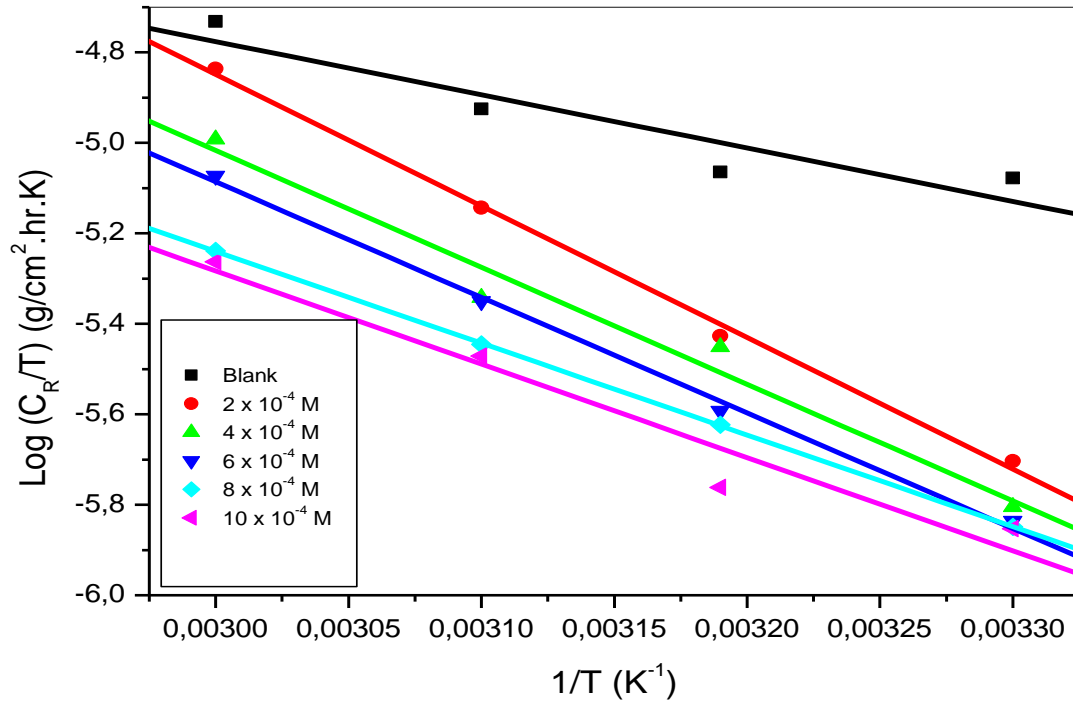


Figure 4.141: Transition state plots for the corrosion of zinc in 1.5 M  $\text{CH}_3\text{COOH}$  in the absence and presence of various concentrations of 3CYC.

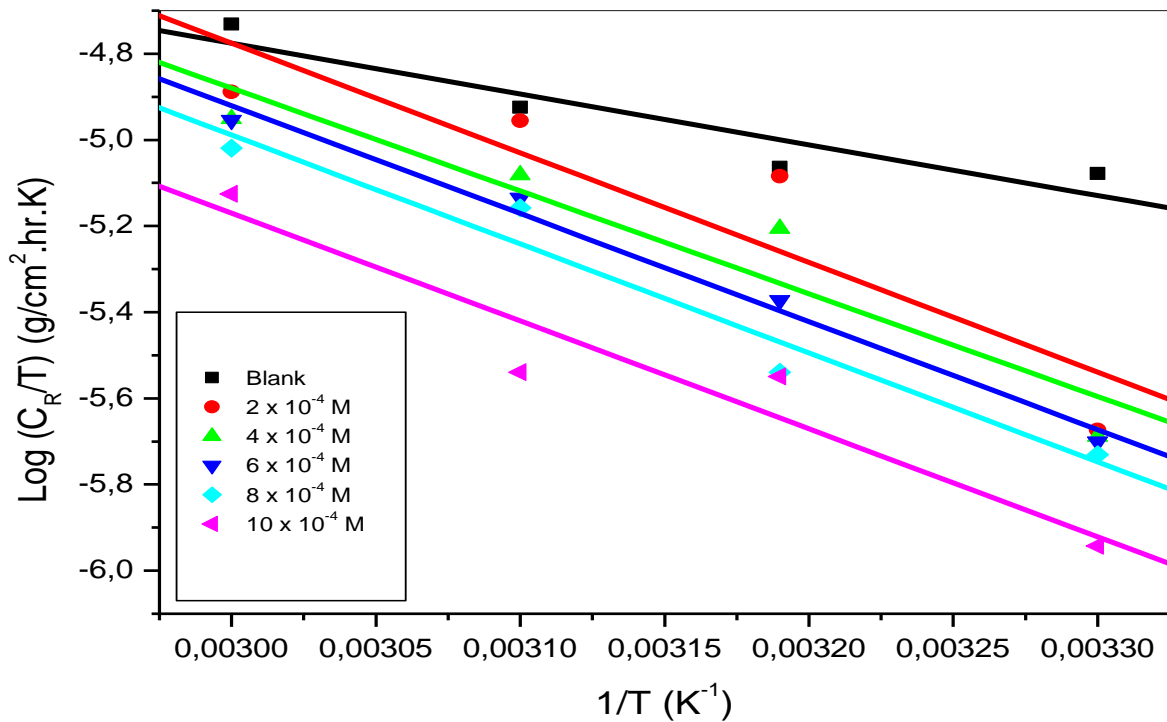


Figure 4.142: Transition state plots for the corrosion of zinc in 1.5 M  $\text{CH}_3\text{COOH}$  in the absence and presence of various concentrations of 6MCH.

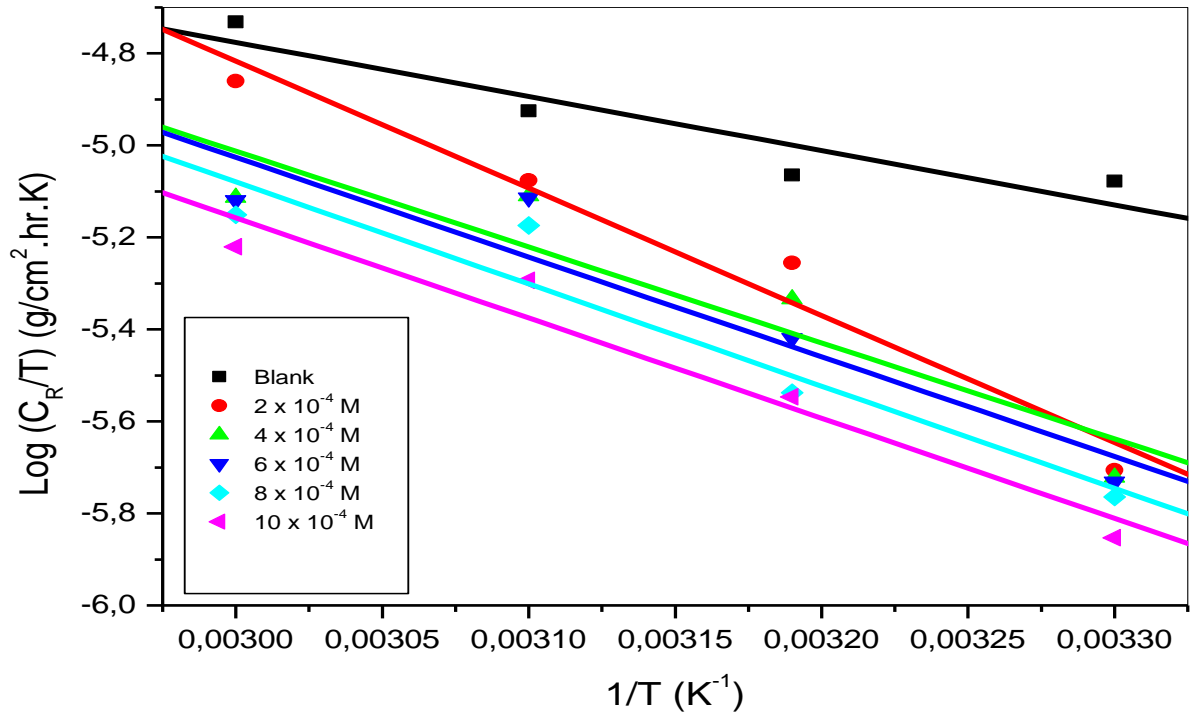


Figure 4.143: Transition state plots for the corrosion of zinc in 1.5 M CH<sub>3</sub>COOH in the absence and presence of various concentrations of 6MC2C.

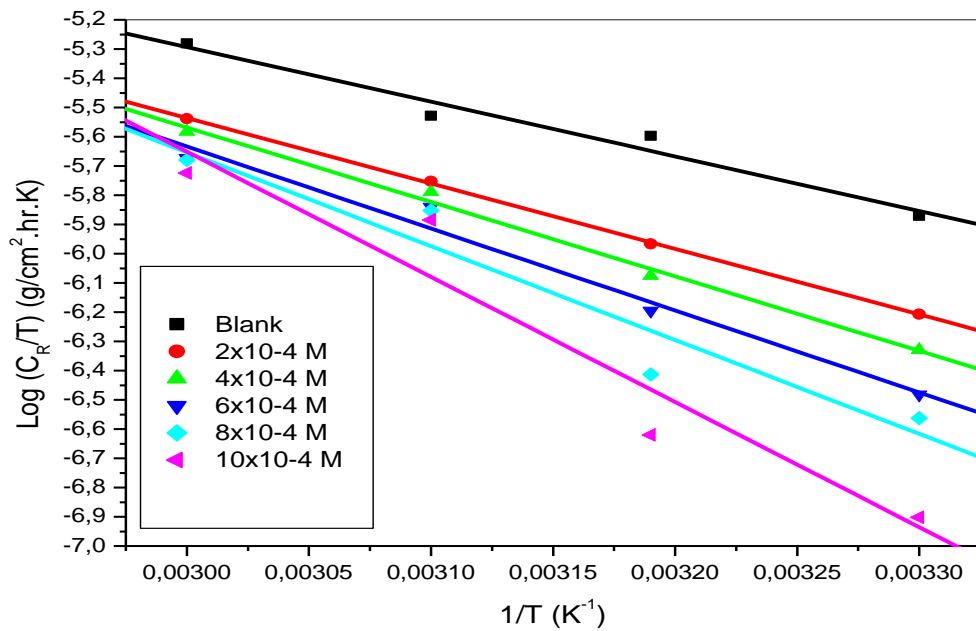


Figure 4.144: Transition state plots for the corrosion of aluminium in 1.5 M HNO<sub>3</sub> in the absence and presence of various concentrations of 3CYC.

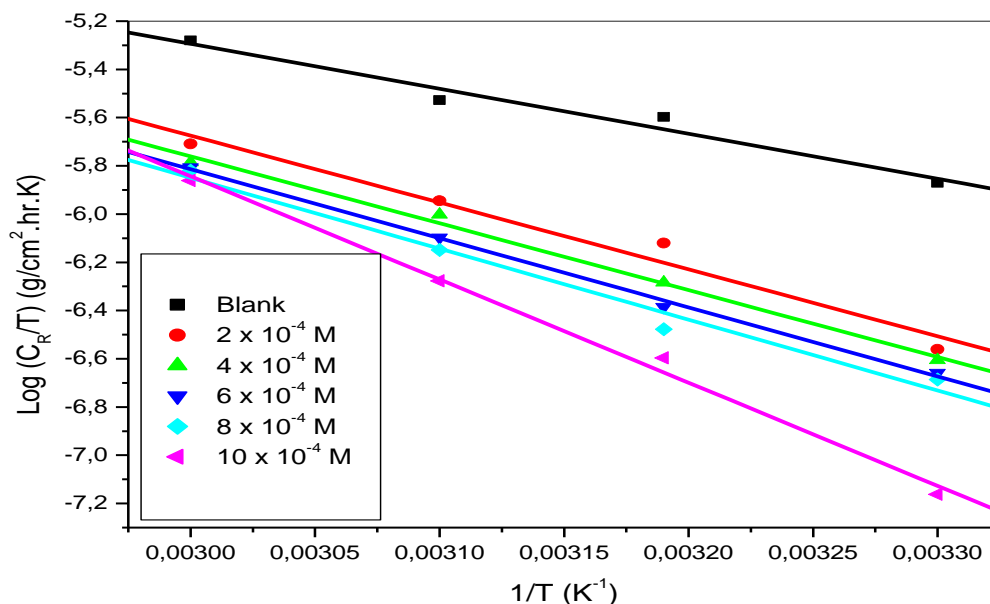


Figure 4.145: Transition state plots for the corrosion of aluminium in 1.5 M HNO<sub>3</sub> in the absence and presence of various concentrations of 6MCH.

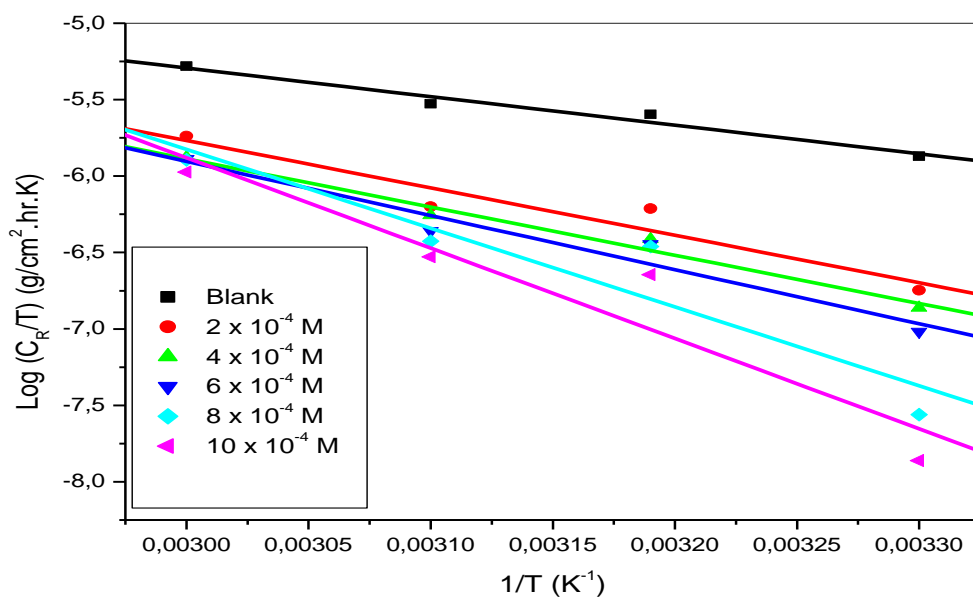


Figure 4.146: Transition state plots for the corrosion of aluminium in 1.5 M HNO<sub>3</sub> in the absence and presence of various concentrations of 6MC2C.

Tables 4.52–4.56 display valid information about the activation energy, change in enthalpy and change in entropy. The activation energy of uninhibited metal appears to be lower compared to the inhibited metal. This trend deviates at Table 4.54 where the uninhibited metal has activation energy of 35.08kJ/mol, the presence of inhibitor had little or minor impact especially on Table 4.52 because the activation energy of uninhibited metal is higher than when

inhibitor is presence. The higher activation energy implies that the reaction takes much time to complete [39]. Table 4.55 shows that the entropy of blank is higher compared to the entropy in the presence of studied inhibitors, thus, the state of disorder was minimised by the presence of inhibitors [39, 40]. The values of activation energy are closer to the values of change in enthalpy, thus, similar trend observed in activation energy values were presence in values of change in enthalpy.

Table 4.52: Kinetic and activation parameters for mild steel in 1.5 M H<sub>2</sub>SO<sub>4</sub> in the absence and presence of various concentrations of inhibitors.

Inhibitor	Concentration (M)	E <sup>a</sup> (kJ.mol <sup>-1</sup> )	ΔH* (kJ.mol <sup>-1</sup> )	-ΔS* (JK <sup>-1</sup> mol <sup>-1</sup> )
Blank	0.00	35.14	32.50	196.08
3CYC	2x10 <sup>-4</sup>	61.84	59.20	192.36
	4x10 <sup>-4</sup>	78.10	75.61	189.85
	6x10 <sup>-4</sup>	76.30	73.66	190.31
	8x10 <sup>-4</sup>	81.13	78.49	189.61
	10x10 <sup>-4</sup>	84.54	81.90	189.24
6MCH	2x10 <sup>-4</sup>	45.17	42.53	145.85
	4x10 <sup>-4</sup>	43.12	40.48	152.73
	6x10 <sup>-4</sup>	43.52	45.85	137.44
	8x10 <sup>-4</sup>	45.30	42.66	146.34
	10x10 <sup>-4</sup>	56.87	54.23	111.54
6MC2C	2x10 <sup>-4</sup>	60.88	58.23	242.45
	4x10 <sup>-4</sup>	128.40	59.02	221.52
	6x10 <sup>-4</sup>	110.58	107.94	199.80
	8x10 <sup>-4</sup>	139.13	136.49	203.57
	10x10 <sup>-4</sup>	147.93	145.29	188.98

Table 4.53: Kinetic and activation parameters for mild steel in 1.5 M CH<sub>3</sub>COOH in the absence and presence of various concentrations of inhibitors.

Inhibitor	Concentration (M)	E <sup>a</sup> (kJ.mol <sup>-1</sup> )	ΔH* (kJ.mol <sup>-1</sup> )	-ΔS* (JK <sup>-1</sup> mol <sup>-1</sup> )
Blank	0.00	36.28	33.64	197.62
3CYC	2x10 <sup>-4</sup>	54.66	52.02	194.96
	4x10 <sup>-4</sup>	53.60	50.96	195.21
	6x10 <sup>-4</sup>	55.08	52.44	195.02
	8x10 <sup>-4</sup>	58.44	55.80	194.59
	10x10 <sup>-4</sup>	65.36	62.71	193.50
	2x10 <sup>-4</sup>	41.59	55.53	138.24
	4x10 <sup>-4</sup>	45.22	42.58	174.77

6MCH	$6 \times 10^{-4}$	44.55	41.91	177.44
	$8 \times 10^{-4}$	57.97	55.33	136.59
	$10 \times 10^{-4}$	60.84	58.20	129.11
6MC2C	$2 \times 10^{-4}$	57.08	54.44	194.31
	$4 \times 10^{-4}$	56.75	54.11	194.42
	$6 \times 10^{-4}$	53.81	51.17	194.97
	$8 \times 10^{-4}$	55.81	53.17	194.68
	$10 \times 10^{-4}$	53.87	51.23	195.07

Table 4.54: Kinetic and activation parameters for zinc in 1.5 M H<sub>2</sub>SO<sub>4</sub> in the absence and presence of various concentrations of inhibitors.

Inhibitor	Concentration (M)	E <sup>a</sup> (kJ.mol <sup>-1</sup> )	ΔH* (kJ.mol <sup>-1</sup> )	-ΔS* (JK <sup>-1</sup> mol <sup>-1</sup> )
Blank	0.00	35.08	32.44	195.89
3CYC	$2 \times 10^{-4}$	39.72	37.08	195.69
	$4 \times 10^{-4}$	34.97	32.33	196.53
	$6 \times 10^{-4}$	32.35	29.71	197.00
	$8 \times 10^{-4}$	29.21	26.57	197.55
	$10 \times 10^{-4}$	26.27	23.63	198.07
6MCH	$2 \times 10^{-4}$	36.08	33.44	196.20
	$4 \times 10^{-4}$	36.97	34.33	196.07
	$6 \times 10^{-4}$	36.59	33.95	196.15
	$8 \times 10^{-4}$	34.99	32.35	196.43
	$10 \times 10^{-4}$	34.60	31.96	196.51
6MC2C	$2 \times 10^{-4}$	39.52	36.88	158.13
	$4 \times 10^{-4}$	38.55	35.91	161.27
	$6 \times 10^{-4}$	40.45	37.81	155.59
	$8 \times 10^{-4}$	40.19	37.55	156.56
	$10 \times 10^{-4}$	62.77	60.13	088.73

Table 4.55: Kinetic and activation parameters for mild steel in 1.5 M CH<sub>3</sub>COOH in the absence and presence of various concentrations of inhibitors.

Inhibitor	Concentration (M)	E <sup>a</sup> (kJ.mol <sup>-1</sup> )	ΔH* (kJ.mol <sup>-1</sup> )	-ΔS* (JK <sup>-1</sup> mol <sup>-1</sup> )
Blank	0.00	25.18	22.54	198.82
3CYC	$2 \times 10^{-4}$	58.32	55.68	193.69
	$4 \times 10^{-4}$	52.11	49.47	194.84
	$6 \times 10^{-4}$	51.53	48.89	194.99
	$8 \times 10^{-4}$	41.48	38.84	196.73
	$10 \times 10^{-4}$	42.16	39.52	196.66
	$2 \times 10^{-4}$	32.84	48.73	142.81
	$4 \times 10^{-4}$	29.80	45.69	153.94

6MCH	$6 \times 10^{-4}$	32.10	47.99	147.82
	$8 \times 10^{-4}$	32.53	48.42	147.83
	$10 \times 10^{-4}$	50.58	47.94	152.07
6MC2C	$2 \times 10^{-4}$	55.54	52.90	131.09
	$4 \times 10^{-4}$	42.55	39.91	173.82
	$6 \times 10^{-4}$	44.14	41.50	169.29
	$8 \times 10^{-4}$	45.15	42.51	167.30
	$10 \times 10^{-4}$	44.33	41.69	171.25

Table 4.56: Kinetic and activation parameters for aluminium in 1.5 M HNO<sub>3</sub> in the absence and presence of various concentrations of inhibitors.

Inhibitor	Concentration (M)	E <sup>a</sup> (kJ.mol <sup>-1</sup> )	ΔH* (kJ.mol <sup>-1</sup> )	-ΔS* (JK <sup>-1</sup> mol <sup>-1</sup> )
Blank	0.00	38.42	35.79	191.56
3CYC	$2 \times 10^{-4}$	45.55	42.91	174.85
	$4 \times 10^{-4}$	51.42	48.78	157.85
	$6 \times 10^{-4}$	56.33	53.69	144.36
	$8 \times 10^{-4}$	64.11	61.47	121.40
	$10 \times 10^{-4}$	84.61	81.97	059.88
6MCH	$2 \times 10^{-4}$	38.43	35.79	191.31
	$4 \times 10^{-4}$	55.72	53.08	146.79
	$6 \times 10^{-4}$	55.74	53.10	148.39
	$8 \times 10^{-4}$	57.52	54.80	144.06
	$10 \times 10^{-4}$	58.96	56.32	140.43
6MC2C	$2 \times 10^{-4}$	38.43	35.79	191.56
	$4 \times 10^{-4}$	62.03	59.39	129.83
	$6 \times 10^{-4}$	63.08	60.44	128.97
	$8 \times 10^{-4}$	70.44	67.80	107.21
	$10 \times 10^{-4}$	10.13	98.70	013.04



---

## CONCLUSIONS

### Conclusions

The assessment of the effect of the three (3) inhibitors was carried out utilizing weight loss measurement, atomic absorption spectroscopy (AAS), Fourier Transform Infrared Spectroscopy (FT-IR), 3D Optical microscopy (3DOP) and electrochemical procedures which included: Potentiodynamic polarization (PDP) and electrochemical impedance spectroscopy (EIS). In an effort to minimise rate of corrosion, therefore the following can be drawn from this study.

- (1) The weight loss measurement shows that the activation energy increases with increase in concentration of corrosion inhibitors. This trend implies that the presence of 3CYC, 6MCH, and 6MC2C delayed corrosion process by forming thin protective layer to MS, Zn, and Al. This statement can be supported by  $K_{ad}$  adsorption value obtained at 303K, large  $K_{ad}$  adsorption value imply greater adsorption of inhibitors onto metal surface. In this study, a decrease in temperature contributed toward increase in  $K_{ad}$  adsorption meaning that at low temperature (303K) maximum IE% were obtained. The conclusion drawn from the values of  $\Delta G^\circ$  reveal that the interactions of Al-inhibitor possess covalent nature and monolayer indicating chemisorption because the  $\Delta G^\circ$  values were  $-45.93\text{kJ/mol}$  to  $-199.83\text{kJ/mol}$ . It further shows physisorption character on Zn-inhibitor and MS-inhibitor with  $\Delta G^\circ$  values below  $-20\text{kJ/mol}$ .
- (2) The rise in temperature contributed towards an increase in rate of reaction. From the weight loss measurements it can be seen that compounds 3CYC, 6MCH, and 6MC2C minimised corrosion rate of MS, Zn, and Al metal in 1.5M  $\text{H}_2\text{SO}_4$ ,  $\text{CH}_3\text{COOH}$ , and  $\text{HNO}_3$  at various temperatures.
- (3) AAS was successful in detecting the concentration of Al, Zn, and MS in solutions in the presence and absence of corrosion inhibitors. The IE% from AAS indicate that the extent at which the inhibitors minimise metal dissolution ranges between 54.18 to 98.60%. Among three tested inhibitors, 3CYC immersed in sulphuric acid shows better inhibition efficiency for zinc.

- (4) The  $i_{\text{corr}}$  values were high in the absence of inhibitors and lower in the presence of inhibitors. This implies that 3CYC, 6MC2C, and 6MCH successfully minimise current resulting in high inhibition efficiency. Surface coverage increase when concentration of inhibitors increases, implying noticeably higher protection of Al, Zn, and MS.
- (5) The charge transfer resistance ( $R_{\text{ct}}$ ) values obtained were lower in the absence of inhibitors and higher in the presence of inhibitor resulting in noticeably higher inhibition efficiency. This high IE% implies that 3CYC, 6MCH, and 6MC2C successfully minimised corrosion of Al, Zn, and MS in  $\text{HNO}_3$ ,  $\text{H}_2\text{SO}_4$ , and  $\text{CH}_3\text{COOH}$ .
- (6) FTIR successfully confirmed the interaction between inhibitors and metal surface that occurred through formation and disappearance of some functional groups. This form of interaction correlate with  $K_{\text{ad}}$  values obtained from weight loss measurements confirms that there exist interaction between inhibitor and metal surface resulting in the successfulness of 3CYC, 6MCH, and 6MC2C inhibiting corrosion.
- (7) 3DOM clearly showed the rough and damaged surface of the metal exposed in the absence of inhibitors, however, in the presence of inhibitors metal surface was less damage indicating that 3CYC, 6MCH, and 6MC2C had minimised the metal damage.
- (8) Overall, the comparison was made to investigate which inhibitor works best under certain conditions. It is clear that 3CYC effectively minimise corrosion rate of MS in  $\text{H}_2\text{SO}_4$ . Among the three tested inhibitors, 3CYC displayed higher IE% on MS in  $\text{H}_2\text{SO}_4$ , this is due to its characteristic such as CN amino group. 3CYC can be recommended to be the best corrosion inhibitor for MS exposed in  $\text{H}_2\text{SO}_4$  at 303K.

## CHAPTER 6

### FUTURE WORK

This study focused on studying 3CYC, 6MCH, and 6MC2C inhibitors in MS, Zn, and Al metals immersed in  $\text{H}_2\text{SO}_4$ ,  $\text{CH}_3\text{COOH}$ , and  $\text{HNO}_3$  only. It would be beneficial to test this compound in basic medium rather than acidic only. Other metals such as copper may be used to test this compound. Temperature ranges may also be increased from 273K up to 333K. Combining these three acids and repeat same procedures would also be interesting to find the outcomes.

## CHAPTER 7

### REFERENCES

- 1) Ahmad, Z., *Principles of corrosion engineering and corrosion control*. Butterworth Heinemann, Oxford, UK, (2006) 1-8.
- 2) Murulana, L. C., M. M. Kabanda, and E. E. Ebenso, *Journal of Molecular Liquids*, **Elsevier**. (2016) 2.
- 3) Fouda, A.E., M.M. Farahat, and M. Abdallah, *Cephalosporin antibiotics as new corrosion inhibitors for nickel in HCl solution*. **Research on Chemical Intermediates**. 40 (2014) 1249-1266.
- 4) Laidler, K.J., *Chemical Kinetics*, Third Edition, Harper & Row. (1987) 42.
- 5) Laidler, K.J., and J.H. Meiser, *Physical chemistry* 1<sup>st</sup> ed. Benjamin/Cummings. (1982) 83-378.
- 6) Yunus A., and M.A. Boles, *Thermodynamics- An Engineering Approach*. McGraw-Hill Series in mechanical Engineering (3<sup>rd</sup> ed) Boston, MA.: McGraw-Hill. (1998). ISBN 978-0-07-011927-7.
- 7) Bauer, T., P. Lunkenheimer, and A. Loidl, *cooperativity and the freezing of Molecular Motion at the Glass Transition*, **physical review Letters**. (2013) 111 (22): 225702.
- 8) Thompson N.G., M. Yunovich and D. Dunmire, *Cost of corrosion and corrosion maintenance strategies*. **Corrosion Reviews**. 25(4) (2007) 247-262.
- 9) Obot I.B., N.O. Obi-Egbedi., and S.A. Umoren, *Antifungal drugs as corrosion inhibitors for aluminium in 0.1 M HCl*, **Corrosion Science**. 51(8) (2009) 1868-1875.
- 10) Agarwal, P., and D. Landolt, *Effect of anions on the efficiency of aromatic carboxylic acid corrosion inhibitors in near neutral media: Experimental investigation and theoretical modeling*. **Corrosion Science**. 40 (1998) 673-691.
- 11) Talbot D., and J. Talbot, *Corrosion science and technology*. Florida: CRC Press. (2000) 82-96.
- 12) Uhlig, H.H., and R.W., Revie, *Corrosion and Corrosion Control. An introduction to Corrosion Science and Engineering, 3rd Ed.*, **John Wiley & Sons, New York**. (1985) 114-133.
- 13) Callister, W.D., *Materials Science and Engineering. An Introduction, 7th Ed.*, **John Wiley & Sons, Inc.** (2007) 338-461.

- 14) Smith, L., *Control of corrosion in oil and gas production tubing*. **British Corrosion Journal**. (1999) 34-247.
- 15) Villamizar, W., M. Casales, J.G. Gonzalez-Rodriguez, and L. Martinez, *CO<sub>2</sub> corrosion inhibition by hydroxyethyl, aminoethyl, and amidoethyl imidazolines in water–oil mixtures*. **Journal of Solid State Electrochemistry**. 11 (2007) 619-620.
- 16) Koch, G.H., M.P.H. Brongers, N.G. Thompson, Y.P. Virmani, and J.H. Payer, *Handbook of environmental degradation of materials*, 2nd Ed., William Andrew, **Norwich, New York**. (2005) 560-667.
- 17) Chaudhari, A., P. Tatiya, R. Hedao, R. Kulkarni, and V. Gite, *Polyurethane prepared from neem oil polyesteramides for self-healing anticorrosive coatings*. **Industrial Engineering Chemistry Research**. (2013) 101-189.
- 18) Ebenso, E., H. Alemu, S. Umoren, and I. Obot, *Inhibition of mild steel corrosion in sulphuric acid using alizarin yellow GG dye and synergistic iodide additive*. **International Journal of Electrochemical Science**. 3 (2008) 1325-1339.
- 19) El-Maksoud, S.A., *The influence of some Arylazobenzoyl acetonitrile derivatives on the behaviour of carbon steel in acidic media*. **Applied Surface Science**. 206 (2003) 129-136.
- 20) Hassan, R.M. and I.A. Zaafarany, *Kinetics of corrosion inhibition of aluminum in acidic media by water-soluble natural polymeric pectates as anionic polyelectrolyte inhibitors*. **Materials**. 6 (2013) 2436-2451.
- 21) Touham, F., A. Aouniti, Y. Abed, B. Hammouti, S. Kertit, and A. Ramdani, *New pyrazolic compounds as corrosion inhibitors for Iron Armco in HCl media*. **Bulletin of Electrochemistry**. 16 (2000) 245-249.
- 22) Gomma, G.K. and M.H. Wahdan, *Schiff bases as corrosion inhibitors for aluminium in hydrochloric acid solution*. **Materials Chemistry and Physics**. 39 (1995) 209-213.
- 23) Blin, F., S.G. Leary, G.B. Deacon, P. C. Junk, and M. Forsyth, *The nature of the surface film on steel treated with cerium and lanthanum cinnamate based corrosion inhibitors*. **Corrosion Science**. (2006) 404.

- 24) Quraishi, M.A., J. Rawat, *Corrosion inhibiting action of tetramethyl-dithia-octaazacyclotetradeca-hexaene (MTAH) on corrosion of mild steel in hot 20% sulfuric acid. **Materials Chemistry and Physics.** (2002) 43.*
- 25) Felhosi, I., J. Telegdi, G. Palinkas, and E. Kalman, *Kinetics of self-assembled layer formation on iron. **Electrochimica Acta.** (2002) 2335.*
- 26) Felhösi, I., E. Kálmán, and P. Póczik, *Corrosion protection by self-assembly. **Russian Journal of Electrochemistry.** (2002) 230.*
- 27) Quraishi, M.A., and D. Jamal, Technical note: CAHMT. A New and eco-friendly acidizing corrosion inhibitor. **Corrosion Science.** (2000) 983.
- 28) Walton, J. C., G. Cragnoia, and S.K. Kalandros, *A numerical model of crevice corrosion for passive and active metals. **Corrosion science.** (1996) 11-21.*
- 29) Hoff, G., G. Langbein, and H. Rieger, *Material destruction due to liquid impact, in erosion by cavitation or impingent. **American Society for Testing and Materials.** (1967) 42-44.*
- 30) Jones, D.A. *Principles and prevention of corrosion.* Prentice-Hall International, United Kingdom. (1996) 862-889.
- 31) Koch G., M. Brongers, N. Thompson, Y. P. Virmani, and J.H. Payer, *Corrosion Cost and Preventive Strategies in the United States.* Publication No. FHWA-RD-01-156. **NACE International.** 231-565.
- 32) Edeleanu, C., and J.G. Hines, *Modeling approach to corrosion prediction. **Materials Performance.** (1990) 63-75.*
- 33) Revie, W., and H.H. Uhlig, *Corrosion and corrosion control: An introduction to corrosion science and engineering. **Wiley-Interscience.** (2008) 537-566.*
- 34) Donnelly, B., T.C. Downie, R. Gzeskowiak, H.R. Hamburg, and D. Short, *Study of the inhibiting properties of some derivatives of thiourea. **Corrosion Science.** (1977) 109.*
- 35) Thomas, J.G.N., *Proceedings of the 5th European symposium on corrosion inhibitors. **Annali dell Universita Ferrara, Italy.** (1980) 453-488.*

- 36) Revie R.W., and H.H. Uhlig, *Corrosion handbook*, **John Wiley and Sons, New York City, New York.** (2000) 219-452.
- 37) Murulana, L. C., M. M. Kabanda, and E. E. Ebenso, *Experimental and theoretical studies on the corrosion inhibition of mild steel by some sulphonamides in aqueous HCl*. **Royal Society of Chemistry Advances.** (2015) 28743-28761.
- 38) Myles, K. *Corrosion control. Principles and practice.* **Myles Publications.** (1995) 220.
- 39) Hluchan, V., B.L Wheeler, and N. Hackerman, *Amino acids as corrosion inhibitors in hydrochloric acid solutions.* **Werkstoffe and Korrosion.** 39 (1988). 512.
- 40) Shukla, S.K., and M.A. Quraishi, *Cefotaxime sodium: A new and efficient corrosion inhibitor for mild steel in hydrochloric acid solution*, **Corrosion Science.** 51 (2009) 1007– 1011.
- 41) Hassan, H.H., E. Abdelghani, and M.A. Amin, *Inhibition of mild steel corrosion in hydrochloric acid solution by triazole derivatives: Part I. Polarization and EIS studies* **Electrochim. Acta.** 52 (2007) 6359 – 6366.
- 42) El Azhar, M., B. Mernari, M. Traisnel, F. Bentiss, and M. Lagrenee, *Corrosion inhibition of mild steel by the new class of inhibitors [2,5-bis(n-pyridyl)-1,3,4-thiadiazoles] in acidic media*, **Corrosion Science.** 43 (2001) 2229 – 2238.
- 43) Hmamou, D.B., R. Salghi, A. Zarrouk, H. Zarrok, S.S. Al-Deyab, O. Benali, and B. Hammouti, *The Inhibited effect of Phenolphthalein towards the corrosion of C38 Steel in Hydrochloric Acid*, **International Journal of Electrochemical Science.** 7 (2012) 8988–9003.
- 44) Yadav, M., D. Behera, S. Kumar, and R. Sinha, *Experimental and Quantum Chemical Studies on the Corrosion Inhibition Performance of Benzimidazole Derivatives for Mild Steel in HCl*, **Industrial and Engineering Chemistry Research.** 52 (2013) 6318– 6328.
- 45) Coates, J., *Interpretation of Infrared Spectra, A Practical Approach*, in: R.A. Meyers (Ed.), *Encyclopaedia of Analytical Chemistry*, **John Wiley and Sons Ltd, Chichester.** (2000) 10815 – 10837.

- 46) Saji, V., *Contemporary developments in corrosion inhibitors-review of Patents. Recent Patents on Corrosion Science*. 1 (2011) 63-71.
- 47) Villamizar, W., M. Casales, J. Gonzalez-Rodriguez, and L. Martinez, *CO<sub>2</sub> corrosion inhibition by hydroxyethyl, aminoethyl, and amidoethyl imidazolines in water-oil mixtures*. **Journal of Solid State Electrochemistry**. 11 (2007) 619-629.
- 48) Yahaya, N., N.M. Noor, M.M. Din, and S.H.M. Nor, *Prediction of CO<sub>2</sub> corrosion growth in submarine pipelines*. **Malaysian Journal of Civil Engineering**. 21 (2009) 69-81.
- 49) Zardasti, L., N.M. Hanafiah, N.M. Noor, Y. Nordin, and A.S.A. Rashid. *The consequence assessment of gas pipeline failure due to corrosion*. in *Solid State Phenomena*. 2015. **Trans Tech Publications**.
- 50) Zarrouk, A., B. Hammouti, T. Lakhlifi, M. Traisnel, H. Vezin, and F. Bentiss, *New 1H-pyrrole-2, 5-dione derivatives as efficient organic inhibitors of carbon steel corrosion in hydrochloric acid medium: electrochemical, XPS and DFT studies*. **Corrosion Science**. 90 (2015) 572-584.
- 51) Ghasemi, O., I. Danaee, G. Rashed, M. RashvandAvei, and M. Maddahy, *Inhibition effect of a synthesized N, N'-bis (2-hydroxybenzaldehyde)-1, 3-propandiimine on corrosion of mild steel in HCl*. **Journal of Central South University**. 20 (2013) 301-311.
- 52) Morad, M. and A.K. El-Dean, *2, 2'-Dithiobis (3-cyano-4, 6-dimethylpyridine): A new class of acid corrosion inhibitors for mild steel*. **Corrosion Science**. 48 (2006) 3398-3412.
- 53) Popova, A., M. Christov, and A. Vasilev, *Mono-and dicationic benzothiazolic quaternary ammonium bromides as mild steel corrosion inhibitors. Part III: influence of the temperature on the inhibition process*. **Corrosion Science**. 94 (2015) 70-78
- 54) El-Awady, A., B. Abd-El-Nabey, and S. Aziz, *Kinetic-thermodynamic and adsorption isotherms analyses for the inhibition of the acid corrosion of steel by cyclic and open-chain amines*. **Journal of the Electrochemical Society**. 139 (1992) 2149-2154.
- 55) Kern, P. and D. Landolt, *Adsorption of an organic corrosion inhibitor on iron and gold studied with a rotating EQCM*. **Journal of the Electrochemical Society**. 148 (2001) B228-B235.



- 56) Obot, I., N. Obi-Egbedi, and S. Umoren, *Adsorption characteristics and corrosion inhibitive properties of clotrimazole for aluminium corrosion in hydrochloric acid*. **International Journal of Electrochemical Science**. 4 (2009) 863-877.
- 57) Thiraviyam, P. and K. Kannan, *Inhibition of aminocyclohexane derivative on mild steel corrosion in 1 N HCl*. **Arabian Journal for Science and Engineering**. 38 (2013) 1757-1767.
- 58) Noor, E.A. and A.H. Al-Moubaraki, *Thermodynamic study of metal corrosion and inhibitor adsorption processes in mild steel/1-methyl-4 [4'(-X)-styryl pyridinium iodides/hydrochloric acid systems*. **Materials Chemistry and Physics**. 110 (2008) 145-154.
- 59) Avci, G., *Corrosion inhibition of indole-3-acetic acid on mild steel in 0.5 M HCl*. **Colloids and Surfaces A: Physicochemical and Engineering Aspects**. 317 (2008) 730-736.
- 60) Langmuir, I., *The constitution and fundamental properties of solids and liquids. Part I. Solids*. **Journal of the American Chemical Society**. 38 (1916) 2221-2295.
- 61) Ituen, E. and U. Udo, *Phytochemical profile, adsorptive and inhibitive behaviour of Costus afer extracts on aluminium corrosion in hydrochloric acid*. **Der Chemica Sinica**. 3 (2012) 1394-1405.
- 62) Yadav, D.K., M. Quraishi, and B. Maiti, *Inhibition effect of some benzylidenes on mild steel in 1 M HCl: an experimental and theoretical correlation*. **Corrosion Science**. 55 (2012) 254-266.
- 63) Loveday, D., P. Peterson, and B. Rodgers, *Evaluation of organic coatings with electrochemical impedance spectroscopy. Part 3: Protocols for testing coatings with EIS*. **JCT coatingstech**. 2 (2005) 22-27.
- 64) Nomenclature, M.C.E.-o. and Definitions. *Compilation of ASTM standard definitions*. 1976. American Society for Testing and Materials.
- 65) Goldstein, J.I., D.E. Newbury, J.R. Michael, N.W. Ritchie, J.H.J. Scott, and D.C. Joy, *Scanning electron microscopy and X-ray microanalysis*. 2017: **Springer**.



- 66) Krishnegowda, P.M., V.T. Venkatesha, P.K.M. Krishnegowda, and S.B. Shivayogiraju, *Acalypha torta* leaf extract as green corrosion inhibitor for mild steel in hydrochloric acid solution. **Industrial & Engineering Chemistry Research**. 52 (2013) 722-728.
- 67) Wassilkowska, A. and W. Dąbrowski, *Zastosowanie mikroskopii elektronowej do badania rur żeliwnych. Cz. 1, Struktura wykładziny z zaprawy cementowej*. **Gaz, Woda i Technika Sanitarna**. (2012) 154-159.
- 68) Stupnisek-Lisac, E., A. Brnada, and A.D. Mance, *Secondary amines as copper corrosion inhibitors in acid media*. **Corrosion Science**. 42 (2000) 243-257.
- 69) Amin, M.A., S.S.A. El-Rehim, E. El-Sherbini, and R.S. Bayoumi, *The inhibition of low carbon steel corrosion in hydrochloric acid solutions by succinic acid: Part I. Weight loss, polarization, EIS, PZC, EDX and SEM studies*. **Electrochimica Acta**. 52 (2007) 3588-3600.
- 70) Bastidas, D.M., E. Cano, and E. Mora, *Volatile corrosion inhibitors: a review*. **Anti-Corrosion Methods And Materials**. 52 (2005) 71-77.
- 71) Rammelt, U., S. Koehler, and G. Reinhard, *Use of vapour phase corrosion inhibitors in packages for protecting mild steel against corrosion*. **Corrosion Science**. 51 (2009) 921-925
- 72) Kondo, H., *Protic ionic liquids with ammonium salts as lubricants for magnetic thin film media*. **Tribology Letters**. 31 (2008) 211-218.
- 73) Vuorinen, E. and W. Skinner, *Amine carboxylates as vapour phase corrosion inhibitors*. **British Corrosion Journal**. 37 (2002) 159-160.
- 74) Kohler, F., R. Gopal, G. Goetze, H. Atrops, M. Demeriz, E. Liebermann, E. Wilhelm, F. Ratkovics, and B. Palagyi, *Molecular interactions in mixtures of carboxylic acids with amines. 2. Volumetric, conductimetric, and NMR properties*. **The Journal of Physical Chemistry**. 85 (1981) 2524-2529.
- 75) Kohler, F., H. Atrops, H. Kalali, E. Liebermann, E. Wilhelm, F. Ratkovics, and T. Salamon, *Molecular interactions in mixtures of carboxylic acids with amines. 1. Melting curves and viscosities*. **The Journal of Physical Chemistry**. 85 (1981) 2520-2524.

- 76) Soeda, K. and T. Ichimura, *Present state of corrosion inhibitors in Japan*. **Cement and Concrete Composites**. 25 (2003) 117-122.
- 77) Sagoe-Crentsil, K., V. Yilmaz, and F.P. Glasser, *Corrosion inhibition of steel in concrete by carboxylic acids*. **Cement and Concrete Research**. 23 (1993) 1380-1388.
- 78) Žerjav, G. and I. Milošev, *Carboxylic acids as corrosion inhibitors for Cu, Zn and Brasses in Simulated Urban Rain*. **International Journal of Electrochemical Science**. 9 (2014) 2696-2715.
- 79) Bouzidi, D., A. Chetouani, B. Hammouti, S. Kertit, M. Taleb, and S. Al-Deyab, *Electrochemical corrosion behaviour of iron rotating disc electrode in physiological medium containing amino acids and amino esters as an inhibitors*. **International Journal of Electrochemical Science**. 7 (2012) 2334-2348.
- 80) Khaled, K., N. Abdel-Shafi, and N. Al-Mobarak, *Understanding corrosion inhibition of iron by 2-thiophenecarboxylic acid methyl ester: Electrochemical and computational study*. **International Journal of Electrochemical Science**. 7 (2012) 1027-1044.
- 81) Helen, L., A. Rahim, B. Saad, M. Saleh, and P.B. Raja, *Aquilaria crassna leaves extracts—a green corrosion inhibitor for mild steel in 1 M HCl medium*. **International Journal of Electrochemical Science**. 9 (2014) 830-846.
- 82) Manamela, K.M., L.C. Murulana, M.M. Kabanda, and E.E. Ebenso, *Adsorptive and DFT studies of some imidazolium based ionic liquids as corrosion inhibitors for zinc in acidic medium*. **International Journal of Electrochemical Science**. 9 (2014) 3029-3046.
- 83) Hassan, H.M., A. Eldesoky, R. Younis, and W.A. Zordok, *Density Functional Theory (DFT) Studies on sulfa dimedine azo derivatives as green inhibitors for C-steel in 0.5 MH<sub>3</sub>PO<sub>4</sub> Solutions*. **International Journal**. 2 (2014) 550-568.
- 84) Madram, A.R., F. Shokri, M.R. Sovizi, and H. Kalhor, *Aromatic Carboxylic Acids as Corrosion Inhibitors for Aluminium in Alkaline Solution*. **Portugaliae Electrochimica Acta**. 34 (2016) 395-405.
- 85) Andreev, N., E. Starovoitova, and N. Lebedeva, *Steel corrosion inhibition by benzoic acid salts in calcium hydroxide solutions*. **Protection of Metals**. 44 (2008) 688-691.

- 86) Wranglen, G., *An introduction to corrosion and protection of metals*. 1985: Chapman and Hall.
- 87) Spek, A.L., *Structure validation in chemical crystallography*. **Acta Crystallographica Section D: Biological Crystallography**. 65 (2009) 148-155.
- 88) Meyer, R., T.-k. Ha, H. Frei, and H. Günthard, *Acetic acid monomer: Ab initio study, barrier to proton tunnelling, and infrared assignment*. **Chemical Physics**. 9 (1975) 393-402.
- 89) Atta, A., G. El-Mahdy, H. Al-Lohedan, and A. Ezzat, *A new green ionic liquid-based corrosion inhibitor for steel in acidic environments*. **Molecules**. 20 (2015) 11131-11153.
- 90) Likhanova, N.V., M.A. Domínguez-Aguilar, O. Olivares-Xometl, N. Nava-Entzana, E. Arce, and H. Dorantes, *The effect of ionic liquids with imidazolium and pyridinium cations on the corrosion inhibition of mild steel in acidic environment*. **Corrosion Science**. 52 (2010) 2088-2097.
- 91) Brycki, B.E., I.H. Kowalczyk, A. Szulc, O. Kaczerewska, and M. Pakiet, *Organic Corrosion Inhibitors*, in *Corrosion Inhibitors, Principles and Recent Applications*. **IntechOpen**. (2017)
- 92) Lin, P.-C., I.-W. Sun, J.-K. Chang, C.-J. Su, and J.-C. Lin, *Corrosion characteristics of nickel, copper, and stainless steel in a Lewis neutral chloroaluminate ionic liquid*. **Corrosion Science**. 53 (2011) 4318-4323.
- 93) Antonijevic, M. and M. Petrovic, *Copper corrosion inhibitors. A review*. **International Journal of Electrochemical Science**. 3 (2008) 1-28.
- 94) Levy, M., *Anodic Behavior of Titanium and Commercial Alloys in Sulfuric Acid*. **Corrosion**. 23 (1967) 236-244.
- 95) Vatsala, S., V. Bansal, D. Tuli, M. Rai, S. Jain, S. Srivastava, and A. Bhatnagar, *Gas chromatographic determination of residual hydrazine and morpholine in boiler feed water and steam condensates*. **Chromatographia**. 38 (1994) 456-460.
- 96) Dahmani, M., A. Et-Touhami, S. Al-Deyab, B. Hammouti, and A. Bouyanzer, *Corrosion inhibition of C38 steel in 1M HCl: A comparative study of Black pepper*

- extract and its isolated piperine. International Journal of Electrochemical Science.* 5 (2010) 1060-1069.
- 97) Amira, W.E., A. Rahim, H. Osman, K. Awang, and P.B. Raja, *Corrosion inhibition of mild steel in 1 M HCl solution by Xylopia ferruginea leaves from different extract and partitions. International Journal of Electrochemical Science.* 6 (2011) 2998-3016.
- 98) Osokogwu, U. and E. Oghenekaro, *Evaluation of corrosion inhibitors effectiveness in oilfield production operations. International journal of scientific & technology research.* 1 (2012) 19-23.
- 99) Karthik, R., P. Muthukrishnan, S.-M. Chen, B. Jeyaprabha, and P. Prakash, *Anti-corrosion inhibition of mild steel in 1M hydrochloric acid solution by using Tiliacora acuminate leaves extract. International Journal of Electrochemical Science.* 10 (2015) 3707-3725.
- 100) Anbarasi, M., S. Rajendran, M. Pandiarajan, and A. Krishnaveni, *An encounter with corrosion inhibitors. European Chemical Bulletin.* 2 (2013) 197-207.
- 101) Jiajian, C., C. Dianzhen, and C. Chu'nan, *Inhibition and desorption behaviour of N, N-dipropoxy methyl amine trimethyl phosphonate in hydrochloric acid. Bulletin of Electrochemistry.* 13 (1997) 13-17.
- 102) Lazarova, E., T., Yankova, G. Neykov, *Electrochemical study of the adsorption of n-phenylmaleimide and its p-substituted derivatives on iron in sulfuric acid solutions. Bulgarian Chemical Communications.* 28 (1995) 647-660.
- 103) Kairi, N.I., and J. Kassim, *The effect of temperature on the corrosion inhibition of mild steel in 1 M HCl solution by curcuma longa extract. International Journal of Electrochemical Science.* 8 (2013) 7138-7155.
- 104) Foley, R., *Role of the chloride ion in iron corrosion. Corrosion.* 26 (1970) 58-70.
- 105) Beaunier, L., *Corrosion of grain boundaries: initiation processes and testing. Le Journal de Physique Colloques.* 43 (1982) C6-271-C6-282.

- 106) Al-Amoudi, O.S.B., M. Maslehuddin, A. Lashari, and A.A. Almusallam,,  
*Effectiveness of corrosion inhibitors in contaminated concrete. Cement and Concrete Composites.* 25 (2003) 439-449.